TESIS DOCTORAL

Biología celular y molecular

Joaquín Caro Astorga

2018

UNIVERSIDAD DE MÁLAGA

Universidad de Málaga. Facultad de Ciencias
Departamento de Microbiología

Tesis doctoral

Programa de doctorado:
Biología celular y molecular

Study of the molecular bases governing biofilm formation in *Bacillus cereus*

Joaquín Caro Astorga

Málaga 2018

UNIVERSIDAD DE MÁLAGA

IHSM La Mayora
Instituto de Hortofruticultura Subtropical y Mediterránea

Director: Diego Francisco Romero Hinojosa

UNIVERSIDAD DE MÁLAGA

Departamento de Microbiología

Facultad de Ciencias

Study of the molecular bases governing biofilm formation in *Bacillus cereus*

TESIS DOCTORAL

Joaquín Caro Astorga

Málaga, 2018

AUTOR: Joaquín Caro Astorga

http://orcid.org/0000-0003-4650-6376

EDITA: Publicaciones y Divulgación Científica. Universidad de Málaga

UNIVERSIDAD DE MÁLAGA

Departamento de Microbiología

Facultad de Ciencias

Study of the molecular bases governing biofilm formation in *Bacillus cereus*

Memoria presentada por **D. Joaquín Caro Astorga** para optar al grado de Doctor por la Universidad de Málaga

UNIVERSIDAD DE MÁLAGA

Departamento de Microbiología

Facultad de Ciencias

D. JUAN JOSÉ BORREGO GARCÍA, Director del Departamento de Microbiología de la Universidad de Málaga.

INFORMA:

Que **D. JOAQUÍN CARO ASTORGA** ha realizado en los laboratorios de este departamento el trabajo experimental conducente a la elaboración de la presente Memoria de Tesis Doctoral.

Y para que así conste, y tenga los efectos que correspondan, en cumplimiento de la legislación vigente, expido el presente informe,

En Málaga, 28 de mayo de 2018.

Fdo. D. Juan José Borrego García

UNIVERSIDAD DE MÁLAGA

Departamento de Microbiología

Facultad de Ciencias

D. DIEGO FRANCISCO ROMERO HINOJOSA, Profesor Contratado Doctor del Departamento de Microbiología de la Universidad de Málaga.

INFORMA:

Que, **D. JOAQUÍN CARO ASTORGA** ha realizado bajo mi dirección el trabajo experimental conducente a la elaboración de la presente Memoria de Tesis Doctoral.

Y para que así conste, y tenga los efectos que correspondan, en cumplimiento de la legislación vigente, expedimos el presente informe,

En Málaga, 28 de mayo de 2018.

Fdo. D. Diego Francisco Romero Hinojosa

Este trabajo ha sido subvencionado por:

- Plan Nacional de I+D+I del Ministerio de Ciencia e Innovación AGL-2012-31968, AGL2016-78662-R y cofinanciado con fondos europeos FEDER (UE).
- Ayudas para Contratos Predoctorales para la formación de doctores: BES-2

Agradecimientos:

La realización de una tesis doctoral implica la participación de multitud de personas que directa o indirectamente participan en su desarrollo en los aspectos académico, científico o personal. Tan atrás podría ir como a mi profesora de biología del instituto y su excelente motivación en sus explicaciones. O en las clases de genética en 2º de Ambientales que Cayo Ramos daba también con excelente motivación. Me dejo muchas menciones atrás de la etapa del Máster en Biotecnología, y salto hasta la persona que considero como mi madre científica, Kika. No hay palabras para agradecer su disposición a ayudar en todo lo que estuviera en su mano, para ofrecer todo lo que fuese beneficioso para mí en lo académico, en lo científico y también en lo personal. Kika es también el enlace con mi tesis, pasando de trabajar con la Synucleína a TasA. Todo se queda entre amiloides.

Tras mi buenísima experiencia en el Dpto. de bioquímica, comienza mi tesis doctoral en el Dpto. de microbiología, y aquí mis mayores agradecimientos van a mi director de tesis, Diego Romero. Gracias por confiar en mí desde el día de la entrevista, por ser tan cercano y por tanto trabajo juntos. Por los congresos y las oportunidades de las estancias en Groningen y Boston. Por los laboratorios nuevos. Por la obsesión del trabajo bien hecho y por todo lo que he aprendido bajo tu dirección. Grandes también los agradecimientos a Antonio de Vicente, el padre que supervisa todo en la sombra y que nos cuida sin hacer mucho ruido, o haciéndolo cuando hace falta en los entresijos administrativos de la Universidad de Málaga. Gracias también por tantos seminarios y tantas recomendaciones, donde hay que incluir de

nuevo a Cayo Ramos, y seguir con Alejandro Pérez, Francisco Cazorla y Juan Antonio Torés, siempre atentos para contribuir a mejorar el trabajo, el enfoque, las técnicas y la exposición.

Los comienzos en el laboratorio siempre son de mucha sensación de desorientación. Aunque la ayuda siempre estuvo en todas partes, recuerdo especialmente la atención de Irene, Houda y Laura G durante las primeras semanas. Y sigo con Irene, por tu paciencia, por tu trabajo y por tu amistad, has sido una persona muy importante todos estos años. Para Jesús, David y Alvarito también tengo mención especial en lo académico, lo científico y lo personal. Tantas discusiones científicas, vuestra ayuda con los papeleos, en la escritura y en las aventuras en los congresos, sin olvidar el ChoniLab®, que marcó un antes y un después. Gracias también a todos los compañeros que siempre estuvieron ahí para resolver problemas, para las fiestas del laboratorio, para el Harlem Shake, para organizar eventos o para dar apoyo. Seguro que se me olvida alguien, pero en esto se me vienen a la mente Lola, Guti, Eva, Nuria, Eloy, Pilar, Isa, Isa P, Carmen, Mariqui, Claudia, France, Nacho, Davinia, Víctor, Milena, Alberto, Sandra, Yandira, Zahira, Cristina, Alejandra, Laura, Jorge, Fernando y Belén. Todos formáis parte de esta etapa vital que siempre imprimirá una sonrisa inmediata cuando me vengan recuerdos. A destacar la ayuda de Víctor en ese gran momento de mi charla sorpresa en el Congreso FEMS en Maastricht.

Trabajo en la sombra, pero imprescindible. Gracias a Irene, Saray, Cristina y Yandira por tener siempre todo a punto en todos los

laboratorios para cuando hiciera falta, por arreglar nuestros caos y por preocuparos por que todo funcione.

Gracias también a Edgar, Zahira y Rafa por lo que aprendí de vosotros mientras os enseñaba en vuestras prácticas como técnico, TFGs y TFMs.

La mudanza al PTA también fue un punto de inflexión. El equipo *Bacillus* creció con el BacBio y uno a uno se fueron incorporando Mario, Jesús H, Marisa, Jesús C, Saray, Elena, Yurena, Carlos, Sara, Ana y Mari Luz. Y María que ya mismo se incorpora oficialmente. Aquí también me gustaría remarcar la especial influencia de todos en lo académico, lo científico y lo personal. Os voy a echar mucho de menos. Dar de comer a los patos, los pitufos mixtos, los cafés, las comidas, las cenas, los Fatty Wensdays, los debates políticos y científicos, las ideas de los nenúfares y la nieve carbónica, y el apoyo cuando las cosas se nos complican. Mención especial a Jesús C por el trabajo en el laboratorio compartiendo diariamente todas las preguntas y respuestas del día a día. Y a María Cuaresma y Amparito, por lo grandes que sois.

Hay también agradecimientos a los que fueron importantes en mis estancias. Fueron grandes experiencias en todos los aspectos y aunque también hay muchísima gente a la que nombrar, destacar a Oscar Kuipers y Roberto Kolter como IPs de los laboratorios de acogida. A Elrike, por su ayuda en el laboratorio de Oscar; A Manolo, Bárbara, David, Peter, Daso y Leandro por las aventuras por Holanda; a Jorge y Mónica por vuestra ayuda en el laboratorio de Roberto; y a

Emma, Rocío, Juanlu, Rubén, Larimar, Jorge y Sandra por todas las aventuras de Boston.

Y para finalizar, muchas gracias al apoyo técnico de David, Goyo, Adolfo, Casimiro, Auxi, Merche, Zafra y Reme de los Servicios de Apoyo a la Investigación de la Universidad de Málaga. Y a John, Juan Félix, Luisa, Reyes, Yoana y Juan Antonio Guadix de Bionand. Sin duda, gran parte de esta tesis no hubiera sido posible sin vuestra colaboración, y os estoy especialmente agradecido por enseñarme a manejar todos vuestros cacharritos.

Me dejo atrás personas y anécdotas, pero el olvido es del momento.

Gracias a todos

INDEX

SUMMARY IN SPANISH

La contaminación por bacterias de alimentos frescos, almacenados y envasados continúa siendo una amenaza importante para la seguridad alimentaria en los países desarrollados, ya que disminuyen la vida útil del producto y causan intoxicaciones alimentarias. Los síntomas de intoxicación alimentaria pueden ser leves, como vómitos y diarrea, o más graves como bacteriemia, que en casos severos puede causar la muerte de los pacientes. Las cepas bacterianas de *Escherichia coli, Salmonella, Enterococcus, Lysteria y Bacillus cereus* son agentes etiológicos recurrentes en estos brotes de intoxicación, siendo este último uno de los menos estudiados. Los estudios epidemiológicos revelan que la contaminación del producto ocurre antes del paso industrial, estando asociadas al producto en origen.

B. cereus es un habitante natural del suelo, se aísla con frecuencia de verduras frescas y de alimentos preparados listos para el consumo, y causa dos tipos principales de intoxicación: emética y diarreica. La intoxicación emética se asocia con la producción de cereulide, una toxina lipofílica. Esta toxina es extremadamente estable al calor y puede producirse en alimentos contaminados por *B. cereus*. Cereulide puede persistir en el cuerpo por un largo período, afectando diferentes órganos y eventualmente llevando a la muerte del paciente La intoxicación diarreica es causada por otro grupo de toxinas: la enterotoxina Hemolysin BL (HBL), la enterotoxina no hemolítica (NHE) y la citotoxina (CytK). Además, *B. cereus* posee una larga lista de otras toxinas y enzimas degradativas que contribuyen a la gravedad de la patología.

La colonización y la persistencia de *B. cereus* en vegetales y frutas frescas es un elemento indispensable para la intoxicación. *B. cereus* produce esporas altamente resistentes a ambientes estresantes y puede sobrevivir al calor, las condiciones secas, los procedimientos de desinfección y los tratamientos de los alimentos procesados.

Las bacterias se agregan en comunidades bacterianas llamadas biofilm o biopelículas. Estudios en la especie relacionada *B. subtilis* revelan que los biofilms son reservorios naturales de esporas (Branda, 2005). La formación de biofilm requiere una vía regulación compleja que coordina la expresión de los componentes estructurales implicados en el ensamblaje de una matriz extracelular protectora. En *B. subtilis*, la matriz extracelular está compuesta de exopolisacáridos, la proteína hidrofobina BslA y la proteína amiloide TasA entre otros elementos (Hobley, 2013, n.º 218; Romero, 2013, n.º 309).

En las últimas cuatro décadas, los biofilms han sido uno de los temas que más han llamado la atención de la comunidad científica en el ámbito de la microbiología, no solo desde un enfoque biológico sino también desde un punto de vista de salud pública (McCoy et al., 1981; Rittmann y McCarty, 1982; Dasgupta y Costerton, 1989). Durante estos años, se ha acumulado un gran conocimiento sobre el desarrollo del biofilm, fisiología, ecología y biología molecular, especialmente sobre bacterias modelo como *E. coli*, como patógena gram-negativa, o *B. subtilis* en el grupo de los gram-positivos (Tan et al. 2017; Lo et al. 2017; Mielich-Süss y Lopez 2015).

Aunque los modelos han revelado las pautas generales de ensamblaje de un biofilm, existen muchas particularidades en cada especie bacteriana. Hasta la fecha, se han descrito 2552 géneros y alrededor de 14,000 especies de bacterias, lo que da una idea de cuán variable pueden ser los biofilms en términos de estructura, propiedades físicas, regulación y funciones asociadas a este estado fisiológico. (Clasificación de Bacterias - Patrocinado por Ribocon GmbH n.d.). Aunque la formación de biofilms se ha estudiado en detalle en *B. subtilis*, no se sabe mucho acerca de este programa de desarrollo en *B. cereus*.

La distancia evolutiva entre *B. cereus* y el organismo modelo *B. subtilis* se puede evidenciar en su ecología, ya que *B. subtilis* vive como un saprófito en el suelo y en asociación con plantas, mientras que *B. cereus* también es un patógeno de mamíferos, que además puede vivir en el intestino de los insectos. En términos de diferencias moleculares, hay varios elementos estructurales y de regulación implicados en la formación de biofilm que son diferentes: i) el operón de formación de exopolisacáridos de *B. subtilis* muestra poca similitud con el homólogo en *B. cereus* ; ii) la ausencia de la proteína TapA, necesaria para el ensamblaje de la fibra de tipo amiloide en *B. subtilis*, iii) la presencia de dos parálogos de TasA en *B. cereus* ; iv) la ausencia en *B. cereus* de la proteína hidrofóbica de revestimiento del biofilm BslA (Hobley et al., 2013); v) las diferencias en las redes reguladoras de formación del biofilm, que carecen de las subredes reguladoras II y III, y la ganancia del regulador pleiotrópico PlcR, involucrado en virulencia y formación de biofilm (Gohar et al., 2008); vii) la ausencia en *B. cereus* de la

lipoproteína Med asociada a la actividad de fosforilación de KinD que desencadena la formación de biofilms (Banse, Hobbs y Losick 2011). Estas son algunas de las diferencias que evidencian la necesidad de un mayor conocimiento para tener una imagen clara del desarrollo del biofilm en *B. cereus*.

La multicelularidad es una característica común en todas las especies de bacterias, que incluso cruza la frontera de los reinos biológicos. Los hongos y las algas también pueden ensamblar biofilms e incluso pueden formar biofilms compuestos por organismos de distintos reinos (Dutton et al., 2014; Rajendran y Hu 2016; García-Meza, Barrangue, y Admiraal 2005; Barranguet et al., 2005; Fanning y Mitchell, 2012). Este hecho no puede ser casual dado que dicha estrategia está ampliamente distribuida, proporcionando un amplio abanico de beneficios en términos de adhesión, colonización, competencia, adaptación, resiliencia, virulencia, defensa, supervivencia, división de funciones, eficiencia e intercambio genético (Jefferson 2004, Watnick y Kolter 2000). Los estudios sobre el biofilm de *B. cereus* son escasos y la mayoría de ellos se centran en la descripción de fenotipos de distintas cepas, con pocos estudios en el campo de la biología molecular. Acerca de los componentes estructurales generales de los biofilms, solo se había estudiado en detalle el DNA extracelular, que en *B. cereus* es esencial para la formación de biofilm (Vilain et al., 2006). El componente proteico y los polisacáridos no ha sido estudiado hasta el momento, siendo desconocido el origen de estos elementos y su importancia relativa en la estructura del biofilm.

Durante el desarrollo de esta tesis, aparecieron algunos estudios sobre la formación de biofilm en *B. cereus*. La confirmación de que la región homóloga en *B. cereus* a la región de síntesis de EPS en *B. subtilis* no es relevante para la formación de biofilms (Gao et al., 2015a) abrió preguntas importantes sobre cuál es el exopolisacárido que realmente funciona como un elemento estructural y de adhesión en biofilm. Por otro lado, si esa región no está involucrada en la formación de biofilm, ¿cuál es la función de esa región genómica?

En este escenario, esta tesis se ha centrado en estudiar esas particularidades en la formación de biofilm de *B. cereus* debido a las múltiples preocupaciones sobre esta bacteria, ya que es un patógeno humano responsable de brotes de intoxicación alimentaria, un agente causal habitual de deterioro de producto y maquinaria en la industria, y un aislado recurrente en infecciones nosocomiales (Tewari y Abdullah 2015; Dohmae et al., 2008). Un conocimiento más profundo sobre la formación de biofilm de esta bacteria nos permitirá comprender mejor su comportamiento, sus debilidades y fortalezas, una información muy útil para desarrollar estrategias para prevenir, reducir o manejar problemas y amenazas con un origen en el biofilm de *B. cereus*. Por otro lado, *B. cereus* vive en el suelo como un saprofito o en asociación con plantas en la rizosfera, suponiendo una doble preocupación como reservorio de esporas y células vegetativas y como una bacteria beneficiosa para las plantas, ambas consideraciones asociadas con la formación de biofilm.

En cuanto al conocimiento del ensamblaje del biofilm de *B. cereus*, hasta ahora no se había desarrollado ningún estudio sobre los

componentes proteicos. En *B. subtilis*, la peptidasa señal SipW reconoce los péptidos señal en la posición N-terminal de las proteínas TapA y TasA, y las secreta al medio, donde se polimerizan en fibras, principalmente formadas por la proteína TasA y donde TapA juega un papel de anclaje de las fibras, nucleación y aceleración de la cinética de polimerización. Estos tres genes están codificados en un mismo operón en *B. subtilis*. La búsqueda en el genoma de *B. cereus* de proteínas similares a TasA y TapA produjo tres genes con similitud considerada con TasA, identificados como *BC1279, BC1281 y BC4868*, y también se encontró un homólogo de sipW, identificado como *BC1278*. Aunque, no se encontró ningún gen con homología con *tapA*. Como la estructura genética de *BC1278* (*sipW*) y *BC1279* (*tasA*) se parece a la del operón de *B. subtilis*, y *BC1281* (*calY*) es una duplicación de *BC1279*, lanzamos la hipótesis de que esta región (*sipW*-hasta-*claY*) es responsable de la formación de fibras amiloides en la formación de biofilm en *B. cereus*. El análisis bioinformático de la proteína codificada por *BC4868* (anotada como una metaloproteasa) revela que: i) la secuencia de la proteína es muy similar a TasA y CalY; ii) la predicción de la estructura secundaria con el software SOPMA revela un patrón casi idéntico; iii) el análisis con el programa Pasta 2.0 muestra incluso más regiones amiloidogénicas para BC4868 que para TasA y CalY. Sin embargo, esta proteína no está bajo el control del master regulador de biofilm SinR (Fagerlund et al., 2014), lo que sugiere que, aunque esta proteína probablemente retiene todo el potencial para comportarse como una proteína amiloide, no debe estar involucrada en la formación de fibras amiloides en biofilm.

Para estudiar el papel de la región *sipW*-hasta-*calY* en la formación de biofilm, se realizaron mutantes. Los mutantes simples en *sipW* dieron como resultado una baja biomasa de biofilm, con una pobre adherida a la pared del pocillo y que además no mostró fibras en la visualización por microscopía electrónica de transmisión (TEM). Por otro lado, los mutantes en *tasA* mostraron una mayor biomasa de biofilm, pero poco adheridos; y el mutante *calY* mostró un desarrollo similar a la cepa silvestre pero también con una adhesión reducida. Ambos mutantes en *tasA* y *calY* mostraron la formación de fibras en visualización en TEM, aunque fueron más abundantes y más gruesas en el mutante *calY*, lo que sugiere una mayor contribución de TasA a la formación de fibras. Estos resultados también sugieren que ambas proteínas están involucradas en la formación de biofilm ya que la adhesión se ve afectada tanto en mutantes en *tasA* como en *calY*.

Para responder a las preguntas sobre el papel individual de estas proteínas y aclarar si otros elementos juegan un papel relevante en la formación de fibras en *B. cereus*, se realizó expresión heteróloga de los genes de *B. cereus* en una cepa de *B. subtilis* que carece del operón *tapA* y otra que carece sólo de *tasA*. Estas cepas no forman la típica película flotante y arrugada producida por la cepa silvestre, que une el colorante rojo congo (CR) cuando se agrega al medio de cultivo. La expresión heteróloga de *tasA* y *calY* de *B. cereus* en una cepa mutante de *B. subtilis* mutante en *tasA* revelaría si alguna de estas proteínas cumple una función principal. Inesperadamente, ninguna de ellas restauró el fenotipo, lo que nos llevó a preguntarnos si las pequeñas diferencias en el péptido señal harían que cada ortólogo *sipW* fuera

específico sobre los péptidos señales de las proteínas de su mismo genoma. Ciertamente, la expresión heteróloga de *sipW-tasA* en un mutante en *tasA* restauró la formación de película, la tinción de CR y la formación de fibras, aunque el fenotipo arrugado no se restauró. La expresión de la fusión *sipW-calY* en un mutante *en tasA* dio como resultado el mismo efecto, aunque la película era considerablemente más delgada.

La expresión heteróloga en un mutante *sipW-tapA-tasA* completo de *B. subtilis* reveló que TapA estaba interactuando con las proteínas de *B. cereus,* promoviendo su polimerización. La expresión heteróloga en la cepa de *B. subtilis* que carece del operón *tapA* completo dio resultados diferentes. La expresión de *sipW-tasA* o *sipW-calY* no restauró la película ni la adhesión de CR, aunque se observaron algunas fibras en TEM en el caso de *sipW-tasA*. Solo la expresión de la región completa *sipW*-hasta-*calY* fue capaz de restaurar completamente los fenotipos de película, arrugas, adhesión de CR y la observación de fibras en TEM. Estos resultados confirmaron que esta región es responsable de la síntesis de la formación de fibras estructurales en *B. cereus* biofilm. También reveló que este sistema amiloide ha evolucionado a un modo de acción independiente de una proteína accesoria para el anclaje y la polimerización como TapA. Aunque, dentro de esta región se incluye el gen *BC1280*, anotado como una proteína hipotética. Inicialmente, el análisis de RT-PCR mostró que este gen no se expresó en nuestras condiciones experimentales a pesar de que los resultados de RNAseq e iTRAQ revelaron que este gen está sobreexpresado en biofilm. El análisis bioinformático también reveló que esta proteína posee incluso

más regiones amiloidogénicas que TasA y CalY. De hecho, los mutantes en *BC1280* muestran el mismo fenotipo que los mutantes en la región completa o en *sipW*, lo que sugiere que esta proteína podría tener un papel importante en la polimerización de las fibras. Estos nuevos resultados mantendrían en entre dicho la función de *calY* en la formación de fibras. Sin embargo, la caracterización de las proteínas TasA y CalY y su interacción demostró su papel en la formación de fibras, aunque el estudio de la proteína BC1280 no se ha incluido en esta tesis.

La expresión y purificación de las proteínas TasA y CalY en cultivos bacterianos de *E. coli* es una técnica habitual para la caracterización de proteínas, lo que nos permitió el estudio *in vitro* de la estructura secundaria, las propiedades amiloides, el perfil de polimerización y la interacción de ambas proteínas TasA y CalY.

El uso de varias herramientas bioinformáticas junto con los resultados de los mutantes en *B. cereus* y la expresión heteróloga de TasA y CalY en *B. subtilis* sugirieron que estas proteínas probablemente poseen propiedades amiloides. Ambas proteínas mostraron un alto porcentaje de secuencia de aminoácidos no estructurados, regiones con una tendencia a convertirse en estructuras secundarias de láminas β debido a las interacciones internas de la proteína y con otras unidades de TasA o CalY, de forma similar a lo que ocurre, por ejemplo, con la proteína CsgA en la formación de las estructuras amiloides que forman el pili en *E. coli* (Van Gerven et al., 2015).

La confirmación de las propiedades amiloides de TasA y CalY se basa en los resultados de los espectros Thioflavin T y Congo Red de emisión de fluorescencia y absorbancia respectivamente, que son las principales pruebas utilizadas para determinar las propiedades amiloides de una proteína (Girych et al., 2016).

Resultados adicionales obtenidos con ATR-FTIR (Attenuated Total Reflectance- Fourier Transformed Infra Red) y ECD (Electronic Circular Dicroism) demostraron el enriquecimiento en estructuras secundarias de láminas β en proteínas polimerizadas y en láminas β intermoleculares. Las imágenes de TEM nos llevaron a confirmar que la polimerización de fibras también ocurre *in vitro* cuando ambas proteínas están aisladas y que lo hacen de forma diferente, ya que TasA es propensa a formar fibras grandes y CalY tiene tendencia a formar polímeros con forma de rejilla o fibras muy ramificadas.

En *B. subtilis*, la mezcla de TapA y TasA resulta en una polimerización más rápida que la de TasA por aislada, con una emisión fluorescente más alta en la mezcla, revelando que la interacción de ambas proteínas aumenta su patrón de plegamiento amiloide (Romero et al., 2014). La interacción in vitro de TasA y CalY a pH 6 con CR dio lugar a grandes agregados visibles al ojo, que no se formaron en las proteínas puras, lo que sugiere un comportamiento similar a las interacciones TasA y TapA. Sin embargo, la emisión fluorescente de las mezclas no se incrementó y siempre estuvieron dentro de un rango entre los valores de TasA y CalY por separado de acuerdo con sus concentraciones relativas. La interacción se confirmó en TEM, revelando que solo un

10% de CalY inducía a TasA a polimerizar en un patrón de rejilla; y también en DLS, donde la mezcla de las dos proteínas mostró una mejor progresión de la polimerización.

La confirmación final del papel colaborativo entre TasA y CalY surgió con experimentos *in vivo* en los que la adición de ambas proteínas a un mutante en *tasA* indujo la formación de una gran biomasa de biofilm flotante. El proceso de polimerización debe estar finamente regulado, ya que la adición de estas proteínas a un cultivo de la cepa silvestre no produce ningún cambio en el desarrollo del biofilm. Las características de un mutante en *tasA*, que no desensambla completamente el flagelo en biofilm y muestra un mayor número de bacterias encadenadas, también pueden explicar por qué la adición de material amiloidogénico da como resultado una biomasa de biofilm mucho mayor.

Ambas formas de polimerización en rejillas y en forma de fibra son compatibles biológicamente y pueden desempeñar una función protectora. Hemos visto que ambas proteínas pueden producir ambas tipologías *in vivo*. Aunque TasA parece ser más propenso a formar fibras y CalY a formar rejillas, la polimerización de amiloides es un proceso complejo, influenciado por la concentración de proteína, el pH, la temperatura, el tiempo y la presencia de otras moléculas con las que interactúan. Las condiciones locales en las cuales *B. cereus* produce amiloides estructurales son difíciles de determinar y reproducir *in vitro*. La comparación de imágenes de fibras *in vivo* con aquellas formadas *in vitro*, muestra que ambas coexisten *in vivo* y son similares a las formadas *in vitro*.

Sin embargo, las estructuras proteicas del biofilm son solo uno de los elementos estructurales, que en sí no implican un biofilm. La multicelularidad bacteriana implica un cambio radical de estilo de vida. Las células flotantes son nadadoras y se mueven respondiendo a gradientes de nutrientes que actúan como quimioatrayentes o como quimiorepelentes, por ejemplo, compuestos tóxicos (Yamamoto, Macnab e Imae 1990, Pandey y Jain 2002, Eisenbach Michael 2001). El estilo de vida sésil requiere lidiar con la imposibilidad de moverse hacia los nutrientes o huir de los tóxicos, pero requiere un menor consumo de energía dedicado al movimiento. En contrapartida, el ensamblaje de la matriz extracelular del biofilm supone una redistribución del flujo metabólico para la síntesis de todos los elementos.

La brecha en el conocimiento sobre los cambios fisiológicos sufridos por el cambio de estilo de vida nos llevó a explorar cómo *B. cereus* enfrenta el desafío de una forma de vida sésil. En primer lugar, desarrollamos una metodología para separar eficientemente el biofilm de las células planctónicas, evitando la contaminación de la población sumergida de biofilm que podría introducir ruido o incluso enmascarar las diferencias entre ambas poblaciones. Con la ayuda de técnicas de secuenciación masiva, realizamos la secuenciación total de ARNm y el análisis proteómico usando espectrometría de masas iTRAQ sobre ambas poblaciones de bacterias, y las comparamos para buscar diferencias que revelen su estado fisiológico. Debido a la mayor sensibilidad y las ventajas de la reproducibilidad, la transcriptómica fue nuestro experimento de referencia, utilizando la proteómica como una

herramienta para confirmar la gran cantidad de entradas obtenidas del experimento de ARNseq, en lugar de utilizar qRT-PCR o Western Blot, que no son eficientes para confirmar datos masivos (Łabaj y Kreil 2016). Además, la qRT-PCR solo confirma los niveles de transcripción. En las bacterias, la transcripción y la traducción se asocian eficientemente, aunque la vida media del ARNm y el reciclado de proteínas pueden alterar las cantidades finales, dando una idea sesgada de la configuración funcional de las bacterias (Gowrishankar y Harinarayanan 2004; Kristoffersen et al., 2012).

El análisis de los cambios en la expresión relativa se hizo usando un umbral conservador de log2 (fold change)> | 2 |, que rindió como resultado 1292 genes con expresión diferencial, que representan el 23,5% de los genes totales anotados en el genoma de *B. cereus* ATCC1457. Este número da una idea de la complejidad de los cambios que sufren las células planctónicas cuando se convierten en habitantes del biofilm.

Todos los cambios encontrados se pueden resumir en tres grupos que comprenden i) elementos necesarios para construir la estructura del biofilm; ii) elementos para atacar a los competidores y sobrevivir a su ataque; iii) y elementos para las interacciones bacteria-huésped, que incluyen también ataque y defensa. Las estrategias utilizadas por las células de biofilm de *B. cereus* generalmente proporcionan múltiples ventajas para varios propósitos. Por ejemplo, el exopolisacárido funciona como una adhesina, sirve como elemento estructural, retiene moléculas antimicrobianas y puede proteger contra el ataque del huésped (Nwodo, Green y Okoh 2012). Producir todos estos elementos

supone un cambio en el requerimiento de nutrientes y energía, produciéndose en la bacteria un redireccionamiento de los flujos metabólicos.

Entre los elementos estructurales encontramos varios cambios arquitectónicos. La pared celular bacteriana juega un papel importante en la fisiología bacteriana, como una barrera que protege la célula. Además, en un estado de biofilm la pared celular es la plataforma a la que se anclan los exopolisacáridos y las fibras de proteína. En nuestros resultados, encontramos que las células de biofilm de *B. cereus* aumentan el espesor de la pared celular en un 33%. Nuestra hipótesis es que esta estrategia permite a las bacterias soportar las fuerzas físicas que se producen por el apilamiento de bacterias y las fuerzas transmitidas a través de los polímeros de proteínas y sacáridos anclados a la pared celular. Las proteínas TasA y CalY, como se ve en el capítulo II, funcionan también como adhesinas. Además de estos elementos, también encontramos la sobreexpresión de proteínas tipo colágeno y proteínas de adhesión al colágeno, adhesinas que nunca antes se habían descrito en *B. cereus* y que han sido descritas en biofilm en otras especies con un papel importante en la adhesión, agregación, colonización del hospedador, persistencia y formación de biofilm (Abranches et al., 2011; Miller et al., 2015; Tang, et al., 2016; Zhao, et al., 2015). En cuanto a los exopolisacáridos, encontramos que la región *eps1* no se sobreexpresa en células de biofilm, de acuerdo con resultados previos de mutantes en esta región que no mostraron un fenotipo en biofilm (Gao et al., 2015b). La sobreexpresión de la región *eps2* anotada como biosíntesis de exopolisacárido capsular

sugirió que esta región estaba implicada en la formación de biofilm, lo que se confirmó adicionalmente mediante el ensayo de biofilm sobre cepas con esta región deleccionada. Los resultados con estos exopolisacáridos nos llevaron a investigar sus funciones, cuyo resultado se analizará más adelante. El tercer componente general de la matriz extracelular del biofilm es el ADN extracelular, cuya maquinaria de síntesis se sobreexpresa en las células biofilm, con un patrón específico en el tiempo. Se sobreexpresó principalmente en las primeras etapas de la formación del biofilm y volvió a los niveles normales en etapas posteriores en el caso de la síntesis de pirimidinas, quedando la vía de biosíntesis de purinas activa a todos los tiempos, probablemente por la necesidad de síntesis de mensajeros secundarios implicados en la formación de biofilm e interacciones bacteria-huésped como son ppGpp, C-di-GMP o c-GMP-AMP (Jenal et al., 2017).

En la naturaleza, los biofilms suelen ser multiespecíficos, cohabitando una multitud de especies diferentes en el mismo espacio (Yang et al., 2011, Elias y Banin 2012, Yadav et al., 2017). *B. cereus* es un habitante común del suelo, la rizosfera o el intestino de los animales, nichos en los que viven miles de especies diferentes que compiten por la colonización del espacio y los nutrientes (Majed et al., 2016). La competencia en estos entornos se puede traducir en una lucha perpetua que resulta en el desarrollo de estrategias de ataque y defensa. Se encontró que las células de biofilm de *B. cereus* sobreexpresan regiones relacionadas con la síntesis de antimicrobianos, como la tiocilina, cuya síntesis fue confirmada en biofilm por espectrometría de masas, señalando el estado de ánimo de

ataque del biofilm frente a los competidores. Por otro lado, el ARNseq reveló una estrategia compleja para sobrevivir al ataque de los competidores, incluyendo: i) la sobreexpresión de genes anotados como genes de resistencia a antimicrobianos; ii) mejora de la rigidez de la membrana celular aumentando su proporción en cardiolipina, lo que confiere resistencia contra la surfactina, un surfactante producido por *B. subtilis* (Dubois-Brissonnet, Trotier y Briandet 2016; Seydlová et al., 2013); iii) estrategia de prevención de la muerte mediada por ROS por efecto de antimicrobianos (Van Acker y Coenye 2017), que incluye la sobreexpresión del complejo I de la cadena de transporte de electrones, regulación negativa del complejo II, regulación negativa del ciclo del TCA, regulación al alza del *shunt* del TCA, aumento de las concentraciones de NAD^+, la sobreexpresión de la maquinaria de detoxificación de ROS y el mantenimiento de un entorno reducido; iv) la síntesis de la matriz extracelular, que secuestra los antimicrobianos por sorpción y evita así su penetración en el citoplasma o reduce su constante de difusión (Stewart 2015; Tseng et al., 2013; Potera 1999); v) aumento del espesor de la pared celular, lo que puede proporcionar una posición ventajosa frente a los antimicrobianos β-lactámicos (Bush 2012). La sobreexpresión de la esporulación completa las estrategias de supervivencia, lo que permite producir una subpoblación de formas resistentes y muy adherentes que pueden germinar en lugares alejados de la localización original de la colonia. Sobre la esporulación, encontramos una progresión de esporulación controlada en el tiempo, con una parada a las 72 h de desarrollo de biofilm, controlado por cantidades reducidas del regulador Spo0A, la regulación positiva de la

fosfatasa del activador SpoOA-P y regulación positiva del inhibidor de la esporulación, que comprende un grupo completo de elementos para controlar la detención de esporulación de forma eficaz.

En el campo de las interacciones bacteria-huésped se obtuvieron hallazgos interesantes, cambiando nuestra visión del estado atacante de las bacterias, que depende de su estado fisiológico. Las células planctónicas sobreexpresan los genes de síntesis de toxinas, orientadas a lograr un ataque rápido y eficiente contra el huésped, de acuerdo con algunos casos clínicos descritos en los que solo 13 h después de la ingestión de un plato de ensalada contaminado con *B. cereus* fue suficiente para matar a un paciente e inducir un pronóstico clínico grave a otros miembros de la misma familia (Dierick et al., 2005). La gran mayoría de estos factores de virulencia se regula negativamente en las células de biofilm, con la única excepción de la hemolisina III, cuya regulación es independiente del regulador PlcR. Este comportamiento especial podría tener implicaciones en las interacciones biofilm-células eucariotas, tal vez en las interacciones con las raíces de las plantas, contra hongos o para extraer nutrientes de un epitelio sobre el que se forma un biofilm. Se ha descrito que la internalización de *B. cereus* ocurre a una tasa baja, lo que sugiere que solo una subpoblación adquiere esta estrategia de invasión. También encontramos que las células planctónicas sobreexpresan sphingomyelin phosphodiesterasa y 1-phosphatidylinositol phosphodiesterasa, enzimas implicadas en la liberación del fagolisosoma (Faulstich et al., 2015; Shivanna, Kim y Chang 2015; Wei, Zenewicz, y Goldfine 2005). Por otro lado, las células del biofilm son

más propensas a defenderse del ataque del huésped, sobreexpresando beta-lisina acetiltransferasa, que neutraliza la beta-lisina producida por plaquetas contra bacterias gram-positivas (Hamzeh-Cognasse et al., 2015), y varios inhibidores inmunológicos que degradan los factores humorales de insectos atacinas y cecropinas (Lövgren et al., 1990; Pflughoeft et al., 2014).

Hay elementos expresados por las células planctónicas que no son necesarios para vivir en comunidades multicelulares. Como era de esperar, el flagelo se regula negativamente en biofilm, pero también encontramos un evento interesante relacionado con la S-layer. Ésta cubierta externa había sido estudiada en *B. cereus* concluyendo que la capacidad de sintetizar la S-layer se correlaciona inversamente con la formación de biofilm (Auger et al., 2009). En *B. thuringiensis* se encontró un desprendimiento de la S-layer al entrar en la fase estacionaria de crecimiento, que se propuso como el resultado del recambio de la pared celular (Luckevich y Beveridge, 1989). La cepa de *B. cereus* ATCC14579 no ensambla la S-layer porque carece de algunos de los genes estructurales principales, aunque conserva otros que presumiblemente también conservan su regulación, lo que nos lleva a proponer la S-layer como un impedimento físico que controla el reclutamiento, más allá de sus funciones ya descritas.

Todos estos hallazgos producidos por el análisis molecular de biofilm y células planctónicas representan una imagen detallada de todos los procesos implicados en la formación de biofilm. De todos los resultados, hay uno especialmente notable que es la sofisticada y

amplia estrategia de células de biofilm para prevenir el daño de ROS. Esta podría ser una pista que revela la debilidad de los biofilm, apuntando a un nuevo objetivo para diseñar compuestos antimicrobianos o potenciadores de ROS combinados con antimicrobianos comerciales y agentes anti biofilm para prevenir su formación o reducir su resiliencia frente a los antibióticos.

Aunque este estudio supone un gran avance a nivel molecular, se ignoraba también el proceso de desarrollo microscópico del biofilm de *B. cereus*. Al sumergir parcialmente un cubreobjetos de vidrio en un cultivo líquido, se obtuvo un modelo de biofilm de interfase aire-líquido fácil de recuperar para la observación al microscopio. Después de la inoculación del cultivo, las observaciones se realizaron cada dos horas, lo que nos llevó a describir los diferentes pasos de la formación del biofilm.

La adhesión inicial se produce verticalmente por uno de los polos de la bacteria y de manera reversible, de forma similar a la descrita en otras bacterias (Sjollema et al., 2017; Caiazza y O'Toole 2004). La adhesión progresa con la fijación horizontal a la superficie, lo que ocurre en una escala de tiempo de minutos. La formación de microcolonias se lleva a cabo de dos formas diferentes, formadas por bacterias ordenadas o desordenadas que finalmente conducen al mismo empaquetamiento y formación de biofilm. A medida que crece, se desarrollan largas cadenas bacterianas ancladas al biofilm, que flotan en el cultivo líquido y en las cuales se reclutan grupos de células planctónicas, integrándose luego en el biofilm. La esporulación se produce principalmente en la parte superior del biofilm, cerca del aire y más

expuesta a la desecación. El aplastamiento parcial del biofilm reveló una estructura interna de largas cadenas, probablemente con un origen en las cadenas celulares que reclutan células planctónicas, que funcionan como un soporte estructural para el biofilm. La maduración del biofilm después de las 72 h resulta en áreas internas de células muertas, una condición descrita en otras especies de bacterias (Asally et al., 2012; Webb et al., 2003).

En el primer capítulo, se describió un fenotipo característico de formación de biofilm en la cepa mutante en *tasA*, que muestra una mayor formación de biofilm a pesar de la falta de una adhesina importante implicada en la formación de fibras estructurales, lo que sugiere una desregulación en la expresión génica y de otros factores que generan una mayor biomasa. Para buscar genes desregulados, realizamos RNAseq e iTRAQ sobre biofilms de la cepa mutante *tasA* y comparamos los datos con los obtenidos en la cepa silvestre. El análisis mostró que las células de biofilm en el mutante en *tasA* regulan negativamente la proteína de división celular *ftsH*, una proteína cuya mutación origina en *B. subtilis* un fenotipo de crecimiento en largas cadenas (Wehrl, Niederweis y Schumann 2000; Deuerling et al., 1997). Este resultado está en línea con las observaciones de la progresión del desarrollo del biofilm del mutante en *tasA*, en el que destaca un fenotipo de alta filamentación, mientras que todas las demás características de crecimiento se desarrollan normalmente. También se vio que las células de biofilm del mutante en *tasA* se encontraban en un estado fisiológico intermedio entre las células de biofilm y las células planctónicas de la cepa silvestre, lo que hace que estas células

retengan las estructuras del flagelo o al menos en una proporción mayor. Se ha descrito que el flagelo es esencial para el reclutamiento (Houry et al., 2010), lo que combinado con el encadenamiento celular resultaría en un aumento en el reclutamiento de agregados de células planctónicas. Esta hipótesis se confirmó midiendo la densidad óptica de cultivos líquidos de las dos cepas, mostrando alrededor de la mitad de la concentración de bacterias en el mutante en *tasA*.

El estudio de la actividad del promotor proporcionó información sobre el momento en que se expresa *tasA* y, por tanto, cuándo se ejerce el efecto regulador de la proteína. La expresión de *tasA* no se detectó hasta que se formaron micro colonias, lo que revela que *tasA* no está involucrado en las etapas iniciales de adhesión que conducen al ensamblaje del biofilm. Estudios adicionales sobre las condiciones ambientales que pueden desencadenar, retrasar o bloquear la expresión de *tasA* confirmaron que diferentes nichos podrían condicionar su expresión y de esta manera pueden modular la fisiología del biofilm de *B. cereus*. A pesar de esta modulación, el biofilm siempre se desarrolla, pero con características fisiológicas que pueden oscilar a un estado más cercano a las células planctónicas o a una situación en la que los genes de biofilm están incluso más sobreexpresados. Esta modulación es general en el biofilm de otras especies (Toyofuku et al., 2016).

El estudio de los cambios fisiológicos y la maquinaria molecular implicada en la formación de biofilm de *B. cereus* condujo a evidenciar el bajo número de estudios sobre los exopolisacáridos en *B. cereus*. En *B. subtilis*, se ha estudiado en detalle el operón *epsA-O,* involucrado en

la síntesis de exopolisacáridos, jugando un papel determinante en la formación de biofilm ya que los mutantes en esta región no pueden ensamblar una película flotante (Elsholz, Wacker y Losick 2014) En *B. cereus* hay una región con cierta homología (*eps1*) que ha sido eliminado en otros trabajos sin mostrar ningún fenotipo de biofilm (Gao et al., 2015b). Los resultados de los datos de RNAseq que comparan biofilm y células planctónicas confirmaron que el patrón de expresión de esta región no cambia durante la formación del biofilm. Aunque, otras regiones de biosíntesis de exopolisacáridos mostraron una regulación al alza. Dos de ellos están relacionados con polisacáridos asociados con estructuras de la espora (Li et al. 2017). Y también una región (*eps2*), compuesta de varios genes anotados como biosíntesis de exopolisacárido capsular. El hecho de que *B. cereus* ATCC14579 carezca de cápsula nos llevó a la hipótesis de un papel de este exopolisacárido como un componente estructural del biofilm.

Se obtuvieron cepas con ambos *eps1 y eps2* deleccionados, así como mutantes dobles para buscar sus funciones. Los ensayos de biofilm en placas de agar, cultivos líquidos sin agitación y cultivo líquido con agitación confirmaron nuestra hipótesis del papel en el biofilm de la región *eps2*. Los mutantes en *eps2* muestran una formación reducida de biofilm en cultivos con agitación y una reducción de la tinción con rojo congo en cultivos líquidos y placas de agar que contienen el colorante. La observación microscópica del medio planctónico también reveló que *eps2* está involucrado en la cohesión de los grumos planctónicos.

El estudio del patrón de expresión de ambas regiones mostró una expresión relativamente estable de la región *eps1*, en contraste con *eps2*, que muestra una expresión drásticamente disminuida a 37ºC. Este comportamiento se asemeja al comportamiento de la expresión de *tasA* en diferentes condiciones ambientales, en las cuales a 37ºC se produjo la inhibición de la expresión en la mayoría de las condiciones evaluadas. *B. cereus* es un patógeno humano, por lo general con una estrategia muy agresiva cuando está en contacto con el huésped, produciendo una plétora de toxinas principalmente por células en un estado planctónico como revelan los análisis transcriptómico y proteómico. Dado que *B. cereus* tiene una baja tendencia a colonizar las estructuras del huésped, nuestra hipótesis estaría cargada de sentido ya que a 37ºC se evita el estado de biofilm, con una preferencia por un estado planctónico, propenso a atacar al huésped.

Varios trabajos indican que algunos exopolisacáridos desempeñan un papel en la motilidad bacteriana (Berleman et al., 2016; Zhou Tianyi y Nan Beiyan, 2016). Para explorar un posible papel de *eps1* y *eps2* en la motilidad, realizamos experimentos de motilidad de swimming y swarming, lo que reveló un efecto negativo de *eps2* en el swimming y un papel positivo en *eps1* en el swarming. En ambos experimentos, los dobles mutantes muestran un mayor efecto, lo que sugiere cierta colaboración o sinergia entre ambos exopolisacáridos. Este efecto de sinergia fue también patente en los resultados del ensayo de agregación, revelando que la falta de alguno de ellos induce la agregación y la sedimentación. Este experimento sugiere un equilibrio de cargas entre ambos exopolisacáridos que se altera por la falta de

alguno de ellos. Además, los ensayos de motilidad y agregación revelan que a pesar de que *eps2* desempeña un papel importante en la formación de biofilm, la expresión basal da como resultado estructuras funcionales que afectan tareas desarrolladas típicamente por células planctónicas como el swimming o tienen un efecto en la agregación y sedimentación de células planctónicas.

Un estudio de componentes principales sobre cepas caracterizadas como aislados no patógenos, aislados de intoxicaciones alimentarias y cepas clínicas demuestra un agrupamiento de las cepas patógenas en relación con la adhesión y la citotoxicidad (Kamar et al., 2013). Los exopolisacáridos también están implicados en la adhesión a superficies bióticas. Las verduras son uno de los principales orígenes de la intoxicación alimentaria causada por *B. cereus* (Flores-Urbán et al., 2014; Kim, Lee y Paik, 2004). Utilizando hojas de melón como modelo para evaluar la adhesión a los vegetales de las cepas mutantes en las regiones de *eps* en comparación con el tipo silvestre, comprobamos que la mutación simple en *eps1* dio como resultado una mayor adhesión, mientras que la eliminación de *eps2* redujo drásticamente la unión bacteriana. El doble mutante recuperó las propiedades de adhesión. En este caso, la interacción entre los exopolisacáridos parece tener un efecto opuesto, que desaparece en las cepas que carecen de ambas regiones, adquiriendo más relevancia otras adhesinas que podrían estar enmascaradas por los polisacáridos. Por otro lado, la región *eps1* parece no tener ningún efecto en la colonización de células humanas epiteliales, siendo *eps2* la región responsable en esta función. En el análisis transcriptómico del biofilm,

encontramos un grupo de genes anotados como proteínas de adhesión a colágeno y proteínas tipo colágeno. A primera vista, es fácil pensar que las proteínas de adhesión de colágeno deberían tener la propiedad de adherirse al colágeno de mamífero, pero al revisar estos resultados, la estructura del colágeno de mamífero y las proteínas similares al colágeno bacteriano deben ser considerablemente diferentes ya que las proteínas de adhesión a colágeno no juegan un papel importante en la adhesión a las células epiteliales dado que cuando se elimina *eps2* prácticamente desaparece la adhesión.

De la misma manera, mediante experimentos de adhesión al intestino de pez cebra hemos demostrado la implicación de la región *eps2* en la adhesión a tejidos complejos. El pez cebra ha sido usado tradicionalmente como modelo de intestino humano, donde hay múltiples tipos celulares, células de defensa, un ambiente mucoso y la presencia de otras bacterias que pueden interferir en la adhesión de *B. cereus* al intestino humano. Este modelo se usa como paso previo al uso de mamíferos superiores, por su facilidad de reproducción y mantenimiento, así como por las múltiples similitudes que presenta con el intestino humano.

La maquinaria molecular de la formación de biofilm comprende varias estrategias para sobrevivir al ataque de otros competidores, generalmente compuestos antimicrobianos. Sin embargo, la resistencia antimicrobiana se ha atribuido generalmente a la matriz extracelular, aunque el ADN extracelular es un factor principal en la protección contra la actividad de aminoglucósidos, fluoroquinolonas y péptidos antimicrobianos (Chiang et al., 2013, Johnson et al., 2013, Lewenza

2013, Tetz, Artemenko y Tetz, 2009). Con el propósito de evaluar el perfil de resistencia y sensibilidad de los mutantes en las regiones de *eps* hicimos experimentos de crecimiento en presencia de antibióticos. Encontramos cierta colaboración entre ambos exopolisacáridos, lo que resulta en sensibilidades más altas cuando ambas regiones están ausentes.

La resistencia a los antimicrobianos de cepas patógenas es una importante preocupación pública que está atrayendo muchos esfuerzos científicos. Aunque no era el objetivo original de este trabajo, hemos señalado nuevas dianas para desarrollar nuevas estrategias contra bacterias patógenas. Del mismo modo que se resolvió la resistencia a los antibióticos betalactámicos incluyendo en los preparados inhibidores de la enzima que degrada el antimicrobiano, sería interesante explorar estrategias similares, incluyendo inductores de ROS. En *B. cereus,* el ADN extracelular protege a las bacterias de los aminoglicósidos, que también podría ser atacado. La aplicación de DNAsa a las prótesis en combinación con aminoglucósidos puede ser una estrategia exitosa para prevenir la resistencia a las bacterias y la fijación del biofilm en los implantes.

Esta tesis ha cubierto importantes vacíos en el conocimiento de la formación de biofilm de *B. cereus*, y también en las especies cercanas relacionadas que comprenden el grupo *B. cereus*. Nuestros resultados arrojan luz sobre los componentes de proteína y exopolisacáridos de la matriz extracelular. Además, estudiamos la maquinaria molecular implicada en la formación de biofilm. Partiendo de un enfoque

molecular, se hace una perspectiva global con el enfoque micro y macroscópico en el desarrollo del biofilm de *B. cereus*.

REFERENCIAS

Abranches, J., Miller, J.H., Martinez, A.R., Simpson-Haidaris, P.J., Burne, R.A., and Lemos, J.A. (2011). The Collagen-Binding Protein Cnm Is Required for Streptococcus mutans Adherence to and Intracellular Invasion of Human Coronary Artery Endothelial Cells. Infect. Immun. *79*, 2277–2284.

Asally, M., Kittisopikul, M., Rué, P., Du, Y., Hu, Z., Çağatay, T., Robinson, A.B., Lu, H., Garcia-Ojalvo, J., and Süel, G.M. (2012). Localized cell death focuses mechanical forces during 3D patterning in a biofilm. Proc. Natl. Acad. Sci. *109*, 18891–18896.

Auger, S., Ramarao, N., Faille, C., Fouet, A., Aymerich, S., and Gohar, M. (2009). Biofilm Formation and Cell Surface Properties among Pathogenic and Nonpathogenic Strains of the Bacillus cereus Group. Appl. Environ. Microbiol. *75*, 6616–6618.

Banse, A.V., Hobbs, E.C., and Losick, R. (2011). Phosphorylation of Spo0A by the Histidine Kinase KinD Requires the Lipoprotein Med in Bacillus subtilis ▿. J. Bacteriol. *193*, 3949–3955.

Barranguet, C., Veuger, B., Beusekom, S.A.M.V., Marvan, P., Sinke, J.J., and Admiraal, W. (2005). Divergent composition of algal-bacterial biofilms developing under various external factors. Eur. J. Phycol. *40*, 1–8.

Berleman, J.E., Zemla, M., Remis, J.P., Liu, H., Davis, A.E., Worth, A.N., West, Z., Zhang, A., Park, H., Bosneaga, E., et al. (2016). Exopolysaccharide microchannels direct bacterial motility and organize multicellular behavior. ISME J. *10*, 2620–2632.

Bush, K. (2012). Antimicrobial agents targeting bacterial cell walls and cell membranes. Rev. Sci. Tech. Int. Off. Epizoot. *31*, 43–56.

Caiazza, N.C., and O'Toole, G.A. (2004). SadB is required for the transition from reversible to irreversible attachment during biofilm formation by Pseudomonas aeruginosa PA14. J. Bacteriol. *186*, 4476–4485.

Chiang, W.-C., Nilsson, M., Jensen, P.O., Hoiby, N., Nielsen, T.E., Givskov, M., and Tolker-Nielsen, T. (2013). Extracellular DNA Shields against

Aminoglycosides in Pseudomonas aeruginosa Biofilms. Antimicrob. Agents Chemother. *57*, 2352–2361.

Dasgupta, M.K., and Costerton, J.W. (1989). Significance of biofilm-adherent bacterial microcolonies on Tenckhoff catheters of CAPD patients. Blood Purif. *7*, 144–155.

Deuerling, E., Mogk, A., Richter, C., Purucker, M., and Schumann, W. (1997). The ftsH gene of Bacillus subtilis is involved in major cellular processes such as sporulation, stress adaptation and secretion. Mol. Microbiol. *23*, 921–933.

Dierick, K., Van Coillie, E., Swiecicka, I., Meyfroidt, G., Devlieger, H., Meulemans, A., Hoedemaekers, G., Fourie, L., Heyndrickx, M., and Mahillon, J. (2005). Fatal Family Outbreak of Bacillus cereus-Associated Food Poisoning. J. Clin. Microbiol. *43*, 4277–4279.

Dohmae, S., Okubo, T., Higuchi, W., Takano, T., Isobe, H., Baranovich, T., Kobayashi, S., Uchiyama, M., Tanabe, Y., Itoh, M., et al. (2008). Bacillus cereus nosocomial infection from reused towels in Japan. J. Hosp. Infect. *69*, 361–367.

Dubois-Brissonnet, F., Trotier, E., and Briandet, R. (2016). The Biofilm Lifestyle Involves an Increase in Bacterial Membrane Saturated Fatty Acids. Front. Microbiol. *7*.

Dutton, L.C., Nobbs, A.H., Jepson, K., Jepson, M.A., Vickerman, M.M., Alawfi, S.A., Munro, C.A., Lamont, R.J., and Jenkinson, H.F. (2014). O-Mannosylation in Candida albicans Enables Development of Interkingdom Biofilm Communities. MBio *5*, e00911-14.

Eisenbach Michael (2001). Bacterial Chemotaxis. ELS.

Elias, S., and Banin, E. (2012). Multi-species biofilms: living with friendly neighbors. FEMS Microbiol. Rev. *36*, 990–1004.

Elsholz, A.K.W., Wacker, S.A., and Losick, R. (2014). Self-regulation of exopolysaccharide production in Bacillus subtilis by a tyrosine kinase. Genes Dev. *28*, 1710–1720.

Fagerlund, A., Dubois, T., Økstad, O.-A., Verplaetse, E., Gilois, N., Bennaceur, I., Perchat, S., Gominet, M., Aymerich, S., Kolstø, A.-B., et al. (2014). SinR Controls Enterotoxin Expression in Bacillus thuringiensis Biofilms. PLoS ONE *9*.

Fanning, S., and Mitchell, A.P. (2012). Fungal Biofilms. PLOS Pathog. *8*, e1002585.

Faulstich, M., Hagen, F., Avota, E., Kozjak-Pavlovic, V., Winkler, A.-C., Xian, Y., Schneider-Schaulies, S., and Rudel, T. (2015). Neutral sphingomyelinase 2 is a key factor for PorB-dependent invasion of Neisseria gonorrhoeae. Cell. Microbiol. *17*, 241–253.

Flores-Urbán, K.A., Natividad-Bonifacio, I., Vázquez-Quiñones, C.R., Vázquez-Salinas, C., and Quiñones-Ramírez, E.I. (2014). Detection of toxigenic Bacillus cereus strains isolated from vegetables in Mexico City. J. Food Prot. *77*, 2144–2147.

Gao, T., Foulston, L., Chai, Y., Wang, Q., and Losick, R. (2015a). Alternative modes of biofilm formation by plant-associated *Bacillus cereus*. MicrobiologyOpen *4*, 452–464.

Gao, T., Foulston, L., Chai, Y., Wang, Q., and Losick, R. (2015b). Alternative modes of biofilm formation by plant-associated *Bacillus cereus*. MicrobiologyOpen *4*, 452–464.

García-Meza, J.V., Barrangue, C., and Admiraal, W. (2005). Biofilm formation by algae as a mechanism for surviving on mine tailings. Environ. Toxicol. Chem. *24*, 573–581.

Girych, M., Gorbenko, G., Maliyov, I., Trusova, V., Mizuguchi, C., Saito, H., and Kinnunen, P. (2016). Combined thioflavin T-Congo red fluorescence assay for amyloid fibril detection. Methods Appl. Fluoresc. *4*, 034010.

Gohar, M., Faegri, K., Perchat, S., Ravnum, S., Økstad, O.A., Gominet, M., Kolstø, A.-B., and Lereclus, D. (2008). The PlcR Virulence Regulon of Bacillus cereus. PLoS ONE *3*, e2793.

Gowrishankar, J., and Harinarayanan, R. (2004). Why is transcription coupled to translation in bacteria? Mol. Microbiol. *54*, 598–603.

Hamzeh-Cognasse, H., Damien, P., Chabert, A., Pozzetto, B., Cognasse, F., and Garraud, O. (2015). Platelets and Infections – Complex Interactions with Bacteria. Front. Immunol. *6*.

Hobley, L., Ostrowski, A., Rao, F.V., Bromley, K.M., Porter, M., Prescott, A.R., MacPhee, C.E., van Aalten, D.M.F., and Stanley-Wall, N.R. (2013). BslA is a self-assembling bacterial hydrophobin that coats the Bacillus subtilis biofilm. Proc. Natl. Acad. Sci. U. S. A. *110*, 13600–13605.

Houry, A., Briandet, R., Aymerich, S., and Gohar, M. (2010). Involvement of motility and flagella in Bacillus cereus biofilm formation. Microbiology *156*, 1009–1018.

Jefferson, K.K. (2004). What drives bacteria to produce a biofilm? FEMS Microbiol. Lett. *236*, 163–173.

Jenal, U., Reinders, A., and Lori, C. (2017). Cyclic di-GMP: second messenger extraordinaire. Nat. Rev. Microbiol. *15*, 271–284.

Johnson, L., Horsman, S.R., Charron-Mazenod, L., Turnbull, A.L., Mulcahy, H., Surette, M.G., and Lewenza, S. (2013). Extracellular DNA-induced antimicrobial peptide resistance in Salmonella enterica serovar Typhimurium. BMC Microbiol. *13*, 115.

Kamar, R., Gohar, M., Jéhanno, I., Réjasse, A., Kallassy, M., Lereclus, D., Sanchis, V., and Ramarao, N. (2013). Pathogenic Potential of Bacillus cereus Strains as Revealed by Phenotypic Analysis. J. Clin. Microbiol. *51*, 320–323.

Kim, H.-J., Lee, D.S., and Paik, H.-D. (2004). Characterization of Bacillus cereus isolates from raw soybean sprouts. J. Food Prot. *67*, 1031–1035.

Kristoffersen, S.M., Haase, C., Weil, M.R., Passalacqua, K.D., Niazi, F., Hutchison, S.K., Desany, B., Kolstø, A.-B., Tourasse, N.J., Read, T.D., et al. (2012). Global mRNA decay analysis at single nucleotide resolution reveals segmental and positional degradation patterns in a Gram-positive bacterium. Genome Biol. *13*, R30.

Łabaj, P.P., and Kreil, D.P. (2016). Sensitivity, specificity, and reproducibility of RNA-Seq differential expression calls. Biol. Direct *11*.

Lewenza, S. (2013). Extracellular DNA-induced antimicrobial peptide resistance mechanisms in Pseudomonas aeruginosa. Front. Microbiol. *4*.

Li, Z., Mukherjee, T., Bowler, K., Namdari, S., Snow, Z., Prestridge, S., Carlton, A., and Bar-Peled, M. (2017). A Four-gene Operon in Bacillus cereus Produces Two Rare Spore-decorating Sugars. J. Biol. Chem. jbc.M117.777417.

Lo, A.W., Moriel, D.G., Phan, M.-D., Schulz, B.L., Kidd, T.J., Beatson, S.A., and Schembri, M.A. (2017). “Omic” Approaches to Study Uropathogenic Escherichia coli Virulence. Trends Microbiol. *25*, 729–740.

Lövgren, A., Zhang, M., Engström, A., Dalhammar, G., and Landén, R. (1990). Molecular characterization of immune inhibitor A, a secreted virulence protease from Bacillus thuringiensis. Mol. Microbiol. *4*, 2137–2146.

Luckevich, M.D., and Beveridge, T.J. (1989). Characterization of a dynamic S layer on Bacillus thuringiensis. J. Bacteriol. *171*, 6656–6667.

Majed, R., Faille, C., Kallassy, M., and Gohar, M. (2016). Bacillus cereus Biofilms—Same, Only Different. Front. Microbiol. *7*.

McCoy, W.F., Bryers, J.D., Robbins, J., and Costerton, J.W. (1981). Observations of fouling biofilm formation. Can. J. Microbiol. *27*, 910–917.

Mielich-Süss, B., and Lopez, D. (2015). Molecular mechanisms involved in Bacillus subtilis biofilm formation. Environ. Microbiol. *17*, 555–565.

Miller, J.H., Avilés-Reyes, A., Scott-Anne, K., Gregoire, S., Watson, G.E., Sampson, E., Progulske-Fox, A., Koo, H., Bowen, W.H., Lemos, J.A., et al. (2015). The Collagen Binding Protein Cnm Contributes to Oral Colonization and Cariogenicity of Streptococcus mutans OMZ175. Infect. Immun. *83*, 2001–2010.

Nwodo, U.U., Green, E., and Okoh, A.I. (2012). Bacterial Exopolysaccharides: Functionality and Prospects. Int. J. Mol. Sci. *13*, 14002–14015.

Okshevsky Mira, Louw Matilde Greve, Lamela Elena Otero, Nilsson Martin, Tolker-Nielsen Tim, and Meyer Rikke Louise (2017). A transposon mutant library of Bacillus cereus ATCC 10987 reveals novel genes required for biofilm formation and implicates motility as an important factor for pellicle-biofilm formation. MicrobiologyOpen *0*, e00552.

Oosthuizen, M.C., Steyn, B., Theron, J., Cosette, P., Lindsay, D., von Holy, A., and Brözel, V.S. (2002). Proteomic Analysis Reveals Differential Protein Expression by Bacillus cereus during Biofilm Formation. Appl. Environ. Microbiol. *68*, 2770–2780.

Pandey, G., and Jain, R.K. (2002). Bacterial Chemotaxis toward Environmental Pollutants: Role in Bioremediation. Appl. Environ. Microbiol. *68*, 5789–5795.

Pflughoeft, K.J., Swick, M.C., Engler, D.A., Yeo, H.-J., and Koehler, T.M. (2014). Modulation of the Bacillus anthracis Secretome by the Immune Inhibitor A1 Protease. J. Bacteriol. *196*, 424–435.

Potera, C. (1999). Forging a Link Between Biofilms and Disease. Science *283*, 1837–1839.

Rajendran, A., and Hu, B. (2016). Mycoalgae biofilm: development of a novel platform technology using algae and fungal cultures. Biotechnol. Biofuels *9*, 112.

Rittmann, B.E., and McCarty, P.L. (1982). Model of steady-state-biofilm kinetics. Biotechnol. Bioeng. *24*, 2291.

Romero, D., Vlamakis, H., Losick, R., and Kolter, R. (2014). Functional analysis of the accessory protein TapA in Bacillus subtilis amyloid fiber assembly. J. Bacteriol. *196*, 1505–1513.

Rosano, G.L., and Ceccarelli, E.A. (2014). Recombinant protein expression in Escherichia coli: advances and challenges. Front. Microbiol. *5*.

Seydlová, G., Fišer, R., Čabala, R., Kozlík, P., Svobodová, J., and Pátek, M. (2013). Surfactin production enhances the level of cardiolipin in the

cytoplasmic membrane of Bacillus subtilis. Biochim. Biophys. Acta BBA - Biomembr. *1828*, 2370–2378.

Shivanna, V., Kim, Y., and Chang, K.-O. (2015). Ceramide formation mediated by acid sphingomyelinase facilitates endosomal escape of caliciviruses. Virology *483*, 218–228.

Sjollema, J., van der Mei, H.C., Hall, C.L., Peterson, B.W., de Vries, J., Song, L., Jong, E.D. de, Busscher, H.J., and Swartjes, J.J.T.M. (2017). Detachment and successive re-attachment of multiple, reversibly-binding tethers result in irreversible bacterial adhesion to surfaces. Sci. Rep. *7*, 4369.

Stewart, P.S. (2015). Antimicrobial Tolerance in Biofilms. Microbiol. Spectr. *3*.

Tan, C.H., Lee, K.W.K., Burmølle, M., Kjelleberg, S., and Rice, S.A. (2017). All together now: experimental multispecies biofilm model systems. Environ. Microbiol. *19*, 42–53.

Tang, Q., Yin, K., Qian, H., Zhao, Y., Wang, W., Chou, S.-H., Fu, Y., and He, J. (2016). Cyclic di-GMP contributes to adaption and virulence of Bacillus thuringiensis through a riboswitch-regulated collagen adhesion protein. Sci. Rep. *6*, 28807.

Tetz, G.V., Artemenko, N.K., and Tetz, V.V. (2009). Effect of DNase and Antibiotics on Biofilm Characteristics. Antimicrob. Agents Chemother. *53*, 1204–1209.

Tewari, A., and Abdullah, S. (2015). Bacillus cereus food poisoning: international and Indian perspective. J. Food Sci. Technol. *52*, 2500–2511.

Toyofuku, M., Inaba, T., Kiyokawa, T., Obana, N., Yawata, Y., and Nomura, N. (2016). Environmental factors that shape biofilm formation. Biosci. Biotechnol. Biochem. *80*, 7–12.

Tseng, B.S., Zhang, W., Harrison, J.J., Quach, T.P., Song, J.L., Penterman, J., Singh, P.K., Chopp, D.L., Packman, A.I., and Parsek, M.R. (2013). The extracellular matrix protects Pseudomonas aeruginosa biofilms by limiting the penetration of tobramycin. Environ. Microbiol. *15*, 2865–2878.

Van Acker, H., and Coenye, T. (2017). The Role of Reactive Oxygen Species in Antibiotic-Mediated Killing of Bacteria. Trends Microbiol. *25*, 456–466.

Van Gerven, N., Klein, R.D., Hultgren, S.J., and Remaut, H. (2015). Bacterial amyloid formation: structural insights into curli biogensis. Trends Microbiol. *23*, 693–706.

Vilain, S., Luo, Y., Hildreth, M.B., and Brozel, V.S. (2006). Analysis of the Life Cycle of the Soil Saprophyte Bacillus cereus in Liquid Soil Extract and in Soil. Appl. Environ. Microbiol. *72*, 4970–4977.

Watnick, P., and Kolter, R. (2000). Biofilm, City of Microbes. J. Bacteriol. *182*, 2675–2679.

Webb, J.S., Thompson, L.S., James, S., Charlton, T., Tolker-Nielsen, T., Koch, B., Givskov, M., and Kjelleberg, S. (2003). Cell death in Pseudomonas aeruginosa biofilm development. J. Bacteriol. *185*, 4585–4592.

Wehrl, W., Niederweis, M., and Schumann, W. (2000). The FtsH protein accumulates at the septum of Bacillus subtilis during cell division and sporulation. J. Bacteriol. *182*, 3870–3873.

Wei, Z., Zenewicz, L.A., and Goldfine, H. (2005). Listeria monocytogenes phosphatidylinositol-specific phospholipase C has evolved for virulence by greatly reduced activity on GPI anchors. Proc. Natl. Acad. Sci. *102*, 12927–12931.

Yadav, M.K., Chae, S.-W., Go, Y.Y., Im, G.J., and Song, J.-J. (2017). In vitro Multi-Species Biofilms of Methicillin-Resistant Staphylococcus aureus and Pseudomonas aeruginosa and Their Host Interaction during In vivo Colonization of an Otitis Media Rat Model. Front. Cell. Infect. Microbiol. *7*.

Yamamoto, K., Macnab, R.M., and Imae, Y. (1990). Repellent response functions of the Trg and Tap chemoreceptors of Escherichia coli. J. Bacteriol. *172*, 383–388.

Yang, L., Liu, Y., Wu, H., Høiby, N., Molin, S., and Song, Z. (2011). Current understanding of multi-species biofilms. Int. J. Oral Sci. *3*, 74–81.

Zhao, X., Wang, Y., Shang, Q., Li, Y., Hao, H., Zhang, Y., Guo, Z., Yang, G., Xie, Z., and Wang, R. (2015). Collagen-Like Proteins (ClpA, ClpB, ClpC, and ClpD) Are Required for Biofilm Formation and Adhesion to Plant Roots by Bacillus amyloliquefaciens FZB42. PLOS ONE *10*, e0117414.

Zhou Tianyi, and Nan Beiyan (2016). Exopolysaccharides promote Myxococcus xanthus social motility by inhibiting cellular reversals. Mol. Microbiol. *103*, 729–743.

Classification of bacteria - sponsored by Ribocon GmbH.

CHAPTER I

GENERAL INTRODUCTION AND THESIS OBJECTIVES

Coexistent with the macroscopic world, there is a whole microbial universe which have beautifully diversified to live in all known environmental conditions. Microbes have developed an intriguing molecular machinery which senses a variety of signals further integrated in efficient responses (Jayaraman and Wood, 2008). Life in community, conceived as an efficient way of life which evolved to the appearance of macro-organisms, have developed itself to respond to changeable environmental conditions, a strategy which is also outstandingly achieved in the microbial world in the form of biofilms.

In the XVII century, Anton van Leeuwenhoek owned a draper shop in Delft, The Nederland. Motivated for having a more detailed view of the thread of the fabrics he dealt with, he learned how to build and, most importantly, improve his own lenses. He constructed at least 25 microscopes, some of them able to magnify the samples over 500 times. However, his interest in fabrics diluted as soon as he entered into the new world of the "animalcules", the name that he gave to the microbes that he saw with his first microscope:

> *<< …my work, which I've done for a long time, was not pursued in order to gain the praise I now enjoy, but chiefly from a craving for knowledge, which I notice resides in me more than in most other men. And therewithal, whenever I found out anything remarkable, I have thought it my duty to put down my discovery on paper, so that all ingenious people might be informed thereof.>>*
>
> *Antony van Leeuwenhoek. Letter of 12th of June 1716.*

The interest for the study of these “animalcules” that invaded Leeuwenhoek’s life worth him the name of “The father of microbiology”. Since these pioneer observations, the attraction of the humankind for the study of the microbial world has grown continuously, reaching deeper interest into the nano and molecular scales of knowledge.

The study of bacteria led the taxonomic scientific community to stablish parameters for their proper classification, what constituted the first stage in the study of groups of taxons. The diversity of bacterial species inhabiting our world makes difficult the study of microorganisms, however, some of them, the so called “model organisms” have been routinely used in studies aimed at understanding basic aspects of bacteriology. Among the most renowned, *Escherichia coli* is considered the paradigm within the group of the gram-negative bacteria, as so *Bacillus subtilis* for the gram-positive group (Borriss et al., 2017). The accumulated knowledge obtained from these studies has constituted solid foundations which are accelerating our understanding of the entire microbial universe.

Bacillus cereus is a low-GC content gram-positive bacterium able to form spores very resistant to a variety of stresses (Su et al., 2012). This bacterium was firstly isolated by the end of XIX century from the air in a cow shed and it is considered the type strain of *B. cereus.* This strain is actually deposited in several culture collections, and classified with the code ATCC14579 in the American Type Culture Collection and CECT148 in the ¨Colección Española de Cultivos Tipo¨ (Frankland and Frankland, 1887). Pioneers works on *Bacillus* were carried out by

Ferdinad Cohn, in which it was described his observations of bacteria growing in groups. He beautifully drew bacterial cells organizations that remind biofilm structures, filaments and bacteria containing spores. These studies worth him the consideration of the father of *Bacillus* (Fig. 1).

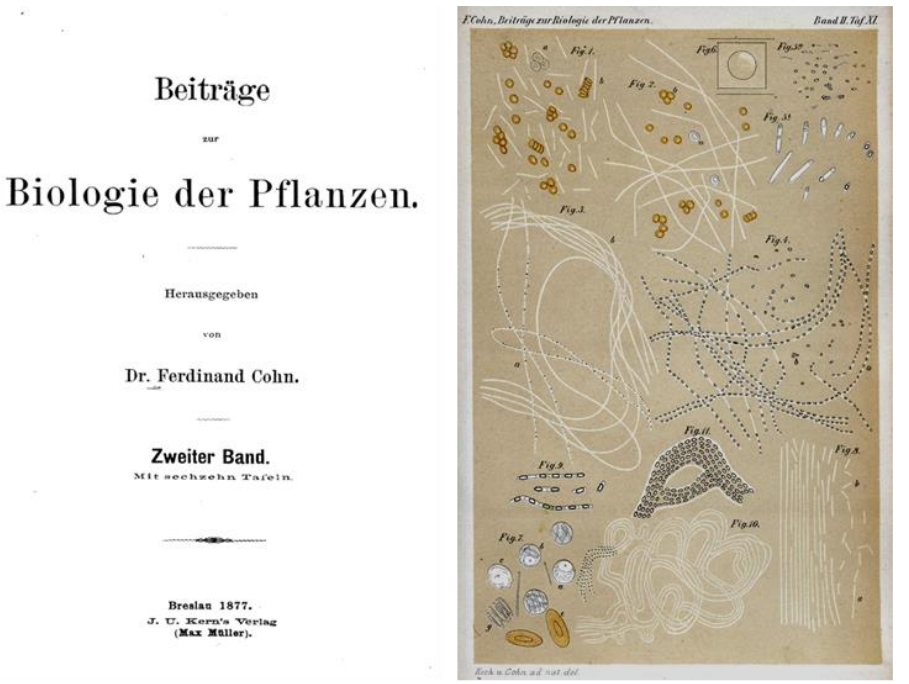
Beiträge

zur

Biologie der Pflanzen.

Herausgegeben

von

Dr. Ferdinand Cohn.

Zweiter Band.

Mit sechzehn Tafeln.

Breslau 1877.
J. U. Kern's Verlag
(Max Müller).

Figure 1. Ferdinand Cohn works describing bacterial cells organizations of *Bacillus*.

More than one hundred and thirty years later, our knowledge on *Bacillus spp.* is still quite incomplete, especially in some species different from the model organism *Bacillus subtilis*. *B. cereus* has evolved from a close ancestor which is also the origin of a wide variety of highly similar bacteria species which share multiple characteristics (Rasko et al., 2005).

1. Taxonomy of the *B. cereus* group

Belonging to the Phylum *Firmicutes* and the Family *Bacilliales*, the genus *Bacillus* is a widely diverse group of strictly aerobic or facultative anaerobic rod-shape bacteria which sporulate under certain environmental conditions (Higgins and Dworkin, 2012). The intrinsic diversity of the genus makes difficult the taxonomy of the group. This is especially striking between closely related with *Bacillus cereus* species, a group integrated by a collection of very similar strains with a wide variability in toxins productions, host specificity or biofilm formation (Ceuppens et al., 2013; Senesi and Ghelardi, 2010), a situation leading the scientific community to use the term "*Bacillus cereus group"* to refer to all of these species. New sequencing technology and more robust bioinformatics tools has help clarifying partially the controversial taxonomic classification within the *B. cereus group.* However, this terminology is still in use to refer to this group of different but closely related bacteria species highly similar at genetics and physiological level (Priest et al., 2004).

The group of *B. cereus* is nowadays composed of 15 species: *B. thuringiensis,* an entomopathogenic bacteria used as a bio pesticide (Rosas-García, 2009); *B. anthracis,* the etiological agent of anthrax (Spencer, 2003); *B. weihenstephanensis*, a phsycrotolerant species (Lechner et al. 1998); *B. toyonensis*, a probiotic species used since 1988 in animal nutrition including birds, mammals and fishes, that stabilizes intestinal microbiota and improves nutrient digestion (Jiménez et al., 2013); *B. mycoides,* with some strains providing a wide protection

to plants against phytopathogens; *B. pseudomycoides*, isolated from soil (Nakamura, 1998); *B. citotoxicus*, a thermotolerant bacteria occasionally associated with food poisoning (Guinebretiere et al., 2013); *B. manliponensis* and *B. gaemokensis*, isolated from foreshore tidal flat sediment from the Yellow Sea (Jung et al., 2011); *B. bombisepticus*, a pathogen of the main sink worm *Bombyx mori,* producing Black Chest Septicemia (Cheng et al., 2014); *B. bingmayonensis*, isolated from the pit soil of Emperor Qin's Terra-cotta warriors in China and *B. wiedmanii*, which is psychrotolerant and cytotoxic (Miller et al., 2016).

Within the *B. cereus* group, several genetic studies have confirmed such level of similarity among *B. cereus*, *B. thuringiensis* and *B. anthracis* genomes, having stated that they should be considered the same species. Indeed, strains lacking their specific plasmids become indistinguishable (Helgason et al., 2000). Although, the pathogenic properties of each strain have outweighed taxonomic considerations and they are still conceived as different species (Okinaka and Keim, 2016). To refer to all these similar bacterium group of species it is used the term *B. cereus sensu lato*, leaving the term *B. cereus sensu stricto* to refer strictly to *B. cereus*. Despite the last taxonomic studies, *B. cereus* remains as an example of a taxonomic quandary (Fiedoruk et al., 2017; Liu et al., 2015; Okinaka and Keim, 2016; Zwick et al., 2012).

2. Natural environments of *B. cereus* group

The soil is a highly variable niche in physic-chemical conditions such as water content, chemical composition, organic material, pH, temperature

or osmolarity. The combination of changes in these parameters results in a plethora of different environmental conditions which can be optimal for specific bacterial community's survival, affecting the species composition or even its presence. *B. cereus* group is highly diverse at genomic level and also in terms of the presence of plasmids, from 2kb to 500kb, which may harbour genes that increase the fitness and adaptability to these variable environmental conditions (Zheng et al., 2015). Diverse strains have been reported to be isolated from environments as variable as 7°C to 50°C, spanning from alpine to hot thermal environments. This phenotype can be classified within thermotypes, and is not congruent with the species classification within the *B. cereus* group, except *B. wheistphanensis,* which comprises all the strains able to survive at 4°C (von Stetten et al., 1999). This ecological skill is also a very important issue for the food industry, given that refrigeration is the most important factor to keep under consideration for food conservation.

Focusing on *B. cereus sensu stricto* (henceforth *B. cereus*), multiple strains have been described to live in association with the guts of arthropods (Wenzel et al., 2002), earthworms (Schuch et al., 2010), isopoda (Swiecicka and Mahillon, 2006), and plants rhizosphere (Hu et al., 2017). These are very competitive niches in which *B. cereus* has evolved the ability to efficiently deal with, deploying an arsenal of tools directed to: i) defence, represented mainly by sporulation, antibiotic resistance and biofilm formation; and ii) offense, inflicted by production of secondary metabolites (surfactants or antimicrobials), degradative enzymes and toxins (Bottone, 2010).

As previously indicated, a distinctive characteristic of the *Bacillus* genus is its ability to sporulate, which let bacteria survive in highly changeable environments and overcome successfully long lasting periods of unfavourable conditions (Higgins and Dworkin, 2012). The recalcitrance of the spores is indeed responsible for their successful spread to different niches, not only as a saprophyte but also in association with different hosts. This is of special interest with pathogenic strains of *B. cereus,* which are able to survive through the digestive tube, were the acid of the stomach or the biliary salts of the upper part of the small intestine would destroy vegetative bacterial cells (Ceuppens et al., 2012).

3. *B. cereus* in anthropic environments

The adaptability acquired by *B. cereus* in evolution can be considered a perfect training to live in the anthropic world. Humans have changed drastically most of the surfaces worldwide and have created new niches that never existed before. Many of these niches are highly hostile to most bacteria species, but *B. cereus* is able to adapt to many of them.

Although not recurrent, episodes of *B. cereus* bacteraemia outbreaks in hospitals has been reported, which presumably had the origin in biofilms formed inside the laundry machines. Spores released from the biofilms in contaminated towels or blankets reached catheters, causing further systemic infections and eventually death of immune-suppressed patients (Kusama et al., 2015; Sasahara et al., 2011).

The main material used in the food industry is stainless steel due to the consideration of its stability to oxidation and ease to cleaning. However, *B. cereus* is commonly isolated from pipes and tanks, where this bacteria is able to form strong biofilms, a lifestyle apparently favoured by the abundant availability of iron (Cherif-Antar et al., 2016). Besides, the previously introduced psychrotolerance of many strains is a complementary feature contributing to their survival during refrigeration, the conservation strategy routinely used for storage and distribution of food, especially of dairy products and semi cooked food (Choma et al., 2000; Guinebretiere and Nguyen-The, 2003; Larsen and Jørgensen, 1997). Pasteurization, or dehydration are also strategies used to preserve food from contamination, however, certain *B. cereus* strains are also able to survive the aggressiveness of both strategies. As result of this contamination, food spoilage or further human intoxications are major problems with additional negative economic impact (Becker et al., 1994; Lin et al., 1998).

4. *B. cereus* as a pathogen

Within the *B. cereus* group, *B. cereus sensu lato* includes several pathogenic strains. *B. citotoxicus* has been occasionally associated with food poisoning outbreaks (Guinebretiere et al., 2013). *B. anthracis* is the etiological agent of anthrax disease in humans and is considered a zoonotic disease. The disease is mainly associated to herbivores and domestic animals in regions with low vaccination control, and although relatively uncommon in humans, constitutes a public health thread

because its potential use as bioweapon (Goel, 2015). *B. thuringiensis* is an entomopathogenic specie which toxicity is mainly related to the production of the cry toxins (Bravo et al., 2013). The efficiency and specificity of the toxins have been determinant for the implementation of *B. thuringiensis* as a bio pesticide, or the design of transgenic crops of potato, maize and cotton, expressing this toxin to fight insect's plagues (Koch et al., 2015). The species that gives the name to the group, *B. cereus sensu stricto*, possesses a complete panel of toxins responsible for pathogenesis in humans and other mammals (Table 1). Among them, cereulide is the only one specific of *B. cereus*, it is codified in a megaplasmid and it is responsible of the emetic condition (Ehling-Schulz et al., 2006). All the other toxins are widely distributed in *B. cereus sensu lato* species, although, the presence of genes codifying the toxin synthesis machinery does not correlate with pathogenicity. Nevertheless, and given the recent description of many of the isolates of the group, there is still a blurred vision of their pathogenicity potential (Miller et al., 2018).

In *B. cereus* group, PlcR is a pleiotropic regulator, which plays a positive control over the expression of virulence genes including most of the toxins listed in Table 1 (Gohar et al., 2008). Interestingly, *B. anthracis* possesses a truncated version of *plcR* which encodes a non-functional regulator, leading to the low expression of these toxins and other virulent factors (Slamti et al., 2004). Pathogenicity of *B. anthracis* is given by two plasmids pXO1 and pXO2, which harbours genes codifying for a tripartite toxin: the lethal factor, the edema factor and a third

component codified in the genome, the protective antigen (Mock and Mignot, 2003; Turk, 2007).

Table 1. Toxins described in *B. cereus.*

Toxin	Simptom	Action	Gene Localization	Target	Ref.
Cereolysin O	Diarrhoea	Pore forming	Genome	Erythrocytes	(Brillard and Lereclus 2007)
Hemolysin II	Diarrhoea	Pore forming	Genome	Macrophage, monocytes, erythrocytes, Caco2	(Tran and Ramarao 2013)
Hemolysin III	Diarrhoea	Pore forming	Genome	Erythrocytes	(Baida and Kuzmin 1996)
Cytotoxin K	Diarrhoea	Pore forming	Genome	Erythrocytes, necrotic	(Castiaux et al. 2015; Lund, De Buyser, and Granum 2000)
Hemolysin A		Pore forming	Genome	Unknown	Not studied yet
Hemolysin BL	Diarrhoea	Pore forming	Genome	Erythrocytes, cytotoxic, dermonecrotic, vascular permeability	(McDowell and Friedman 2017; Beecher, Schoeni, and Wong 1995)
Hemolysin XhlA		Pore forming	Genome	Insect immune cells and erythrocytes	(Frey and Falquet 2015)
Enterotoxin CwpFM	Diarrhoea	Pore forming	Genome	MHC complex	(Asano et al. 1997)
Cereulide	Emetic	Potassium channel	Plasmid	Host cells	(Teplova et al. 2006)
InhA1		Metalloprotease	Genome	Scape of spores from macrophages	(Ramarao and Lereclus 2005)

Non-Hemolytic Enterotoxin	Diarrhoea	Pore forming	Genome	Erythrocytes	(McDowell and Friedman 2017)
Collagenase		Collagen cleavage	Genome	Collagen	(Abfalter et al. 2016)
Lysophospho-lipase L2		Membranes damage	Genome	Phospholipids	Not studied yet
Phospholipase C		Phospholipid cleavage	Genome	Phospholips	(Kuppe et al. 1989)
Sphingomye-linase		Membranes damage	Genome	Sphingolipids, erythrocytes	(Oda et al. 2010)

These plasmids also harbour the genes for the synthesis of a poly-γ-D-glutamic acid capsule which mask bacteria, preventing its recognition by macrophages (Ezzell and Welkos, 1999; Okinaka et al., 1999).

5.1. Gastrointestinal diseases

Several studies point to a common asymptomatic presence of *B. cereus* in low numbers in the human gastrointestinal track (GI) and faeces associated with spore ingestion or vegetative cells living on the surface of products (Ghosh, 1978; Turnbull and Kramer, 1985). The most common health problem elicited by *B. cereus* is food poisoning, which virulence depends on the strain, pathogen doses and host variables, which explain why the physical presence of *B. cereus* is not determinant to pathogenesis (Kamar et al., 2013). The incidence of pathogenesis is elusive varying between 2 and 22% of total gastroenteritis cases reported, with a few data restricted only to a small group in developed

countries (Dodd et al., 2017). However, its incidence is considered underestimated due to accumulative reasons: i) *B. cereus* generally produces low-mild symptoms, cases that do not need medical assistance and remain unnoticed in statistics; ii) the symptoms may be caused by thermostable toxins produced during food storage by bacteria which die in the digestive tube, making difficult to define the causal agent; iii) the presence of this bacteria in tests has been usually considered a contamination of samples; and iv) the 45-60% of GI infections in hospitals are undefined (Tompkins et al., 1999). In France, between 2006 and 2013, *B. cereus* food poisoning was considered the second most frequent after *Staphylococcus aureus* (Glasset et al., 2016). Rice dishes have been commonly associated with food poisoning of *B. cereus*, however, cases of intoxications has been also reported with origin in milk, meat, vegetables, potatoes, pasta, soups, spices and dehydrated meals. Attending to the symptoms, food poisoning caused by *B. cereus* can be classified in emetic or diarrheic conditions, depending on the toxins involved. Nevertheless, other uncommon but severe cases include fulminant liver failure, necrotizing gastritis or pancreatitis (Dierick et al., 2005; Drobniewski, 1993; Le Scanff et al., 2006; Mahler et al., 1997; Saleh et al., 2012).

5.2.1 Emetic disease

The emetic illness shows symptoms within 30 minutes to 6 hours and it is caused by the toxin cereulide, which shows multiple isoforms (Marxen

et al., 2015). The genetic cluster involved in the synthesis of cereulide is hosted in a megaplasmid which is only present in some strains of *B. cereus*. Cereulide is a ionophore toxin, with a high affinity for potassium cations (Mikkola et al., 1999). The toxin is soluble in membranes and causes loss of the membrane potential by transporting K^+ ions and uncoupling the oxidative phosphorylation chain when reaches the mitochondria (Makarasen et al., 2009). This toxin is non-ribosomaly synthetized and it is outstandingly resistant to acidic pH, proteolytic activity and heat (126°C 90 min). The physic-chemical properties of cereulide determine the physiopathology of this disorder, usually caused by the consumption of improperly conserved food with a subsequent bacteria proliferation and toxin production (ref). Other toxins can be present, but none of them survive heating, the acidic pH of the stomach or proteolysis. The symptoms generally resolve within 12 hours without medical assistance as there is no treatment against the toxin (Ehling-Schulz et al., 2005).

5.2.2 Diarrhoeic disease

Vegetative cells of *B. cereus* are susceptible to the acidic pH of the stomach, what make this disease mainly produced by spores germinating in the intestine, which proliferate and produce the diarrhoeic toxins (Table 1). Within these toxins, haemolysin BL, non-haemolytic enterotoxin and cytotoxic K are the main pore forming proteins implicated in this illness, although other toxins influence the virulence grade in combination with host variables (Kamar et al., 2013).

This condition takes 8-16 hour to show the first symptoms and usually solve within the next 24 hours (Drobniewski, 1993).

5.2. Non-gastrointestinal diseases

Although the pathologies related to *B. cereus* are mainly GI syndromes, *B. cereus* is also responsible of many different human infections, some of them severely virulent or even lethal (Shimoyama et al., 2017). Nosocomial infections are the most commons among non-gastrointestinal diseases, and are apparently related with the presence of vegetative cells or spores in hospital bed dressing, towels or uniforms. Further contamination of instruments or catheters permit *B. cereus* to reach immune depressed patients, although several cases have also been reported on non-immunocompromised patients (Gurler et al., 2012). Nevertheless, other infections have their origin out of the hospital facilities and affect healthy patients that suffer highly virulent infections which evolve rapidly, leaving severe sequels, especially in ocular infections. Non- gastrointestinal diseases can be classified in local or systemic diseases.

5.2.1. Local diseases

Local diseases are commonly originated after surgical intervention, traumatic wounds, burns or ocular infections. Although local infections are usually mild, many cases of deep infections have been reported,

which result in necrotizing fasciitis and gangrene (Sada et al., 2009). In a study on patients after hip arthroplasty it was reported that 25% of infections were produced by *B. cereus*, leading to suspect on the plaster cast as the origin of the contamination (Akesson et al., 1991). Plaster contaminated have also been described as a source of infection in orthopaedic cases with wounds, pointing to plaster as a common source of *B. cereus* infections (Rutala et al., 1986).

B. cereus can cause severe keratitis, panophthalmitis and endophthalmitis, which can result in loss of retinal structure and function within 12-18h. Although these pathologies are usually related to a previous trauma, ocular infections originated in blood infection or contact lens are also common (Pinna et al., 2001). A myriad of skin infections caused by *B. cereus* have been also reported, with typical necrotic bulla symptoms. Among others, an outbreak of cutaneous infections affected 90 cadets in a military program in US or a case of widespread necrotising skin infection in a diabetic patient (Michelotti and Bodansky, 2015).

B. cereus has also been isolated from periodontal infections, in which a biofilm was formed in the tooth-gum interface. However, *B. cereus* is not the initial causal agent of this kind of infection, since it participates as a recruited specie in a previously established biofilm (Majed et al., 2016a).

5.2.2. Systemic diseases

In general, systemic diseases are related to an active entry of bacteria into the host, proliferating and causing the disease. Entries into the blood stream causing bacteraemia are not clinically significant and are usually easy to resolve unless there is a malignant background like immunocompromised patients, drug abusers, neonates or patients receiving haemodialysis (Chou et al., 2016; Cotton et al., 1987; Hilliard et al., 2003; Magnussen et al., 2016; Patrick et al., 1989). Bacteraemia may evolve to a complicated medical chart of endocarditis and ocular or pulmonary infections. Endocarditis is more common in intravenous drug abusers and patients with valve diseases or pacemarker, which sometimes results fatal (Thomas et al., 2012).

Respiratory system infections are also uncommon, but tend to be severe. This group of pathologies caused by *B. cereus* includes pneumonia, lung infection and pleura infection that can evolve to life threatening complications (Miller et al., 1997). The strain *B. cereus* G9241 was isolated from a patient with anthrax-like disease. This strain harbours a plasmid similar to pXO1 presents in *B. anthracis*, which codifies the anthrax toxin among other genes (Wilson et al., 2011).

Central nervous system infections are rare and comprise cases of meningitis and encephalitis in adults, children and neonates. This cases are commonly related with spinal anaesthesia or spinal shunts in patients with reduced immunity state (Stevens et al., 2012).

6. *B. cereus* is also beneficial to humankind

Related to the genetic diversity and versatility of *B. cereus*, some strains can be used in benefit of humankind. As natural inhabitants of the soil, *B. cereus* may reach the plant rhizosphere and maintain a symbiotic relation in which bacteria improve the access of the plant to nutrients and reciprocally plants exudate complex molecules are beneficial to bacteria, which also modulate bacterial behaviour (Haichar et al., 2008). There are examples of *B. cereus* strains which contribute in a multifaceted way to the health of plants, improving the yield of crops like *B. cereus* F-6, which has been described to promote plant growth in vanilla plants (Zhao et al., 2015a).

All microorganisms living in the rhizosphere interact among them in a way that can also benefit plants, given that some strains inhibit pathogenic species (Doornbos et al., 2012). There are different mechanisms for this antipathogenic effect: i) biofilms allow bacteria to colonize the space, impeding pathogens attach to the plant structures; ii) active molecules produced by these beneficial bacteria communities targets the pathogen; iii) activation of the defence system of plants, which is enhanced in advance against a coming pathogen attack. We can find that *B. cereus* strains can biocontrol pathogens through one or all of the three mechanisms. *B. cereus* UW85 produces two antifungal molecules, zwittermicin A and kanosamine, which are known to inhibit the growth of for example *Phytophthora medicaginis*, an oomycetes responsible for the disease called dumping-off of alfalfa (Silo-Suh et al., 1994). *B. cereus* O-9 is an endophyte able to form biofilms in the plant

rhizosphere, impeding the infection caused by the fungus *Rhizoctonia cerealis*, the causal agent of the sharp eyespot in wheat (Xu et al., 2014). *Bacillus cereus* C1L combines several useful characteristic for crop improvement: i) it is a biocontrol agent against fungal infections in monocot plants, inducing the plant immune system, and ii) it also promotes plant growth (Huang et al., 2017; Liu et al., 2008).

In the same way, complex interactions take place in the gut of mammals, in which microorganisms interact. Some of these interactions are beneficial for the host in terms of stimulation of the immune system, colonization of the space and growth inhibition of pathogens (Kechagia et al., 2013). These kind of beneficial organisms are called probiotics, which include some strains of *B. cereus*. An example of probiotic used in birds is *B. cereus toyoi*, which induces a reduction in fat accumulation and an increase of muscle mass (Homma and Shinohara, 2004). Several commercial probiotics based on *B. cereus* are found on the market in some specific countries like China and Brazil for human and cattle consumption, despite the controversial use of these strains due to their pathogenic potential (Cutting, 2011; Zhu et al., 2016).

Other bacterial species can be used to develop biotechnological applications to deal with environmental problems but in a cost effective and nature friendly manner (de Alencar et al., 2017). In the last decades, strategies aimed at the use of bacteria for bioremediation of natural environments contaminated with organic and inorganic compounds have emerged (Kang et al., 2016). In this scenario, strains of *B. cereus* TA2 or TA4, possessing metal detoxification properties, has been

isolated from geothermal springs in Himalaya and are able to reduce the oxidative stage of chrome and selenium (Ghalib et al., 2014). In another example, the *B. cereus* NSPA8 isolate was tested for lead bioremediation, providing a 78% of lead biosorption from a medium contaminated with 1000 ppm of lead acetate (Syed and Chinthala, 2015). Similarly, biomineralization of Pb-II into Pb-hydroxyapatite crystals was achieved by *B. cereus* 12-2, which is able to accumulate them inside the cells. *B. cereus* also possess oil and grasses degradation properties that are apparently more efficient compared to previously used bacterial species (Mr and Sd, 2017). Many other isolates have been reported to be effective for degradation of organic compounds, including the insecticide chlorpyrifos, the explosive glycerol trinitrate, petroleum wastewater (*B. cereus* AKG1 MTCC9817 and AKG2 MTCC9818), phenol (*B. cereus* Jp-A), or complex organic efflux of a palm oil mill (*B. cereus* 103 PB) (Banerjee and Ghoshal, 2016; Li et al., 2006; Liu et al., 2011; Meng et al., 1995; Nwuche et al., 2014).

7. The bacterial social communities called biofilms

Biofilm formation seemed to appear early in bacterial evolution since they have been found in 3 billion years old fossils (Hall-Stoodley et al., 2004). Accumulated studies with diverse bacterial species have demonstrated that their life cycle comprises basically two stages characterized by their motility stage (Mikkelsen et al., 2007). Planktonic stage, with cells moving individually and freely in an aqueous medium, or sedentary, when bacterial cells find an adequate surface, attaching

and developing a sessile lifestyle that includes several relevant changes ending in the formation of a community: First, the initiation of a cell differentiation program leading to an outstanding division of labours inside the community (van Gestel et al., 2015) and second the production of an extracellular matrix which serves the entire community with a myriad of benefits, including protection and physically cohesion (Dragoš and Kovács, 2017). These bacterial communities are called biofilms and they are believed to constitute a usual step in any bacterial life cycle.

The switch from planktonic to biofilm is the result of a sophisticated developmental program governed by an intricate regulation network able to integrate internal and external signals which leads to cell differentiation (Kirov et al., 2007). Besides the species specific variations, there are general steps of biofilm formation, exemplified in Figure 2 from studies with *Bacillus subtilis*. Initial reversible attachment is followed by a cell differentiation process into matrix producers, preventing detachment and favouring the formation of micro colonies. Further maturation steps lead to the three dimensional growth of the community and control of the cell differentiation. In sporulating species, the process is triggered in a subpopulation within the biofilm. The cycle is completed with total or partial dispersion of biofilm of single individuals able to initiate a new planktonic phase (Fig. 2) (Vlamakis et al., 2013a).

Warmed by the relevance of biofilms, hundreds of studies have been directed at elucidating how bacteria sense signals, communicate and

assemble the extracellular matrix; and how all this cellular machinery is regulated (Kearns, 2008; McLoon et al., 2011). Up to date, most of the efforts to understand biofilm formation have been done with bacterial strains isolated *in vitro* and in controlled environmental conditions, what involve a clear bias compared with real environments.

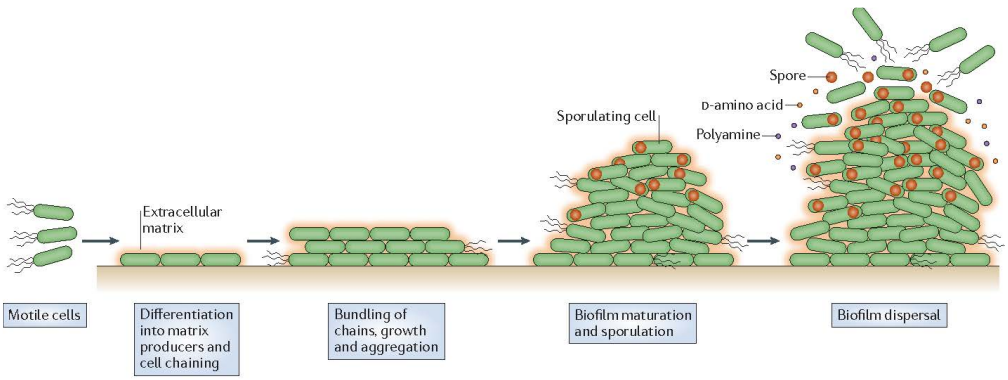

Figure 2. Life cycle of *B. subtilis* biofilm. Motile cells attach to a surface, switching to a sessile life style characterised by chained growth of bacteria and differentiation into matrix producers. Maturation of the biofilm produces differentiation of a subpopulation into sporulating cells. Fully mature biofilms partially disassemble to colonize other niches and initiate a new life cycle. Taken from (Vlamakis et al., 2013b).

Nevertheless, this approach has yielded invaluable knowledge leading to understand the basis of biofilm formation, physiology and ecology. *B. subtilis* is one of the most studied species in the gram positive group, serving as a model organism for studies of sporulation, gene regulation or biofilm formation of motile bacteria. *Streptococcus pneumonia* or *Staphylococcus aureus* are human pathogens and constitute a

paradigm in the study of biofilm formation of non-motile gram-positive bacteria (Chao et al., 2014; Moormeier and Bayles, 2017)

However, in nature, it is believed that biofilms grow in a multispecies specific manner, introducing a new level of complexity (Røder et al., 2016). In the last years some studies have been done in this direction with synthetic multispecies communities assembled *in vitro,* using a reduced number of strains as a model to mimic natural environments (Niu et al., 2017).

7.1. Biofilm architecture: The multifunctional extracellular matrix

The main characteristic and visible feature of a bacterial biofilm is the presence of an extracellular matrix surrounding the cells, which provides the community with outstanding stability and protection against external aggressions (López et al., 2010). The general elements of the extracellular matrix are typically exopolysaccharides, proteins and extracellular DNA (eDNA). However, for different bacterial species, each of these structural elements acquires a particular relevance in the final architecture of the biofilm and thus the way they coordinate to form such architecture. For instance, matrix exopolysaccharides are very variable among species in terms of sugar composition of the main chain, chain length, ramification pattern, sugar composition of the ramifications or additional sugar modifications (Schurr, 2013; Sutherland, 2001). Such variability provides with different properties of adhesion to the surface, cohesion of the community, rheology properties, or level of

hydrophobicity, all of them affecting the matrix performance in different environmental conditions (Hussain et al., 2017). As introduced earlier, *B. subtilis*, closely related to *B. cereus*, constitutes the most relevant model organism for studies of biofilm formation in gram-positive bacteria and a reference in the study of biofilms in related species. Mutants in the *epsA-O* region -in charge of the synthesis of the biofilm exopolysaccharides- results in the absence of biofilm in liquid culture, revealing the importance of this component to the final biofilm architecture of floating pellicles or colony morphology in agar plates (Branda et al., 2004).

In motile bacterial species, flagella are a very important structures for biofilm formation, playing a dual role either as: i) an element of the biofilm structure or ii) indirectly as a necessary functional element to reach the surface and generate the mechanical force for attachment, recruitment of new individuals or the formation of galleries inside the biofilm (Houry et al., 2010). In a myriad of species, secretion systems structures have been described as important elements for adhesion and bacteria interactions requireed to formation of biofilm (Gallique et al., 2017; Hernandes et al., 2013; Piepenbrink and Sundberg, 2016; Yoshida et al., 2017; Zimaro et al., 2014). As an example of other elements, proteins with type collagen domains have been found essential for adhesion and biofilms in some *Bacillus* species (Oliver-Kozup et al., 2011; Zhao et al., 2015b).

Pellicles formed by *B. subtilis* show a wrinkled phenotype and robust resistance which is also conferred by the presence of other structural

components, the amyloid proteins TasA and TapA. These two proteins are involved in the formation of rigid and resistant amyloid fibers (Diehl et al., 2018; Romero et al., 2010a). Amyloids were firstly described in neurodegenerative diseases in humans, Alzheimer and Parkinson diseases, as a protein misfolding resulting in accumulative aggregates inducing neuron toxicity. However, multiple amyloids have been reported to be associated with biological functions in all kingdoms, receiving the name of functional amyloids (Dueholm et al., 2010; Fowler et al., 2006; Som Chaudhury and Das Mukhopadhyay, 2018). Other example of functional amyloid with role in biofilm formation is the protein Curli in *E. coli*, the paradigm of functional amyloid in gram-negative bacteria (Chapman et al., 2002).

Besides the amyloid protein and exopolysaccharides, biofilms of *B. subilis* are also formed by the hydrophobic protein BslA. Studies on this protein have shown the connection among hydrophobicity of BslA and its putative role providing protection against external aggressions (Hobley et al., 2013; Kobayashi, 2007a). This protein forms a plastic-like cover of the biofilm community, which has been proposed as a raincoat protection against aquous solutions in the soil when is polymerised. Besides, another function has been reported as an structural element of the matrix when is in a monomeric form (Arnaouteli et al., 2016, 2017).

Besides the protein and the exopolysaccharides, eDNA is being also reported to be part of the extracellular matrix. This element was firstly associated with competence and DNA exchange, although, recent

studies associated eDNA with colony morphology in *B. subtilis,* affecting the spread of the community (Zafra et al., 2012). Furthermore, in other species eDNA plays a determinant role in biofilm architecture as happens in *B. cereus* (Vilain et al., 2009).

Other components of the extracellular matrix of *B. subtilis* biofilm include the poly-γ-glutamic acid, one of the major secreted polymeric compounds which, however, is not determinant for biofilm formation. Although, an alternative important role in rhizosphere colonization has been proposed for this polymer (Yu et al., 2016).

In the assumption of the essentiality of biofilm in bacterial life cycle, such a complex developmental program should provide substantial benefits to bacteria (Watnick and Kolter, 2000). The three elements of the extracellular matrix cited above possesses adhesive and structural properties, however, it can be noticed additional advantages of living in community. Polysaccharides usually tend to retain water, reducing or retarding desiccation (Ophir and Gutnick, 1994; Wozniak et al., 2015). These polysaccharides can also be a carbon resource in a sudden change of environmental conditions (Costa Oliveira et al., 2017). Polysaccharides and eDNA have also shown ability to specifically interact with antimicrobials, and other toxic compounds as heavy metals, preventing their entrance and deleterious effect in bacterial cells (Priester et al., 2006; Stewart, 2002; Teitzel and Parsek, 2003).

These multilayer communities are organized three dimensionally, which might also be associated with some benefits and detriments in an equilibrium that assure species perpetuation. Although biofilm

architecture usually includes internal channels, biofilms are piled and are exposed to nutrient gradients within the big structure and within the distance to a channel. Though, those gradients also exist in the case of adversities coming from the outside including desiccation, radiation, predation or chemical attack and antimicrobials (McLean et al., 2008). In the genus *Bacillus*, biofilms are also associated with sporulation, yielding resistant forms of life that can survive extreme conditions and constitute a perfect craft for bacterial dispersion (Branda et al., 2001a).

This wide variability found even among closely related species in the assembly elements of biofilm formation should be thus perceived as the result of the adaptation of each specie to their specific niches or life particularities. Thus, species-specific studies are required to get a detailed and more comprehensive knowledge of biofilm architecture.

7.2. General molecular mechanism of biofilm regulation in Bacillus

The variety of elements implicated in formation of biofilms obligates bacterial cells to mobilize a sophisticated regulatory network that coordinate specific gene expression, leading to cell differentiation and the assembly of final architecture (Orell et al., 2018; Renner and Weibel, 2011; Stanley and Lazazzera, 2004). The intricate regulatory networks have been very well studied in *B. subtilis* (Fig. 3A). A variety of sensors are exposed in the cell surfaces that sense changes in the environment or population messages; or internal signals related to the population physiological stage. Among them, the most investigated are Kinases A-

E, especially because of their involvement in triggering the phospohorelay implicated in the formation of the endospore and biofilm (LeDeaux et al., 1995; McLoon et al., 2011). Each of these kinases have acquired the ability to efficiently respond to specific signals. Starvation or desiccation are physical conditions sensed by kinases A and E. Kinase A and B have been proposed as sensors of internal signals related to cellular redox stage, oxygen availability and (NAD(+))/NADH ratio (Kolodkin-Gal et al., 2013). Exudates of tomato roots are specifically detected by KinD, inducing the formation of biofilm (Chen et al., 2012). KinD is also in charge of sensing the osmotic pressure (Rubinstein et al., 2012). Despite the effort, the entire cellular response is still far from being fully understood.

After sensing their specific signals, kinases activate a regulatory cascade known as phosphorelay, starting with the phosphorylation of Spo0F, which pass the phosphoryl group to Spo0B and progressively to different intermediates culminating with the phosphorylation of the master regulator Spo0A (Jiang et al., 2000). The increase levels of Spo0A-P activates a cascade of regulators that exclusively ends in biofilm or sporulation cell fates, a dichotomy resolved with the relative concentration of Spo0A-P within cells (Molle et al., 2003). The higher levels of Spo0A-P are conducive to sporulation in matrix producer cells (Fujita et al., 2005). Spo0A-P induces the expression of the anti-repressor SinI, a specific inhibitor of the repressor SinR, which negatively control the expression of the operon *epsA-O* necessary for the production of exopolysaccharides, and the operon *tapA-sipW-tasA* implicated in the production of the constituents of the amyloid fibrils of

the extracellular matrix (Branda et al., 2006; Diehl et al., 2018; Flemming and Wingender, 2010; Romero et al., 2010b). This regulatory cascade is mostly conserved in the *Bacillus* genus, although the operons for the production of exopolysaccharides or the amyloid fibres vary among species as well as certain regulators that are alternatively present or absent in different species.

Part of these internal network respond to environmental conditions through the sensing of nutrients or physical parameters, while others are connected with *quorum sensing* systems and paracrine comunication. *Rap-Phr* family is involved in competence, sporulation, and biofilm formation. *Phr* codifies a peptide, which is secreted, processed out of the cell and transported again into the cell through the oligopeptide-permease (Opp) complex. Once inside the cell, Phr interacts with their cognates Rap proteins, which exert the regulatory function. Spo0A controls the expression of several *phr* genes, forming a complex regulatory network of multiple interactions (Bendori et al., 2015). The ComX pheromone is a peptide of the ComX-ComP-ComA quorum-sensing pathway, which works in a similar way than Rap-Phr-Opps and controls physiological changes, extracellular matrix and colonization functions (Comella and Grossman, 2005). *Quorum sensing* signalling affects the global gene expression of the entire bacterial population. Although, there are other signals considered a paracrine signalling, affecting a subpopulation within the community which is different from the population that sends the signal. This communication flux has been described in *B. subtilis* and relies on the surfactant molecule surfactin, which triggers the expression of rthe extracellular

matrix genes through Kinase C and the phosphorylation of Spo0A. Interestingly, the expression of surfactin synthesis genes are under the control of ComX pheromone contained in the surfacing synthesis operon (López et al., 2009).

7.3. Biofilm and sporulation

One of the distinctive features of the *Bacillus* genus is the formation of endospores under certain conditions like nutrient starvation or stress. Spores are resistant forms of bacteria that harbours a DNA copy and a reduced portion of the mother cell cytoplasm and some other particularities, like the accumulation of dipicolinic acid and divalent cations (Setlow et al., 2006). Spores maintain an exceptional low basal metabolic activity which granted to survive extreme environmental conditions of temperature, desiccation, oxidizing agents or ionizing radiation (Ghosh et al., 2015; Nicholson et al., 2000; Segev et al., 2012; Setlow, 2014). Representative of their resilience is the remarkable recovery of spores of *Bacillus sphericus* from the gut of a bee fossilised inside a piece of amber since at least 25 mills of years (Cano and Borucki, 1995).

Some particularities characterize spores of each *Bacillus* species, but the most studied is *B. subtilis* spore, a knowledge that seeds the study in other species. The differentiation of the spore initiates with the asymmetric cell division induced by high levels of the master regulator

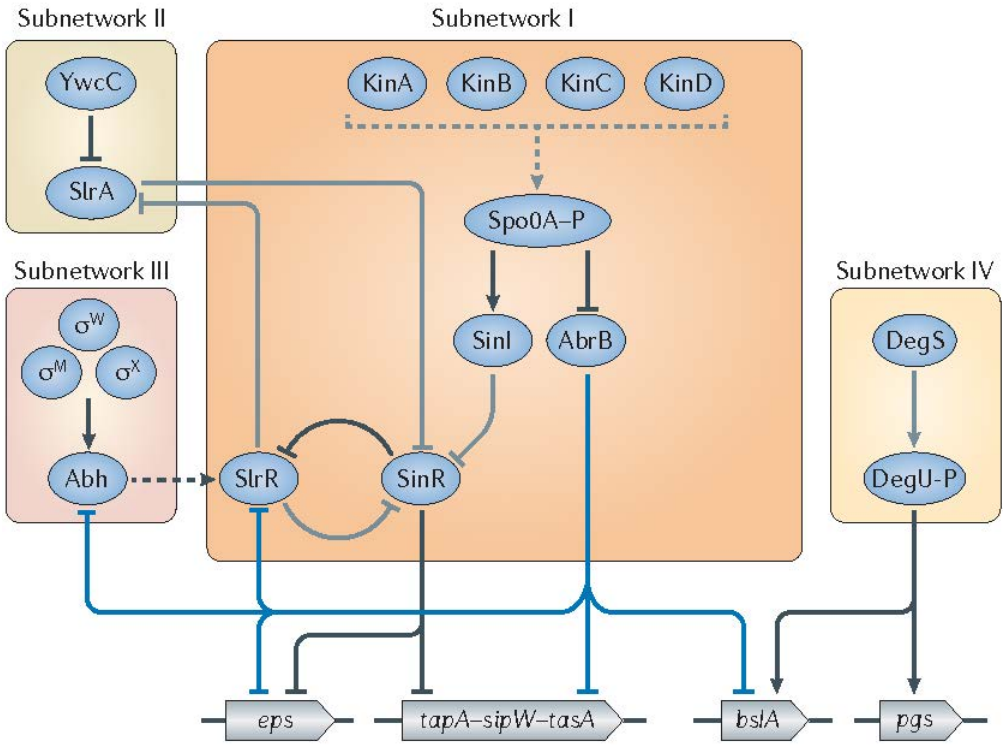

Figure 3. *B. subtilis* sporulation. Diagram of the main regulatory cascades implicated in biofilm formation in *B. subtilis*. KinA-D sensor environmental conditions, phosphorylating Spo0A, that induces the expression of the genes for the synthesis of the components of the extracellular matrix. Scheme taken from (Vlamakis et al., 2013b).

Spo0A-P (Jiang et al., 2000). Once the septum is formed and before asymmetric cell division induced by high levels of the master regulator Spo0A-P (Jiang et al., 2000). Once the septum is formed and before cells separation, the mother cells engulf the daughter cell, maintaining communication and synthetizing the different layers of the final spore (Fig. 4) (McKenney et al., 2013). The core is characterized by

maintaining a gel condition, with low water content, high concentration of dipicolinic acid and the DNA saturated with small acid soluble proteins (SASP) protecting it from damage (Leyva-Illades et al., 2007; Setlow et al., 1992, 2006). Surrounding the core of the spore is the cortex, composed of a chemically modified peptidoglycan compared with the cell wall (Warth and Strominger, 1969). Externally to the peptidoglycan multiple layers of proteins constitute the spore coat (Kim et al., 2006). Finally, additional outer layers called exosporium are present in certain *B. cereus* strains (Fig. 5C), and a polysaccharide outer decorations or an S-layer. All of these structural elements define the physic-chemical characteristics of the final spore including the high hydrophobicity and the adhesion to specific surfaces (Fig. 5) (Driks, 1999; Stewart, 2015).

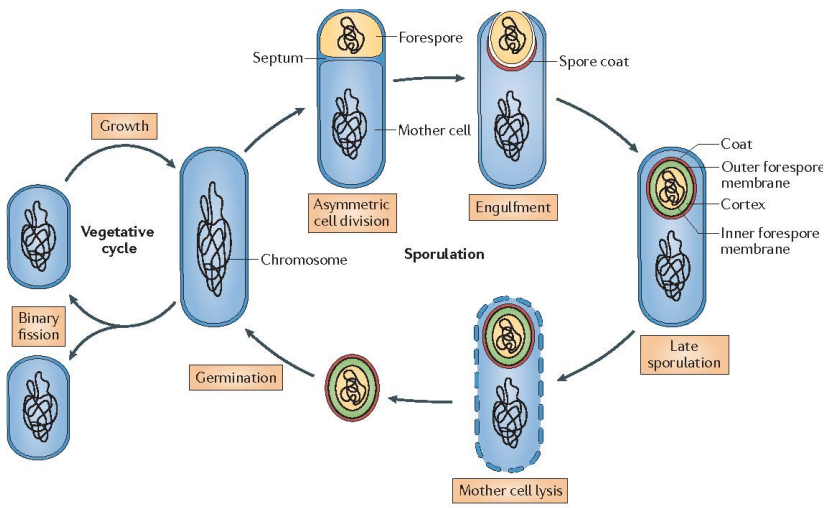

Figure 4. Bacillus sporulation. Scheme of the connection of the sporulation and germination steps in the cell cycle of *B. subtilis* (McKenney et al., 2013).

Each layer provides specific resistance properties to the spore against physical parameters, radiation, oxidants or biocides from environment or human origin (Fig. 5).

Similar to biofilm formation, the complexity of sporulation requires a tight regulation, with multiple regulators specifically dedicated to control the right timing of the different steps of the spore formation (Lindsay et al., 2005). It is therefore not surprising to find sporulation cells in the population that constitute a bacterial biofilm. Indeed, the anatomical studies done in *B. subtilis* showed that this population occupies the outer layers of the colony in a differentiated structure called fruiting bodies, reminiscent of the siblings in fungi (Branda et al., 2001b; Vlamakis et al., 2013a). Additionally, disruption of biofilm formation may also affect sporulation as both processes are connected. Cell differentiation into biofilm formation cell types is controlled by the levels of Spo0A-P, which induces sporulation when this level is high. Given that an impairment in biofilm formation may maintain SpoA in a non-phosphorylated stage, biofilm disruption may affect sporulation (Fujita and Losick, 2005).

7.4. Biofilm in the B. cereus group

Although much is known of the bases of biofilm formation in *B. subtilis*, specific research in other bacteria species are required to confirm the conservation of certain patterns during evolution. Particularities in protein function, interactions and regulation define the specific

developmental program of different species (Majed et al., 2016b). Due to the genetic similarities inside de *B. cereus* group, particularities in biofilm formation are as subtle as those found among strains of the same species, therefore, knowledge in this bacterium is rationally extensive to the entire group, or at least may serve as a more reliable model than *B. subtilis*. Unfortunately, there are insufficient studies focused on biofilm formation in this bacterial species rather than the visual characterization of biofilm phenotypes.

Among the three general components of the extracellular matrix of biofilms, eDNA has been studied in detail only in *B. cereus* (Vilain et al., 2009). Other studies conclude the presence of exopolysaccharides although its origin is unknown (Gao et al., 2015; Houry et al., 2012). No studies in exopolysaccharides were found in other *B. cereus* group species, apart from those related with the capsule of *B. anthracis.* In the same way, the presence of amyloid fibres in the biofilm of the *B. cereus* group had not been explored yet. Although *B. anthracis* is able to form biofilms, only studies on phenotypes were found (Lee et al., 2007).

In *B. thuringiensis,* it has been characterized the cell type differentiation into undifferentiated, virulent, necrotrophic and sporulating cells within the biofilm, reflective of the diversity and highly regulated genetic circuitry necessary to adapt to all these divergent environmental destinies (Verplaetse et al., 2015). Unfortunately, cell differentiation within its biofilm in *B. cereus* group specie is still poorly understood.

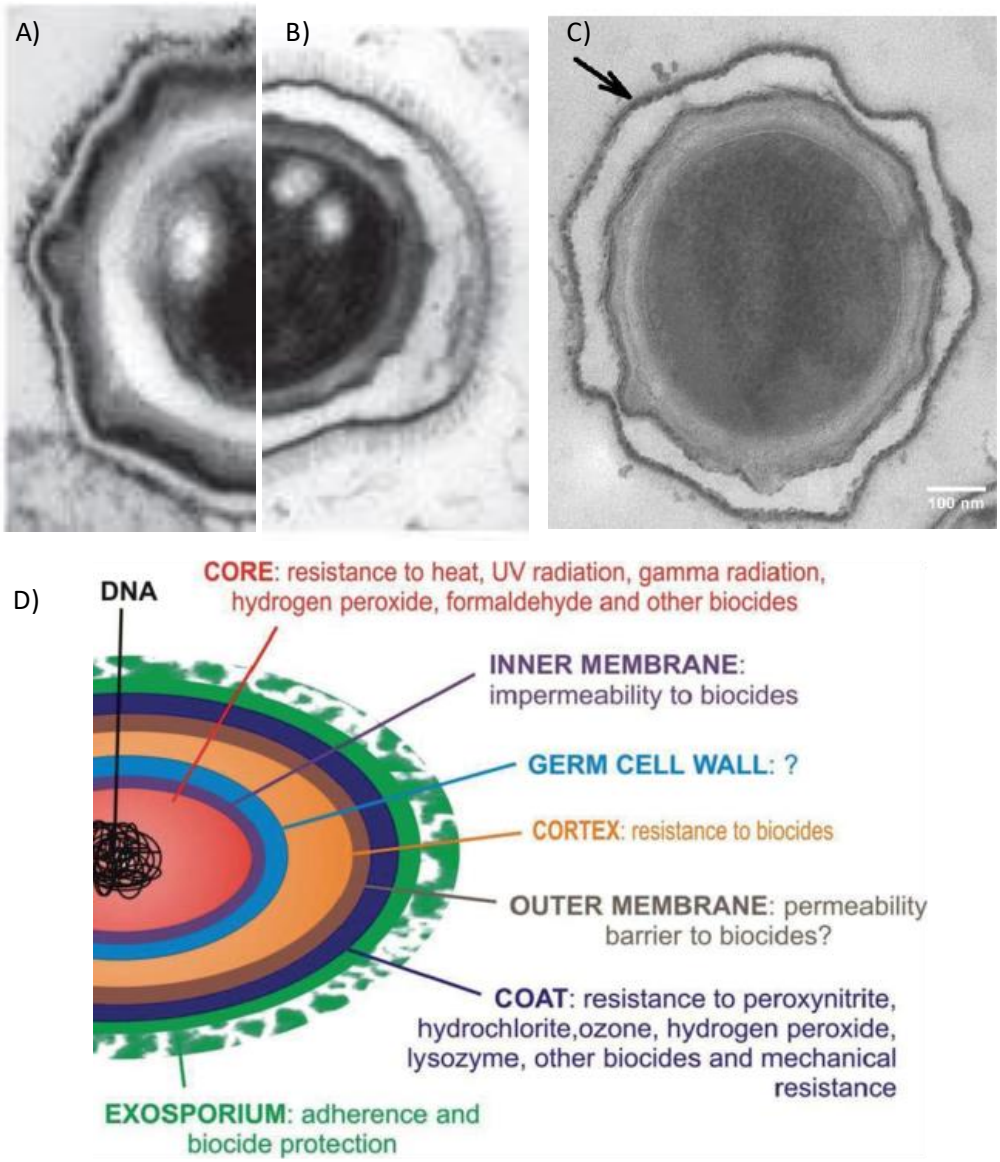

Figure 5. **Bacillus spores.** TEM images of cross-sections of spores of A) *B. subtilis*, B) *B. anthracis* and C) *B. cereus ATCC14579.* Arrow indicates exosporium. D) Scheme of the spore layers of *B. cereus* and their implication in stressing conditions. Pictures taken from (McKenney et al., 2010, 2013; Venir et al., 2014).

Comparatively with *B. subtilis,* the regulatory factors in *B. cereus* group are less understood. Although, several studies in *B. cereus* group species has revealed that the main regulatory routes conducing to biofilm formation are conserved. The phosphorelay that involve Spo0A is conserved, as well as the regulator AbrB and the antirepressor/repressor SinI/SinR. Nevertheless, the regulons present some differences, as the exopolysaccharide biosynthesis operon *epsA-O* is not under the control of SinR (Fagerlund et al., 2014; Kearns et al., 2005). Instead of surfactin, the lipopeptide involved in biofilm formation is the molecule kurstakin, which is included in the SinR regulon (Gélis-Jeanvoine et al., 2017).

PlcR regulator is absent in *B. subtilis*. It is in charge of sensing external signals life nutrients and population density through the peptide PapR. Its regulon comprise most of the virulent factors (Gohar et al., 2008) and it also regulates biofilm formation through the activation of the necrotrophic factor NprR, which induces kurstakin expression (Dubois et al., 2012). The autoinducer AI-2 plays a positive effect on biofilm formation in *B. subtilis,* however, in *B. cereus* it plays a contrary effect and induces bacteria liberation from the biofilm to the liquid medium (Auger et al., 2006; Duanis-Assaf et al., 2016).

Even within the *B. cereus* group there are several differences in the regulation of biofilm formation. In *B. anthracis*, PlcR is truncated (Sastalla et al., 2010) and in *B. cereus* ATCC14579 is reported to repress biofilm formation due to the interruption by a transposon of the *nprR* gene (Gélis-Jeanvoine et al., 2017). Similar situation happens with

CodY, a regulator reported to repress biofilm formation in the type strain and induce it in *B. cereus* UW101C (Hsueh et al., 2006; Lindbäck et al., 2012).

In *B. subtilis*, the subnetwork II and IV controlling biofilm formation involves the proteins SlrA and DegU (Kobayashi, 2007b, 2008), however both proteins has no homologue in *B. cereus.*

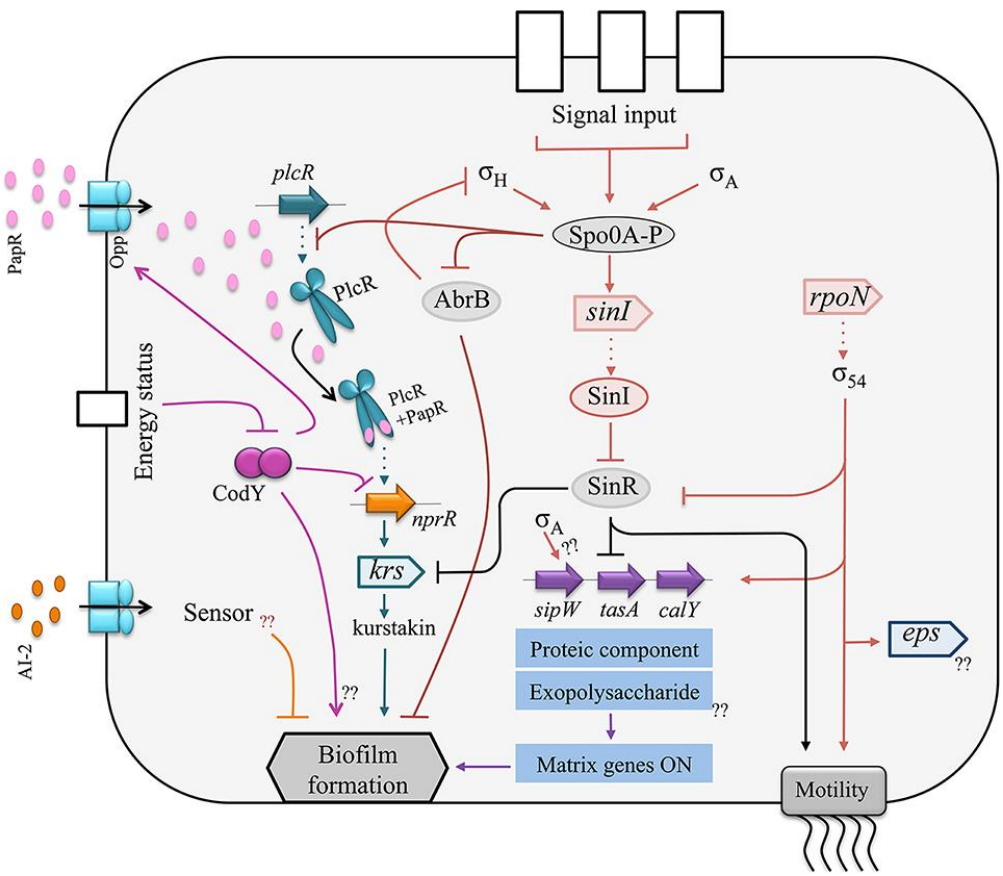

Figure 6. *B. cereus* biofilm. Diagram of the general regulatory networks goberning biofilm formation wihin the *B. cereus* group. Taken from (Majed et al., 2016b).

8. *B. cereus* life cycle

B. cereus life cycle can be resumed as the convergence of several interconnected basic cycles of spore germination, planktonic cells, biofilm formation and sporulation (Fig.7). This basic cycle potentially occurs in any of the niches in which *B. cereus* can be found, exemplified in previous sections. Individual cells from the population of planktonic cells or spores are able to jump among the different niches to initiate and complete a new cycle (Vilain et al., 2006).

B. cereus is commonly isolated from soil, where it lives as a saprophyte. Under adverse environmental conditions, sporulation is triggered and spores will further germinate with the rise of humidity or nutrients availability (Abee et al., 2011; Setlow, 2014). The resulting vegetative cells from germinating spores may form a biofilm if low nutrient availability prevails, an environmental condition which is also inducer of sporulation, leading to the completion of a branch of the foreseen life cycle (Vilain et al., 2006).

Plants are in close contact with soils, which may also host *Bacillus* cells. Plant surfaces, as the rhizosphere, are alternatively supplier of additional nutrients and high humidity conditions, permitting *Bacillus* to live as commensal or in symbiosis, either as epiphyte or endophyte (Peterson et al., 2006; Stabb et al., 1994). Natural niches in plant are not only found in the rhizosphere. *B. cereus* cells may also reach the aerial part of the plants, either because of the above mentioned endophyte lifestyle, because of contamination of the growing tails and

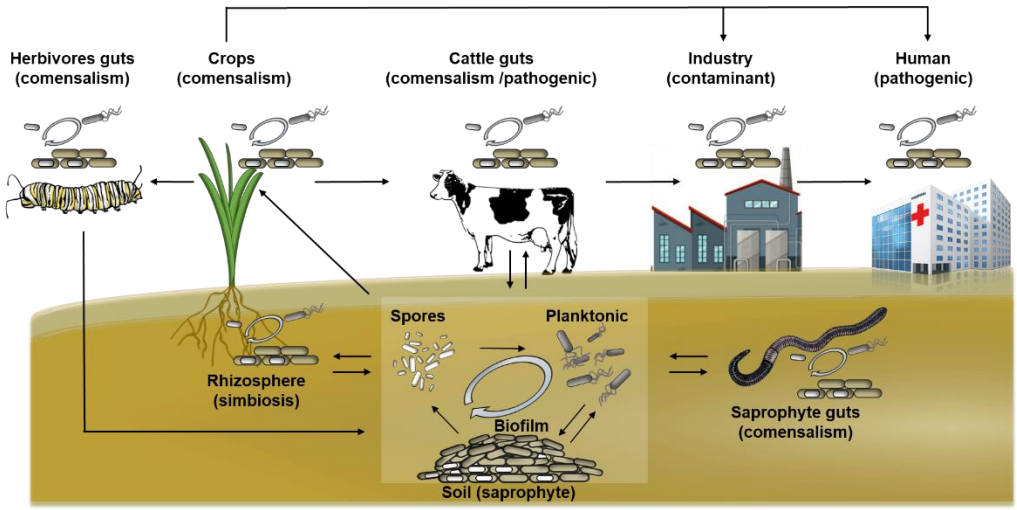

Figure 7. Life cycle of *B. cereus*. The general cycle of spore germination-planktonic-biofilm-sporulation is reproduced in all the niches and lifestyles described in the text. *B. cereus* niches are not isolated and bacteria or spores can move within the complete system.

leaves which contact with spores or vegetative cells present in the soils, or by deposition of dust containing cells or spores.

Once the plants are colonized, herbivores including mammals or insects, can ingest *B. cereus* cells, either as free leaving, spores or encased in biofilm. Thorns of plants can also harbour pathogenic bacteria which may permit bacterial cells to reach the animal host (Halpern et al., 2007). The cells that further reach and colonize the host guts can live as commensal and contaminate the faeces, contributing to the spread of *Bacillus* (Feinberg et al., 1999). Sensible herbivores in combination with highly virulent strains may result in a pathologic process ending in the host death. Other organisms living as

saprophytes in the soil can ingest debris of death plants or those death herbivores contaminated with *B. cereus*, reproducing a similar cycle in their guts.

Vegetable products or animals with guts or paws contaminated with *B. cereus* spores or vegetative cells are also vectors that introduce *B. cereus* into the food industry, nutrient-rich artificial niches that eventually support the same cycle of spore germination, planktonic lifestyle, biofilm formation and sporulation. Spores may contaminate the final products, reaching the human host and as explained in previous sections, *Bacillus* may live as a commensal or a pathogen, depending on the strain and the immunological stage of the host among other factors (Bottone, 2010).

9. *B. cereus* biofilm, host interactions and human concerns

As seen above, *B. cereus* strains are the causative agents of multiple human pathologies, food spoilage, damage of conducts and tanks, biofouling on ship hulls and alternatively be beneficial promoting plant growth, displaying biocontrol activity or as probiotic of animals. All of these effects are believed to be directly or indirectly related to the assembly of biofilms and sporulation.

Biofilms work as a reservoir of protected vegetative cells, which under certain conditions are liberated and reprogramed to initiate a planktonic lifestyle. Besides, a subpopulation of cells sporulate within the biofilm, constituting an extra-reservoir that contribute to the resilience of this

mega-architecture (Branda et al., 2001a). Biofilms create problems in the industry, where spores and biofilms of *B. cereus* are a continuous source of contamination and biofilm can damage facilities. In hospitals, biofilms of *B. cereus* on catheters are found frequently, and spores liberated from biofilms can be the origin of new systemic infections. On the other hand, biofilms are also implicated directly in human concerns as it has been described in the colonization of gut mice for periods of 18 days (Duc et al., 2004) or the biofilm stablished in endocarditis (Wright, 2016). Plant root colonization is also dependent on biofilm formation, conditioning growth enhancement and specially in biocontrol, given that space colonization is one of the key conditions in this beneficial contribution to plants (Gao et al., 2015). All these situations explains the increase interest on the study of *B. cereus,* and specifically the two interconnected aspects, biofilm formation and sporulation (Fig.8). Thus a deeper knowledge of biofilm structural elements, regulations, additional factors, and the complete molecular machinery, which drives the assembly of a biofilm are needed to further develop better tools for an improved control of biofilm formation.

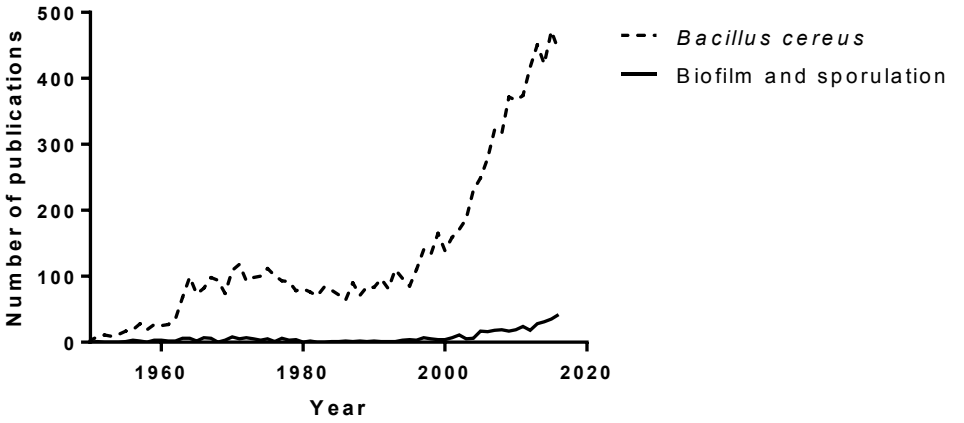

Figure 8. *B. cereus* publications. Number of articles published between 1950 and 2016 on *B. cereus* (dot line) and specifically on biofilms and sporulation (continuous line). Data from Medline PubMed.

General objectives of the thesis.

Previous studies in *B. cereus* have demonstrated the differences with the closely related species *B. subtilis* in the way they assemble a biofilm. It might be thus hypothesized that this divergence is reflective of the variability of ecological niches that *B. cereus* occupies, or how it interacts with its hosts. The extracellular matrix is essential to the viability of bacterial biofilms, and the outer part of the biofilm in contact with the environment. It is thus necessary to study the composition of the extracellular matrix of biofilms of *B. cereus* to understand its contribution to bacterial fitness, adaptability and interaction with hosts. To do so, we planned the next specific aims in this thesis:

1. To study the functionality of protein homologous to amyloid fibers of *B. subtilis*, in the formation of biofilm of *B. cereus* ATCC14579, and their biochemical characterization.

2.- To define the global molecular and structural changes that define the developmental program leading the transition from planktonic to sedentary biofilm in *B. cereus* ATCC14579.

3.- To characterize the role of exopolysaccharides in the multicellular lifestyle of *B. cereus* ATCC14579.

REFERENCES

Abee, T., Groot, M.N., Tempelaars, M., Zwietering, M., Moezelaar, R., and van der Voort, M. (2011). Germination and outgrowth of spores of Bacillus cereus group members: diversity and role of germinant receptors. Food Microbiol. *28*, 199–208.

Akesson, A., Hedström, S.A., and Ripa, T. (1991). Bacillus cereus: a significant pathogen in postoperative and post-traumatic wounds on orthopaedic wards. Scand. J. Infect. Dis. *23*, 71–77.

de Alencar, F.L.S., Navoni, J.A., and do Amaral, V.S. (2017). The use of bacterial bioremediation of metals in aquatic environments in the twenty-first century: a systematic review. Environ. Sci. Pollut. Res. Int. *24*, 16545–16559.

Arnaouteli, S., MacPhee, C.E., and Stanley-Wall, N.R. (2016). Just in case it rains: building a hydrophobic biofilm the Bacillus subtilis way. Curr. Opin. Microbiol. *34*, 7–12.

Arnaouteli, S., Ferreira, A.S., Schor, M., Morris, R.J., Bromley, K.M., Jo, J., Cortez, K.L., Sukhodub, T., Prescott, A.R., Dietrich, L.E.P., et al. (2017). Bifunctionality of a biofilm matrix protein controlled by redox state. Proc. Natl. Acad. Sci. U. S. A. *114*, E6184–E6191.

Auger, S., Krin, E., Aymerich, S., and Gohar, M. (2006). Autoinducer 2 affects biofilm formation by Bacillus cereus. Appl. Environ. Microbiol. *72*, 937–941.

Banerjee, A., and Ghoshal, A.K. (2016). Biodegradation of real petroleum wastewater by immobilized hyper phenol-tolerant strains of Bacillus cereus in a fluidized bed bioreactor. 3 Biotech *6*.

Becker, H., Schaller, G., Wiese, W., and Terplan, G. (1994). Bacillus cereus in infant foods and dried milk products. Int. J. Food Microbiol. *23*, 1–15.

Bendori, S.O., Pollak, S., Hizi, D., and Eldar, A. (2015). The RapP-PhrP Quorum-Sensing System of Bacillus subtilis Strain NCIB3610 Affects Biofilm Formation through Multiple Targets, Due to an Atypical Signal-Insensitive Allele of RapP. J. Bacteriol. *197*, 592–602.

Borriss, R., Danchin, A., Harwood, C.R., Médigue, C., Rocha, E.P.C., Sekowska, A., and Vallenet, D. (2017). Bacillus subtilis, the model Gram-positive bacterium: 20 years of annotation refinement. Microb. Biotechnol. *11*, 3–17.

Bottone, E.J. (2010). Bacillus cereus, a volatile human pathogen. Clin. Microbiol. Rev. *23*, 382–398.

Branda, S.S., Gonzalez-Pastor, J.E., Ben-Yehuda, S., Losick, R., and Kolter, R. (2001a). Fruiting body formation by Bacillus subtilis. Proc. Natl. Acad. Sci. *98*, 11621–11626.

Branda, S.S., Gonzalez-Pastor, J.E., Ben-Yehuda, S., Losick, R., and Kolter, R. (2001b). Fruiting body formation by Bacillus subtilis. Proc. Natl. Acad. Sci. *98*, 11621–11626.

Branda, S.S., González-Pastor, J.E., Dervyn, E., Ehrlich, S.D., Losick, R., and Kolter, R. (2004). Genes involved in formation of structured multicellular communities by Bacillus subtilis. J. Bacteriol. *186*, 3970–3979.

Branda, S.S., Chu, F., Kearns, D.B., Losick, R., and Kolter, R. (2006). A major protein component of the Bacillus subtilis biofilm matrix. Mol. Microbiol. *59*, 1229–1238.

Bravo, A., Gómez, I., Porta, H., García-Gómez, B.I., Rodriguez-Almazan, C., Pardo, L., and Soberón, M. (2013). Evolution of Bacillus thuringiensis Cry toxins insecticidal activity. Microb. Biotechnol. *6*, 17–26.

Cano, R.J., and Borucki, M.K. (1995). Revival and identification of bacterial spores in 25- to 40-million-year-old Dominican amber. Science *268*, 1060–1064.

Ceuppens, S., Uyttendaele, M., Drieskens, K., Heyndrickx, M., Rajkovic, A., Boon, N., and Van de Wiele, T. (2012). Survival and Germination of Bacillus cereus Spores without Outgrowth or Enterotoxin Production during In Vitro Simulation of Gastrointestinal Transit. Appl. Environ. Microbiol. *78*, 7698–7705.

Ceuppens, S., Boon, N., and Uyttendaele, M. (2013). Diversity of Bacillus cereus group strains is reflected in their broad range of pathogenicity and diverse ecological lifestyles. FEMS Microbiol. Ecol. *84*, 433–450.

Chao, Y., Marks, L.R., Pettigrew, M.M., and Hakansson, A.P. (2014). Streptococcus pneumoniae biofilm formation and dispersion during colonization and disease. Front. Cell. Infect. Microbiol. *4*, 194.

Chapman, M.R., Robinson, L.S., Pinkner, J.S., Roth, R., Heuser, J., Hammar, M., Normark, S., and Hultgren, S.J. (2002). Role of Escherichia coli curli operons in directing amyloid fiber formation. Science *295*, 851–855.

Chen, Y., Cao, S., Chai, Y., Clardy, J., Kolter, R., Guo, J., and Losick, R. (2012). A Bacillus subtilis sensor kinase involved in triggering biofilm formation on the roots of tomato plants: Root-associated biofilm formation. Mol. Microbiol. *85*, 418–430.

Cheng, T., Lin, P., Jin, S., Wu, Y., Fu, B., Long, R., Liu, D., Guo, Y., Peng, L., and Xia, Q. (2014). Complete Genome Sequence of Bacillus bombysepticus, a Pathogen Leading to Bombyx mori Black Chest Septicemia. Genome Announc. *2*, e00312-14-e00312-14.

Cherif-Antar, A., Moussa–Boudjemâa, B., Didouh, N., Medjahdi, K., Mayo, B., and Flórez, A.B. (2016). Diversity and biofilm-forming capability of bacteria recovered from stainless steel pipes of a milk-processing dairy plant. Dairy Sci. Technol. *96*, 27–38.

Choma, C., Guinebretière, M.H., Carlin, F., Schmitt, P., Velge, P., Granum, P.E., and Nguyen-The, C. (2000). Prevalence, characterization and growth of Bacillus cereus in commercial cooked chilled foods containing vegetables. J. Appl. Microbiol. *88*, 617–625.

Chou, Y.-L., Cheng, S.-N., Hsieh, K.-H., Wang, C.-C., Chen, S.-J., and Lo, W.-T. (2016). Bacillus cereus septicemia in a patient with acute lymphoblastic leukemia: A case report and review of the literature. J. Microbiol. Immunol. Infect. *49*, 448–451.

Comella, N., and Grossman, A.D. (2005). Conservation of genes and processes controlled by the quorum response in bacteria: characterization of

genes controlled by the quorum-sensing transcription factor ComA in Bacillus subtilis. Mol. Microbiol. *57*, 1159–1174.

Costa Oliveira, B.E., Cury, J.A., and Ricomini Filho, A.P. (2017). Biofilm extracellular polysaccharides degradation during starvation and enamel demineralization. PLOS ONE *12*, e0181168.

Cotton, D.J., Gill, V.J., Marshall, D.J., Gress, J., Thaler, M., and Pizzo, P.A. (1987). Clinical features and therapeutic interventions in 17 cases of Bacillus bacteremia in an immunosuppressed patient population. J. Clin. Microbiol. *25*, 672–674.

Cutting, S.M. (2011). Bacillus probiotics. Food Microbiol. *28*, 214–220.

Diehl, A., Roske, Y., Ball, L., Chowdhury, A., Hiller, M., Molière, N., Kramer, R., Stöppler, D., Worth, C.L., Schlegel, B., et al. (2018). Structural changes of TasA in biofilm formation of Bacillus subtilis. Proc. Natl. Acad. Sci. 201718102.

Dierick, K., Van Coillie, E., Swiecicka, I., Meyfroidt, G., Devlieger, H., Meulemans, A., Hoedemaekers, G., Fourie, L., Heyndrickx, M., and Mahillon, J. (2005). Fatal Family Outbreak of Bacillus cereus-Associated Food Poisoning. J. Clin. Microbiol. *43*, 4277–4279.

Dodd, C.E., Aldsworth, T.G., and Stein, R.A. (2017). Foodborne Diseases (Academic Press).

Doornbos, R.F., Loon, L.C. van, and Bakker, P.A.H.M. (2012). Impact of root exudates and plant defense signaling on bacterial communities in the rhizosphere. A review. Agron. Sustain. Dev. *32*, 227–243.

Dragoš, A., and Kovács, Á.T. (2017). The Peculiar Functions of the Bacterial Extracellular Matrix. Trends Microbiol. *25*, 257–266.

Driks, A. (1999). Bacillus subtilis spore coat. Microbiol. Mol. Biol. Rev. MMBR *63*, 1–20.

Drobniewski, F.A. (1993). Bacillus cereus and related species. Clin. Microbiol. Rev. *6*, 324–338.

Duanis-Assaf, D., Steinberg, D., Chai, Y., and Shemesh, M. (2016). The LuxS Based Quorum Sensing Governs Lactose Induced Biofilm Formation by Bacillus subtilis. Front. Microbiol. *6*.

Dubois, T., Faegri, K., Perchat, S., Lemy, C., Buisson, C., Nielsen-LeRoux, C., Gohar, M., Jacques, P., Ramarao, N., Kolstø, A.-B., et al. (2012). Necrotrophism is a quorum-sensing-regulated lifestyle in Bacillus thuringiensis. PLoS Pathog. *8*, e1002629.

Duc, L.H., Hong, H.A., Barbosa, T.M., Henriques, A.O., and Cutting, S.M. (2004). Characterization of Bacillus Probiotics Available for Human Use. Appl. Environ. Microbiol. *70*, 2161–2171.

Dueholm, M.S., Petersen, S.V., Sønderkær, M., Larsen, P., Christiansen, G., Hein, K.L., Enghild, J.J., Nielsen, J.L., Nielsen, K.L., Nielsen, P.H., et al. (2010). Functional amyloid in Pseudomonas. Mol. Microbiol. *77*, 1009–1020.

Ehling-Schulz, M., Vukov, N., Schulz, A., Shaheen, R., Andersson, M., Martlbauer, E., and Scherer, S. (2005). Identification and Partial Characterization of the Nonribosomal Peptide Synthetase Gene Responsible for Cereulide Production in Emetic Bacillus cereus. Appl. Environ. Microbiol. *71*, 105–113.

Ehling-Schulz, M., Fricker, M., Grallert, H., Rieck, P., Wagner, M., and Scherer, S. (2006). Cereulide synthetase gene cluster from emetic Bacillus cereus: Structure and location on a mega virulence plasmid related to Bacillus anthracis toxin plasmid pXO1. BMC Microbiol. *6*, 20.

Ezzell, null, and Welkos, null (1999). The capsule of bacillus anthracis, a review. J. Appl. Microbiol. *87*, 250.

Fagerlund, A., Dubois, T., Økstad, O.-A., Verplaetse, E., Gilois, N., Bennaceur, I., Perchat, S., Gominet, M., Aymerich, S., Kolstø, A.-B., et al. (2014). SinR Controls Enterotoxin Expression in Bacillus thuringiensis Biofilms. PLoS ONE *9*.

Feinberg, L., Jorgensen, J., Haselton, A., Pitt, A., Rudner, R., and Margulis, L. (1999). Arthromitus (Bacillus cereus) symbionts in the cockroach Blaberus

giganteus: dietary influences on bacterial development and population density. Symbiosis Phila. Pa *27*, 109–123.

Fiedoruk, K., Drewnowska, J.M., Daniluk, T., Leszczynska, K., Iwaniuk, P., and Swiecicka, I. (2017). Ribosomal background of the *Bacillus cereus* group thermotypes. Sci. Rep. *7*, 46430.

Flemming, H.-C., and Wingender, J. (2010). The biofilm matrix. Nat. Rev. Microbiol. *8*, 623–633.

Fowler, D.M., Koulov, A.V., Alory-Jost, C., Marks, M.S., Balch, W.E., and Kelly, J.W. (2006). Functional amyloid formation within mammalian tissue. PLoS Biol. *4*, e6.

Frankland, G.C., and Frankland, P.F. (1887). Studies on Some New Micro-Organisms Obtained from Air. Philos. Trans. R. Soc. B Biol. Sci. *178*, 257–287.

Fujita, M., and Losick, R. (2005). Evidence that entry into sporulation in Bacillus subtilis is governed by a gradual increase in the level and activity of the master regulator Spo0A. Genes Dev. *19*, 2236–2244.

Fujita, M., Gonzalez-Pastor, J.E., and Losick, R. (2005). High- and Low-Threshold Genes in the Spo0A Regulon of Bacillus subtilis. J. Bacteriol. *187*, 1357–1368.

Gallique, M., Decoin, V., Barbey, C., Rosay, T., Feuilloley, M.G.J., Orange, N., and Merieau, A. (2017). Contribution of the Pseudomonas fluorescens MFE01 Type VI Secretion System to Biofilm Formation. PLOS ONE *12*, e0170770.

Gao, T., Foulston, L., Chai, Y., Wang, Q., and Losick, R. (2015). Alternative modes of biofilm formation by plant-associated *Bacillus cereus*. MicrobiologyOpen *4*, 452–464.

Gélis-Jeanvoine, S., Canette, A., Gohar, M., Caradec, T., Lemy, C., Gominet, M., Jacques, P., Lereclus, D., and Slamti, L. (2017). Genetic and functional analyses of krs, a locus encoding kurstakin, a lipopeptide produced by Bacillus thuringiensis. Res. Microbiol. *168*, 356–368.

van Gestel, J., Vlamakis, H., and Kolter, R. (2015). From cell differentiation to cell collectives: Bacillus subtilis uses division of labor to migrate. PLoS Biol. *13*, e1002141.

Ghalib, A.K., Yasin, M., and Faisal, M. (2014). Characterization and Metal Detoxification Potential of Moderately Thermophilic Bacillus cereus from Geothermal Springs of Himalaya. Braz. Arch. Biol. Technol. *57*, 554–560.

Ghosh, A.C. (1978). Prevalence of Bacillus cereus in the faeces of healthy adults. J. Hyg. (Lond.) *80*, 233–236.

Ghosh, S., Korza, G., Maciejewski, M., and Setlow, P. (2015). Analysis of Metabolism in Dormant Spores of Bacillus Species by 31P Nuclear Magnetic Resonance Analysis of Low-Molecular-Weight Compounds. J. Bacteriol. *197*, 992–1001.

Glasset, B., Herbin, S., Guillier, L., Cadel-Six, S., Vignaud, M.-L., Grout, J., Pairaud, S., Michel, V., Hennekinne, J.-A., Ramarao, N., et al. (2016). *Bacillus cereus* -induced food-borne outbreaks in France, 2007 to 2014: epidemiology and genetic characterisation. Eurosurveillance *21*.

Goel, A.K. (2015). Anthrax: A disease of biowarfare and public health importance. World J. Clin. Cases WJCC *3*, 20–33.

Gohar, M., Faegri, K., Perchat, S., Ravnum, S., Økstad, O.A., Gominet, M., Kolstø, A.-B., and Lereclus, D. (2008). The PlcR Virulence Regulon of Bacillus cereus. PLoS ONE *3*, e2793.

Guinebretiere, M.-H., and Nguyen-The, C. (2003). Sources of Bacillus cereus contamination in a pasteurized zucchini purÃ©e processing line, differentiated by two PCR-based methods. FEMS Microbiol. Ecol. *43*, 207–215.

Guinebretiere, M.-H., Auger, S., Galleron, N., Contzen, M., De Sarrau, B., De Buyser, M.-L., Lamberet, G., Fagerlund, A., Granum, P.E., Lereclus, D., et al. (2013). Bacillus cytotoxicus sp. nov. is a novel thermotolerant species of the Bacillus cereus Group occasionally associated with food poisoning. Int. J. Syst. Evol. Microbiol. *63*, 31–40.

Gurler, N., Oksuz, L., Muftuoglu, M., Sargin, F., and Besisik, S. (2012). Bacillus Cereus Catheter Related Bloodstream Infection in a Patient with Acute Lymphoblastic Leukemia. Mediterr. J. Hematol. Infect. Dis. *4*.

Haichar, F. el Z., Marol, C., Berge, O., Rangel-Castro, J.I., Prosser, J.I., Balesdent, J., Heulin, T., and Achouak, W. (2008). Plant host habitat and root exudates shape soil bacterial community structure. ISME J. *2*, 1221–1230.

Hall-Stoodley, L., Costerton, J.W., and Stoodley, P. (2004). Bacterial biofilms: from the Natural environment to infectious diseases. Nat. Rev. Microbiol. *2*, 95–108.

Halpern, M., Raats, D., and Lev-Yadun, S. (2007). The Potential Anti-Herbivory Role of Microorganisms on Plant Thorns. Plant Signal. Behav. *2*, 503–504.

Helgason, E., Okstad, O.A., Caugant, D.A., Johansen, H.A., Fouet, A., Mock, M., Hegna, I., and Kolstø, A.B. (2000). Bacillus anthracis, Bacillus cereus, and Bacillus thuringiensis--one species on the basis of genetic evidence. Appl. Environ. Microbiol. *66*, 2627–2630.

Hernandes, R.T., De la Cruz, M.A., Yamamoto, D., Girón, J.A., and Gomes, T.A.T. (2013). Dissection of the Role of Pili and Type 2 and 3 Secretion Systems in Adherence and Biofilm Formation of an Atypical Enteropathogenic Escherichia coli Strain. Infect. Immun. *81*, 3793–3802.

Higgins, D., and Dworkin, J. (2012). Recent progress in Bacillus subtilis sporulation. FEMS Microbiol. Rev. *36*, 131–148.

Hilliard, N.J., Schelonka, R.L., and Waites, K.B. (2003). Bacillus cereus Bacteremia in a Preterm Neonate. J. Clin. Microbiol. *41*, 3441–3444.

Hobley, L., Ostrowski, A., Rao, F.V., Bromley, K.M., Porter, M., Prescott, A.R., MacPhee, C.E., van Aalten, D.M.F., and Stanley-Wall, N.R. (2013). BslA is a self-assembling bacterial hydrophobin that coats the Bacillus subtilis biofilm. Proc. Natl. Acad. Sci. U. S. A. *110*, 13600–13605.

Homma, H., and Shinohara, T. (2004). Effects of probiotic Bacillus cereus toyoi on abdominal fat accumulation in the Japanese quail (Coturnix japonica). Anim. Sci. J. *75*, 37–41.

Houry, A., Briandet, R., Aymerich, S., and Gohar, M. (2010). Involvement of motility and flagella in Bacillus cereus biofilm formation. Microbiology *156*, 1009–1018.

Houry, A., Gohar, M., Deschamps, J., Tischenko, E., Aymerich, S., Gruss, A., and Briandet, R. (2012). Bacterial swimmers that infiltrate and take over the biofilm matrix. Proc. Natl. Acad. Sci. U. S. A. *109*, 13088–13093.

Hsueh, Y.-H., Somers, E.B., Lereclus, D., and Wong, A.C.L. (2006). Biofilm Formation by Bacillus cereus Is Influenced by PlcR, a Pleiotropic Regulator. Appl. Environ. Microbiol. *72*, 5089–5092.

Hu, H.-J., Chen, Y.-L., Wang, Y.-F., Tang, Y.-Y., Chen, S.-L., and Yan, S.-Z. (2017). Endophytic *Bacillus cereus* Effectively Controls *Meloidogyne incognita* on Tomato Plants Through Rapid Rhizosphere Occupation and Repellent Action. Plant Dis. *101*, 448–455.

Huang, C.-J., Zheng, P.-X., Ou, J.-Y., Lin, Y.-C., and Chen, C.-Y. (2017). Complete Genome Sequence of *Bacillus cereus* C1L, a Plant Growth-Promoting Rhizobacterium from the Rhizosphere of Formosa Lily in Taiwan. Genome Announc. *5*, e01290-17.

Hussain, A., Zia, K.M., Tabasum, S., Noreen, A., Ali, M., Iqbal, R., and Zuber, M. (2017). Blends and composites of exopolysaccharides; properties and applications: A review. Int. J. Biol. Macromol. *94*, 10–27.

Jayaraman, A., and Wood, T.K. (2008). Bacterial quorum sensing: signals, circuits, and implications for biofilms and disease. Annu. Rev. Biomed. Eng. *10*, 145–167.

Jiang, M., Shao, W., Perego, M., and Hoch, J.A. (2000). Multiple histidine kinases regulate entry into stationary phase and sporulation in Bacillus subtilis. Mol. Microbiol. *38*, 535–542.

Jiménez, G., Urdiain, M., Cifuentes, A., López-López, A., Blanch, A.R., Tamames, J., Kämpfer, P., Kolstø, A.-B., Ramón, D., Martínez, J.F., et al. (2013). Description of Bacillus toyonensis sp. nov., a novel species of the Bacillus cereus group, and pairwise genome comparisons of the species of the group by means of ANI calculations. Syst. Appl. Microbiol. *36*, 383–391.

Jung, M.Y., Kim, J.-S., Paek, W.K., Lim, J., Lee, H., Kim, P.I., Ma, J.Y., Kim, W., and Chang, Y.-H. (2011). Bacillus manliponensis sp. nov., a new member of the Bacillus cereus group isolated from foreshore tidal flat sediment. J. Microbiol. *49*, 1027–1032.

Kamar, R., Gohar, M., Jéhanno, I., Réjasse, A., Kallassy, M., Lereclus, D., Sanchis, V., and Ramarao, N. (2013). Pathogenic Potential of Bacillus cereus Strains as Revealed by Phenotypic Analysis. J. Clin. Microbiol. *51*, 320–323.

Kang, C.-H., Kwon, Y.-J., and So, J.-S. (2016). Bioremediation of heavy metals by using bacterial mixtures. Ecol. Eng. *89*, 64–69.

Kearns, D.B. (2008). Division of labour during Bacillus subtilis biofilm formation. Mol. Microbiol. *67*, 229–231.

Kearns, D.B., Chu, F., Branda, S.S., Kolter, R., and Losick, R. (2005). A master regulator for biofilm formation by Bacillus subtilis. Mol. Microbiol. *55*, 739–749.

Kechagia, M., Basoulis, D., Konstantopoulou, S., Dimitriadi, D., Gyftopoulou, K., Skarmoutsou, N., and Fakiri, E.M. (2013). Health Benefits of Probiotics: A Review. ISRN Nutr. *2013*.

Kim, H., Hahn, M., Grabowski, P., McPherson, D.C., Otte, M.M., Wang, R., Ferguson, C.C., Eichenberger, P., and Driks, A. (2006). The Bacillus subtilis spore coat protein interaction network. Mol. Microbiol. *59*, 487–502.

Kirov, S.M., Webb, J.S., O'may, C.Y., Reid, D.W., Woo, J.K.K., Rice, S.A., and Kjelleberg, S. (2007). Biofilm differentiation and dispersal in mucoid Pseudomonas aeruginosa isolates from patients with cystic fibrosis. Microbiol. Read. Engl. *153*, 3264–3274.

Kobayashi, K. (2007a). Bacillus subtilis Pellicle Formation Proceeds through Genetically Defined Morphological Changes. J. Bacteriol. *189*, 4920–4931.

Kobayashi, K. (2007b). Gradual activation of the response regulator DegU controls serial expression of genes for flagellum formation and biofilm formation in Bacillus subtilis. Mol. Microbiol. *66*, 395–409.

Kobayashi, K. (2008). SlrR/SlrA controls the initiation of biofilm formation in Bacillus subtilis. Mol. Microbiol. *69*, 1399–1410.

Koch, M.S., Ward, J.M., Levine, S.L., Baum, J.A., Vicini, J.L., and Hammond, B.G. (2015). The food and environmental safety of Bt crops. Front. Plant Sci. *6*.

Kolodkin-Gal, I., Elsholz, A.K.W., Muth, C., Girguis, P.R., Kolter, R., and Losick, R. (2013). Respiration control of multicellularity in Bacillus subtilis by a complex of the cytochrome chain with a membrane-embedded histidine kinase. Genes Dev. *27*, 887–899.

Kusama, Y., Honma, I., Masuda, M., Goto, H., and Onodera, S. (2015). *Bacillus cereus* Outbreak in Normal Neonates at Our Hospital. Jpn. J. Infect. Prev. Control *30*, 385–390.

Larsen, H.D., and Jørgensen, K. (1997). The occurrence of Bacillus cereus in Danish pasteurized milk. Int. J. Food Microbiol. *34*, 179–186.

Le Scanff, J., Mohammedi, I., Thiebaut, A., Martin, O., Argaud, L., and Robert, D. (2006). Necrotizing Gastritis due to Bacillus cereus in an Immunocompromised Patient. Infection *34*, 98–99.

LeDeaux, J.R., Yu, N., and Grossman, A.D. (1995). Different roles for KinA, KinB, and KinC in the initiation of sporulation in Bacillus subtilis. J. Bacteriol. *177*, 861–863.

Lee, K., Costerton, J.W., Ravel, J., Auerbach, R.K., Wagner, D.M., Keim, P., and Leid, J.G. (2007). Phenotypic and functional characterization of Bacillus anthracis biofilms. Microbiology *153*, 1693–1701.

Leyva-Illades, J.F., Setlow, B., Sarker, M.R., and Setlow, P. (2007). Effect of a Small, Acid-Soluble Spore Protein from Clostridium perfringens on the Resistance Properties of Bacillus subtilis Spores. J. Bacteriol. *189*, 7927–7931.

Li, S., Chen, Z., Qui, L., Wu, J., and Lai, Z. (2006). [Isolation and identification of Bacillus cereus strain Jp-A and its capability in phenol degradation]. Ying Yong Sheng Tai Xue Bao J. Appl. Ecol. *17*, 920–924.

Lin, S., Schraft, H., Odumeru, J.A., and Griffiths, M.W. (1998). Identification of contamination sources of Bacillus cereus in pasteurized milk. Int. J. Food Microbiol. *43*, 159–171.

Lindbäck, T., Mols, M., Basset, C., Granum, P.E., Kuipers, O.P., and Kovács, Á.T. (2012). CodY, a pleiotropic regulator, influences multicellular behaviour and efficient production of virulence factors in Bacillus cereus. Environ. Microbiol. *14*, 2233–2246.

Lindsay, D., Brözel, V.S., and von Holy, A. (2005). Spore formation in Bacillus subtilis biofilms. J. Food Prot. *68*, 860–865.

Liu, Y., Lai, Q., Göker, M., Meier-Kolthoff, J.P., Wang, M., Sun, Y., Wang, L., and Shao, Z. (2015). Genomic insights into the taxonomic status of the Bacillus cereus group. Sci. Rep. *5*.

Liu, Y.-H., Huang, C.-J., and Chen, C.-Y. (2008). Evidence of Induced Systemic Resistance Against *Botrytis elliptica* in Lily. Phytopathology *98*, 830–836.

Liu, Z.Y., Chen, X., Shi, Y., and Su, Z.C. (2011). Bacterial Degradation of Chlorpyrifos by *Bacillus cereus*. Adv. Mater. Res. *356–360*, 676–680.

López, D., Fischbach, M.A., Chu, F., Losick, R., and Kolter, R. (2009). Structurally diverse natural products that cause potassium leakage trigger multicellularity in Bacillus subtilis. Proc. Natl. Acad. Sci. U. S. A. *106*, 280–285.

López, D., Vlamakis, H., and Kolter, R. (2010). Biofilms. Cold Spring Harb. Perspect. Biol. *2*.

Magnussen, E.T., Vang, A.G., á Steig, T., and Gaini, S. (2016). Relapsing peritonitis with *Bacillus cereus* in a patient on continuous ambulatory peritoneal dialysis. BMJ Case Rep. bcr2015212619.

Mahler, H., Pasi, A., Kramer, J.M., Schulte, P., Scoging, A.C., Bär, W., and Krähenbühl, S. (1997). Fulminant Liver Failure in Association with the Emetic Toxin of *Bacillus cereus*. N. Engl. J. Med. *336*, 1142–1148.

Majed, R., Faille, C., Kallassy, M., and Gohar, M. (2016a). Bacillus cereus Biofilms—Same, Only Different. Front. Microbiol. *7*.

Majed, R., Faille, C., Kallassy, M., and Gohar, M. (2016b). Bacillus cereus Biofilms—Same, Only Different. Front. Microbiol. *7*.

Makarasen, A., Yoza, K., and Isobe, M. (2009). Higher structure of cereulide, an emetic toxin from Bacillus cereus, and special comparison with valinomycin, an antibiotic from Streptomyces fulvissimus. Chem. Asian J. *4*, 688–698.

Marxen, S., Stark, T.D., Frenzel, E., Rütschle, A., Lücking, G., Pürstinger, G., Pohl, E.E., Scherer, S., Ehling-Schulz, M., and Hofmann, T. (2015). Chemodiversity of cereulide, the emetic toxin of Bacillus cereus. Anal. Bioanal. Chem. *407*, 2439–2453.

McKenney, P.T., Driks, A., Eskandarian, H.A., Grabowski, P., Guberman, J., Wang, K.H., Gitai, Z., and Eichenberger, P. (2010). A distance-weighted interaction map reveals a previously uncharacterized layer of the Bacillus subtilis spore coat. Curr. Biol. CB *20*, 934–938.

McKenney, P.T., Driks, A., and Eichenberger, P. (2013). The Bacillus subtilis endospore: assembly and functions of the multilayered coat. Nat. Rev. Microbiol. *11*, 33–44.

McLean, J.S., Majors, P.D., Reardon, C.L., Bilskis, C.L., Reed, S.B., Romine, M.F., and Fredrickson, J.K. (2008). Investigations of structure and metabolism within Shewanella oneidensis MR-1 biofilms. J. Microbiol. Methods *74*, 47–56.

McLoon, A.L., Kolodkin-Gal, I., Rubinstein, S.M., Kolter, R., and Losick, R. (2011). Spatial Regulation of Histidine Kinases Governing Biofilm Formation in Bacillus subtilis. J. Bacteriol. *193*, 679–685.

Meng, M., Sun, W.Q., Geelhaar, L.A., Kumar, G., Patel, A.R., Payne, G.F., Speedie, M.K., and Stacy, J.R. (1995). Denitration of glycerol trinitrate by resting cells and cell extracts of Bacillus thuringiensis/cereus and Enterobacter agglomerans. Appl. Environ. Microbiol. *61*, 2548–2553.

Michelotti, F., and Bodansky, H.J. (2015). *Bacillus cereus* causing widespread necrotising skin infection in a diabetic person. Pract. Diabetes *32*, 169-170a.

Mikkelsen, H., Duck, Z., Lilley, K.S., and Welch, M. (2007). Interrelationships between Colonies, Biofilms, and Planktonic Cells of Pseudomonas aeruginosa. J. Bacteriol. *189*, 2411–2416.

Mikkola, R., Saris, N.E., Grigoriev, P.A., Andersson, M.A., and Salkinoja-Salonen, M.S. (1999). Ionophoretic properties and mitochondrial effects of cereulide: the emetic toxin of B. cereus. Eur. J. Biochem. *263*, 112–117.

Miller, J.M., Hair, J.G., Hebert, M., Hebert, L., Roberts, F.J., and Weyant, R.S. (1997). Fulminating bacteremia and pneumonia due to Bacillus cereus. J. Clin. Microbiol. *35*, 504–507.

Miller, R.A., Beno, S.M., Kent, D.J., Carroll, L.M., Martin, N.H., Boor, K.J., and Kovac, J. (2016). Bacillus wiedmannii sp. nov., a psychrotolerant and cytotoxic Bacillus cereus group species isolated from dairy foods and dairy environments. Int. J. Syst. Evol. Microbiol. *66*, 4744–4753.

Miller, R.A., Jian, J., Beno, S.M., Wiedmann, M., and Kovac, J. (2018). Intraclade Variability in Toxin Production and Cytotoxicity of Bacillus cereus Group Type Strains and Dairy-Associated Isolates. Appl. Environ. Microbiol. *84*.

Mock, M., and Mignot, T. (2003). Anthrax toxins and the host: a story of intimacy. Cell. Microbiol. *5*, 15–23.

Molle, V., Fujita, M., Jensen, S.T., Eichenberger, P., González-Pastor, J.E., Liu, J.S., and Losick, R. (2003). The Spo0A regulon of Bacillus subtilis. Mol. Microbiol. *50*, 1683–1701.

Moormeier, D.E., and Bayles, K.W. (2017). Staphylococcus aureus biofilm: a complex developmental organism. Mol. Microbiol. *104*, 365–376.

Mr, K., and Sd, A. (2017). Isolation of Marine Bacteria From Visakhapatnam Coast For Degradation of Oil. J. Bioremediation Biodegrad. *08*.

Nakamura, L.K. (1998). Bacillus pseudomycoides sp. nov. Int. J. Syst. Bacteriol. *48*, 1031–1035.

Nicholson, W.L., Munakata, N., Horneck, G., Melosh, H.J., and Setlow, P. (2000). Resistance of Bacillus endospores to extreme terrestrial and extraterrestrial environments. Microbiol. Mol. Biol. Rev. MMBR *64*, 548–572.

Niu, B., Paulson, J.N., Zheng, X., and Kolter, R. (2017). Simplified and representative bacterial community of maize roots. Proc. Natl. Acad. Sci. U. S. A. *114*, E2450–E2459.

Nwuche, C.O., Aoyagi, H., and Ogbonna, J.C. (2014). Treatment of Palm Oil Mill Effluent by a Microbial Consortium Developed from Compost Soils. Int. Sch. Res. Not. *2014*, 1–8.

Okinaka, R.T., and Keim, P. (2016). The Phylogeny of Bacillus cereus sensu lato. Microbiol. Spectr. *4*.

Okinaka, R.T., Cloud, K., Hampton, O., Hoffmaster, A.R., Hill, K.K., Keim, P., Koehler, T.M., Lamke, G., Kumano, S., Mahillon, J., et al. (1999). Sequence and organization of pXO1, the large Bacillus anthracis plasmid harboring the anthrax toxin genes. J. Bacteriol. *181*, 6509–6515.

Oliver-Kozup, H.A., Elliott, M., Bachert, B.A., Martin, K.H., Reid, S.D., Schwegler-Berry, D.E., Green, B.J., and Lukomski, S. (2011). The streptococcal collagen-like protein-1 (Scl1) is a significant determinant for biofilm formation by group A Streptococcus. BMC Microbiol. *11*, 262.

Ophir, T., and Gutnick, D.L. (1994). A role for exopolysaccharides in the protection of microorganisms from desiccation. Appl. Environ. Microbiol. *60*, 740–745.

Orell, A., Tripp, V., Aliaga-Tobar, V., Albers, S.-V., Maracaja-Coutinho, V., and Randau, L. (2018). A regulatory RNA is involved in RNA duplex formation and biofilm regulation in Sulfolobus acidocaldarius. Nucleic Acids Res. *46*, 4794–4806.

Patrick, C.C., Langston, C., and Baker, C.J. (1989). Bacillus species infections in neonates. Rev. Infect. Dis. *11*, 612–615.

Peterson, S.B., Dunn, A.K., Klimowicz, A.K., and Handelsman, J. (2006). Peptidoglycan from Bacillus cereus Mediates Commensalism with Rhizosphere Bacteria from the Cytophaga-Flavobacterium Group. Appl. Environ. Microbiol. *72*, 5421–5427.

Piepenbrink, K.H., and Sundberg, E.J. (2016). Motility and adhesion through type IV pili in Gram-positive bacteria. Biochem. Soc. Trans. *44*, 1659–1666.

Pinna, A., Sechi, L.A., Zanetti, S., Usai, D., Delogu, G., Cappuccinelli, P., and Carta, F. (2001). Bacillus cereus keratitis associated with contact lens wear. Ophthalmology *108*, 1830–1834.

Priest, F.G., Barker, M., Baillie, L.W.J., Holmes, E.C., and Maiden, M.C.J. (2004). Population structure and evolution of the Bacillus cereus group. J. Bacteriol. *186*, 7959–7970.

Priester, J.H., Olson, S.G., Webb, S.M., Neu, M.P., Hersman, L.E., and Holden, P.A. (2006). Enhanced Exopolymer Production and Chromium Stabilization in Pseudomonas putida Unsaturated Biofilms. Appl. Environ. Microbiol. *72*, 1988–1996.

Rasko, D.A., Altherr, M.R., Han, C.S., and Ravel, J. (2005). Genomics of the Bacillus cereus group of organisms. FEMS Microbiol. Rev. *29*, 303–329.

Renner, L.D., and Weibel, D.B. (2011). Physicochemical regulation of biofilm formation. MRS Bull. Mater. Res. Soc. *36*, 347–355.

Røder, H.L., Sørensen, S.J., and Burmølle, M. (2016). Studying Bacterial Multispecies Biofilms: Where to Start? Trends Microbiol. *24*, 503–513.

Romero, D., Aguilar, C., Losick, R., and Kolter, R. (2010a). Amyloid fibers provide structural integrity to Bacillus subtilis biofilms. Proc. Natl. Acad. Sci. *107*, 2230–2234.

Romero, D., Aguilar, C., Losick, R., and Kolter, R. (2010b). Amyloid fibers provide structural integrity to Bacillus subtilis biofilms. Proc. Natl. Acad. Sci. U. S. A. *107*, 2230–2234.

Rosas-García, N.M. (2009). Biopesticide production from Bacillus thuringiensis: an environmentally friendly alternative. Recent Pat. Biotechnol. *3*, 28–36.

Rubinstein, S.M., Kolodkin-Gal, I., McLoon, A., Chai, L., Kolter, R., Losick, R., and Weitz, D.A. (2012). Osmotic pressure can regulate matrix gene expression in Bacillus subtilis. Mol. Microbiol. *86*, 426–436.

Rutala, W.A., Saviteer, S.M., Thomann, C.A., and Wilson, M.B. (1986). Plaster-associated Bacillus cereus wound infection. A case report. Orthopedics *9*, 575–577.

Sada, A., Misago, N., Okawa, T., Narisawa, Y., Ide, S., Nagata, M., and Mitsumizo, S. (2009). Necrotizing fasciitis and myonecrosis “synergistic necrotizing cellulitis” caused by Bacillus cereus. J. Dermatol. *36*, 423–426.

Saleh, M., Al Nakib, M., Doloy, A., Jacqmin, S., Ghiglione, S., Verroust, N., Poyart, C., and Ozier, Y. (2012). Bacillus cereus, an unusual cause of fulminant liver failure: diagnosis may prevent liver transplantation. J. Med. Microbiol. *61*, 743–745.

Sasahara, T., Hayashi, S., Morisawa, Y., Sakihama, T., Yoshimura, A., and Hirai, Y. (2011). Bacillus cereus bacteremia outbreak due to contaminated hospital linens. Eur. J. Clin. Microbiol. Infect. Dis. *30*, 219–226.

Sastalla, I., Maltese, L.M., Pomerantseva, O.M., Pomerantsev, A.P., Keane-Myers, A., and Leppla, S.H. (2010). Activation of the latent PlcR regulon in Bacillus anthracis. Microbiology *156*, 2982–2993.

Schuch, R., Pelzek, A.J., Kan, S., and Fischetti, V.A. (2010). Prevalence of Bacillus anthracis-Like Organisms and Bacteriophages in the Intestinal Tract of the Earthworm Eisenia fetida. Appl. Environ. Microbiol. *76*, 2286–2294.

Schurr, M.J. (2013). Which Bacterial Biofilm Exopolysaccharide Is Preferred, Psl or Alginate? J. Bacteriol. *195*, 1623–1626.

Segev, E., Smith, Y., and Ben-Yehuda, S. (2012). RNA dynamics in aging bacterial spores. Cell *148*, 139–149.

Senesi, S., and Ghelardi, E. (2010). Production, Secretion and Biological Activity of Bacillus cereus Enterotoxins. Toxins *2*, 1690–1703.

Setlow, P. (2014). Germination of Spores of Bacillus Species: What We Know and Do Not Know. J. Bacteriol. *196*, 1297–1305.

Setlow, B., Sun, D., and Setlow, P. (1992). Interaction between DNA and alpha/beta-type small, acid-soluble spore proteins: a new class of DNA-binding protein. J. Bacteriol. *174*, 2312–2322.

Setlow, B., Atluri, S., Kitchel, R., Koziol-Dube, K., and Setlow, P. (2006). Role of Dipicolinic Acid in Resistance and Stability of Spores of Bacillus subtilis with or without DNA-Protective α/β-Type Small Acid-Soluble Proteins. J. Bacteriol. *188*, 3740–3747.

Shimoyama, Y., Umegaki, O., Ooi, Y., Agui, T., Kadono, N., and Minami, T. (2017). Bacillus cereus pneumonia in an immunocompetent patient: a case report. Ja Clin. Rep. *3*.

Silo-Suh, L.A., Lethbridge, B.J., Raffel, S.J., He, H., Clardy, J., and Handelsman, J. (1994). Biological activities of two fungistatic antibiotics produced by Bacillus cereus UW85. Appl. Environ. Microbiol. *60*, 2023–2030.

Slamti, L., Perchat, S., Gominet, M., Vilas-Boas, G., Fouet, A., Mock, M., Sanchis, V., Chaufaux, J., Gohar, M., and Lereclus, D. (2004). Distinct Mutations in PlcR Explain Why Some Strains of the Bacillus cereus Group Are Nonhemolytic. J. Bacteriol. *186*, 3531–3538.

Som Chaudhury, S., and Das Mukhopadhyay, C. (2018). Functional amyloids: interrelationship with other amyloids and therapeutic assessment to treat neurodegenerative diseases. Int. J. Neurosci. *128*, 449–463.

Spencer, R.C. (2003). Bacillus anthracis. J. Clin. Pathol. *56*, 182–187.

Stabb, E.V., Jacobson, L.M., and Handelsman, J. (1994). Zwittermicin A-producing strains of Bacillus cereus from diverse soils. Appl. Environ. Microbiol. *60*, 4404–4412.

Stanley, N.R., and Lazazzera, B.A. (2004). Environmental signals and regulatory pathways that influence biofilm formation. Mol. Microbiol. *52*, 917–924.

von Stetten, F., Mayr, R., and Scherer, S. (1999). Climatic influence on mesophilic Bacillus cereus and psychrotolerant Bacillus weihenstephanensis populations in tropical, temperate and alpine soil. Environ. Microbiol. *1*, 503–515.

Stevens, M.P., Elam, K., and Bearman, G. (2012). Meningitis due to Bacillus cereus: A case report and review of the literature. Can. J. Infect. Dis. Med. Microbiol. J. Can. Mal. Infect. Microbiol. Medicale *23*, e16-19.

Stewart, G.C. (2015). The Exosporium Layer of Bacterial Spores: a Connection to the Environment and the Infected Host. Microbiol. Mol. Biol. Rev. *79*, 437–457.

Stewart, P.S. (2002). Mechanisms of antibiotic resistance in bacterial biofilms. Int. J. Med. Microbiol. *292*, 107–113.

Su, L., Zhou, T., Zhou, L., Fang, X., Li, T., Wang, J., Guo, Y., Chang, D., Wang, Y., Li, D., et al. (2012). Draft Genome Sequence of Bacillus cereus Strain LCT-BC244. J. Bacteriol. *194*, 3549.

Sutherland, I.W. (2001). Biofilm exopolysaccharides: a strong and sticky framework. Microbiology *147*, 3–9.

Swiecicka, I., and Mahillon, J. (2006). Diversity of commensal Bacillus cereus sensu lato isolated from the common sow bug (Porcellio scaber, Isopoda):

Diversity of commensal Bacillus cereus isolated from the sow bug. FEMS Microbiol. Ecol. *56*, 132–140.

Syed, S., and Chinthala, P. (2015). Heavy Metal Detoxification by Different *Bacillus* Species Isolated from Solar Salterns. Scientifica *2015*, 1–8.

Teitzel, G.M., and Parsek, M.R. (2003). Heavy Metal Resistance of Biofilm and Planktonic Pseudomonas aeruginosa. Appl. Environ. Microbiol. *69*, 2313–2320.

Thomas, B.S., Bankowski, M.J., and Lau, W.K.K. (2012). Native Valve Bacillus cereus Endocarditis in a Non-Intravenous-Drug-Abusing Patient. J. Clin. Microbiol. *50*, 519–521.

Tompkins, D.S., Hudson, M.J., Smith, H.R., Eglin, R.P., Wheeler, J.G., Brett, M.M., Owen, R.J., Brazier, J.S., Cumberland, P., King, V., et al. (1999). A study of infectious intestinal disease in England: microbiological findings in cases and controls. Commun. Dis. Public Health *2*, 108–113.

Turk, B.E. (2007). Manipulation of host signalling pathways by anthrax toxins. Biochem. J. *402*, 405–417.

Turnbull, P.C., and Kramer, J.M. (1985). Intestinal carriage of Bacillus cereus: faecal isolation studies in three population groups. J. Hyg. (Lond.) *95*, 629–638.

Venir, E., Del Torre, M., Cunsolo, V., Saletti, R., Musetti, R., and Stecchini, M.L. (2014). Involvement of alanine racemase in germination of Bacillus cereus spores lacking an intact exosporium. Arch. Microbiol. *196*, 79–85.

Verplaetse, E., Slamti, L., Gohar, M., and Lereclus, D. (2015). Cell Differentiation in a Bacillus thuringiensis Population during Planktonic Growth, Biofilm Formation, and Host Infection. MBio *6*, e00138-00115.

Vilain, S., Luo, Y., Hildreth, M.B., and Brozel, V.S. (2006). Analysis of the Life Cycle of the Soil Saprophyte Bacillus cereus in Liquid Soil Extract and in Soil. Appl. Environ. Microbiol. *72*, 4970–4977.

Vilain, S., Pretorius, J.M., Theron, J., and Brozel, V.S. (2009). DNA as an Adhesin: Bacillus cereus Requires Extracellular DNA To Form Biofilms. Appl. Environ. Microbiol. *75*, 2861–2868.

Vlamakis, H., Chai, Y., Beauregard, P., Losick, R., and Kolter, R. (2013a). Sticking together: building a biofilm the Bacillus subtilis way. Nat. Rev. Microbiol. *11*, 157–168.

Vlamakis, H., Chai, Y., Beauregard, P., Losick, R., and Kolter, R. (2013b). Sticking together: building a biofilm the Bacillus subtilis way. Nat. Rev. Microbiol. *11*, 157–168.

Warth, A.D., and Strominger, J.L. (1969). Structure of the peptidoglycan of bacterial spores: occurrence of the lactam of muramic acid. Proc. Natl. Acad. Sci. U. S. A. *64*, 528–535.

Watnick, P., and Kolter, R. (2000). Biofilm, City of Microbes. J. Bacteriol. *182*, 2675–2679.

Wenzel, M., Schönig, I., Berchtold, M., Kämpfer, P., and König, H. (2002). Aerobic and facultatively anaerobic cellulolytic bacteria from the gut of the termite Zootermopsis angusticollis. J. Appl. Microbiol. *92*, 32–40.

Wilson, M.K., Vergis, J.M., Alem, F., Palmer, J.R., Keane-Myers, A.M., Brahmbhatt, T.N., Ventura, C.L., and O'Brien, A.D. (2011). Bacillus cereus G9241 Makes Anthrax Toxin and Capsule like Highly Virulent B. anthracis Ames but Behaves like Attenuated Toxigenic Nonencapsulated B. anthracis Sterne in Rabbits and Mice. Infect. Immun. *79*, 3012–3019.

Wozniak, D.J., Limoli, D.H., and Jones, C.J. (2015). Bacterial Extracellular Polysaccharides in Biofilm Formation and Function. In Microbial Biofilms, 2nd Edition, P.K. Mukherjee, M. Ghannoum, M. Whiteley, and M. Parsek, eds. (American Society of Microbiology), pp. 223–247.

Wright, W.F. (2016). Central Venous Access Device-Related *Bacillus Cereus* Endocarditis: A Case Report and Review of the Literature. Clin. Med. Res. *14*, 109–115.

Xu, Y.-B., Chen, M., Zhang, Y., Wang, M., Wang, Y., Huang, Q., Wang, X., and Wang, G. (2014). The phosphotransferase system gene *ptsI* in the endophytic bacterium *Bacillus cereus* is required for biofilm formation, colonization, and biocontrol against wheat sharp eyespot. FEMS Microbiol. Lett. *354*, 142–152.

Yoshida, K., Toyofuku, M., Obana, N., and Nomura, N. (2017). Biofilm formation by Paracoccus denitrificans requires a type I secretion system-dependent adhesin BapA. FEMS Microbiol. Lett. *364*.

Yu, Y., Yan, F., Chen, Y., Jin, C., Guo, J.-H., and Chai, Y. (2016). Poly-γ-Glutamic Acids Contribute to Biofilm Formation and Plant Root Colonization in Selected Environmental Isolates of Bacillus subtilis. Front. Microbiol. *7*.

Zafra, O., Lamprecht-Grandío, M., Figueras, C.G., and González-Pastor, J.E. (2012). Extracellular DNA Release by Undomesticated Bacillus subtilis Is Regulated by Early Competence. PLoS ONE *7*, e48716.

Zhao, Q., Wang, H., Zhu, Z., Song, Y., and Yu, H. (2015a). Effects of <i>Bacillus cereus</i> F-6 on Promoting Vanilla (<i>Vanilla planifolia</i> Andrews.) Plant Growth and Controlling Stem and Root Rot Disease. Agric. Sci. *06*, 1068–1078.

Zhao, X., Wang, Y., Shang, Q., Li, Y., Hao, H., Zhang, Y., Guo, Z., Yang, G., Xie, Z., and Wang, R. (2015b). Collagen-Like Proteins (ClpA, ClpB, ClpC, and ClpD) Are Required for Biofilm Formation and Adhesion to Plant Roots by Bacillus amyloliquefaciens FZB42. PLOS ONE *10*, e0117414.

Zheng, J., Guan, Z., Cao, S., Peng, D., Ruan, L., Jiang, D., and Sun, M. (2015). Plasmids are vectors for redundant chromosomal genes in the Bacillus cereus group. BMC Genomics *16*.

Zhu, K., Hölzel, C.S., Cui, Y., Mayer, R., Wang, Y., Dietrich, R., Didier, A., Bassitta, R., Märtlbauer, E., and Ding, S. (2016). Probiotic Bacillus cereus Strains, a Potential Risk for Public Health in China. Front. Microbiol. *7*.

Zimaro, T., Thomas, L., Marondedze, C., Sgro, G.G., Garofalo, C.G., Ficarra, F.A., Gehring, C., Ottado, J., and Gottig, N. (2014). The type III protein

secretion system contributes to Xanthomonas citri subsp. citri biofilm formation. BMC Microbiol. *14*, 96.

Zwick, M.E., Joseph, S.J., Didelot, X., Chen, P.E., Bishop-Lilly, K.A., Stewart, A.C., Willner, K., Nolan, N., Lentz, S., Thomason, M.K., et al. (2012). Genomic characterization of the Bacillus cereus sensu lato species: backdrop to the evolution of Bacillus anthracis. Genome Res. *22*, 1512–1524.

CHAPTER II

A GENOMIC REGION GOVERNING THE FORMATION OF ADHESIN FIBRES IN *B. cereus* BIOFILM.

Caro-Astorga, J., Pérez-García, A., de Vicente, A., and Romero, D.

Published in *Frontiers in microbiology* (2015).

DOI: 10.3389/fmicb.2014.00745

1. INTRODUCTION

A major food-safety problem in developing countries is the contamination of fresh, stored and packaged food by bacteria that decrease the shelf life of the product and cause human poisoning (Burnett and Beuchat, 2001). Consumption of raw vegetables and fruits, milk, eggs, mildly cooked rice or pasta is typically associated with the most common outbreaks of poisoning (Carlin et al., 2000;Kamga Wambo et al., 2011). The symptoms of food poisoning can be mild, such as vomiting and diarrhea, or more severe, such as bacteremia; in severe cases, it can cause death of the patients. Bacterial strains of *Escherichia coli*, *Salmonella*, *Enterococcus*, *Lysteria* and *Bacillus cereus* are recurrent etiological agents of poisoning outbreaks (Berger et al., 2010). Epidemiological studies of these outbreaks have revealed that product contamination occurs before the manufacturing step. Irrigation with wastewater and the use of natural plant strengtheners lead to contamination of vegetables by enteropathogenic *E. coli* and *Salmonella* strains (Berger et al., 2010) .

Several *B. cereus* strains are commonly observed as the etiological agents of poisoning outbreaks, severe bacteremia and septicemia (Bottone, 2010). *B. cereus*, a naturally inhabitant of soils, is frequently isolated from fresh vegetables and ready-to-eat vegetable-based food and is implicated in outbreaks of gastrointestinal diseases, abdominal pains, and watery diarrhea (Elhariry, 2011). *B. cereus* causes two main types of poisoning: emetic and diarrheic. Emetic poisoning is associated with production of cereulide, a lipophilic toxin. This toxin is extremely

heat stable, and it can be produced in food contaminated by *B. cereus* cells. Notably, cereulide may persist in the body for a long period, affecting different organs and eventually leading to patient death (Thorsen et al., 2011). Diarrheic poisoning is caused by another group of toxic molecules: enterotoxin Hemolysin BL (HBL), the non-hemolytic enterotoxin (NHE) and cytotoxin (CytK). However, the specific role of each toxin in symptom development has not been elucidated. NHE and CytK are individually sufficient to induce diarrhea; however, it is not known whether HBL acts similarly. Similar to cereulide, HBL, NHE and CytK can be produced in food contaminated with *B. cereus* cells; however, the sensitivity of these toxins to low pH and digestive proteases prevents the development of diarrheic symptoms. Therefore, poisoning occurs due to enterotoxin production in the small intestine by *B. cereus* cells or spores that have been ingested (McKillip, 2000).

Colonization and persistence of *B. cereus* cells in fresh vegetables and fruits are required for intoxication. *B. cereus* produces spores highly resistant to stressful environments and are able to survive heat, dry conditions, sanitation procedures, and food-processing treatments; and also aggregates in bacterial communities called biofilms (Ball et al., 2008;Shaheen et al., 2010;Elhariry, 2011). Studies on the related bacterial species *B. subtilis* revealed that biofilms are natural reservoirs of spores and are as recalcitrant as spores to eradication therapies (Branda et al., 2005). Biofilm formation requires i) a complex regulatory pathway that coordinates gene expression with external environmental conditions and ii) structural components involved in the assembly of a protective extracellular matrix (Romero, 2013;Vlamakis et al., 2013). In

B. subtilis, the extracellular matrix is composed of exopolysaccharides, the hydrophobin protein BlsA and the amyloid-like protein TasA (Branda et al., 2004;Romero et al., 2010;Kobayashi and Iwano, 2012;Hobley et al., 2013;Romero, 2013). Studies on bacterial ecology have focused on amyloid proteins because: i) they retain the morphological and biochemical features of their pathogenic siblings in humans (Fowler et al., 2007), ii) they are involved in multiple functions relevant to bacterial physiology and ecology (Chapman et al., 2002;Epstein and Chapman, 2008;de Jong et al., 2009;Dueholm et al., 2010;Romero et al., 2010;Schwartz et al., 2012), and iii) they undergo a complex program leading to fibrillation (Blanco et al., 2012). In *B. subtilis* biofilms, TasA amyloid-like fibers constitute the protein skeleton that directs the assembly of the extracellular matrix (Romero et al., 2010).

Although biofilm formation has been studied in detail in *B. subtilis*, not much is known about this developmental program in *B. cereus*. Separate studies revealed that specific *B. cereus* elements are involved in biofilm formation: notably, *sinR* and *sinI*, *spo0A* or *abrB*, major regulators controlling the developmental program ending in biofilm formation of *B. subtilis* has also been demonstrated to play similar roles in biofilm formation of *B. cereus*. The SinR regulon in a strain of *B. thuringiensis* closely related to *B. cereus* contains the loci *sipw-tasA,* as it does in *B. subtilis,* but also the lipopeptide kurstakin, important for biofilm formation (Pflughoeft et al., 2011;Fagerlund et al., 2014). In addition, *B. cereus* appears to form wrinkly colonies and cell bundles in response to glycerol, manganese or milk, and this is proposed to be mediated by the kinase KinD as seen in *B. subtlitis* (Shemesh and Chai,

2013;Pasvolsky et al., 2014). Other two major regulators of *B. cereus* with involvement in biofilm are PlcR, the main virulence regulator, and CodY, a represor of branched aminoacids, which points towards the inevitable connection of virulence with biofilm formation in this bacteria species (Hsueh et al., 2006;Lindback et al., 2012). Besides this knolowledge on the biofilm-dedicated regulatory pathways, other studies have revealed the relevance on motility on adhesion to abiotic surfaces, or the presence of extracellular DNA and other uncharacterized proteins or polysaccharides in the extracellular matrix of biofilms of *B. cereus* (Auger et al., 2009;Vilain et al., 2009;Houry et al., 2010;Karunakaran and Biggs, 2011).

Because amyloid-like fibers are important for biofilm formation in diverse bacterial species, we examined the role of a genomic region encoding two orthologues, TasA and CalY, of the *B. subtilis* TasA amyloid-like protein in biofilm formation by *B. cereus*. Using mutagenesis analysis, we revealed that this region is important for biofilm assembly in *B. cereus* CECT148. Electron microscopy analysis revealed the presence of TasA fibers on the *B. cereus* cell surfaces, similar to those formed by *B. subtilis* TasA. Furthermore, by heterologous expression of *B. cereus* alleles in *B. subtilis* mutants lacking different components required for amyloid-like fiber assembly, we observed that *B. cereus* TasA functions similar to the endogenous *B. subtilis* TasA protein: i) it is involved in the formation of wrinkles in the air-liquid interphase pellicle, a visual feature of mature biofilms, ii) the pellicles are positively stained with the amyloid-specific dye Congo Red and iii) abundant and robust fibers are assembled on cell surfaces.

2. RESULTS

1. *B. cereus* encodes two orthologues of the *B. subtilis* amyloid-like protein TasA

B. subtilis biofilms are mainly composed of exopolysaccharides and the protein TasA. TasA can polymerize to form fibers that are morphologically and biochemically similar to amyloid proteins (Romero et al., 2010). A specific chromosomal region in *B. cereus* is similar to that of *B. subtilis* implicated in biofilm formation; this region encodes an orthologue of *sipW* and two orthologues of *tasA* (*tasA* and *calY*) (Fig. 1A). In *B. subtilis*, the genes *tapA, sipW* and *tasA* constitute an operon ($tapA_{op}$) and we proposed that this organization is conserved in *B. cereus*. To test this hypothesis, we extracted RNA from a 24-h culture of *B. cereus* and performed RT-PCR analysis using primers specific to each gene; we examined the expression of these genes to test whether they were transcribed together. We observed that *sipW* and *tasA* constitute an operon; the locus *bc_1280* was not expressed under our experimental conditions, and *calY* was expressed independently (Fig. 1B).

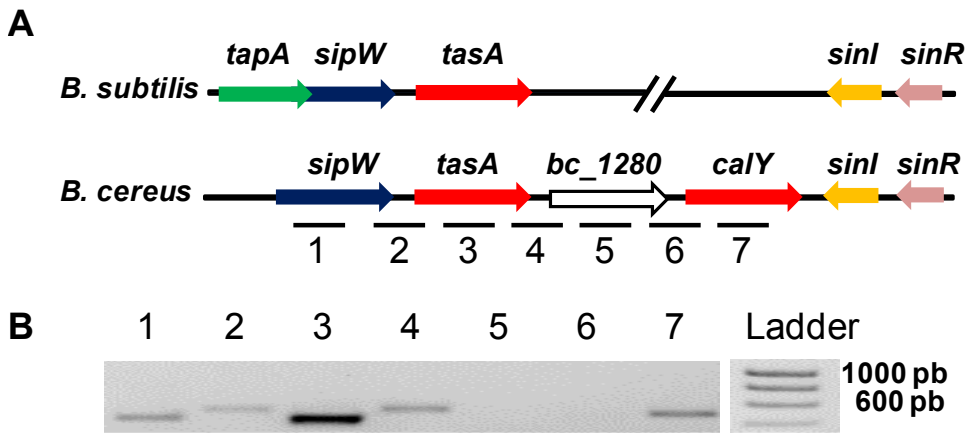

Figure 1. *Bacillus cereus* has genes orthologous to *B. subtilis* genes, which are required for the formation of amyloid-like fibers. A) Comparison of the *B. subtilis* and *B. cereus* genomic regions required for biofilm formation. The *tapA* operon ($tapA_{op}$) is involved in the formation of TasA amyloid-like fibers; TapA (accessory protein for biofilm formation); SipW (signal peptidase that processes immature TapA and TasA); TasA (the major subunit of the amyloid-like fibers). SinR is a negative regulator of the $tapA_{op}$, and SinI antagonizes SinR. The *B. cereus* genomic region contains genes orthologous to *tasA* (*tasA and calY*), *sipW*, *sinI* and *sinR* of *B. subtilis*, but lack *tapA*. B) RT-PCR analysis of RNA purified from a 24 h *B. cereus* culture reveals that *sipW* and *tasA* are co-transcribed but not *bc_1280* or *calY*.

2. SipW-TasA and CalY are involved in *B. cereus* biofilm formation

Because $tapA_{op}$ is important for the assembly of biofilms in *B. subtilis*, we examined the role of *sipW-tasA* and *calY* in *B. cereus* biofilm formation. Biofilms were visualized by performing crystal violet staining on the biomass adhered to well surfaces (Fig. 2). After 24 h of growth, wild-type cells formed visible rings, which grew in thickness up to 72 h.

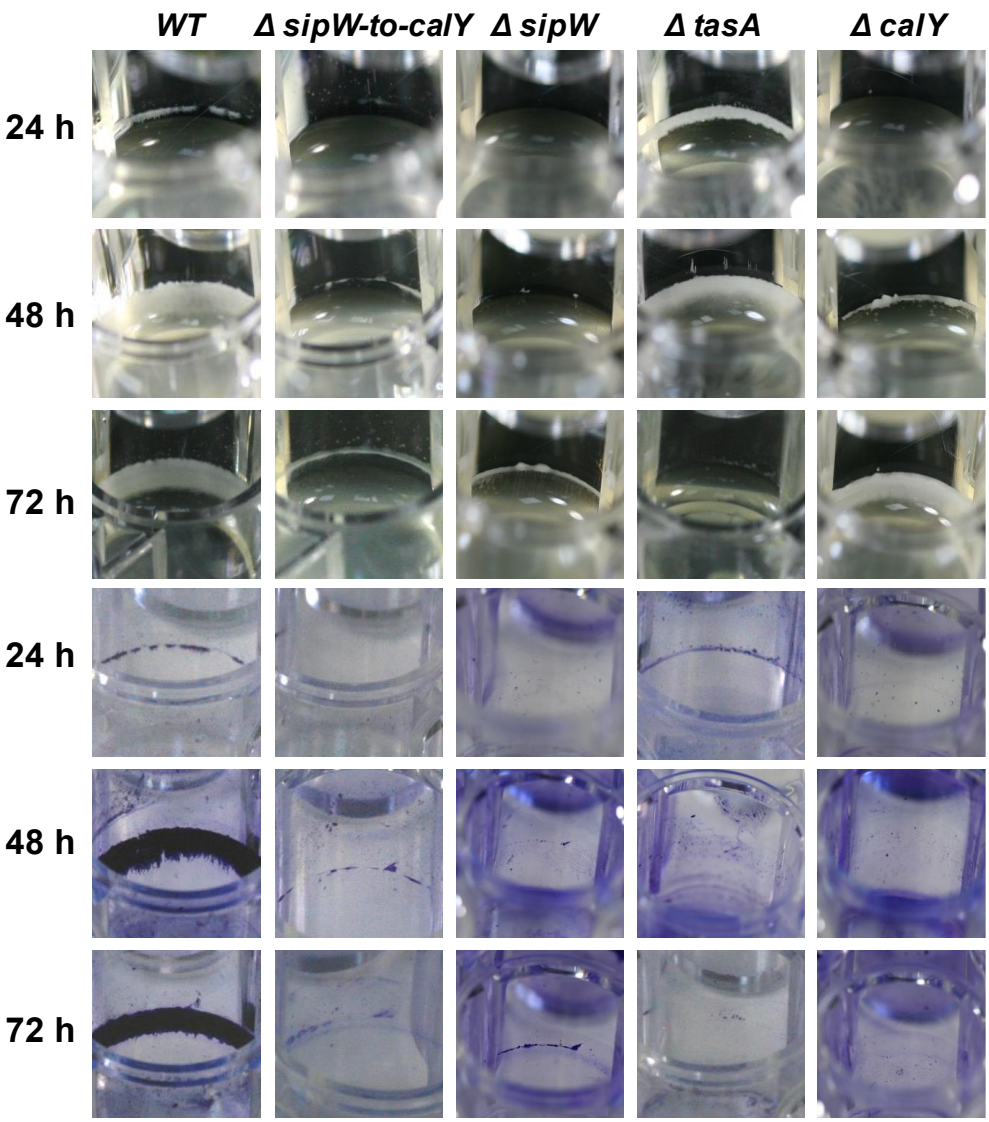

Figure 2. *sipW-tasA* and *calY* play complementary roles in *B. cereus* biofilm formation. Biofilms of *B. cereus* wild type and mutant cells were visualized as rings of biomass adhered to the wells in TY broth at 30ºC without agitation. The biomass-related rings were photographed after and before staining with crystal violet.

At all these stages, the rings of adhered biomass were significantly stained with crystal violet. Deletion of the *sipW-to-calY* region prevented the formation of similar biomass rings; a mutation in *sipW* caused the same phenotype. SipW is a signal peptidase involved in TasA processing, which facilitates efficient secretion of TasA from *B. subtilis* cells (Stover and Driks, 1999b); mutation of *sipW* eliminated biofilm formation ability. Notably, deletion of *tasA* conferred an unexpected phenotype: compared to the wild type strain, a thicker biomass ring was observed in the *tasA* deletion strain at 24 h, which disappeared at 72 h. Upon staining with crystal violet, the biomass was extruded from the wells at each stage. Deletion of *calY* caused a different phenotype: the biomass adhered to the wells was thicker after 72 h of growth; however, similar to the phenotype of the *tasA* mutant, the biomass did not bind tightly to the wells upon crystal violet staining. These observations revealed that this region is important for biofilm formation in *B. cereus* and that *tasA* and *calY* potentially cooperate at different stages of biofilm formation, including initial attachment and maturation.

3. TasA and CalY form morphologically different fibers in *B. cereus* biofilms

The formation of amyloid-like fibers in *B. subtilis* requires the function of two proteins, TasA and the accessory protein TapA (Romero et al., 2014). Bioinformatics analysis revealed that at the amino acid level, TasA and CalY share only 31% and 32% identity to *B. subtilis tasA*, respectively, but share 61% identity with each other. Based on these

observations and the absence of a TapA ortholog in *B. cereus*, we proposed that TasA and CalY do not form fibers. To test this hypothesis, we use transmission electron microscopy to analyze *B. cereus* biomass adhered to wells (Fig. 3, top row).

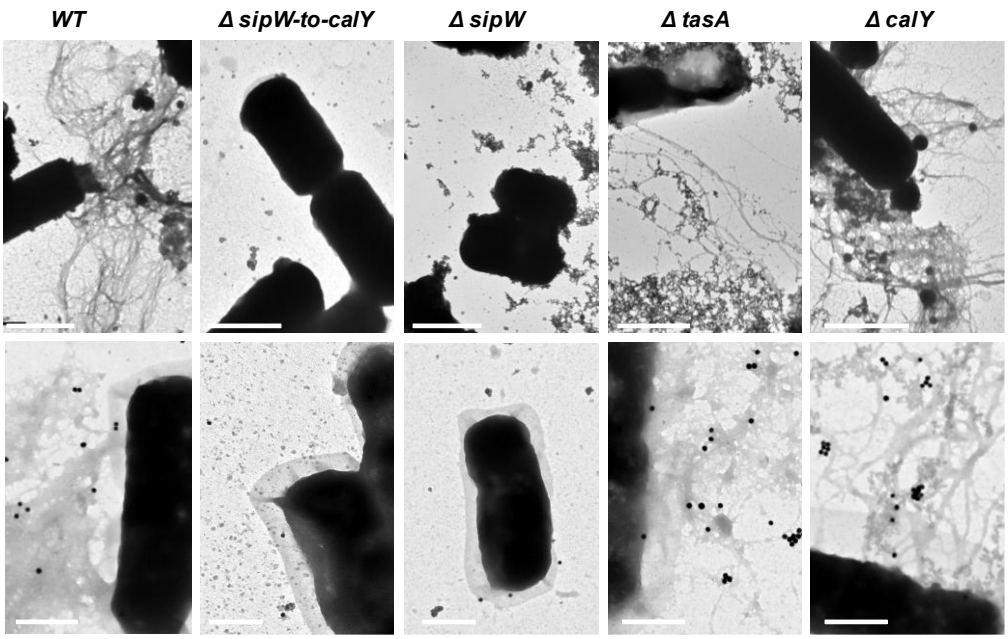

Figure 3. TasA and CalY form morphologically distinct fibers in *B. cereus*. Biomass rings of *B. cereus* strains were isolated after 24 h of growth, contrasted with uranyl acetate and analyzed using transmission electron microscopy (top row), or immunolabeled with primary anti-TasA antibodies (1:150) and secondary antibody conjugated to 40 nm gold particles (1:50) before contrasting with uranyl acetate and visualization (Bottom). Bars equal 1□m (top row images) or 0.5 mm (bottom row images).

Contrary to our hypothesis, *B. cereus* cells appeared highly decorated with fibers; however, cells with a deletion of this genomic region (*ΔsipW-to-calY*) or a mutation in (*sipW*) *ΔsipW* did not form fibers. Consistent with our previous biofilm experiments (Fig. 2), cells of the single *ΔtasA* mutant, which expressed CalY, produced thin and less abundant fibrils compared to the wild type. However, *ΔcalY* mutant cells, which expressed TasA, formed abundant fibers on their surfaces, similar to the wild type. To confirm that TasA or CalY formed fibers, we performed immunoelectron microscopy using anti-TasA antibodies raised against *B. subtilis* TasA (Fig. 3, bottom row). The cross immunoreaction of *B. cereus* TasA with anti-TasA antibodies of *B. subtilis* was previously demonstrated (Pflughoeft et al., 2011). The fibers observed in wild type, *ΔtasA* and *ΔcalY B. cereus* cells immunoreacted with the anti-TasA antibodies; however, no signal was observed in *ΔsipW-to-calY* or *ΔsipW* mutant cells.

Because *B. cereus* TasA forms fibers similar to *B. subtilis* TasA, we proposed that *B. cereus* biofilms would bind to amyloid dyes such as Congo Red. We performed biofilm experiments in 4.5-mm-diameter plates containing TY supplemented with Congo Red (Fig. 4). Similar to the experiments performed with microtiter plates, no pellicles were observed during the initial stages of growth; however, after 5 days, a thin pellicle was visible in the *B. cereus* wild-type and *ΔcalY* strains but not in *ΔsipW-to-calY*, *ΔsipW* or *ΔtasA* mutants. When the medium was removed, the remaining pellicle appeared stained with Congo Red. These observations suggested that i) TasA fibers are more important than CalY fibers for producing pellicles in the air-liquid interphase and

ii) *B. cereus* TasA fibers stain similarly to TasA amyloid-like fibers of *B. subtilis*.

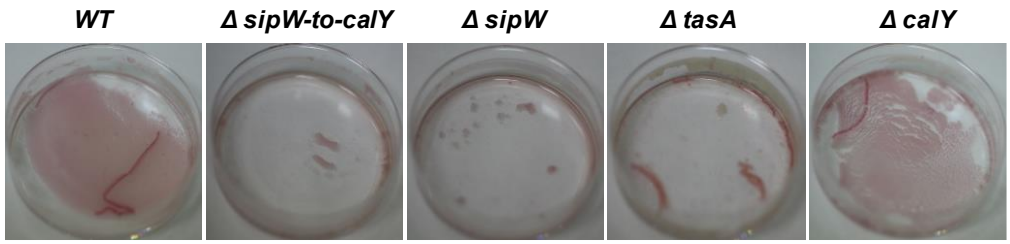

Figure 4. Thin pellicles of *B. cereus* containing TasA bind the amyloid dye Congo Red. Biofilms *of B. cereus* were grown in 4.5 mm diameter plates containing TY supplemented with a solution of Congo Red (20 □g/mL) and Coomassie Brilliant Blue G (10 □g/mL) for 5 days at 30ºC. Top view pictures of pellicles after removing the spending medium.

4. Expression of the *B. cereus sipW-to-calY* region rescues pellicle formation in *B. subtilis*

Our results suggested that the *sipW-tasA* and *calY* are involved in *B. cereus* biofilm formation and that TasA is important for assembly of pellicles in the air-liquid interphase. Therefore, we proposed that *B. cereus* TasA might functionally replace *B. subtilis* TasA. *B. subtilis* forms wrinkly pellicles in the air-liquid interphase; this property facilitates identification of mutants that disrupt assembly of the normal architecture. In *B. subtilis*, deletion of TasA leads to a defect in assembling wrinkly pellicles (Branda et al., 2006). Therefore, we performed heterologous expression of the respective *B. cereus* loci (referred to as $allele_{Bc}$) in *B. subtilis* and examined the pellicle

phenotype (Fig. 5) and the adhesion to abiotic surfaces (Fig. 6). The constructs were ectopically integrated at the *amyE* or *lacA* locus of *B. subtilis*, and their expression was driven by an IPTG-inducible promoter to bypass any potential regulatory processes associated with their native promoters.

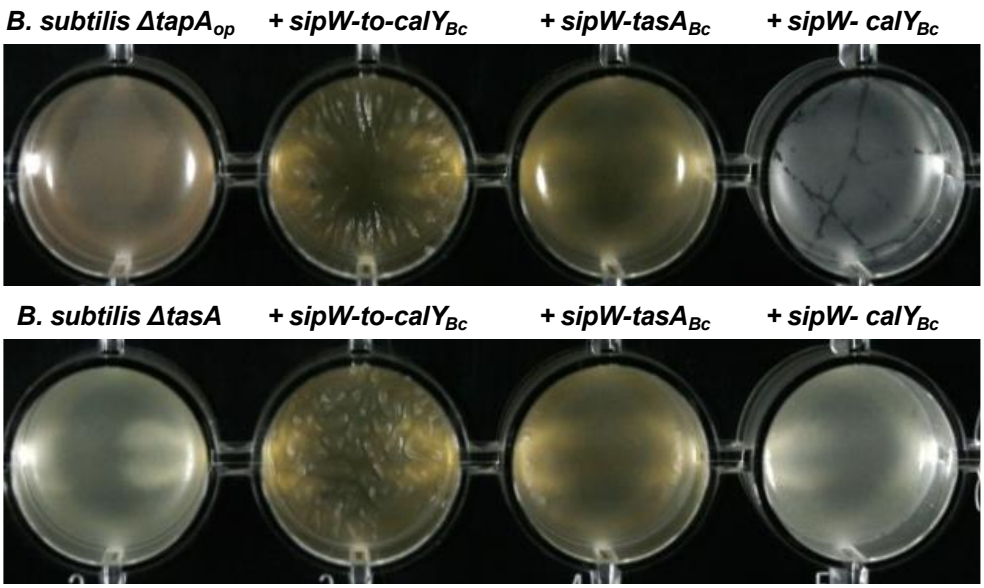

Figure 5. Heterologous expression of *B. cereus sipW-to-tasA* or *sipW-tasA* in *B. subtilis* rescues pellicle formation. Biofilm experiments were performed in static cultures in MSgg broth and induced with 1 mM IPTG in 24-well plates. Top view of pellicles were photographed after 48 h of incubation in MSgg broth at 30°C.

To examine the role of TasA in pellicle formation, we complemented a *B. subtilis* mutant lacking the *tapA* operon (*ΔtapA$_{op}$*) with the *B. cereus sipW*-to-*calY* chromosomal region (*sipW-to-calY$_{Bc}$*). As expected, this *B. cereus* construct rescued the formation of wrinkly pellicles, which

resembled wild-type *B. subtilis* pellicles (Fig. 5); furthermore, this construct notably enhanced the adhesion to the well surfaces in crystal violet assays (Fig. 6A, top row and 6B). Therefore, the *B. cereus sipW*-to-*calY* region is involved in pellicle formation. Next, we examined the specific roles of *tasA* and *calY* in pellicle formation. Expression of either *tasA* or *calY* failed to restore pellicle formation in the *B. subtilis tasA* mutant strain (*ΔtasA)* (Fig. Sup. 1, top and middle rows). We then tested whether these loci must be expressed with the cognate *sipW* gene of *B. cereus*. Expression of *sipW-tasA* in the *B. subtilis* Δ*tasA* mutant strain rescued pellicle formation (Fig. 5, bottom row) and adhesion to abiotic surfaces, although less efficiently that complementation with *sipW-to-calY* (Fig. 6A, bottom row and 6B). Notably, expression of the *sipW-calY* construct failed to restore pellicle formation (Fig. 5, bottom row) or bind to abiotic surfaces (Fig. 6A, bottom row and 6B). Because the *B. subtilis ΔtasA* mutant strain encodes the *tapA* gene, which is required to form pellicles in *B. subtilis* (Romero et al., 2011) we expressed *sipW-tasA* or *sipW-calY* in a *B. subtilis* strain lacking the entire operon $\Delta tapA_{op}$; this strategy eliminated expression of TapA, a protein with no ortholog in *B. cereus* but retained the native *sipW* gene. We observed that *sipW-calY* did not restore the wild-type phenotype (Fig. 5, top row; Fig. 6A, top row and 6B), and *sipW-tasA* complementation resulted in the formation of pellicles but not wrinkles (Fig. 5, top row) and restored adhesion to abiotic surfaces (Fig. 6A, top row and 6B).

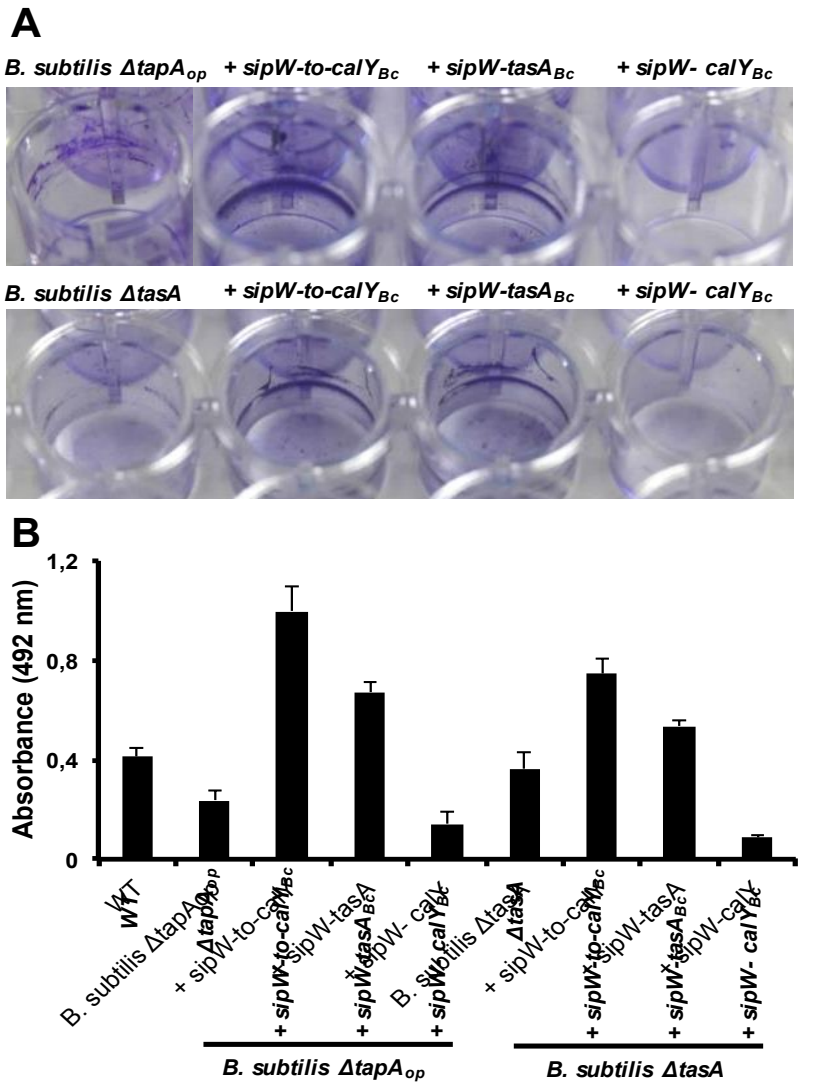

Figure 6. Heterologous expression of *B. cereus sipW-to-tasA* or *sipW-tasA* in *B. subtilis enhances adhesion to abiotic surfaces*. Biofilm experiments were performed in static cultures in MSgg broth and induced with 1 mM IPTG in 24-well plates. A) Adhesion to abiotic surfaces was examined by staining the cultures with Crystal Violet, and pictures were obtained after 48 h of incubation at 30°C. B) Quantification of the amount of crystal violet retained in bacterial biomass.

These results suggested that *B. subtilis tapA* might affect pellicle formation in the *B. subtilis ΔtasA* mutant complemented with *B. cereus sipW-tasA*. Therefore, we examined pellicle formation in a *B. subtilis ΔtapA* mutant strain complemented with the following *B. cereus* regions: *sipW-to-calY*, *sipW-tasA* or *sipW-calY* (Fig. Sup. 2, top and middle rows). We observed that expression of *sipW-to-calY* was required to restore formation of wrinkly pellicles and adhesion to abiotic surfaces. Expression of *sipW-tasA* partially rescued the mutant phenotype, but *sipW-calY* failed to restore any of these phenotypes. Together, these observations confirmed the intrinsic ability of the *B. cereus sipW-to-calY* region to form wrinkly pellicles in the surrogate host *B. subtilis*. Additionally, TasA and CalY might have complementary roles in this phenotype, but the function of TasA is predominant.

5. *B. cereus* TasA mimics the formation of amyloid-like fibers in *B. subtilis* biofilms

Two observations indicated that *B. cereus* TasA has amyloid-like properties: i) *B. cereus* cells contained polymerized fibers (Fig. 3), and ii) the thin pellicles in *B. cereus* cells expressing TasA were stained with Congo Red (Fig. 4). Based on these observations, we proposed that *B. cereus* TasA would display similar behavior and aggregate into amyloid-like fibers when expressed in the surrogate host *B. subtilis*. To test this hypothesis, we grew biofilms from mutant *B. subtilis* cells and cells complemented with different *B. cereus* loci; the cells were grown in TY medium supplemented with the amyloid-specific dye Congo Red (Fig.

7). As expected, the *B. subtilis ΔtapA$_{op}$* and *ΔtasA* mutants did not bind this dye. Staining with Congo Red was stronger in pellicles of *B. subtilis ΔtapA$_{op}$* mutant cells complemented with the entire *sipW-to-calY* region of *B. cereus* (Fig. 7, top row); a strain that, as described above, formed wrinkly pellicles (Fig. 5). The pellicles of *B. subtilis ΔtapA$_{op}$* strains expressing either *sipW-tasA* or *sipW-calY* were stained at low levels (Fig. 7, top row). Notably, complementation of the *B. subtilis ΔtasA* mutant strain with the *sipW-tasA* region or *sipW-to-calY* resulted in similar levels of Congo Red staining; however, complementation with the *sipW-calY* construct resulted in weaker staining (Fig. 7, bottom row).

These data were consistent with the results obtained on pellicle formation and suggested that *B. subtilis tapA* influences cellular staining properties. However, when these experiments were performed using a *B. subtilis ΔtapA* mutant strain, complementation with the entire *B. cereus sipW-to-calY* or *sipW-TasA* but not *sipW-calY* restored Congo Red binding (Fig. Sup. 2, bottom row).

To further examine the amyloid nature of *B. cereus* TasA and CalY, we studied fibrillation of TasA and CalY on the *B. subtilis* cell surfaces (Fig. 8). Transmission electron microscopy analysis revealed that *B. subtilis ΔtasA$_{op}$* and *ΔtasA* mutant cells contained no fibers. Consistent with other experiments *B. subtilis ΔtasA$_{op}$* cells complemented with the *B. cereus sipW-to-calY* or *sipW-tasA* loci appeared decorated with several fibers (Fig. 8, top row). However, complementation with *sipW-calY*,

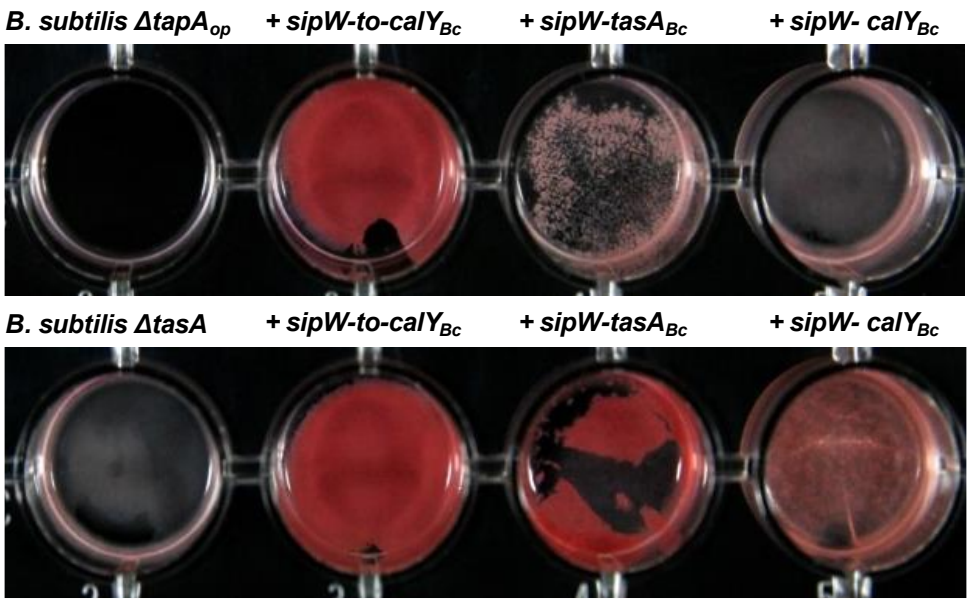

Figure 7. Pellicles of *B. subtilis* complemented with *sipW-to-tasA* or *sipW-tasA of B. cereus* stained with specific amyloid dye Congo Red. Biofilm experiments were performed in static cultures in Ty-Congo Red (20 µg/ml)-Coomassie Blue (20 µg/ml) broth and induced with 1 mM IPTG in 24-well plates. Top-view pictures of pellicles after 24 h of static growth at 30ºC.

which did not restore Congo Red binding, also failed to promote fiber formation (Fig. 8, top row). Expression of the entire *B. cereus sipW-to-calY* region or *sipW-tasA* resulted in the formation of abundant fibers on the surfaces of *B. subtilis ΔtasA* cells; however, expression of the *sipW-calY* promoted less abundant and thinner fibrils formation (Fig. 8, bottom row). Finally, in *B. subtilis ΔtapA* mutant; fibers were formed in *ΔtapA* cells complemented with the entire region or with *sipW-tasA* but not with *sipW-calY* (Fig. Sup. 3). These results indicated that i) the entire region of *B. cereus* drives the formation of fibers with amyloid properties

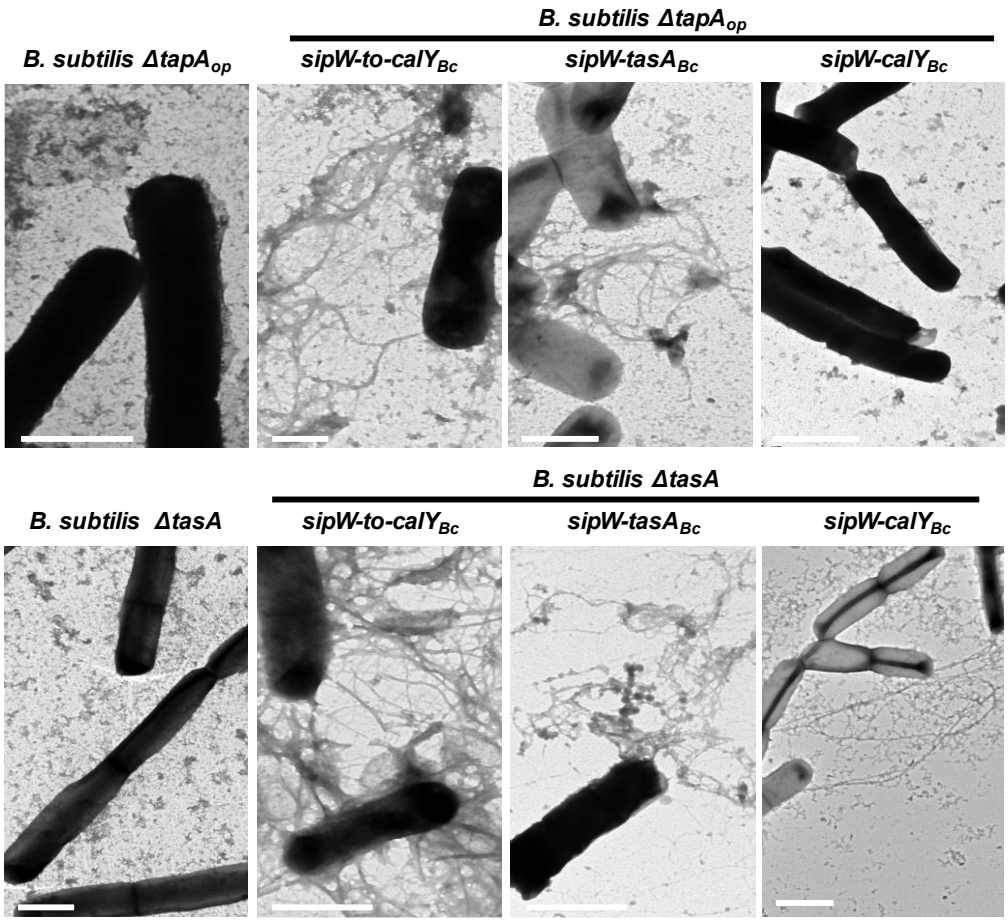

Figure 8. Expression of *B. cereus sipW-tasA* leads to fiber formation in *B. subtilis*. *B. cereus* alleles were ectopically integrated at the *lacA* or *amyE* locus of *B. subtilis* mutants lacking the entire *tapA* operon (*B. subtilis ΔtapA*$_{op}$) or lacking *tasA* alone (*B. subtilis ΔtasA*), and their expression was driven by an IPTG-inducible promoter. The strains were grown in MSgg broth and induced with 1 mM IPTG without shaking at 30ºC. Samples were collected after 12 h, contrasted using uranyl acetate and then analyzed using transmission electron microscopy. Scale bars = 1 µm.

similar to the *tapAop* of *B. subtilis* but does not require a *tapA* orthologue, ii) *B. cereus* TasA and at a lesser extent CalY polymerizes to form fibers similar to *B. subtilis* TasA, and iii) CalY complements the function of TasA in the formation of pellicles and fibers.

3. DISCUSSION

The bacterium *Bacillus cereus* is widely distributed in nature, and several species within this group inhabit soils, colonize arthropod guts or are pathogenic to humans (Bottone, 2010). The intrinsic factors contributing to this versatile ecological distribution include spore and biofilm formation (Auger et al., 2009;Elhariry, 2011). Spores are highly resistant to environmental stresses and are extremely adhesive, facilitating attachment to abiotic and biotic surfaces (Ball et al., 2008;Shaheen et al., 2010). Biofilms are considered to promote adhesion and protect cells from antimicrobials and other external insults and are thus difficult to eradicate (Flemming and Wingender, 2010). In this study, we examined the role of a specific genomic region in *B. cereus* biofilm formation.

Studies on biofilms of the phylogenetically related organism *B. subtilis* have elucidated both the genetic circuits that govern the biofilm developmental program and the structural components that facilitate assembly of the extracellular matrix (Romero, 2013;Vlamakis et al., 2013). The important matrix components of *B. subtilis* biofilms include exopolysaccharides, the hydrophobin BlsA and the amyloid-like protein TasA (Branda et al., 2004;Romero et al., 2010;Ostrowski et al., 2011). TasA, TapA and the signal peptidase SipW are especially important for correct assembly of the extracellular matrix. The studied *B. cereus* genomic region contains two TasA orthologs, TasA and CalY, and an ortholog of the signal peptidase SipW. However, this region lacks the accessory protein TapA. The fact that the expression of *sipW*, *tasA* and

calY of *B. cereus* are under control of the biofilm master regulator SinR (Fagerlund et al., 2014) led to think in their implication in biofilm formation, as the $tapA_{op}$ in *B. subtilis* (Chu et al., 2006), and our data are supportive of this hypothesis (Fig. 2). The divergent patterns of biofilm formation in *tasA* and calY mutants suggested that these proteins function in different stages of biofilm formation: CalY might be more important for initial attachment, and TasA might be required for further maturation. Indeed, pioneer studies demonstrated that CalY could be purified from *B. cereus* cells at mi-log phase of growth (Fricke et al., 2001). In the other hand, this observation is not unprecedented; the interplay of diverse factors in biofilm formation can be observed in other bacteria species. The Gram-negative bacterium *Pseudomonas putida* contains two protein adhesins, LapF and LapA, which are essential for the initiation and maturation of biofilms, respectively (Martinez-Gil et al., 2010). We further propose that CalY and TasA are required for cell-to-cell and cell-to-abiotic surface interactions. However, crystal violet staining and heterologous expression analyses in *B. subtilis* cells revealed that TasA might be more important for the interaction to abiotic surfaces (Fig. 6).

The *B. cereus tasA* mutant cells form an early biomass ring that is loosely bound to abiotic surfaces; therefore, other extracellular matrix components might be over-expressed. Two possible candidates are an exopolysaccharide or CalY. In *B. subtilis*, the absence of TasA increases the expression of the exopolysaccharide by an unknown regulatory pathway (Vlamakis et al., 2008), and a similar imbalance in

the expression of components of the extracellular matrix has been reported in *P. putida* mutants lacking its large adhesin proteins (Martinez-Gil et al., 2013). Consistent with this observation, pellicles of a *B. subtilis tasA* mutant were easy to disrupt and fluid; expression *of B. cereus sipW-tasA* suppressed these defects, and the pellicles resembled those of wild-type *B. subtilis* cells (Fig. 5), indicating that EPS levels might be restored. The genome of *B. cereus* contains a region (*BC_5267* to *BC_5278*) that highly resembles the operon dedicated to the synthesis of EPS in *B. subtilis*, but contrary to this bacteria species, the loci of *B. cereus* do not appear to be part of the *sinR* regulon (Fagerlund et al., 2014). Whether these or additional unknown factors of *B. cereus* are involved in biofilm formation needs to be clarified.

To build the extracellular matrix, *B. subtilis* TasA forms resistant fibers with amyloid properties. This process requires an accessory protein TapA, which contributes to the initiation and growth of TasA fibers (Romero et al., 2011; 2014). Our data from mutagenesis in *B. cereus* and heterologous expression in *B. subtilis* indicate that the *B. cereus sipW-to-calY* region contains all elements required for fiber assembly (Figs. 3 and Fig. 8). We propose that as previously described in *B. subtilis*, SipW functions as a signal peptidase that processes TasA and CalY to their mature forms for secretion (Tjalsma et al., 1998;Stover and Driks, 1999b;a). The rationale for this hypothesis is as follows: first, both proteins contain signal peptides with a canonical sequence that is a substrate for SipW proteolytic activity (Tjalsma et al., 1998;Terra et

al., 2012); second, a *sipW* mutant is completely defective for biofilm formation (Fig. 2); third, *B. cereus* TasA and CalY are not functional in *B. subtilis* unless they are co-expressed with the cognate SipW protein (Fig. 5 and Fig. Sup. 1). Our data suggest that *B. cereus* TasA is the more important for fiber formation than the other *B. subtilis*-TasA orthologous CalY. Abundant TasA fibers are present in wild-type and *calY* mutant *B. cereus* cells (Fig. 3). Furthermore, in heterologous expression experiments, *B. subtilis* mutants lacking *tapA* formed fibers using *B. cereus* TasA (Fig. 8). CalY has 62% identity with *B. cereus* TasA; CalY assembled into thin fibrils in *B. cereus* but failed to form fibers in *B. subtilis* unless TapA was present. One interpretation is that TapA of *B. subtilis* is able to cross seed the assembly of CalY fibers, a phenomenon recently reported in the assembly of the amyloid-like fiber Curli among *Eschirichia coli* and *Salmonella typhimurium* (Zhou et al., 2012).

Besides all our observations, we do not exclude the possibility that CalY has amyloid-like properties. Previous studies have shown that CalY is unusually resistant to SDS and heat treatments, and display high aggregative properties in organic solvent (Fricke et al., 2001); features associated with but not exclusive to amyloid proteins (Greenwald and Riek, 2010). The high sequence identity of CalY and TasA leads to the following mutually exclusive models: i) CalY and TasA cooperate to assemble robust and stable fibers with amyloid properties including binding Congo Red, as described among CsgA and CsgB in assembly of Curli in *E. coli* (Shu et al., 2012); ii) TasA and

CalY form fibers independently, but these two types of fibers are important for biofilm assembly during different environmental conditions. An example of the diversification of amyloid-like proteins is the Gram-positive bacterium *Streptomyces coelicolor*, which has up to eight different chaplin proteins with a propensity to assemble amyloid-like fibers; this suggests the existence of significant plasticity to ensure the completion of complex developmental programs (Di Berardo et al., 2008;Sawyer et al., 2011). Further biochemical and morphological analyses of purified TasA and CalY are required to elucidate their amyloid properties.

In summary, we identified a specific *B. cereus* genomic region, which contains two independent genetic factors, the two-gene operon *sipW-tasA* and the gene *calY*, which are both necessary for *B. cereus* biofilm formation. Directed mutagenesis in *B. cereus* and heterologous expression of the *B. cereus* alleles in *B. subtilis* revealed that TasA and, to a lesser extent, CalY have the intrinsic ability to polymerize and form fibers that are microscopically similar to the TasA amyloid-like fibers of *B. subtilis*. Finally, the Congo Red-binding ability of pellicles in TasA-expressing *B. cereus* cells and in *B. subtilis* cells complemented with *sipW-tasA* and CalY or only *sipW-tasA* point towards the amyloid nature of fibers formed by TasA.

5. METHODS AND MATERIAL

Bacterial strains and culture conditions

The bacteria used in this study are listed in Table 1. Bacteria were routinely grown in Ty broth (1% tryptone, OXOID), 0.5% yeast extract (OXOID), 0.5% NaCl, 10 mM $MgSO_4$, and 1 mM $MnSO_4$). Biofilm assays were performed either in TY or MSgg broth (100 mM morpholinopropanesulfonic acid (MOPS) (pH 7), 0.5% glycerol, 0.5% glutamate, 5 mM potassium phosphate (pH 7), 50 µg/ml tryptophan, 50 µg/ml phenylalanine, 2 mM $MgCl_2$, 700 µM $CaCl_2$, 50 µM FeCl3, 50 µM $MnCl_2$, 2 µM thiamine, and 1 µM $ZnCl_2$) {Branda, 2001 #179}. Antibiotics were used when required at the following concentrations (final): MLS, 1 µg/ml erythromycin, 25 µg/ml lincomycin, spectinomycin 100 µg/ml, chloramphenicol 5 µg/ml, and kanamycin 10 µg/ml.

RNA purification and RT-PCR

A 3 ml culture of *B. cerues* CECT158 in LB was growth without agitation at 30°C. After 24 h, the tube was vortexed to resuspend the ring of biomass adhered to the wells of the tube and centrifuged at 7000 g 1 min to collect cells. The cells were washed and lysed in BirnBoim A solution (10% sucrose; 10mM TrisHCl, pH8.1; 10mM EDTA; 50 mM NaCl), supplemented with 20 µgr lysozyme from chicken egg white (Sigma) for 30 min 37ºC, and eventually sonicated (cycle 0.5, amplitude 20% and 20 pulses). Cells were pelleted at 7000 g 1 min, and the pellet

resuspended in 1 ml of Trizol (Trireagent, Trisure) with 10 µl of proteinase K, and incubated at 60ºC 20 min. After that, 200 µl of chloroform were added to the sample, mixed inverting the tube several times and centrifuged. Supernatant over the interphase containing nucleic acids were collected carefully without disrupting the interphase. The subsequent steps for purification of RNA was performed using a commercial kit (Nucleospin RNA Plant, Macherey-Nagel). The integrity of the RNA extraction was tested by electrophoresis in agarose gel and cDNA was obtained using Titan One RT-PCR System (Roche). To prove which genes constitute an operon was performed PCR with cDNA as template using primers between genes to test which are transcribed in the same ARN molecule; and primers inside each gene to test if they were expressed. Positive controls for each primer pair were included using genomic DNA as template and for negative controls RNA extraction as template to ensure that RNA extraction was not contaminated with genomic DNA. (Specific primers are specified in Sup. Table 1).

Construction of B. cereus mutants

B. cereus mutants were obtained by electroporation using derivatives of the plasmid pMAD (Arnaud et al., 2004). Primers used to generate the mutagenesis constructs are listed in Sup. Table 1. The constructs were created by joining PCR, as previously described (López et al., 2009). In the first step, regions flanking the target genes and antibiotic-resistance cassettes were amplified separately, purified, and used for the joining

PCRs. These PCR products were digested with enzymes BamHI and NcoI and cloned into the pMAD vector digested with the same enzymes (Arnaud et al., 2004). The resulting suicide plasmids were used to transform *B. cereus* electrocompetent cells as described previously (Pflughoeft et al., 2011). Electroporations were performed with 4 µg of plasmids and 100 µL of electrocompetent *B. cereus* in 0.2-mm cuvettes using the following electroporation parameters: voltage 2500 kV, capacitance 25 µF, resistance 350 Ω. The electropored cells were seeded in LB plates supplemented with X-Gal and erythromycin for 72 h at 30°C. Blue colonies were selected and restreaked as previously described to trigger allele replacement (Arnaud et al., 2004). Finally, white colonies that were sensitive to MLS were selected, and deletion of the target gene was verified by colony PCR analysis and sequencing of the amplicons.

Heterologous expression of B. cereus alleles in B. subtilis mutants

B. cereus alleles were amplified with specific primers (Sup. Table 1), digested and cloned into the integrative plasmid pDR111 (for ectopic integration at the *amyE* locus), digested with the same enzyme. When required, fragments containing the $P_{hyperspank}$-promoter and the inserts were sub-cloned into the integrative plasmid pDR183 for ectopic integration at the *lacA* locus (López et al., 2009;Romero et al., 2011). The resulting integrative plasmids were used to transform *B. subtilis* 168 by natural competence; subsequently, using generalized transduction with Spp1 phages, the constructs were introduced into the recipient *B.*

subtilis 3610 strains (Romero et al., 2011). The transformants were selected by antibiotic resistance and tested by PCR.

Biofilm assays

B. subtilis biofilm formation was analyzed in MSgg medium (Branda et al., 2006). For pre-cultures, each strain was grown in LB agar with the required antibiotic at 37°C for 8 h. A colony was resuspended in 1 ml of MSgg, and 10 µl was used to inoculate 1 ml of MSgg in 24-well plates, and the plates were incubated without agitation at 30°C. The pellicles were examined for the presence of wrinkles, a morphological feature of mature *B. subtilis* biofilms (Branda et al., 2006).

B. cereus biofilm formation was monitored by testing bacterial adhesion to abiotic surfaces and staining with crystal violet (O'Toole et al., 1999). Cultures were grown in TY at 30ºC without agitation. One milliliter of a 1% solution of crystal violet in water was added to each well of a 24-well-plate. After 5 minutes of incubation, the plates were rinsed five times by immersion in tap water and were left inverted to dry on the bench for at least 45 minutes. The crystal violet was then resuspended with 50% acetic acid. The resuspended solution was diluted 1/10, and the absorbance was measured at 595 nm.

Congo Red assay

Staining of *B. subtilis* pellicles with the amyloid dye Congo Red was performed as described above but using Ty medium supplemented with Congo Red and Coomassie Brilliant Blue G at final concentrations of 20 µg/ml and 10 µg/ml; the dyes were filtered and added to autoclaved Ty medium (Romero et al., 2010). The same procedures were used to stain *B. cereus* pellicles but grown in 4.5 cm diameter plates.

Immunolabeling and transmission electron microscopy analysis

Each strain was grown in LB agar with the required antibiotic at 37°C for 8 h. A colony was suspended in 1 ml of Ty (*B. cereus* strains) or MSgg (*B. subtilis* strains) and 10 µl was inoculated in 1 ml of Ty or MSgg in 24-well plates; the plates were incubated without agitation at 30°C for 24 h. Cooper Grids for TEM were deposited on the air-liquid interface and incubated overnight. The grids were contrasted using 1% uranyl acetate for 2 minutes, rinsed by submersion in distilled water 2 minutes twice and then dried prior to examination. For immunelabeling assay, samples were floated on blocking buffer (1% non-fat dry milk in PBS with 0.1% Tween20) for 30 min, on anti-TasA of *B. subtilis* 1:150 for 2h, rinsed in PBST 30 min with a buffer change every 5 minutes, floated in goat-anti-rabbit 40nm gold secondary antibody (TedPella) 1:50 at 37ºC 1h, rinsed in PBST and in water 4 times for 5 min each. Samples were dried at RT and contrasted as previously described. Samples were visualized in a JEOL JEM-1400 transmission electron microscope.

6. SUPPLEMENTAL FIGURES

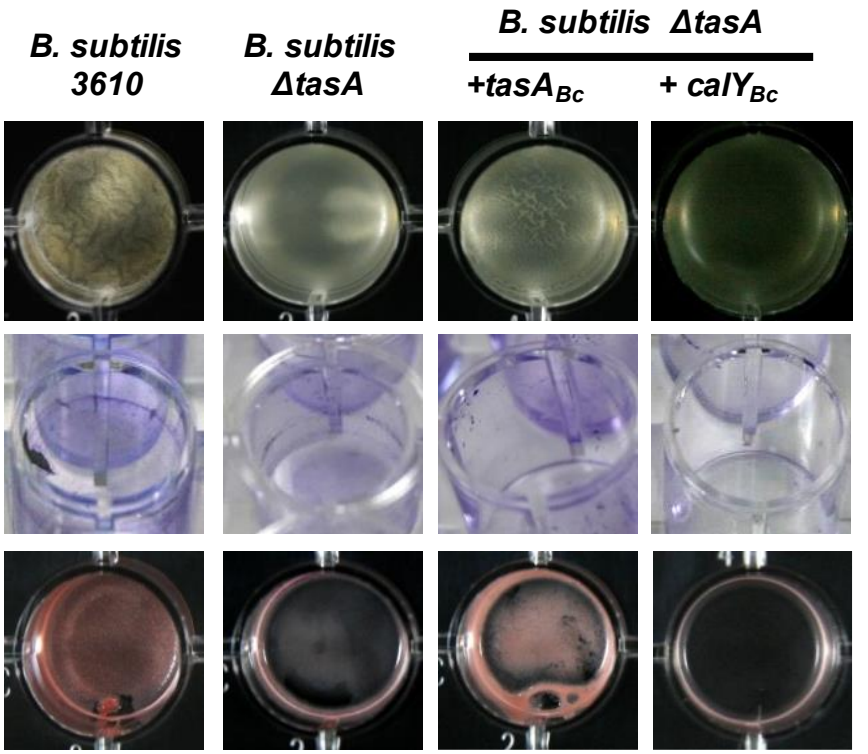

Figure S1. **Heterologous expression of B. cereus tasA or calY in B. subtilis fails to restore pellicle formation, adhesion to abiotic surfaces and amyloid-like staining in biofilms.** The B. cereus tasA and calY alleles were ectopically integrated at the lacA or amyE locus of the B. subtilis ΔtasA mutant strain, and expression of the alleles was driven by an IPTG-inducible promoter. Biofilm experiments were performed in static cultures in MSgg broth and Ty-Congo Red-Coomassie Blue broth and induced with 1 mM IPTG in 24-well plates. Top line: Top view of pellicles photographed after 48 h of incubation at 30ºC. Middle line: The adhesion to abiotic surface was evaluated using the Crystal Violet staining of cultures, and pictures were taken after 48 h of incubation at 30ºC. Bottom line: Top view pictures of pellicles grown in Ty broth supplemented with the amyloid-specific dye Congo Red (20 µg/ml) and Coomassie Blue (10 µg/ml).

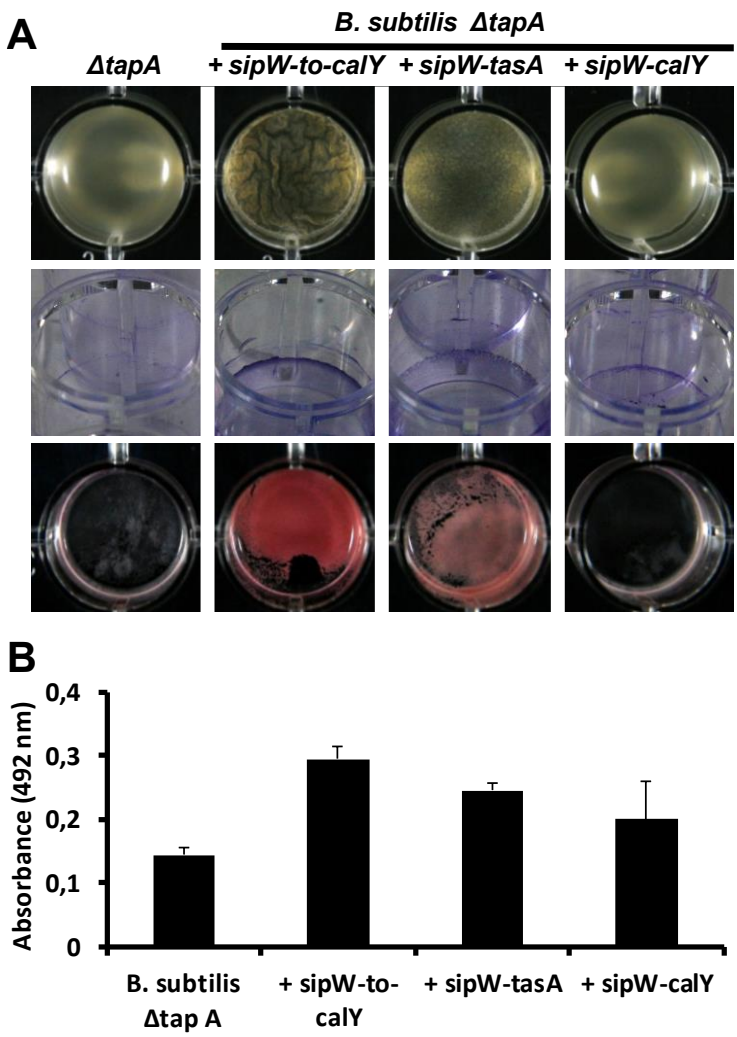

Figure S2. Heterologous expression of *B. cereus sipW-to*-calY, *sipW-tasA* and *sipW-calY* in a *B. subtilis DtapA* mutant strain. A) **Top line:** Top view of pellicles photographed after 48 h of incubation at 30ºC. **Middle line:** The adhesion to abiotic surface was evaluated using the Crystal Violet staining of cultures, and pictures were taken after 48 h of incubation at 30ºC. **Bottom line:** Top view pictures of pellicles grown in Ty broth supplemented with the amyloid-specific dye Congo Red (20 µgr/ml) and Coomassie Blue (10 µgr/ml). B) Quantification of the amount of crystal violet retained in bacterial biomass.

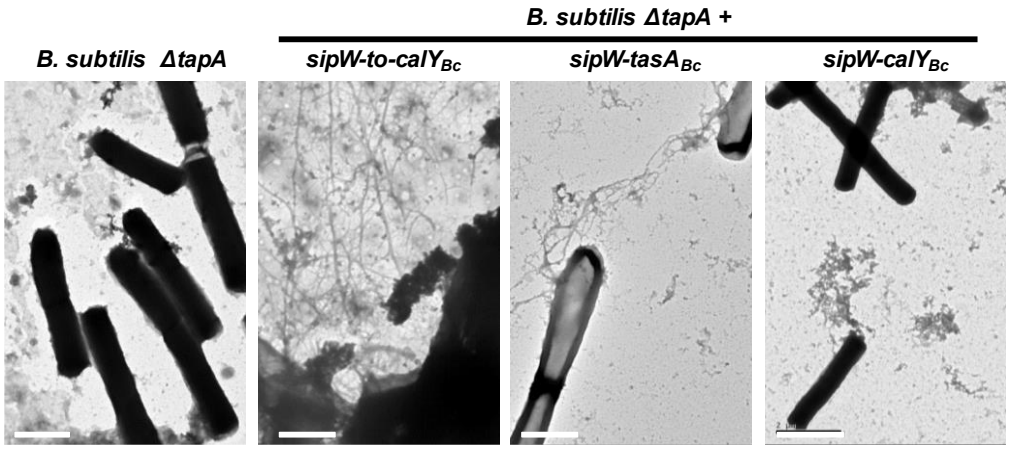

Figure Sup. 3. Heterologous expression of B. cereus *sipW-to-calY*, *sipW-tasA* but not *sipW-calY* leads to fiber formation in a B. subtilis *ΔtapA* mutant. B. cereus alleles were ectopically integrated at the *lacA* locus of a B. subtilis *ΔtapA* mutant strain, and their expression was driven by an IPTG-inducible promoter. The strains were grown in MSgg broth and induced with 1 mM IPTG without shaking at 30ºC. After 12 h, culture samples were contrasted with uranyl acetate, and transmission electron micrographs were obtained. Scale bars equal 1 μm.

7. ANNEX

Table 1. Strains used in this study.

Strain	Derivative strain	Genotype	Reference
B. subtilis 168		Prototroph	(Branda et al. 2001)
B. subtilis NCIB3610		Undomesticated prototroph	(Branda et al. 2001)
B. subtilis 168	SSB149	*(tapA-sipW-tasA)::spc*	(Branda et al. 2004)
B. subtilis NCIB3610		*(tapA-sipW-tasA)::spc*	(Branda et al. 2004)
B. subtilis NCIB3610	FC268	*(tapA-sipW-tasA)::spc, amyE::(tapA::cm-sipW-tasA)::spc*	(Branda et al. 2006)
B. subtilis NCIB3610	CA017	*tasA::km*	(Romero et al. 2010)
B. subtilis NCIB3610	JCA32	*tasA::km, lacA::*$P_{hyperspank}$*-sipW-tasA-bc1280-calY-mls*	This study

B. subtilis NCIB3610	DR6	*tasA::km, lacA::$P_{hyperspank}$-tasA-mls*	(Romero et al. 2010)
B. subtilis NCIB3610	JCA33	*(tapA-sipW-tasA)::spc, amyE::((tapA::cm)-sipW-tasA), lacA::$P_{hyperspank}$-sipW-tasA-bc1280-calY-mls*	This study
B. subtilis NCIB3610	JCA34	*(tapA-sipW-tasA)::spc, lacA::$P_{hyperspank}$-sipW-tasA-bc1280-calY-mls*	This study
B. subtilis NCIB3610	JCA35	*tasA::km, amyE::$P_{hyperspank}$-calY-spc*	This study
B. subtilis NCIB3610	JCA36	*tasA::km, amyE::$P_{hyperspank}$-sipW-tasA-spc*	This study
B. subtilis NCIB3610	JCA56	*(tapA-sipW-tasA)::spc, lacA::$P_{hyperspank}$ sipW-calY-mls*	This study
B. subtilis NCIB3610	JCA57	*(tapA-sipW-tasA)::spc, amyE::(tapA::cm-sipW-tasA), lacA::$P_{hyperspank}$-sipW-calY-mls*	This study
B. subtilis NCIB3610	JCA58	*tasA::km, lacA::$P_{hyperspank}$-sipW-calY-mls*	This study
B. subtilis NCIB3610	JCA90	*(tapA-sipW-tasA)::spc, amyE::$P_{hyperspank}$-sipW-tasA-spc*	This study

B. subtilis NCIB3610	JCA91	*(tapA-sipW-tasA)::spc, amyE::((tapA::cm)-sipW-tasA), lacA::$P_{hyperspank}$-sipW-tasA-mls*	This study
B. subtilis NCIB3610	JCA92	*tasA::Km, amyE::$P_{hyperspank}$-tasA-spc*	This study
B. cereus CECT148		Type strain	Spanish Colection of Type Strains
B. cereus CECT148	JCA110	*sipW::Eri*	This study
B. cereus CECT148	JCA111	*tasA::Km*	This study
B. cereus CECT148	JCA113	*calY::Eri*	This study
B. cereus CECT148	JCA114	*(sipW-tasA-bc_1280-calY)::Eri*	This study

8. REFERENCES

Arnaud, M., Chastanet, A., and Debarbouille, M. (2004). New vector for efficient allelic replacement in naturally nontransformable, low-GC-content, gram-positive bacteria. *Appl Environ Microbiol* 70**,** 6887-6891. doi: 10.1128/AEM.70.11.6887-6891.2004.

Auger, S., Ramarao, N., Faille, C., Fouet, A., Aymerich, S., and Gohar, M. (2009). Biofilm formation and cell surface properties among pathogenic and nonpathogenic strains of the Bacillus cereus group. *Appl Environ Microbiol* 75**,** 6616-6618. doi: AEM.00155-09 [pii] 10.1128/AEM.00155-09.

Ball, D.A., Taylor, R., Todd, S.J., Redmond, C., Couture-Tosi, E., Sylvestre, P., Moir, A., and Bullough, P.A. (2008). Structure of the exosporium and sublayers of spores of the Bacillus cereus family revealed by electron crystallography. *Mol Microbiol* 68**,** 947-958. doi: MMI6206 [pii] 10.1111/j.1365-2958.2008.06206.x.

Berger, C.N., Sodha, S.V., Shaw, R.K., Griffin, P.M., Pink, D., Hand, P., and Frankel, G. (2010). Fresh fruit and vegetables as vehicles for the transmission of human pathogens. *Environ Microbiol* 12**,** 2385-2397. doi: EMI2297 [pii]10.1111/j.1462-2920.2010.02297.x.

Blanco, L.P., Evans, M.L., Smith, D.R., Badtke, M.P., and Chapman, M.R. (2012). Diversity, biogenesis and function of microbial amyloids. *Trends Microbiol* 20**,** 66-73. doi: S0966-842X(11)00208-3 [pii] 10.1016/j.tim.2011.11.005.

Bottone, E.J. (2010). Bacillus cereus, a volatile human pathogen. *Clin Microbiol Rev* 23**,** 382-398. doi: 23/2/382 [pii]10.1128/CMR.00073-09.

Branda, S.S., Chu, F., Kearns, D.B., Losick, R., and Kolter, R. (2006). A major protein component of the *Bacillus subtilis* biofilm matrix. *Mol Microbiol* 59**,** 1229-1238. doi: MMI5020 [pii] 10.1111/j.1365-2958.2005.05020.x.

Branda, S.S., Gonzalez-Pastor, J.E., Ben-Yehuda, S., Losick, R., and Kolter, R. (2001). Fruiting body formation by Bacillus subtilis. *Proc Natl Acad Sci U S A* 98**,** 11621-11626. doi: 10.1073/pnas.191384198 98/20/11621 [pii].

Branda, S.S., Gonzalez-Pastor, J.E., Dervyn, E., Ehrlich, S.D., Losick, R., and Kolter, R. (2004). Genes involved in formation of structured multicellular communities by Bacillus subtilis. *J Bacteriol* 186**,** 3970-3979. doi: 10.1128/JB.186.12.3970-3979.2004 186/12/3970 [pii].

Branda, S.S., Vik, S., Friedman, L., and Kolter, R. (2005). Biofilms: the matrix revisited. *Trends Microbiol* 13**,** 20-26. doi: S0966-842X(04)00260-4 [pii] 10.1016/j.tim.2004.11.006.

Burnett, S.L., and Beuchat, L.R. (2001). Human pathogens associated with raw produce and unpasteurized juices, and difficulties in decontamination. *J Ind Microbiol Biotechnol* 27**,** 104-110. doi: 10.1038/sj/jim/7000199.

Carlin, F., Girardin, H., Peck, M.W., Stringer, S.C., Barker, G.C., Martinez, A., Fernandez, A., Fernandez, P., Waites, W.M., Movahedi, S., Van Leusden, F., Nauta, M., Moezelaar, R., Torre, M.D., and Litman, S. (2000). Research on factors allowing a risk assessment of spore-forming pathogenic bacteria in cooked chilled foods containing vegetables: a FAIR collaborative project. *Int J Food Microbiol* 60**,** 117-135.

Chapman, M.R., Robinson, L.S., Pinkner, J.S., Roth, R., Heuser, J., Hammar, M., Normark, S., and Hultgren, S.J. (2002). Role of *Escherichia coli* curli operons in directing amyloid fiber formation. *Science* 295**,** 851-855. doi: 10.1126/science.1067484 295/5556/851 [pii].

Chu, F., Kearns, D.B., Branda, S.S., Kolter, R., and Losick, R. (2006). Targets of the master regulator of biofilm formation in *Bacillus subtilis*. *Mol Microbiol* 59**,** 1216-1228. doi: MMI5019 [pii] 10.1111/j.1365-2958.2005.05019.x.

De Jong, W., Wosten, H.A., Dijkhuizen, L., and Claessen, D. (2009). Attachment of Streptomyces coelicolor is mediated by amyloidal fimbriae that are anchored to the cell surface via cellulose. *Mol Microbiol*. doi: MMI6838 [pii] 10.1111/j.1365-2958.2009.06838.x.

Di Berardo, C., Capstick, D.S., Bibb, M.J., Findlay, K.C., Buttner, M.J., and Elliot, M.A. (2008). Function and redundancy of the chaplin cell surface proteins in aerial hypha formation, rodlet assembly, and viability in Streptomyces coelicolor. *J Bacteriol* 190**,** 5879-5889. doi: JB.00685-08 [pii] 10.1128/JB.00685-08.

Dueholm, M.S., Petersen, S.V., Sonderkaer, M., Larsen, P., Christiansen, G., Hein, K.L., Enghild, J.J., Nielsen, J.L., Nielsen, K.L., Nielsen, P.H., and Otzen, D.E. (2010). Functional amyloid in Pseudomonas. *Mol Microbiol* 77**,** 1009-1020. doi: MMI7269 [pii] 10.1111/j.1365-2958.2010.07269.x.

Elhariry, H.M. (2011). Attachment strength and biofilm forming ability of Bacillus cereus on green-leafy vegetables: cabbage and lettuce. *Food Microbiol* 28**,** 1266-1274. doi: S0740-0020(11)00116-X [pii] 10.1016/j.fm.2011.05.004.

Epstein, E.A., and Chapman, M.R. (2008). Polymerizing the fibre between bacteria and host cells: the biogenesis of functional amyloid fibres. *Cell Microbiol* 10**,** 1413-1420. doi: CMI1148 [pii] 10.1111/j.1462-5822.2008.01148.x.

Fagerlund, A., Dubois, T., Okstad, O.A., Verplaetse, E., Gilois, N., Bennaceur, I., Perchat, S., Gominet, M., Aymerich, S., Kolsto, A.B., Lereclus, D., and Gohar, M. (2014). SinR controls enterotoxin expression in Bacillus thuringiensis biofilms. *PLoS One* 9**,** e87532. doi: 10.1371/journal.pone.0087532.

Flemming, H.C., and Wingender, J. (2010). The biofilm matrix. *Nat Rev Microbiol* 8**,** 623-633. doi: nrmicro2415 [pii] 10.1038/nrmicro2415.

Fowler, D.M., Koulov, A.V., Balch, W.E., and Kelly, J.W. (2007). Functional amyloid--from bacteria to humans. *Trends Biochem Sci* 32**,** 217-224. doi: S0968-0004(07)00059-X [pii] 10.1016/j.tibs.2007.03.003.

Fricke, B., Drossler, K., Willhardt, I., Schierhorn, A., Menge, S., and Rucknagel, P. (2001). The cell envelope-bound metalloprotease (camelysin) from Bacillus cereus is a possible pathogenic factor. *Biochim Biophys Acta* 1537**,** 132-146.

Greenwald, J., and Riek, R. (2010). Biology of amyloid: structure, function, and regulation. *Structure* 18**,** 1244-1260. doi: S0969-2126(10)00308-4 [pii] 10.1016/j.str.2010.08.009.

Hobley, L., Ostrowski, A., Rao, F.V., Bromley, K.M., Porter, M., Prescott, A.R., Macphee, C.E., Van Aalten, D.M., and Stanley-Wall, N.R. (2013). BslA is a

self-assembling bacterial hydrophobin that coats the Bacillus subtilis biofilm. *Proc Natl Acad Sci U S A* 110**,** 13600-13605. doi: 10.1073/pnas.1306390110.

Houry, A., Briandet, R., Aymerich, S., and Gohar, M. (2010). Involvement of motility and flagella in Bacillus cereus biofilm formation. *Microbiology* 156**,** 1009-1018. doi: mic.0.034827-0 [pii] 10.1099/mic.0.034827-0.

Hsueh, Y.H., Somers, E.B., Lereclus, D., and Wong, A.C. (2006). Biofilm formation by Bacillus cereus is influenced by PlcR, a pleiotropic regulator. *Appl Environ Microbiol* 72**,** 5089-5092. doi: 10.1128/AEM.00573-06.

Kamga Wambo, G.O., Burckhardt, F., Frank, C., Hiller, P., Wichmann-Schauer, H., Zuschneid, I., Hentschke, J., Hitzbleck, T., Contzen, M., Suckau, M., and Stark, K. (2011). The proof of the pudding is in the eating: an outbreak of emetic syndrome after a kindergarten excursion, Berlin, Germany, December 2007. *Euro Surveill* 16.

Karunakaran, E., and Biggs, C.A. (2011). Mechanisms of Bacillus cereus biofilm formation: an investigation of the physicochemical characteristics of cell surfaces and extracellular proteins. *Appl Microbiol Biotechnol* 89**,** 1161-1175. doi: 10.1007/s00253-010-2919-2.

Kobayashi, K., and Iwano, M. (2012). BslA(YuaB) forms a hydrophobic layer on the surface of Bacillus subtilis biofilms. *Mol Microbiol* 85**,** 51-66. doi: 10.1111/j.1365-2958.2012.08094.x.

Lindback, T., Mols, M., Basset, C., Granum, P.E., Kuipers, O.P., and Kovacs, A.T. (2012). CodY, a pleiotropic regulator, influences multicellular behaviour and efficient production of virulence factors in Bacillus cereus. *Environ Microbiol* 14**,** 2233-2246. doi: 10.1111/j.1462-2920.2012.02766.x.

López, D., Vlamakis, H., Losick, R., and Kolter, R. (2009). Paracrine signaling in a bacterium. *Genes Dev* 23**,** 1631-1638. doi: 23/14/1631 [pii] 10.1101/gad.1813709.

Martinez-Gil, M., Quesada, J.M., Ramos-Gonzalez, M.I., Soriano, M.I., De Cristobal, R.E., and Espinosa-Urgel, M. (2013). Interplay between extracellular matrix components of Pseudomonas putida biofilms. *Res Microbiol* 164**,** 382-389. doi: 10.1016/j.resmic.2013.03.021.

Martinez-Gil, M., Yousef-Coronado, F., and Espinosa-Urgel, M. (2010). LapF, the second largest Pseudomonas putida protein, contributes to plant root colonization and determines biofilm architecture. *Mol Microbiol* 77**,** 549-561. doi: 10.1111/j.1365-2958.2010.07249.x.

Mckillip, J.L. (2000). Prevalence and expression of enterotoxins in Bacillus cereus and other Bacillus spp., a literature review. *Antonie Van Leeuwenhoek* 77**,** 393-399.

O'toole, G.A., Pratt, L.A., Watnick, P.I., Newman, D.K., Weaver, V.B., and Kolter, R. (1999). Genetic approaches to study of biofilms. *Methods Enzymol* 310**,** 91-109.

Ostrowski, A., Mehert, A., Prescott, A., Kiley, T.B., and Stanley-Wall, N.R. (2011). YuaB functions synergistically with the exopolysaccharide and TasA amyloid fibers to allow biofilm formation by Bacillus subtilis. *J Bacteriol* 193**,** 4821-4831. doi: 10.1128/JB.00223-11 JB.00223-11 [pii].

Pasvolsky, R., Zakin, V., Ostrova, I., and Shemesh, M. (2014). Butyric acid released during milk lipolysis triggers biofilm formation of Bacillus species. *Int J Food Microbiol* 181**,** 19-27. doi: 10.1016/j.ijfoodmicro.2014.04.013.

Pflughoeft, K.J., Sumby, P., and Koehler, T.M. (2011). Bacillus anthracis sin locus and regulation of secreted proteases. *J Bacteriol* 193**,** 631-639. doi: JB.01083-10 [pii] 10.1128/JB.01083-10.

Romero, D. (2013). Bacterial determinants of the social behavior of Bacillus subtilis. *Res Microbiol* 164**,** 788-798. doi: 10.1016/j.resmic.2013.06.004.

Romero, D., Aguilar, C., Losick, R., and Kolter, R. (2010). Amyloid fibers provide structural integrity to Bacillus subtilis biofilms. *Proc Natl Acad Sci U S A* 107**,** 2230-2234. doi: 0910560107 [pii] 10.1073/pnas.0910560107.

Romero, D., Vlamakis, H., Losick, R., and Kolter, R. (2011). An accessory protein required for anchoring and assembly of amyloid fibres in B. subtilis biofilms. *Mol Microbiol* 80**,** 1155-1168. doi: 10.1111/j.1365-2958.2011.07653.x.

Romero, D., Vlamakis, H., Losick, R., and Kolter, R. (2014). Functional analysis of the accessory protein TapA in Bacillus subtilis amyloid fiber

assembly. *J Bacteriol*. doi: 10.1128/JB.01363-13.

Sawyer, E.B., Claessen, D., Haas, M., Hurgobin, B., and Gras, S.L. (2011). The assembly of individual chaplin peptides from Streptomyces coelicolor into functional amyloid fibrils. *PLoS One* 6**,** e18839. doi: 10.1371/journal.pone.0018839.

Schwartz, K., Syed, A.K., Stephenson, R.E., Rickard, A.H., and Boles, B.R. (2012). Functional amyloids composed of phenol soluble modulins stabilize Staphylococcus aureus biofilms. *PLoS Pathog* 8**,** e1002744. doi: 10.1371/journal.ppat.1002744 PPATHOGENS-D-12-00201 [pii].

Shaheen, R., Svensson, B., Andersson, M.A., Christiansson, A., and Salkinoja-Salonen, M. (2010). Persistence strategies of Bacillus cereus spores isolated from dairy silo tanks. *Food Microbiol* 27**,** 347-355. doi: S0740-0020(09)00262-7 [pii] 10.1016/j.fm.2009.11.004.

Shemesh, M., and Chai, Y. (2013). A combination of glycerol and manganese promotes biofilm formation in Bacillus subtilis via histidine kinase KinD signaling. *J Bacteriol* 195**,** 2747-2754. doi: 10.1128/JB.00028-13.

Shu, Q., Crick, S.L., Pinkner, J.S., Ford, B., Hultgren, S.J., and Frieden, C. (2012). The E. coli CsgB nucleator of curli assembles to beta-sheet oligomers that alter the CsgA fibrillization mechanism. *Proc Natl Acad Sci U S A* 109**,** 6502-6507. doi: 10.1073/pnas.1204161109 1204161109 [pii].

Stover, A.G., and Driks, A. (1999a). Control of synthesis and secretion of the Bacillus subtilis protein YqxM. *J Bacteriol* 181**,** 7065-7069.

Stover, A.G., and Driks, A. (1999b). Secretion, localization, and antibacterial activity of TasA, a *Bacillus subtilis* spore-associated protein. *J Bacteriol* 181**,** 1664-1672.

Terra, R., Stanley-Wall, N.R., Cao, G., and Lazazzera, B.A. (2012). Identification of Bacillus subtilis SipW as a bifunctional signal peptidase that controls surface-adhered biofilm formation. *J Bacteriol* 194**,** 2781-2790. doi: 10.1128/JB.06780-11 JB.06780-11 [pii].

Thorsen, L., Azokpota, P., Munk Hansen, B., Ronsbo, M.H., Nielsen, K.F.,

Hounhouigan, D.J., and Jakobsen, M. (2011). Formation of cereulide and enterotoxins by Bacillus cereus in fermented African locust beans. *Food Microbiol* 28**,** 1441-1447. doi: S0740-0020(11)00159-6 [pii] 10.1016/j.fm.2011.07.003.

Tjalsma, H., Bolhuis, A., Van Roosmalen, M.L., Wiegert, T., Schumann, W., Broekhuizen, C.P., Quax, W.J., Venema, G., Bron, S., and Van Dijl, J.M. (1998). Functional analysis of the secretory precursor processing machinery of Bacillus subtilis: identification of a eubacterial homolog of archaeal and eukaryotic signal peptidases. *Genes Dev* 12**,** 2318-2331.

Vilain, S., Pretorius, J.M., Theron, J., and Brozel, V.S. (2009). DNA as an adhesin: Bacillus cereus requires extracellular DNA to form biofilms. *Appl Environ Microbiol* 75**,** 2861-2868. doi: 10.1128/AEM.01317-08.

Vlamakis, H., Aguilar, C., Losick, R., and Kolter, R. (2008). Control of cell fate by the formation of an architecturally complex bacterial community. *Genes Dev* 22**,** 945-953. doi: 22/7/945 [pii] 10.1101/gad.1645008.

Vlamakis, H., Chai, Y., Beauregard, P., Losick, R., and Kolter, R. (2013). Sticking together: building a biofilm the Bacillus subtilis way. *Nat Rev Microbiol* 11**,** 157-168. doi: 10.1038/nrmicro2960.

Zhou, Y., Smith, D., Leong, B.J., Brannstrom, K., Almqvist, F., and Chapman, M.R. (2012). Promiscuous cross-seeding between bacterial amyloids promotes interspecies biofilms. *J Biol Chem* 287**,** 35092-35103. doi: 10.1074/jbc.M112.383737.

CHAPTER III

BIOCHEMICAL CHARACTERIZATION OF THE PROTEINS TasA AND CalY

INTRODUCTION

Amyloids are a group of proteins with tendency to acquire a particular folding that ends in the formation of fibres with a characteristic quaternary structure enriched in β-sheets, which confers the fibres with outstanding stability and physicochemical properties (Shammas et al., 2011). The assembly of the fibres is a multistep process that although essentially similar among amyloids, may show subtle differences depending on the protein-system (Makin et al., 2005). In general, it can be said that first stages are in some extent reversible, with monomers of protein that interact into several units of aggregates in a process called nucleation, which seed further fibrillation of the protein (Fig.1). Later states of aggregation lead to irreversible polymerized amyloids fibres, and still a secondary nucleation may happen leading to a supra-molecular organization (Linse, 2017), which is the origin of fibre branching. These processes occur as a consequence of the autopolymerisation properties of amyloid proteins (Tjernberg et al., 1999; Wang et al., 2008).

The amyloid stage, fibre or fibrils, is outstandingly insoluble and resistant to protease degradation and detergent denaturation (Masters and Selkoe, 2012). Amyloids are characterized by their enrichment in β-sheets secondary structures, which can: i) be present in the original conformation of the protein ii) be induced by the action of other monomers of the same protein (Imran and Mahmood, 2011), or iii) be induced by other additional proteins and/or physic-chemical environmental conditions (temperature, hydrophobicity, pH or protein concentration) (Cheon et al., 2012; Khurana et al., 2001; Kowalewski

and Holtzman, 1999; Zhu et al., 2002). Additional to the structural stability, the specific folding of amyloids with the enrichment of β-sheets serves to the specific binding of the dyes Congo Red and Thioflavin T, both routinely used in the diagnosis and study of amyloids because of their particular properties of absorbance or fluorescence emissions upon interaction with amyloid proteins (Girych et al., 2016; Maezawa et al., 2008).

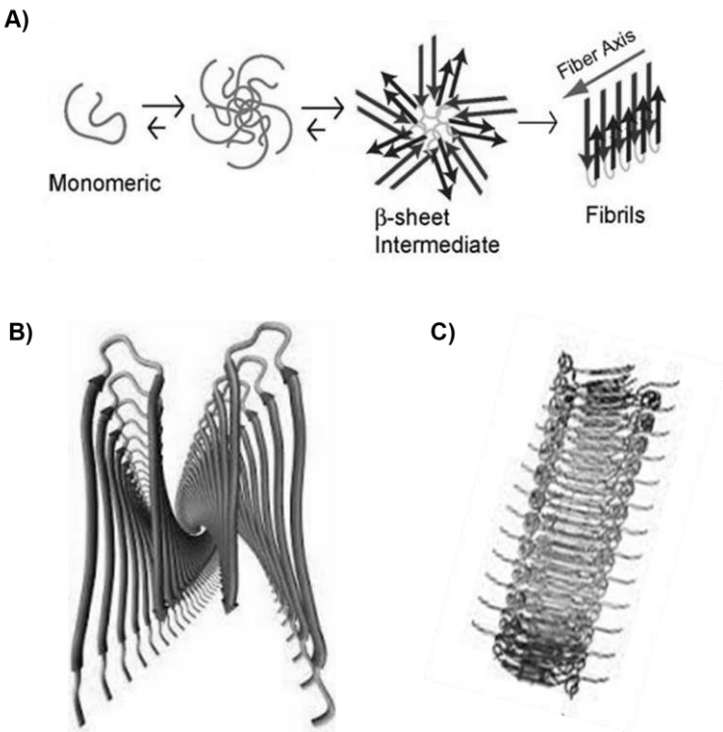

Figure 1. Amyloid polymerization. A) Canonical model of polymerization of amyloids. B) Scheme of intra- and inter-molecular β-sheets interactions. C) Schematic view of an amyloid fiber. Source: Piotr Hanczyc. Chalmers University of Technology.

Amyloids were firstly described in human neurodegenerative diseases, Alzheimer and Parkinson, both affecting the nervous system as a result of the accumulation of toxic amyloid aggregates in the neurons (Forloni et al., 2002). Since their discovery, the number of pathologies related to amyloids has increased, becoming more than 50 different amyloidogenic conditions in humans (Baker and Rice, 2012; Chiti and Dobson, 2006), a reason for the exceptional interest in the study of amyloids. Other kind of amyloids are prions. This is an interesting group of proteins given that the amyloid properties are based in a misfolded isoform of the protein that induces a similar misfolding in another monomer of the same protein upon interaction, propagating the misfolding into a form of a protein with auto polymerization properties and subsequent formation of the amyloid (Sabate et al., 2015; Stöhr et al., 2008).

After the discovery of these pathologies based in protein misfolding, amyloid proteins started to be described with important biological roles in all life kingdoms, a reason to call them functional amyloids (Pham et al., 2014). These functions include: structural role in the silkworm chorion of the eggshell (Iconomidou et al., 2001) or the spider silk (Kenney et al., 2002); structural function in the formation of aerial hyphae formation in *Streptomyces coelicolor* (Claessen et al., 2003); antimicrobial activity (Jang et al., 2011); hormone storage in granules in the pituitary gland (Maji et al., 2009); acceleration of melanin polymerization (Fowler et al., 2006); cell adhesion in the yeast *Candida albicans* and *Saccharomyces cerevisiae* (Ramsook et al., 2010) and in several bacteria (Chapman et al., 2002); hyphae compatibility in

filamentous of *Podospora anserine* (Coustou-Linares et al., 2001); biofilm formation in *Pseudomonas* sp. (Dueholm et al., 2010); control of plasmid replication (Molina-García et al., 2017); toxins produced by several bacteria, inducing cell death in plant cells and as effectors translocators (Choi et al., 2013); peptide LL-37 belongs to the human defense system against biofilm formation, preventing the polymerization of Curli of *E. coli* biofilm fibers and also working as antimicrobial peptide (Kai-Larsen et al., 2010; Sood et al., 2008); or bacteriocins produced from bacteria against other bacteria (Cogen et al., 2010; Shahnawaz and Soto, 2012). Amyloid properties also play roles in protein activity regulation, switching a protein to an inactive form when environmental conditions change. This property is used by *Listeria monocitogenes* producing the active protein LLO to escape from the acidic phagosome. Once the phagosome is lysed, bacteria and the protein LLO are released to the cytoplasm, with a higher pH, where the protein LLO inactivates its own polymerization into amyloid fibers, preventing the disruption of the cell membrane and allowing the bacteria resides inside the host cell (Podobnik et al., 2015). Each of this functional amyloids have a different mechanism of interaction and most of them require the action of accessory proteins that: i) control the cleavage of the original protein to produce the active peptide (Dürr et al., 2006); ii) induce or promote the polymerization (Chapman et al., 2002; Romero et al., 2011); or iii) control the specific localization of the protein (Stöver and Driks, 1999).

These examples evidence the variability within the amyloid systems and although the huge effort done in the study of this kind of proteins, there

are still blind aspects in our knowledge on the amyloid system, especially in the treatment of diseases (Ankarcrona et al., 2016). Further amyloid systems description and deep study would help to fully understand the mechanisms, interactions and how the amyloid formation can be controlled. Besides, functional amyloids are very common in bacteria, including pathogenic species, and a myriad of them, as presented above, are implicated in biofilm, aggression resilience, host defence inactivation and host colonization among other functions.

In *B. subtilis*, the amyloid system encoded in the *tapA* operon is involved in biofilm formation and contains three genes: *tasA*, encoding the protein that polymerizes into fibres; *tapA*, which encodes the accessory protein necessary for efficient polymerization of TasA and anchoring to the cell wall; and the locus *sipW*, codifying for a signal peptidase which recognise a peptide sequence of TasA and TapA for proper secretion (Romero et al., 2011; Stöver and Driks, 1999). As exposed in the previous chapter of this thesis, the proteins TasA and CalY were presented as responsible for fibre formation in *B. cereus*. These proteins are orthologues to the amyloid-like protein TasA of *B. subtilis*, and heterologous expression of TasA and CalY region of *B. cereus* in a *B. subtilis* strain lacking the *tapA* operon rescued the phenotype. Besides, TEM imaging showed similar fibres that disappeared in full mutants in this genomic region. Considering all these precedents we hypothesize that TasA and CalY may also possess amyloid properties. In this study we aimed at characterizing biochemically both proteins to answer whether any of them is the beholder of the amyloid nature.

1. RESULTS

1. Bioinformatic analyses predicts the amyloid nature of TasA and CalY

The identity among TasA of *B. subtilis* and its orthologues in *B. cereus* TasA and CalY is only 38%, and rise to 62% among both paralogues (TasA and CalY) based on Clustal Omega alignments of amino acid sequences of the three proteins (Fig. 2A). This result evidences several deletions affecting both TasA and CalY of *B. cereus* in comparison to TasA of *B. subtilis*, a suggestion of gene duplication before deletion events. This alignment also reveals the presence of amino acid highly conserved, which might be potentially relevant for the proper protein folding. This was evident at the N-terminal position of the proteins, which hold the signal peptide described in TasA of *B. subtilis* (Fig. 2) which is recognized by the signal peptidase SipW. The search for putative signal peptides on the proteins sequences using the SignalP 4.1 server detected signal peptides at these position in both proteins, suggesting a similar processing events in both bacterial species (Fig. 2B).

It should be considered that the putative amyloidogenic function to form fibres is supported by the secondary structure, what accept variability at amino acid sequence (Shea et al., 1991).Thus, it is not surprising that alignment analyses of these proteins do not show a high level of homology. Indeed, we found an almost perfect correlation of the predicted secondary structure of the three proteins, with the difference

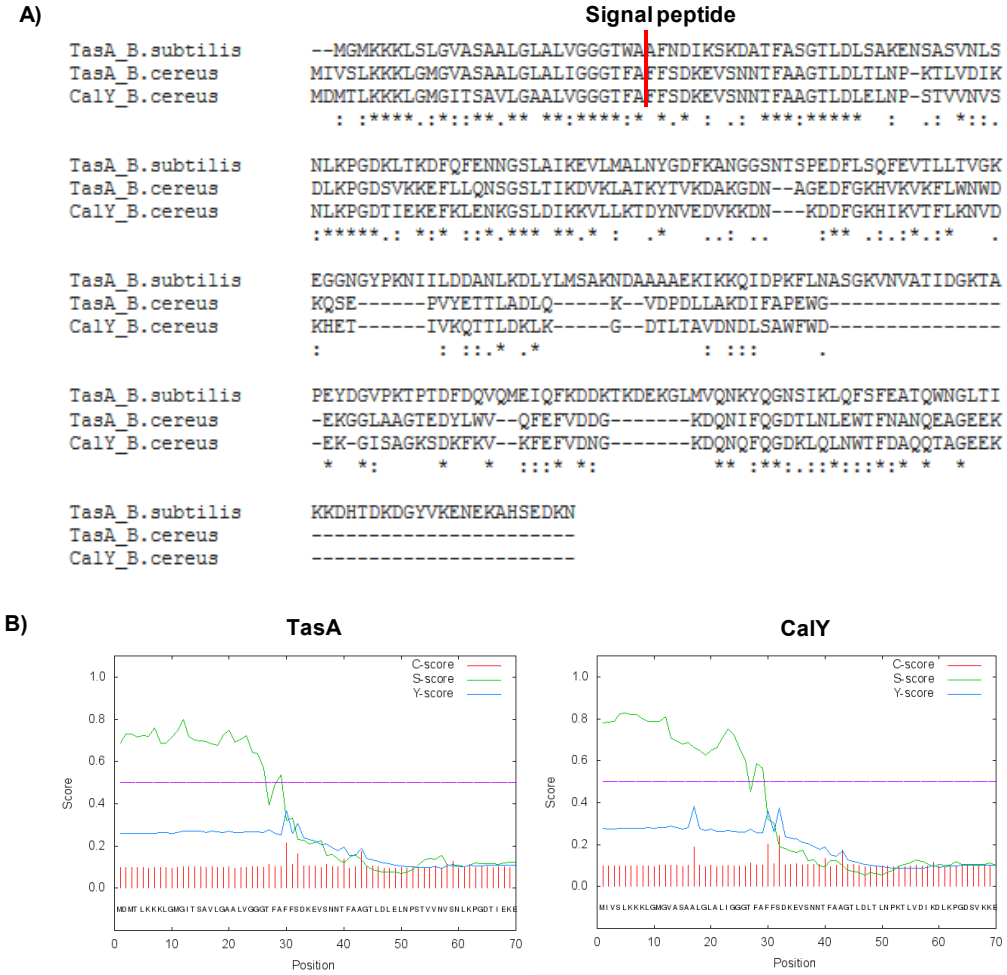

Figure 2. TasA and CalY identity. A) Clustal Omega alignment of the protein TasA from *B. subtilis* and the two orthologues, TasA and CalY in *B. cereus*. Asterisk (*) indicate fully conserved residue, colon (:) indicates conservation between groups of strongly similar properties, dot (.) indicates conservation between groups of weakly similar properties. **B)** SignalP 4.1 Server - prediction of signal peptides. A cleavage site was predicted between the amino acid at positions 29 and 30 in TasA (left) and several possibilities in CalY, with the most probable prediction also between the positions 29 and 30. C-Score and S-Score define the result of neural network processing and Y-score is an integration of both signals.

in the C-terminal region, which is absent in TasA and CalY of *B. cereus* in the C-terminal region, which is absent in TasA and CalY of *B. cereus* compared to TasA of *B. subtilis* (Fig. 3). It is remarkable that this secondary structure pattern has been conserved despite the several deletion events affecting both proteins in *B. cereus* compared to *B. subtilis*.

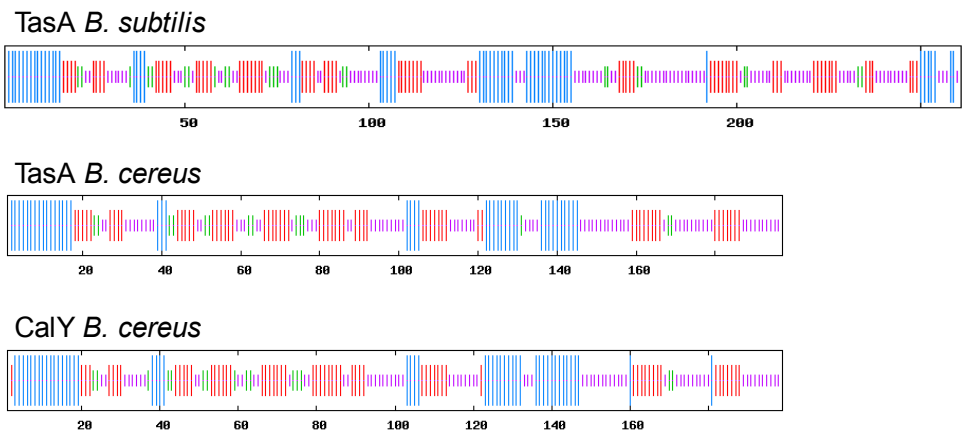

Figure 3. TasA and CalY retain secondary structure similitude with TasA fo *B. subtilis*. Secondary structure prediction of the protein TasA of *B. subtilis* and the two orthologues TasA and CalY in *B. cereus* with SOPMA Software. Colour bars indicate alpha-helix (blue), beta-sheet (red), beta-turn (green). (Institute of Biology and Protein Chemistry Bioinformatic Site).

Given the highly conserved secondary structure prediction pattern, we also considered to run predictions for amyloid properties. There are several amyloid-aggregation-prediction software to do *in silico* studies previous to experimental procedures, which yield information of the secondary structure tendency for putative amyloidogenic regions

(Hamodrakas, 2011). We used the software Pasta 2.0 (Threshold of -4 PEUs, where 1 PEU = 1.192 Kcal/mol) to compare the three proteins without the signal peptide, as this peptide is cleaved before extrusion out of the cell and fibre formation. Under these prediction settings, we found that TasA of *B. subtilis* would possesses 13 amyloidogenic regions, compared to the 22 showed by TasA of *B. cereus*. Besides, the minimum free energy associated to the amyloidogenic regions show a lower tendency for auto-aggregation in TasA of *B. subtilis* compared to the orthologue in *B. cereus*. CalY showed only 4 amyloidogenic regions and a higher free energy, indicative of less propensity to amyloid folding (Table 1).

Table 1. Analysis of protein aggregation (Pasta 2.0 software). Threshold of -4 PEUs, where 1 PEU = 1.192 Kcal/mol. The lesser free energy indicates higher propensity to aggregation.

Protein	Protein length	Amyloid regions	Best energy of amyloid regions	% disorder	% α-helix	% β-strand	% coil
TasA *B.subtilis*	234	13	-5.683288	20.08	12.39	29.91	57.69
TasA *B. cereus*	168	22	-6.14015	14.28	0	47.02	52.98
CalY *B.cereus*	169	4	-4.756513	14.2	3.55	40.83	55.62
Co-aggregation							
TasA *B. cereus*-*CalY B.cereus*			-4.408466				

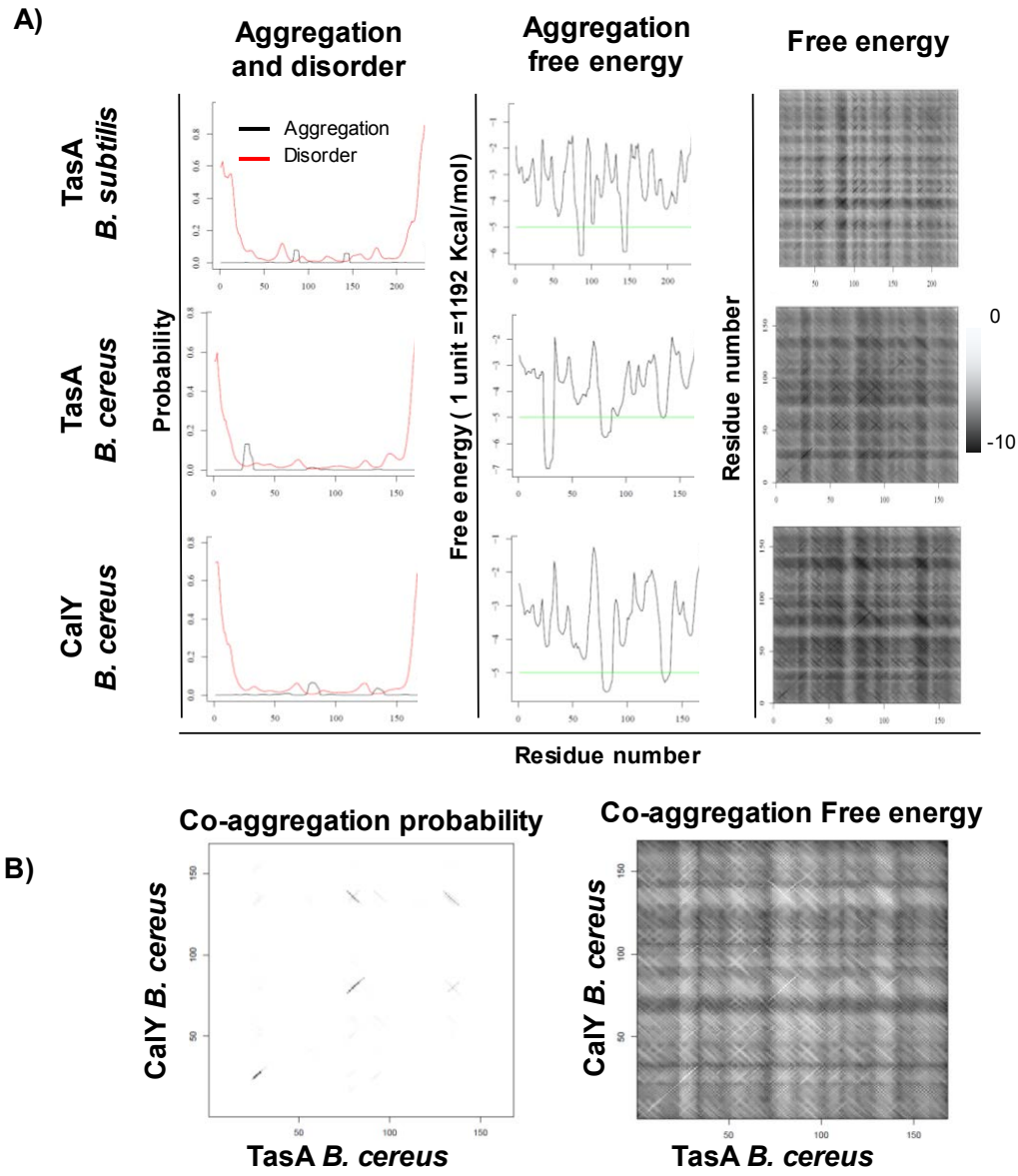

Figure 4. TasA and CalY show similar predicted aggregation patterns. Aggregation analysis of TasA and CalY with Pasta 2.0. A) Auto-aggregation profiles of TasA of *B. subtilis*, TasA and CalY of *B. cereus*. B) Co-aggregation profiles of TasA and CalY of *B. cereus*.

Nevertheless, the free energy of auto-aggregation graph of CalY is plenty of negative value bands (black), indicating that this protein also tends to aggregation (Fig.4 and Table 1). Besides auto-aggregation prediction, we also run co-aggregation predictions among TasA and CalY of *B. cereus* (Table 1), which is lower than those showed by isolated proteins for auto-aggregation but close to the values of CalY. If we consider TasA of *B. subtilis* as the reference, TasA of *B. cereus* has evolved to a more amyloidogenic protein and CalY inversely, suggesting that upon interaction, CalY would reduce the fibre polymerization rate.

2. TasA and CalY expressed and purified in *E. coli* retain properties of amyloid proteins

To characterize biochemically both proteins, we cloned their open reading frames, without signal peptide, in the plasmid PET30b in frame with a histidine tag (6xHis) and under control of an IPTG inducible promoter. After transformation of *E. coli* BL21 DE3, several colonies were inoculated in 300 ml of LB. Diverse trials were done to obtain culture conditions for a high yield of purified protein. The best result was obtained after bacterial growth at OD_{600} 0.7, and induction for 16 h at 16ºC with soft shaking. From these cultures, bacteria were recovered and lysed, and protein was purified in a Ni-column (as described in material and methods).

Fractions from pellets, lysate, column washing and elute were electrophoretically resolved in denaturing agarose gels (Fig. 5). Both

proteins were highly expressed and most of the protein was recovered in the column with low level of contaminants.

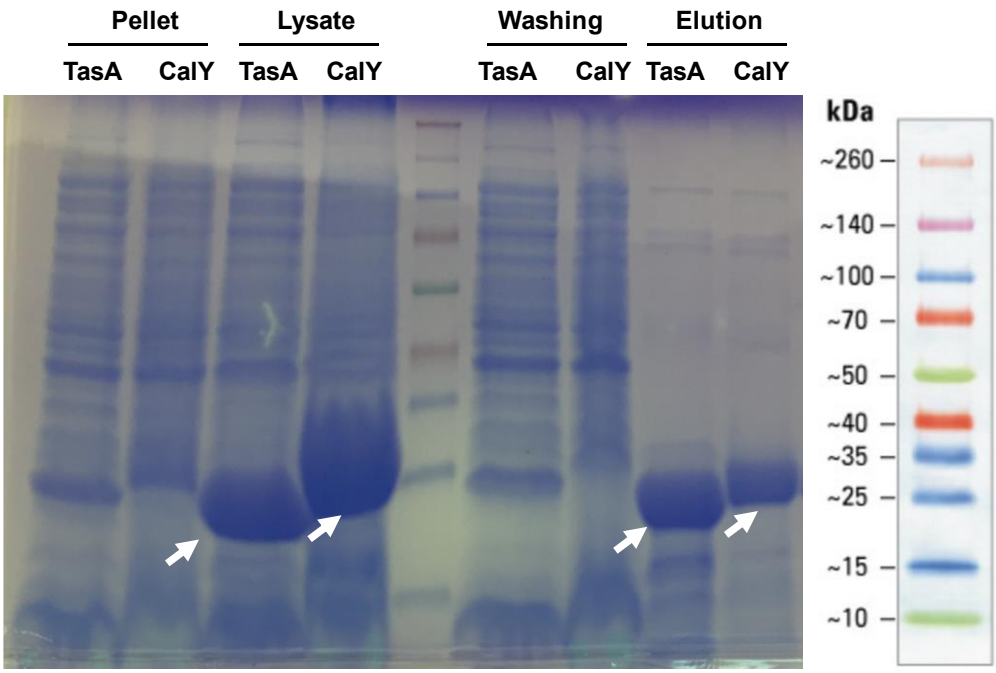

Figure 5. TasA and CalY are efficiently purified from *E. coli* cultures. SDS denaturing electrophoresis of the centrifuged lysate pellet, lysate, and the column washing and elution fractions from *E. coli* BL21 DE3 transformed with the plasmid pET30a-TasA or pET30a-CalY. Arrows indicate the proteins TasA and CalY.

As previously seen in the bioinformatic predictions, TasA and CalY are supposedly enriched in β-sheets (Table 1). In order to determine experimentally the secondary structure profile of these proteins, ECD (Electronic Circular Dichroism) over purified TasA and CalY were done after incubation of protein homogenates for 48 h at 25ºC. This analysis

showed high content of disorder and β-strands and comparatively lower presence of α-helix, which are almost absent in the TasA structure (Fig. 6). Unordered regions seemed to dominate the structure of these proteins at these experimental conditions, which, based on studies with other amyloids, might be prone to β-sheet structures during the process of polymerization (Tompa, 2009).

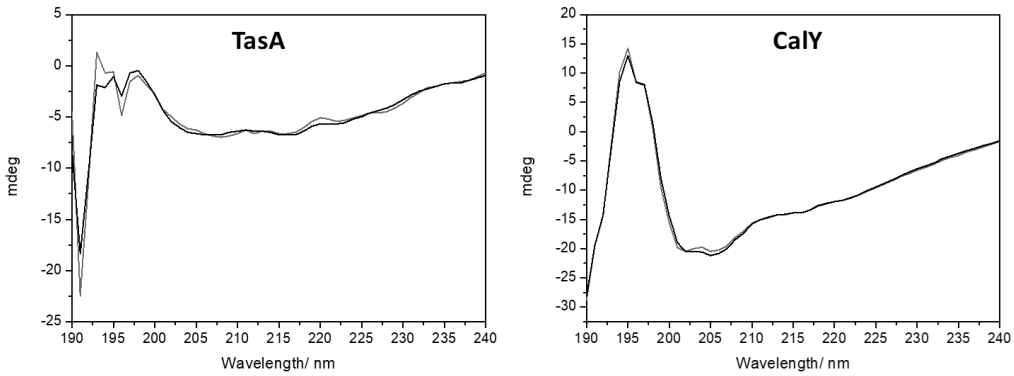

	Helix	Strand	Turns	Unordered
TasA	0.03	0.3	0.18	0.48
CalY	0.17	0.27	0.22	0.33

Figure 6. TasA and CalY show high enrichment in β-strands. ECD spectrums (grey) of TasA (left) and CalY (right) (0.4 mg/ml), compared with the predicted spectrum (Black line). The table resume the content of secondary structures of each protein.

The polymerization process of amyloids is usually dependent on the formation of intermolecular β-sheet. To test experimentally the enrichment in this form of secondary structure we used ATR-FTIR (Attenuated Total Reflectance-Fourier Transformed InfraRed) analysing the amide I region (1700–1600 cm^{-1}) on purified TasA and CalY, both

incubated at room temperature during 48 h to let each protein polymerize (Fig. 7). A band at 1630 $cm^{-1,}$ attributed to β-sheet structures, dominated the spectrums of TasA and CalY (Lefèvre and Subirade, 2003). Interestingly and according to the ECD findings, only CalY showed a small proportion of α-helix. None antiparallel β-sheet structures were found (~1690 cm^{-1}), suggesting that fibrillation might adopt a parallel position.

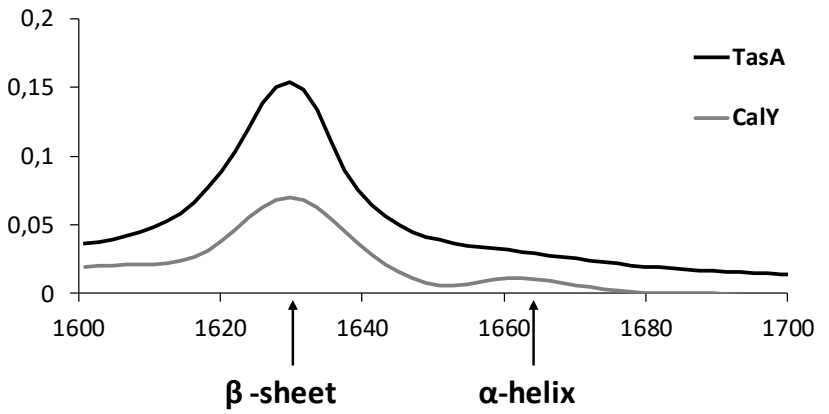

Figure 7. TasA and CalY show high enrichment in β-strands. ATR-FTIR spectrum in the interval of the Amide I, related to amyloid β-sheet singature, of the proteins TasA and CalY (1 mg/ml) after 48 h of incubation at room temperature.

Thioflavin-T (ThT) is one of the most frequently used fluorescent dyes to track the fibrillation of amyloids. The staining of amyloids with ThT provokes a shift from 385 nm to 450 nm in the excitation maximum, and from 445 nm to 490 nm in the emission maximum (LeVine, 1993; Naiki

et al., 1989). Amyloid fibrillation depends among other variables on pH, which determines the charge stage of amino acids and thus their interactions and the secondary structure of the proteins. Homogenates of TasA and CalY were adjusted to pH 5-8, incubated for 48 h and stained with ThT (Fig. 8). The higher emission intensity of TasA than CalY at pH 7 is suggestive of the higher propensity of these proteins to form amyloid aggregates. Values of emission of both proteins at pH5 were closer to the control, revealing that this pH is no favourable to fibrillation, at least under the polymerization conditions used in this study.

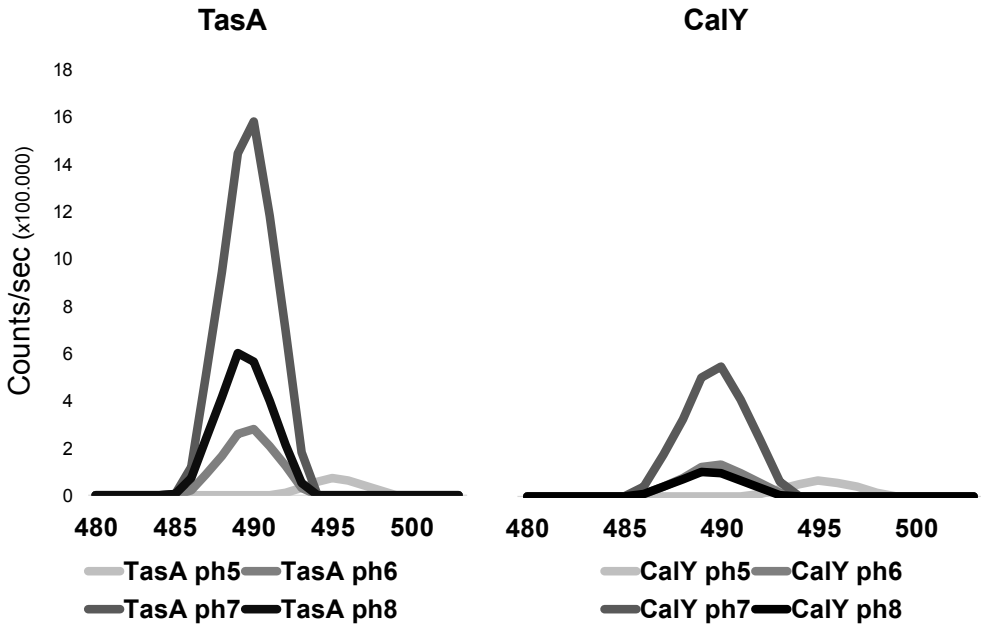

Figure 8. TasA and CalY show amyloid like ThiflavinT fluorescent emission. Emission spectrum of ThT assay of TasA and CalY (1mg/ml) at different pH after 48 h of incubation. TasA shows higher emission intensity than CalY.

To confirm this amyloid staining features we also did experiments of staining with Congo Red, which showed the typical increase in the absorbance of the protein homogenates at 540-550 nm upon binding to amyloids (Kazushige et al., 2010; Wu et al., 2013).

Pervious *in silico* analysis showed 65 % of identity among TasA and CalY, the fact that the two proteins are processed by the same signal peptidase led us to think on a putative collaboration of the two proteins during fibre assembly. Thus, in this analysis, we used different mixtures of the proteins TasA and CalY under different conditions (Fig. 9)

After 72 h of incubation, visible aggregates stained with Congo Red could be observed (Fig.9A). Surprisingly, at pH 6 TasA or CalY alone did not show aggregates, although mixtures of both (except for 90% CalY + 10% TasA) promoted the formation of extensive visible aggregates, confirming that these proteins somehow interact inducing protein aggregation. The same effect was observed at pH7, but in mixtures with higher amount of TasA. Comparison of the absorbance of TasA and CalY pure samples showed a higher score in TasA, in line with the results of ThT assay, suggesting again that TasA possesses a higher amyloid folding tendency (Fig. 9B).

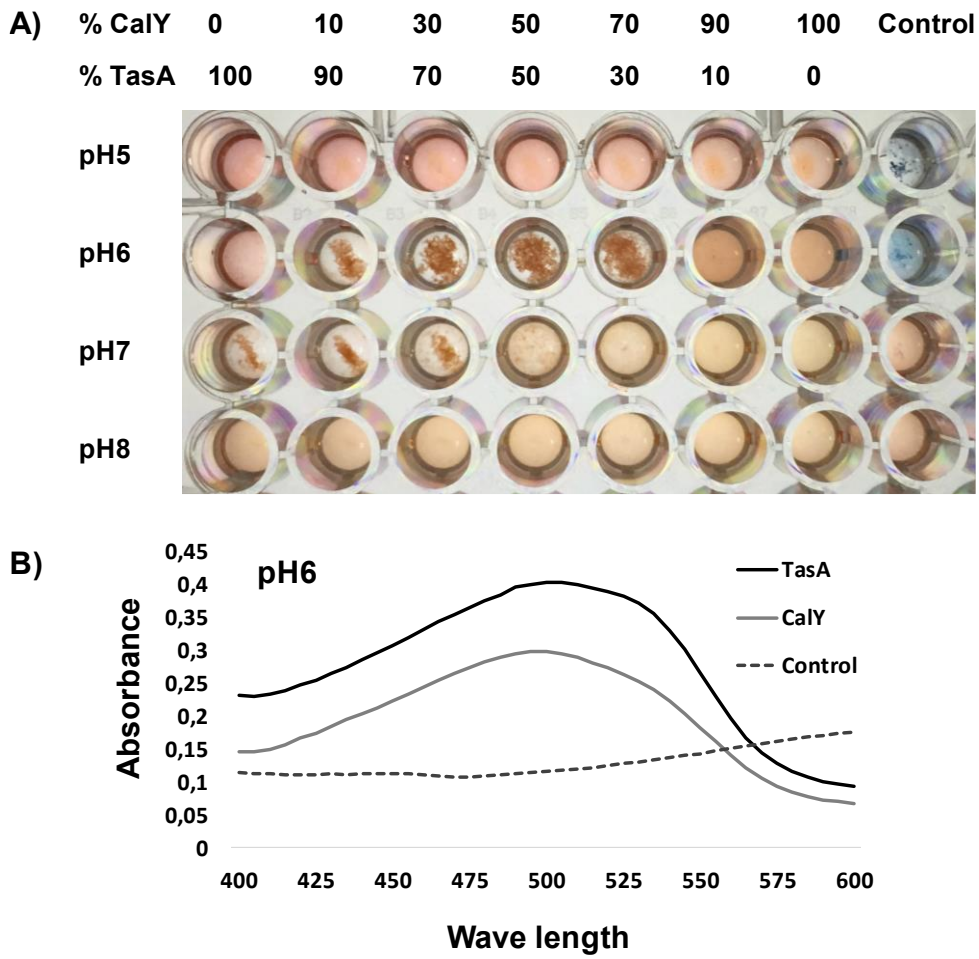

Figure 9. TasA and CalY interaction induce aggregation. A) Aggregation of protein mixtures of TasA and CalY with Congo Red at different pH's after 72 h of incubation at room temperature. B) Absorbance of TasA and CalY with Congo Red at pH 6.

2. TasA and CalY polymerizes in vitro

All previous findings were indicative of the intrinsic amyloid nature of TasA and CalY, thus both proteins should be able to assemble fibres.

Protein samples of TasA and CalY from the aggregation assay with Congo Red at different pH´s were observed at Transmission Electron Microscopy (TEM) to look for fibrillation and check that those aggregates correspond with amyloid fibrillation and not with amorphous aggregates (Fig. 10). TasA formed tangles of large fibres at any pH, although at pH 5 a tendency to assemble amorphous aggregates rather than fibrils was visible in TasA (Fig. 10).

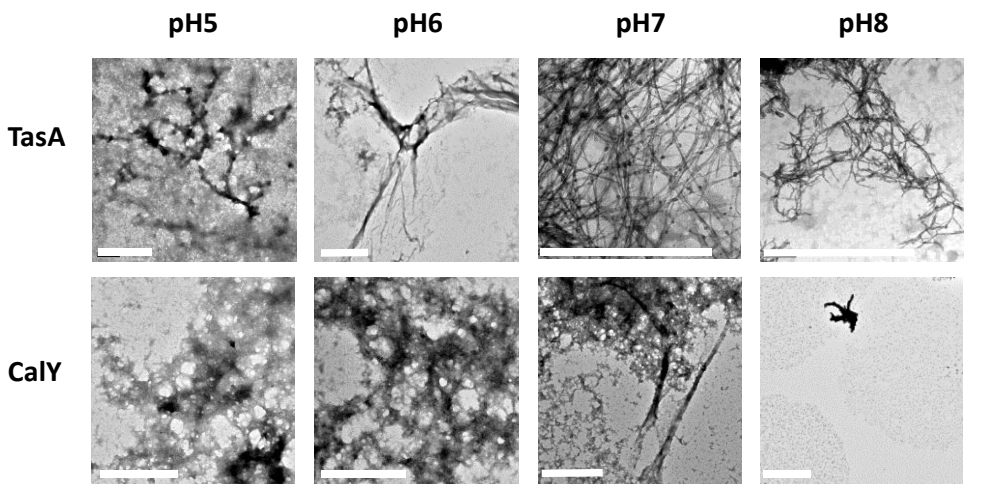

Figure 10. TasA and CalY polymerize independently. Transmission Electron Microscopy (TEM) images of the proteins TasA and CalY incubated during 48 h with Congo Red at different pHs. Bars =1µm.

On the other hand, fibrils were also observed in CalY, but the major conformation observed was a morphology that looks a mixture of fibres and aggregates with amorphous appearance, resulting in a morphology similar to grids. Although, looking in detail that aggregates, it is possible

to see brunches of small fibrils highly interconnected, revealing that they are not amorphous clots. In alignment with the previous results from the ThT assay, we could not visualize fibres of pure CalY at pH 8.

Samples of the protein mixtures at pH 6, which showed aggregation, were also observed at TEM. Surprisingly, all the samples showed similar polymerization pattern with a grid morphology, suggesting that CalY induces over TasA this kind of polymerization (Fig.11). In a process called secondary nucleation, two different fibres can interact and connect each other at any point of the fibre, or a new fibre can grow laterally from other already preformed. The grid morphology seems to be the result of a highly tendency of secondary nucleation, a function we hypothesize to be attributed to CalY, although TasA still retains certain secondary nucleation properties. Only in a 10% of CalY mixture was seen a reduced grid morphology, showing polymers formed by thin fibres with less ramifications. In the other mixtures, it can be observed much more ramification and most of them result in very thin fibres with an aspect of prickles.

Based on the morphology of the aggregates or fibres observed in the protein mixtures at TEM, we wondered if there were differences at a molecular level when the proteins TasA and CalY are mixed at different proportions. In agreement with *in silico* predictions in which high free energy values of the interactions among both proteins, the ThT assay showed that amyloid properties of TasA remain equal in the presence of CalY. Mixtures of proteins at pH7 result in intermediate fluorescent values between pure TasA and pure CalY, and always lower than TasA alone. (Fig. 12).

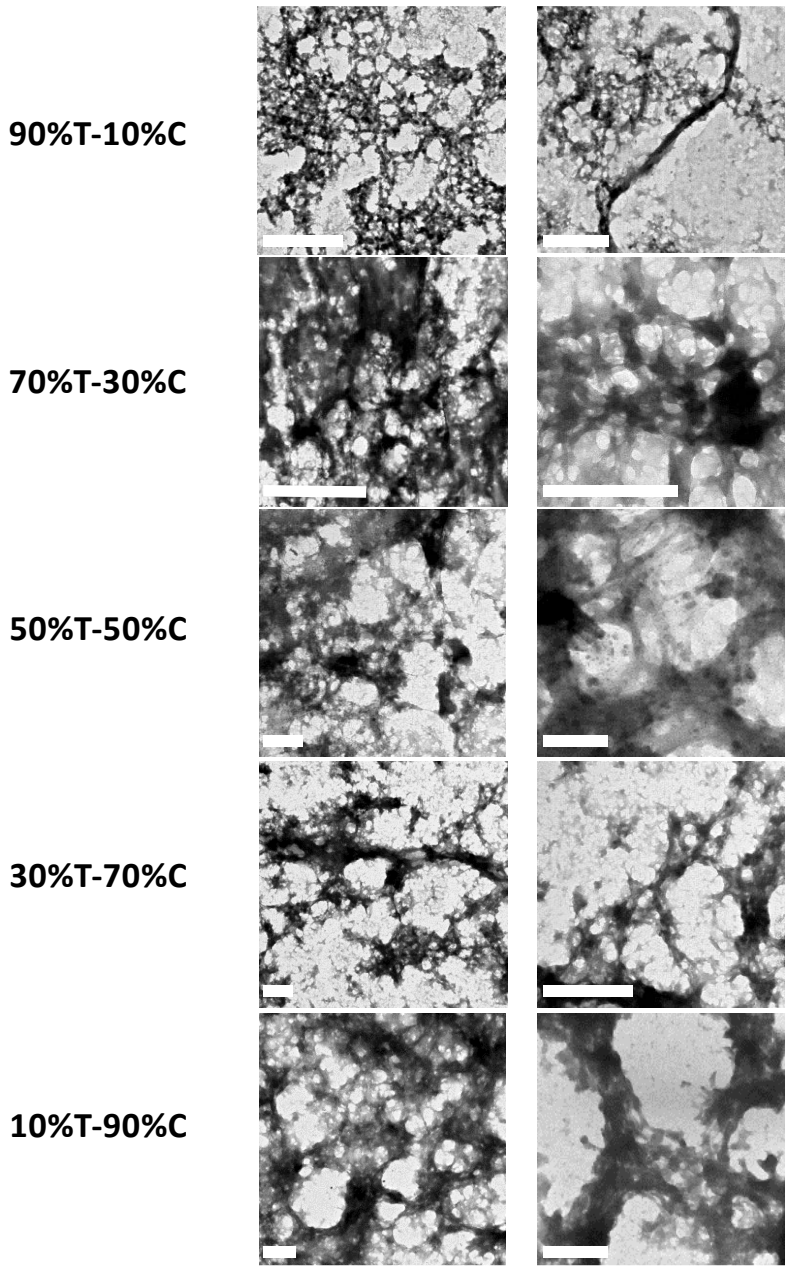

Figure 11. CalY influence TasA polymerization pattern. Transmission Electron Microscopy (TEM) images of mixtures of TasA and CalY incubated during 48 h with Congo Red at pH 6. Bars equal 500 nm. T stands for TasA and C for CalY. Right column images are zoomed areas of left column images.

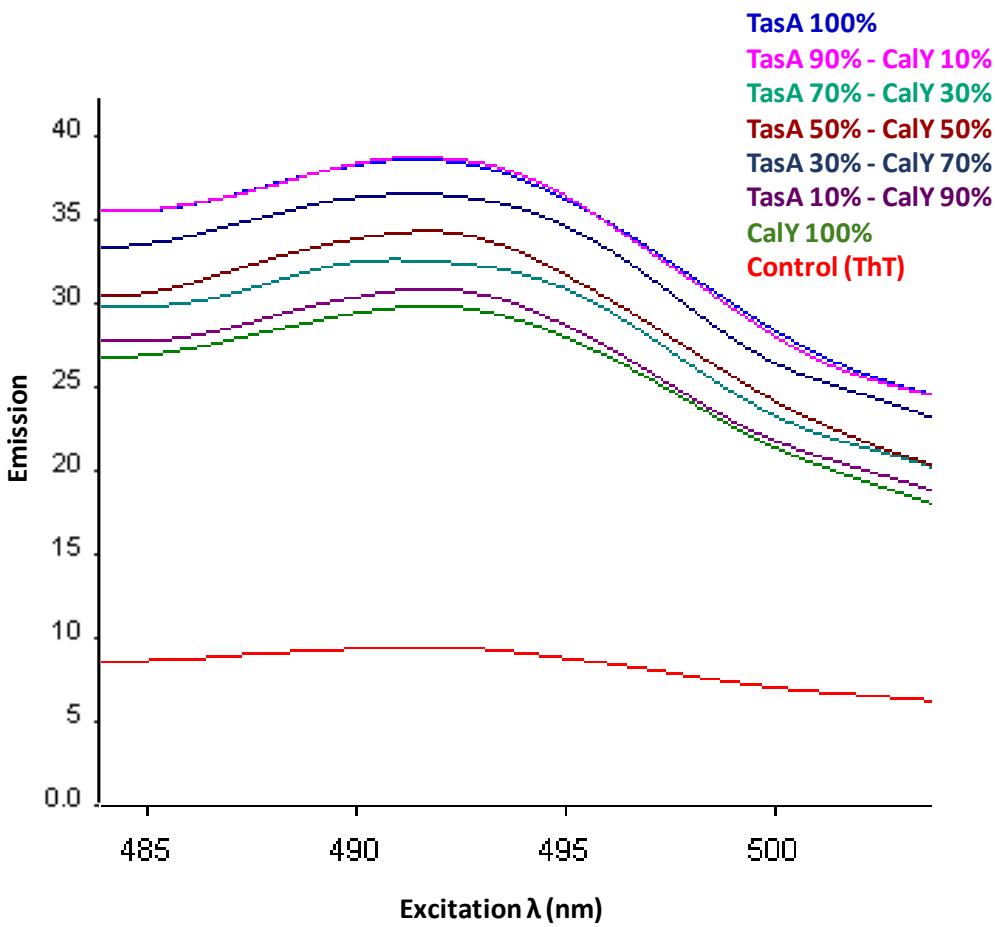

Figure 12. TasA and CalY modify their amyloid properties upon interaction. Thioflavin T emission spectrums of pure TasA and CalY and mixtures of both proteins at pH7 after 48 h of incubation at RT.

Polymerization kinetics of TasA, CalY and mixtures

Polymerization is a complex and ordered process which initiates with the formation of oligomers that interact and aggregate into more and more organized structures, a process which can be monitored using Dynamic Light Scattering (DLS). This technique provides with two parameters, which give an idea of the average size of the aggregates and the diversity of the aggregates size (PDI). It should be noticed that CalY have a high average particle size which decreases over time in contrast to TasA, which maintains a more stable average size (Fig. 13A). It should be also noticed that both proteins show a high polydispersion PDI value (Fig. 13B). PDI values higher than 0.7 indicate a high variability in particle size, what is the case of initial measurements. This parameter falls to 0.3 at the fourth day, indicating the occurrence of protein rearrangement to a regular size particle range (Fig. 13A). Equitably mixtures of TasA and CalY show intermediates values of particle size and PDI at earlier times.

Further measurements on the same samples showed a rearrangement of proteins into a similar particle average (approx. 1µm) and a reduced polydispersion PDI values. Interestingly, equitably mixtures showed an earlier rearrangement of the particle sizes and a faster reduction of PDI, revealing that TasA and CalY interaction improve the process of aggregation.

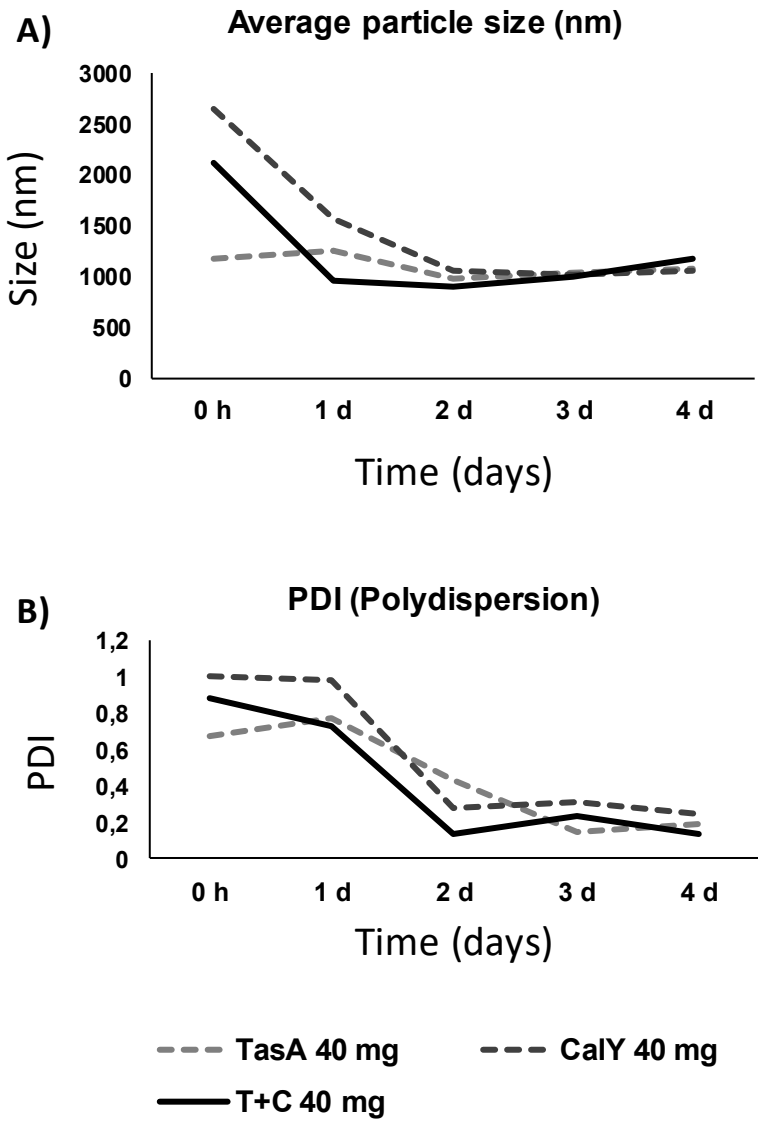

Figure 13. Polymerization kinetic of TasA and CalY. Dynamic Light Scattering kinetics of TasA, CalY and a 50% mixture of both proteins at pH 7. A) Average particle size in nm. B) PDI values, indicative of the polydispersion of the particle size.

3. TasA but not CalY expressed in *E. coli* rescues the formation of biofilm of a *tasA* mutant

Previous studies demonstrated that external addition of TasA to a *tasA* mutant of *B. subtilis* rescued the formation of wrinkly pellicles (Romero et al., 2010). The addition of purified TasA, CalY or both proteins to a culture of *B. cereus* wild type did not change the phenotype compared to controls (Fig. 14). The same results were observed upon addition of pure CalY or a mixture of TasA and CalY to a *calY* mutant. These results may initially lead to the conclusion that CalY is not functional. However, the addition of the mixture to a *tasA* mutant results in a big mass of pellicle biofilm, in contrast with the addition of only TasA, revealing that purified CalY is indeed functional. We speculated that this behaviour could be due to the large amount of protein added given that the total amount of protein raised to 100 µg. Therefore, we carried out an experiment in a *tasA* mutant strain of *B. cereus* adding different quantities of purified protein TasA to assess the putative effect of the amount of protein added (Fig. 15).

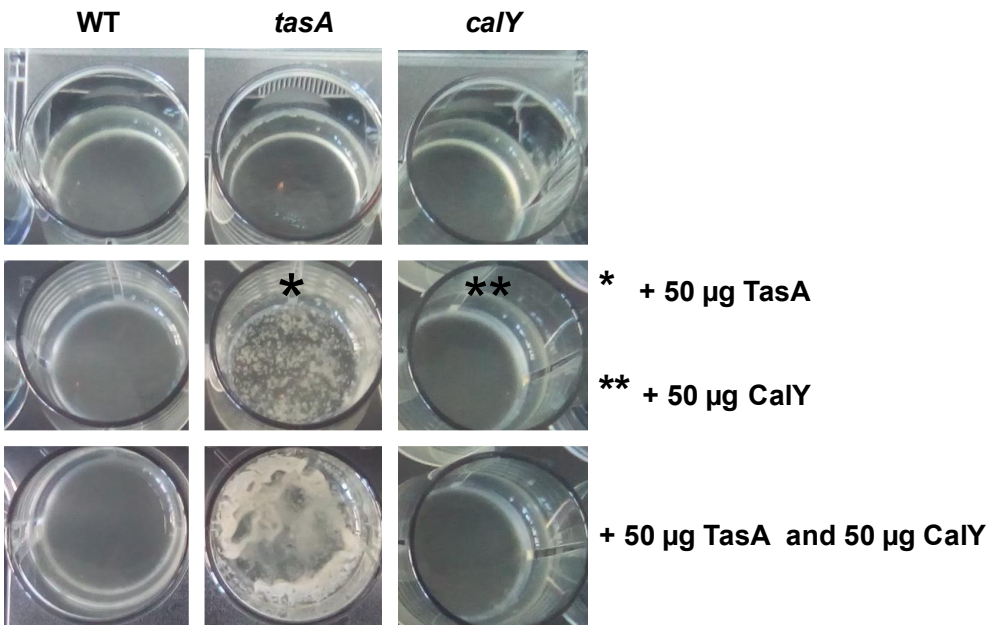

Figure 14. External complementation experiments in biofilms of wild type and mutants in *tasA* and *calY*. Purified TasA and CalY were added to the medium cultures at the beginning of the experiment. Pictures were taken after 24 h of incubation at 28ºC without shaking.

The external complementation of *tasA* mutant with purified TasA at different quantities provided a similar result, the restoration of biofilm formation, revealing that this reversion is quantity independent, and that purified CalY is functional and such huge biofilm pellicle in vivo is due to the interaction with TasA (Fig. 15). After 48 h of culture, *tasA* mutant shows a characteristic phenotype, a thick ring of biomass but loosely attached to the wall of the well. Besides, the liquid culture becomes clear, in contrast to the wild type, in which the medium culture is visibly

turbid. All quantities of TasA added to the cultures resulted in a normal biofilm development and the rescue of the wild type phenotype: adhered biofilm to the wall of the well and similar turbidity of the liquid culture (Fig. 15). These experiments confirmed that the purification method renders protein with ability to fold and conserved functions. Besides, the phenotype of the *tasA* mutant suggests some deregulation of the bacterial physiology, recovered when the protein is externally added.

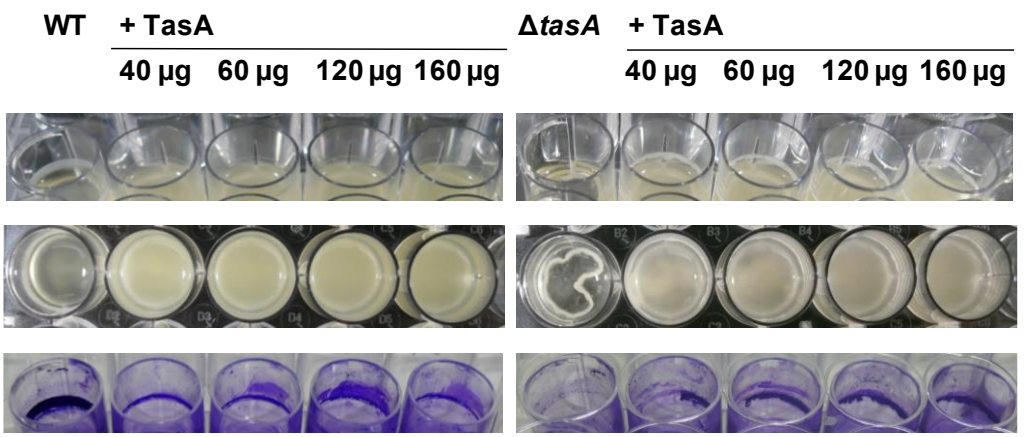

Figure 15. External complementation experiments in biofilms of wild type and *tasA* mutant. Purified TasA was added to the medium cultures at the beginning of the experiment. Pictures were taken after 48 h of incubation at 28ºC without shaking.

3. DISCUSSION

In previous studies, CalY has been reported to be a cell wall metalloprotease able to cleave casein (Fricke et al., 2001; Grass et al., 2004). Domain analysis of CalY and TasA of *B. cereus* and TasA of *B. subtilis* reveals that most of the sequence of the three proteins forms a peptidase M73 superfamily domain. We did not found any previous published work about TasA in *B.* cereus before those included in the chapter II of this thesis, and neither about peptidase activity of TasA of *B. subtilis*. We failed in our attempts to reproduce the previously reported protease activity of these proteins using the azo-casein cleavage assay (Data not shown). Two putative explanations are: i) the absence of such intrinsic protease activity or these proteins, or ii) that in our system, the two proteins evolve rapidly towards amyloid aggregates and fibres, which block the protease activity of the monomeric form. In any case, attending to their amyloid intrinsic nature and as previously seen in other functional amyloids, distinct functions can be driven by different morphological stages of the protein (Maji et al., 2009).

The proteins TasA and CalY can be expressed and purified in *E. coli* BL21 DE3, allowing their study and characterization as amyloids. In the course of this thesis, another paper has been published giving exactly the opposite conclusion, that these proteins as the sibling of *B. subtilis* are not retaining amyloid properties (Erskine et al., 2017) . A possible explanation to this controversy may be given by the important part of unordered sequences in addition to the high proportion of β-sheets in

the native protein. It is known from other amyloids, that the disorders are especially susceptible to be reordered into relevant secondary structures which may participate in the protein folding or in intermolecular interactions, inducing a folding of these regions into β-sheets, which finally contribute to the amyloid formation, as happens in other amyloid systems (Krasnoslobodtsev et al., 2016). The amyloid protein CsgA of *E. coli* forms the pili and shows itself as an unstructured protein in their monomeric form, acquiring the β-sheets structures during the aggregation and polymerization process which is controlled by the accessory proteins that block polymerization in the cytoplasm (CsgC), it secretion (CsgE, CsgG, CsgF) or its external polymerization (CsgB) (Van Gerven et al., 2015). In addition, and in alignment to our conclusions, a recent structural biology paper has unquestionably confirmed the amyloid nature, previously proposed, of TasA from *B. subtilis* (Diehl et al., 2018; Romero et al., 2010), and we do have additional information from NMR studies done in our group that support the amyloid features of the two proteins (Personal Communication).

Aggregation assay and TEM studies suggest that TasA has conserved higher amyloidogenic properties than CalY during the evolution of *B. cereus*. CalY polymerization presents a tendency to be hyper branched, probably as a consequence of the higher propensity to secondary nucleation, which results in a special morphology of the amyloid in a grid shape rather than fibres, as happens in pure TasA polymers. These differences in the behaviour between TasA and CalY can be explained by the differences found in the secondary structure enrichment revealed by ATR-FTIR analysis, that showed the less presence of β-sheets and

the presence of α-helix in CalY, which might interfere with the fibrillary polymerization process. TEM images of the protein mixtures showed a grid morphological pattern even in the presence of 10% of CalY, suggestive of a guiding role of CalY over the polymerization of TasA. However, the ThT experiments suggest that the final structure of the fibres must not be different to those formed by TasA alone. Therefore, there is synergistic or complementary role among the two proteins, that would happen at the very initial stages of polymerization, which is supported by the DLS finding, which overall indicates an acceleration of protein arrangement in the mixture TasA-CalY compared to each one alone.

Complementary functions happen in amyloid systems described in other bacterial species. In *B. subtilis*, the protein TapA has not been reported to possesses amyloid properties, but it accelerates the polymerization of TasA (Romero et al., 2011). *B. cereus* lacks TapA, evolving to a different system in which TasA and CalY complement each other, a fact supported by our findings in external complementation experiments. Amyloid polymerization is an extremely complex process influenced by many factors like concentration, local pH, temperature, time and other molecules in the environment that interact with these proteins, what must be perfectly orchestrated by *B. cereus* to yield an effective polymerization in grids and fibres, with the aim of providing structural stability to the biofilm and protect the bacterial cell community.

4. METHODS AND MATERIAL

Bacterial strains and culture conditions

The strain *E. coli* DH5α was used for plasmid construction and replication. *E. coli* BL21 DE3 was used for protein expression. *B. cereus* strains were grown in TY broth (1% tryptone, OXOID), 0.5% yeast extract (OXOID), 0.5% NaCl, 10 mM $MgSO_4$, and 0.1 mM $MnSO_4$). Antibiotics were used for protein expression at final concentrations of kanamycin 50 µg/ml. For phenotype restoration assays, purified proteins were added to the initial liquid culture.

Plasmids construction

The open reading frames of *tasA* and *calY* without the signal peptide were cloned using the primers listed on Table 1. Restriction sites for Nde I and Xho I were added to the primer tails to direct the cloning of the fragment into the plasmid pET30a (Novagen) cut with same enzymes. The final construct contains the open reading frame cloned in frame with a His-tag at C-terminal and the expression under control of an inducible promoter with IPTG.

Protein purification

E. coli BL21 DE3 was transformed separately with the plasmids pET30a-*tasA* or pET30a-*calY* and the transformation was plated in LB agar plates with kanamycin for selection. Several colonies were stuck into a 300 ml liquid LB and incubated with shaking at 150 rpm until

OD600 reached 0.7, when IPTG was added (1 mM final concentration) for induction of protein expression and incubation for 16h at 16ºC and 70 rpm. Pellet was harvested and suspended in phosphate buffer containing PMSF 1mM, lysozyme 0,2mg/ml and 2ml of cell lytic 10x (Sigma). After 1 h of incubation, three pulses of sonication of 1 min 80% amplitude were applied. After centrifuging at 8000G at 4°C, supernatant was filtered through a 0.45 µm Ø filter. Proteins were then purified in-bach using HIS-Select® Nickel Affinity Gel (Sigma) or in FPLC using HisTrap™ FF Ni-Sepharose columns (Amersham Biosciences) following the manufacturer instructions. Eluate was desalted using Slide-A-Lyzer™ Dialysis Cassettes (Thermo Fisher Scientific) or in FPLC using HiTrap™ Desalting (GE Healthcare). The protein was recovered in phosphate buffer pH8.

Thioflavin T and Congo Red binding assays

Thioflavin T (ThT) fluorescence assay was performed adding 20 µM ThT solution to protein samples and incubation at room temperature for 48 h. Excitation was done at 450 nm and emission was recorded as spectrums with a Fluorimeter FLS920 (Edinburgh Instruments).

Congo Red (CR) binding assay was performed adding 20 µM of CR to 200 µg of protein (2 mg/ml final concentration) and incubated at room temperature for 72 h. Absorbance spectrum was recorded using a Spectrophotometer Eon instrument (BioTek).

Spectroscopy analysis

Attenuated Total Reflectance-Fourier Transformed InfraRed (ATR-FTIR) was performed over desalted samples of proteins and suspended in deionized water at a final concentration of 1mg/ml, using a Spectrophotometer VERTEX 70. The amide I region of the spectrum (1700–1600 cm^{-1}) was used for secondary structure analysis.

Electronic Circular Dicroism (ECD) was performed in samples at 1.5 µgr/ml using a J-1000 Series Circular Dichroism spectrophotometers. Calculated secondary structures percentages were done using Dicroweb software.

Dynamic Light scattering

Protein samples at 400 µg/ml were analysed for evolution of aggregates at room temperature, using a Zetasizer Nano-ZS (Malvernequipment) and routinely protocols. Measurements were taken every 24 hours.

Transmission electron microscopy

Protein samples (5µl) were deposited on Cooper Grids and let dry. The grids were contrasted using 1% solution of uranyl acetate for 2 minutes, rinsed twice in distilled water 2 minutes and then dried prior to examination. Samples were visualized and photographed in a JEOL JEM-1400 transmission electron microscope.

5. Annex

Table 1. Primers for *tasA* and *calY* cloning.

Primer name	Sequence
NdeI.TasA.Fw	ttttt**CATATG**TTTTTCAGTGATAAAGAAGTGTCAAAC
	ttttt**CTCGAG**AGAACCGCGTGGCACCAGTTTTTCTTCA
XhoI.TasA.Rv	CCTGCTGTTTG
NdeI.CalY.Fw	ttttt**CATATG**GCATTGGGGTTAGCTTTAATTGG
	ttttt**CTCGAG**AGAACCGCGTGGCACCAGTTTTTCTTCC
XhoI.CalY.Rv	CCAGCTTCTTG

6. REFERENCES

Ankarcrona, M., Winblad, B., Monteiro, C., Fearns, C., Powers, E.T., Johansson, J., Westermark, G.T., Presto, J., Ericzon, B.-G., and Kelly, J.W. (2016). Current and future treatment of amyloid diseases. J. Intern. Med. *280*, 177–202.

Baker, K.R., and Rice, L. (2012). The Amyloidoses: Clinical Features, Diagnosis and Treatment. Methodist DeBakey Cardiovasc. J. *8*, 3–7.

Chapman, M.R., Robinson, L.S., Pinkner, J.S., Roth, R., Heuser, J., Hammar, M., Normark, S., and Hultgren, S.J. (2002). Role of Escherichia coli curli operons in directing amyloid fiber formation. Science *295*, 851–855.

Cheon, M., Chang, I., and Hall, C.K. (2012). Influence of temperature on formation of perfect tau fragment fibrils using PRIME20/DMD simulations. Protein Sci. Publ. Protein Soc. *21*, 1514–1527.

Chiti, F., and Dobson, C.M. (2006). Protein Misfolding, Functional Amyloid, and Human Disease. Annu. Rev. Biochem. *75*, 333–366.

Choi, M.-S., Kim, W., Lee, C., and Oh, C.-S. (2013). Harpins, multifunctional proteins secreted by gram-negative plant-pathogenic bacteria. Mol. Plant-Microbe Interact. MPMI *26*, 1115–1122.

Claessen, D., Rink, R., de Jong, W., Siebring, J., de Vreugd, P., Boersma, F.G.H., Dijkhuizen, L., and Wosten, H.A.B. (2003). A novel class of secreted hydrophobic proteins is involved in aerial hyphae formation in Streptomyces coelicolor by forming amyloid-like fibrils. Genes Dev. *17*, 1714–1726.

Cogen, A.L., Yamasaki, K., Muto, J., Sanchez, K.M., Crotty Alexander, L., Tanios, J., Lai, Y., Kim, J.E., Nizet, V., and Gallo, R.L. (2010). Staphylococcus epidermidis antimicrobial delta-toxin (phenol-soluble modulin-gamma) cooperates with host antimicrobial peptides to kill group A Streptococcus. PloS One *5*, e8557.

Coustou-Linares, V., Maddelein, M.L., Bégueret, J., and Saupe, S.J. (2001). In vivo aggregation of the HET-s prion protein of the fungus Podospora anserina. Mol. Microbiol. *42*, 1325–1335.

Diehl, A., Roske, Y., Ball, L., Chowdhury, A., Hiller, M., Molière, N., Kramer, R., Stöppler, D., Worth, C.L., Schlegel, B., et al. (2018). Structural changes of TasA in biofilm formation of Bacillus subtilis. Proc. Natl. Acad. Sci. 201718102.

Dueholm, M.S., Petersen, S.V., Sønderkær, M., Larsen, P., Christiansen, G., Hein, K.L., Enghild, J.J., Nielsen, J.L., Nielsen, K.L., Nielsen, P.H., et al. (2010). Functional amyloid in Pseudomonas. Mol. Microbiol. *77*, 1009–1020.

Dürr, U.H.N., Sudheendra, U.S., and Ramamoorthy, A. (2006). LL-37, the only human member of the cathelicidin family of antimicrobial peptides. Biochim. Biophys. Acta *1758*, 1408–1425.

Erskine, E., Morris, R., Schor, M., Earl, C., Gillespie, R.M.C., Bromley, K., Sukhodub, T., Clark, L., Fyfe, P., Serpell, L., et al. (2017). Formation of functional, non-amyloidogenic fibres by recombinant Bacillus subtilis TasA. BioRxiv 188995.

Forloni, G., Terreni, L., Bertani, I., Fogliarino, S., Invernizzi, R., Assini, A., Ribizzi, G., Negro, A., Calabrese, E., Volonté, M.A., et al. (2002). Protein misfolding in Alzheimer's and Parkinson's disease: genetics and molecular mechanisms. Neurobiol. Aging *23*, 957–976.

Fowler, D.M., Koulov, A.V., Alory-Jost, C., Marks, M.S., Balch, W.E., and Kelly, J.W. (2006). Functional amyloid formation within mammalian tissue. PLoS Biol. *4*, e6.

Fricke, B., Drössler, K., Willhardt, I., Schierhorn, A., Menge, S., and Rücknagel, P. (2001). The cell envelope-bound metalloprotease (camelysin) from Bacillus cereus is a possible pathogenic factor. Biochim. Biophys. Acta *1537*, 132–146.

Girych, M., Gorbenko, G., Maliyov, I., Trusova, V., Mizuguchi, C., Saito, H., and Kinnunen, P. (2016). Combined thioflavin T-Congo red fluorescence assay for amyloid fibril detection. Methods Appl. Fluoresc. *4*, 034010.

Grass, G., Schierhorn, A., Sorkau, E., Müller, H., Rücknagel, P., Nies, D.H., and Fricke, B. (2004). Camelysin Is a Novel Surface Metalloproteinase from Bacillus cereus. Infect. Immun. *72*, 219–228.

Hamodrakas, S.J. (2011). Protein aggregation and amyloid fibril formation prediction software from primary sequence: towards controlling the formation of bacterial inclusion bodies. FEBS J. *278*, 2428–2435.

Iconomidou, V.A., Chryssikos, G.D., Gionis, V., Vriend, G., Hoenger, A., and Hamodrakas, S.J. (2001). Amyloid-like fibrils from an 18-residue peptide analogue of a part of the central domain of the B-family of silkmoth chorion proteins. FEBS Lett. *499*, 268–273.

Imran, M., and Mahmood, S. (2011). An overview of human prion diseases. Virol. J. *8*, 559.

Jang, H., Arce, F.T., Mustata, M., Ramachandran, S., Capone, R., Nussinov, R., and Lal, R. (2011). Antimicrobial protegrin-1 forms amyloid-like fibrils with rapid kinetics suggesting a functional link. Biophys. J. *100*, 1775–1783.

Kai-Larsen, Y., Lüthje, P., Chromek, M., Peters, V., Wang, X., Holm, A., Kádas, L., Hedlund, K.-O., Johansson, J., Chapman, M.R., et al. (2010). Uropathogenic Escherichia coli modulates immune responses and its curli fimbriae interact with the antimicrobial peptide LL-37. PLoS Pathog. *6*, e1001010.

Kazushige, Y., Andrew D., F., Amanda R., A., Daniel R., W., and Ruel E., M. (2010). Spectroscopic and calorimetric studies of congo red dye-amyloid peptide complexes. J. Biophys. Chem. *2010*.

Kenney, J.M., Knight, D., Wise, M.J., and Vollrath, F. (2002). Amyloidogenic nature of spider silk. Eur. J. Biochem. *269*, 4159–4163.

Khurana, R., Gillespie, J.R., Talapatra, A., Minert, L.J., Ionescu-Zanetti, C., Millett, I., and Fink, A.L. (2001). Partially folded intermediates as critical precursors of light chain amyloid fibrils and amorphous aggregates. Biochemistry (Mosc.) *40*, 3525–3535.

Kowalewski, T., and Holtzman, D.M. (1999). In situ atomic force microscopy study of Alzheimer's beta-amyloid peptide on different substrates: new insights into mechanism of beta-sheet formation. Proc. Natl. Acad. Sci. U. S. A. *96*, 3688–3693.

Krasnoslobodtsev, A.V., Deckert-Gaudig, T., Zhang, Y., Deckert, V., and Lyubchenko, Y.L. (2016). Polymorphism of amyloid fibrils formed by a peptide from the yeast prion protein Sup35: AFM and Tip-Enhanced Raman Scattering studies. Ultramicroscopy *165*, 26–33.

Lefèvre, T., and Subirade, M. (2003). Formation of intermolecular beta-sheet structures: a phenomenon relevant to protein film structure at oil-water interfaces of emulsions. J. Colloid Interface Sci. *263*, 59–67.

LeVine, H. (1993). Thioflavine T interaction with synthetic Alzheimer's disease beta-amyloid peptides: detection of amyloid aggregation in solution. Protein Sci. Publ. Protein Soc. *2*, 404–410.

Linse, S. (2017). Monomer-dependent secondary nucleation in amyloid formation. Biophys. Rev. *9*, 329–338.

Maezawa, I., Hong, H.-S., Liu, R., Wu, C.-Y., Cheng, R.H., Kung, M.-P., Kung, H.F., Lam, K.S., Oddo, S., Laferla, F.M., et al. (2008). Congo red and thioflavin-T analogs detect Abeta oligomers. J. Neurochem. *104*, 457–468.

Maji, S.K., Perrin, M.H., Sawaya, M.R., Jessberger, S., Vadodaria, K., Rissman, R.A., Singru, P.S., Nilsson, K.P.R., Simon, R., Schubert, D., et al. (2009). Functional amyloids as natural storage of peptide hormones in pituitary secretory granules. Science *325*, 328–332.

Makin, O.S., Atkins, E., Sikorski, P., Johansson, J., and Serpell, L.C. (2005). Molecular basis for amyloid fibril formation and stability. Proc. Natl. Acad. Sci. U. S. A. *102*, 315–320.

Masters, C.L., and Selkoe, D.J. (2012). Biochemistry of Amyloid β-Protein and Amyloid Deposits in Alzheimer Disease. Cold Spring Harb. Perspect. Med. *2*.

Molina-García, L., Moreno-del Álamo, M., Botias, P., Martín-Moldes, Z., Fernández, M., Sánchez-Gorostiaga, A., Alonso-del Valle, A., Nogales, J.,

García-Cantalejo, J., and Giraldo, R. (2017). Outlining Core Pathways of Amyloid Toxicity in Bacteria with the RepA-WH1 Prionoid. Front. Microbiol. *8*.

Naiki, H., Higuchi, K., Hosokawa, M., and Takeda, T. (1989). Fluorometric determination of amyloid fibrils in vitro using the fluorescent dye, thioflavin T1. Anal. Biochem. *177*, 244–249.

Pham, C.L.L., Kwan, A.H., and Sunde, M. (2014). Functional amyloid: widespread in Nature, diverse in purpose. Essays Biochem. *56*, 207–219.

Podobnik, M., Marchioretto, M., Zanetti, M., Bavdek, A., Kisovec, M., Cajnko, M.M., Lunelli, L., Serra, M.D., and Anderluh, G. (2015). Plasticity of Listeriolysin O Pores and its Regulation by pH and Unique Histidine. Sci. Rep. *5*.

Ramsook, C.B., Tan, C., Garcia, M.C., Fung, R., Soybelman, G., Henry, R., Litewka, A., O'Meally, S., Otoo, H.N., Khalaf, R.A., et al. (2010). Yeast cell adhesion molecules have functional amyloid-forming sequences. Eukaryot. Cell *9*, 393–404.

Romero, D., Aguilar, C., Losick, R., and Kolter, R. (2010). Amyloid fibers provide structural integrity to Bacillus subtilis biofilms. Proc. Natl. Acad. Sci. U. S. A. *107*, 2230–2234.

Romero, D., Vlamakis, H., Losick, R., and Kolter, R. (2011). An Accessory Protein Required for Anchoring and Assembly of Amyloid Fibers in B. subtilis Biofilms. Mol. Microbiol. *80*, 1155–1168.

Sabate, R., Rousseau, F., Schymkowitz, J., Batlle, C., and Ventura, S. (2015). Amyloids or prions? That is the question. Prion *9*, 200–206.

Shahnawaz, M., and Soto, C. (2012). Microcin Amyloid Fibrils A Are Reservoir of Toxic Oligomeric Species. J. Biol. Chem. *287*, 11665–11676.

Shammas, S.L., Knowles, T.P.J., Baldwin, A.J., MacPhee, C.E., Welland, M.E., Dobson, C.M., and Devlin, G.L. (2011). Perturbation of the Stability of Amyloid Fibrils through Alteration of Electrostatic Interactions. Biophys. J. *100*, 2783–2791.

Shea, C., Nunley, J.W., Williamson, J.C., and Smith-Somerville, H.E. (1991). Comparison of the adhesion properties of Deleya marina and the exopolysaccharide-defective mutant strain DMR. Appl. Environ. Microbiol. *57*, 3107–3113.

Sood, R., Domanov, Y., Pietiäinen, M., Kontinen, V.P., and Kinnunen, P.K.J. (2008). Binding of LL-37 to model biomembranes: insight into target vs host cell recognition. Biochim. Biophys. Acta *1778*, 983–996.

Stöhr, J., Weinmann, N., Wille, H., Kaimann, T., Nagel-Steger, L., Birkmann, E., Panza, G., Pruºsiner, S.B., Eigen, M., and Riesner, D. (2008). Mechanisms of prion protein assembly into amyloid. Proc. Natl. Acad. Sci. *105*, 2409–2414.

Stöver, A.G., and Driks, A. (1999). Control of synthesis and secretion of the Bacillus subtilis protein YqxM. J. Bacteriol. *181*, 7065–7069.

Tjernberg, L.O., Pramanik, A., Björling, S., Thyberg, P., Thyberg, J., Nordstedt, C., Berndt, K.D., Terenius, L., and Rigler, R. (1999). Amyloid beta-peptide polymerization studied using fluorescence correlation spectroscopy. Chem. Biol. *6*, 53–62.

Tompa, P. (2009). Structural disorder in amyloid fibrils: its implication in dynamic interactions of proteins. FEBS J. *276*, 5406–5415.

Van Gerven, N., Klein, R.D., Hultgren, S.J., and Remaut, H. (2015). Bacterial amyloid formation: structural insights into curli biogensis. Trends Microbiol. *23*, 693–706.

Wang, X., Hammer, N.D., and Chapman, M.R. (2008). The Molecular Basis of Functional Bacterial Amyloid Polymerization and Nucleation. J. Biol. Chem. *283*, 21530–21539.

Wu, J.W., Liu, K.-N., How, S.-C., Chen, W.-A., Lai, C.-M., Liu, H.-S., Hu, C.-J., and Wang, S.S.-S. (2013). Carnosine's effect on amyloid fibril formation and induced cytotoxicity of lysozyme. PloS One *8*, e81982.

Zhu, M., Souillac, P.O., Ionescu-Zanetti, C., Carter, S.A., and Fink, A.L. (2002). Surface-catalyzed Amyloid Fibril Formation. J. Biol. Chem. *277*, 50914–50922.

CHAPTER IV

THE MOLECULAR MACHINERY OF BIOFILM ASSEMBLY OF *B. cereus*. BIOFILM FORMATION DISPLAY INTRINSIC OFFENSIVE AND DEFENSIVE FEATURES

1. INTRODUCTION

Bacillus cereus is a widespread bacterium that is able to colonize a multitude of niches, including soil and seawater, where it survives living as a saprophyte. This bacterium can also be found in association with plant tissues, living as a commensal or in symbiosis as a rhizosphere inhabitant (Hu et al., 2017). Mammalian or arthropod guts are also a niche for *B. cereus,* where it can live as a commensal or a pathogen, either opportunistic or not (Kusama et al., 2015; Swiecicka and Mahillon, 2006). The versatility shown by these bacteria evidence the capacity for resilience to a wide range of extreme environmental conditions (von Stetten et al., 1999). *B. cereus* gives the name to the *B. cereus sensu lato* group composed of, among others, the phylogenetically similar bacterial species *B. thuringiensis* and *B. anthracis*, which are diverse in their impact on insects and human health (Helgason et al., 2000). Some strains of *B.* cereus provide benefits to plants, as a promoter of growth (PGP) or biocontrol against microbial diseases, while others are proposed as probiotics for cattle. By contrast, there are strains responsible for human pathologies mainly caused by food poisoning, contamination of products in the food industry or even food spoilage (Rajasekar and Ting, 2010; Schultz et al., 2011; Wan et al., 2018). Biofouling, clogging and corrosive consequences of *B. cereus* in industrial devices complete the concerns of humans regarding this bacteria species (Rajasekar et al., 2007).

Regardless of the consequences, most of the scenarios listed above are believed to be related to the organization of bacterial cells in

biofilms. The formation of biofilms is considered an important step in the life cycle of most bacterial species, and it is known to be related to outbreaks of diseases, resistance to antimicrobials, or contamination of medical and industrial devices (Gurler et al., 2012). Approximately 65% of bacterial human diseases are estimated to involve bacterial biofilms, thus these multicellular structures might be considered potential targets to fight bacterial diseases (Potera, 1999). Based on the relevance of bacterial biofilms, our research focuses on elucidating the intrinsic factors that *B. cereus* cells employ to transition to this sedentary lifestyle, and which are the possible environmental triggers. In general, it is known that after encountering an adequate surface, motile bacterial cells switch from a floating or planktonic to a sessile lifestyle followed by the assembly of an extracellular matrix. Studies on biofilm formation in the gram-positive bacterium *Bacillus subtilis* have substantially contributed to our understanding of the intricate machinery devoted to efficiently complete this transition (Vlamakis et al., 2013). While studies on biofilm formation by specific *B. cereus* strains indicate that key processes resemble *B. subtilis* biofilm development, clear differences start to be perceived, representative of the evolutionary distance between the two species: i) the minor role of the exopolysaccharide of *B. cereus* homologous to the e*psA-O* of *B. subtilis* in biofilm formation; ii) the absence of homologues to the accessory protein TapA, necessary for amyloid-like fiber assembly in *B. subtilis*, iii) the existence of two paralogs of *subtilis* TasA, i.e., TasA and CalY (Caro-Astorga et al., 2015); iv) the absence of the hydrophobic BlsA protein, which coats the biofilm in *B. subtilis* (Hobley et al., 2013); v) the differences in the

regulatory networks of biofilm formation, lacking the regulatory subnetworks II and III, involving SlrA-SlrR-SinR and Abh, and the gain of the pleiotropic regulator PlcR involved in virulence and biofilm formation; vii) the absence in *B. cereus* of the lipoprotein Med associated with KinD phosphorylation activity that triggers biofilm formation (Banse et al., 2011); and viii) the different adhesive properties of the spores of *B. cereus* (Gao et al., 2015). Therefore, novel in-depth studies are required not only to confirm similarities between the two microbes but also to highlight unexplored differences.

In a previous study, we proved that *B. cereus* ATCC 14579 is able to form a biomass of cells adhering to abiotic surfaces, a process that clearly evolved with time. A genomic region containing the two paralogous proteins TasA and CalY, the signal peptidase SipW and the locus *BC_2180* were proven essential in the transition from planktonic or floating to sedentary and further growth of the biofilm. The differences found in *B. subtilis* in this and other reports led us to investigate which were the additional intrinsic genetic features that permit *B. cereus* to resolve hypothetical environmental situations by the assembly of biofilms. The combination of two high throughput techniques, RNAseq and iTRAQ mass spectrometry, enabled us to acquire solid evidence of the global changes differentiating floating from biofilm programmed cells. First, initial reinforcement of the cell wall prepares cells for further assembly of macromolecules as polysaccharides and other adhesins, and additionally protects the cells individually from external aggressions. Second, biofilm- associated cells are prone to defend against aggression, competitors, antimicrobials, or the host immune

system, while floating cells are more aggressive against the human host. Our findings argue in favor of the metabolic versatility of *B. cereus* and the fine tuning in gene expression that permits this species to maintain the two distinct subpopulations necessary to face changeable environmental conditions. In fact, we also found several metabolic changes and the existence of cooperative metabolic relations among floating and biofilm-associated cells, with members of each cellular phase developing different parts of the same metabolic pathway. We also provide provisional function assignments to some hypothetical proteins with unknown functions that have emerged as being specific for the biofilm-associated lifestyle.

2. RESULTS AND DISCUSSION

1. Changes in gene expression define different stages in biofilm formation

To study the transition of cells from floating to biofilm and its further progression, we used static cultures and developed the experimental setup summarized in Figure 1 (described in detail in the Materials and Methods). Regarding biofilm formation as a developmental program, we considered 24 h cultures as the initial time to do the comparison, when biomass started to be visible and thus suitable for recollection and further analysis. This comparison allowed us to define the initial changes in gene expression that characterize sessile or floating cells in young biofilms.

A further time-course analysis using this comparison as a reference was done to study the changes arising at 48 h, when the biofilm is consolidated in thickness and adherence, and at 72 h, when the biofilm is fully matured (Fig S1.A) (Caro-Astorga, 2015).

Although transcription and translation are intimately associated in bacteria in space and in time (Gowrishankar and Harinarayanan, 2004), there are other factors that can alter the final amount of protein and, subsequently, the final function trusted in those proteins. In *B. cereus*, it has been reported that mRNA decay shows a half-life ranging from 1-15 minutes (Kristoffersen et al., 2012).

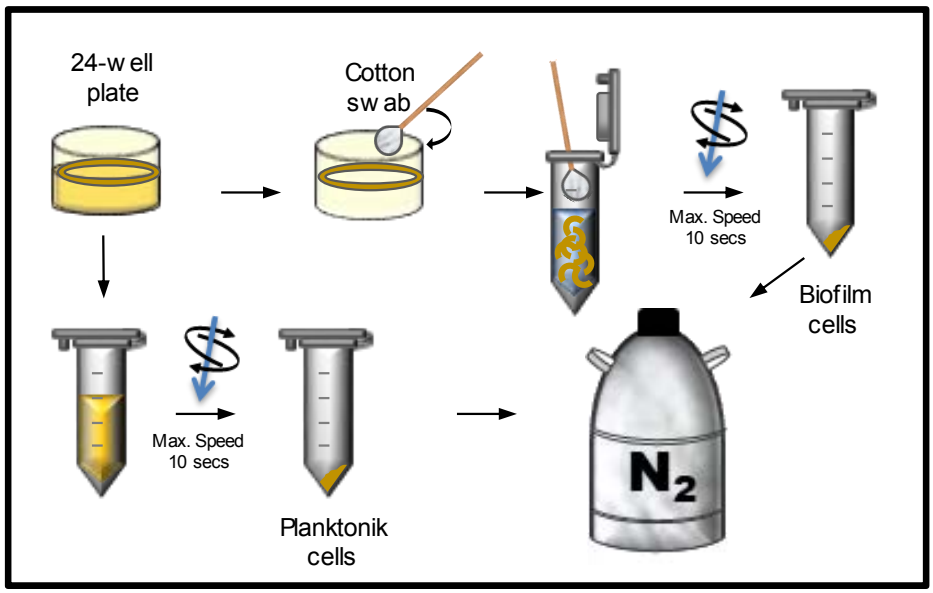

Figure 1. Isolation method of biofilm and floating cells. Biofilms were grown in 24-well plates without agitation at 28ºC. Floating cells were harvested taking only 250-500 µl of the upper part of the medium without disturbing the submerged biofilm. Samples were immediately centrifuged at maximum speed for 10 seconds and frozen in liquid nitrogen after discarding the supernatant. Next, the remaining medium and submerged biofilm was discarded, and the biofilm was collected with sterile cotton swabs, suspended in 1 ml of TY medium, centrifuged at maximum speed for 10 seconds and frozen in liquid nitrogen after discarding the supernatant. The sampling time was less than one minute to prevent RNA degradation and RNA recycling.

Several studies on *Bacillus* species classify the total amount of proteins inside a cell into two protein populations of either a labile fraction or a fraction of long-lived proteins with a turnover ranging from less than one hour to forty hours, which can introduce large differences between mRNA transcripts and protein function (Chaloupka et al., 1981).

Therefore, our samples were analyzed by two complementary quantitative techniques directed to two steps in gene expression: i) sequencing analysis of total mRNA and ii) quantitative proteome analysis using isobaric tags for relative and absolute quantitation (iTRAQ). Like RNAseq, iTRAQ is very accurate in defining quantity differences, although it requires a relatively large amount of protein. Thus, RNAseq data were considered as a reference in our study for gene expression, and the iTRAQ data were used to confirm that variations in gene expression result in the same direction as variations of translation. Henceforth, confirmed bacterial factors will be indicated with an asterisk "*" and discordances with an "x". The absence of a mark means that this protein was not detected by iTRAQ.

The genome of *B. cereus* ATCC 14579 possesses 5490 ORFs, and the RNAseq analysis showed that 1292 genes were differentially expressed (log2<>|2|) in biofilm-associated cells compared to floating cells, meaning 23,5% of the total gene content. These numbers are illustrative of the outstanding genetic machinery dedicated to the developmental program that leads to the formation of a bacterial biofilm (Fig. S1B-C). Proteomic analysis yielded 945 proteins with differential expression (log2>|0.7|). A wider view of the data indicates a good correlation between both techniques in the number of genes with up or down expression levels (Fig. 2A). Although the initial putative suspicion on the relative low concordance of transcription and translation, discordances among mRNA and protein levels were limited to only 43, 9 and 21 hits at 24, 48 and 72 h respectively, a finding that shows a first wide confirmation of data.

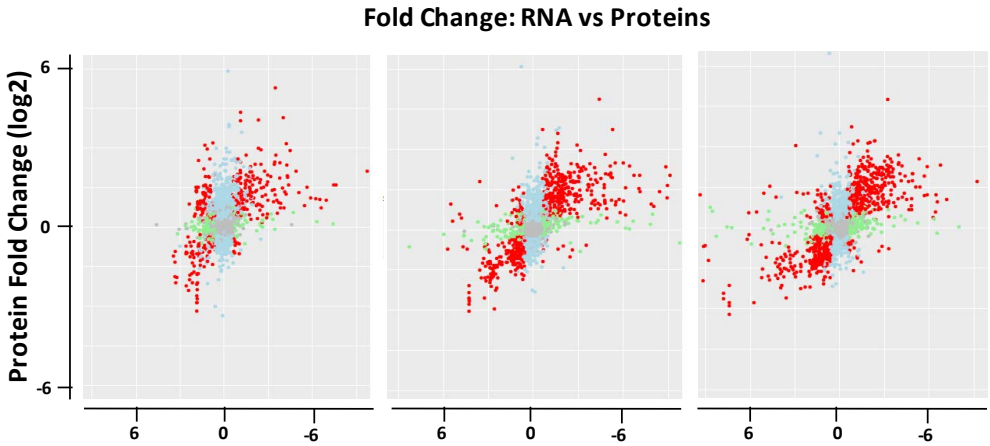

Figure 2. Validation of the variation of gene expression using RNAseq and iTRAQ analyses. The fold change in expression between transcriptomic (RNA-Seq) and proteomic (iTRAQ) results from samples at 24, 48 and 72 h. Points show significant changes (adjusted p-value < 0.05) according to both technologies (red), changes only found in proteomic (blue) or only found in transcriptomic (green). Gray dots represent items detected with no statistically significant changes. The top right and bottom left quadrants show concordant directions of change between both technologies; the top left and bottom right show conflicting directions.

To obtain a detailed view of the major physiological changes, genes with differential expression were sorted into Cluster of Orthologous Groups (COG) categories (Fig. 3). The data showed some foreseen changes such as the downregulation of the COG for flagellum assembly compared to that of floating cells. Delving into more detail, as COG categories ignore many of the individual ORFs that are differentially expressed, manual classification of the 1292 genes into functional groups was performed. Sporulation is also an expected upregulated

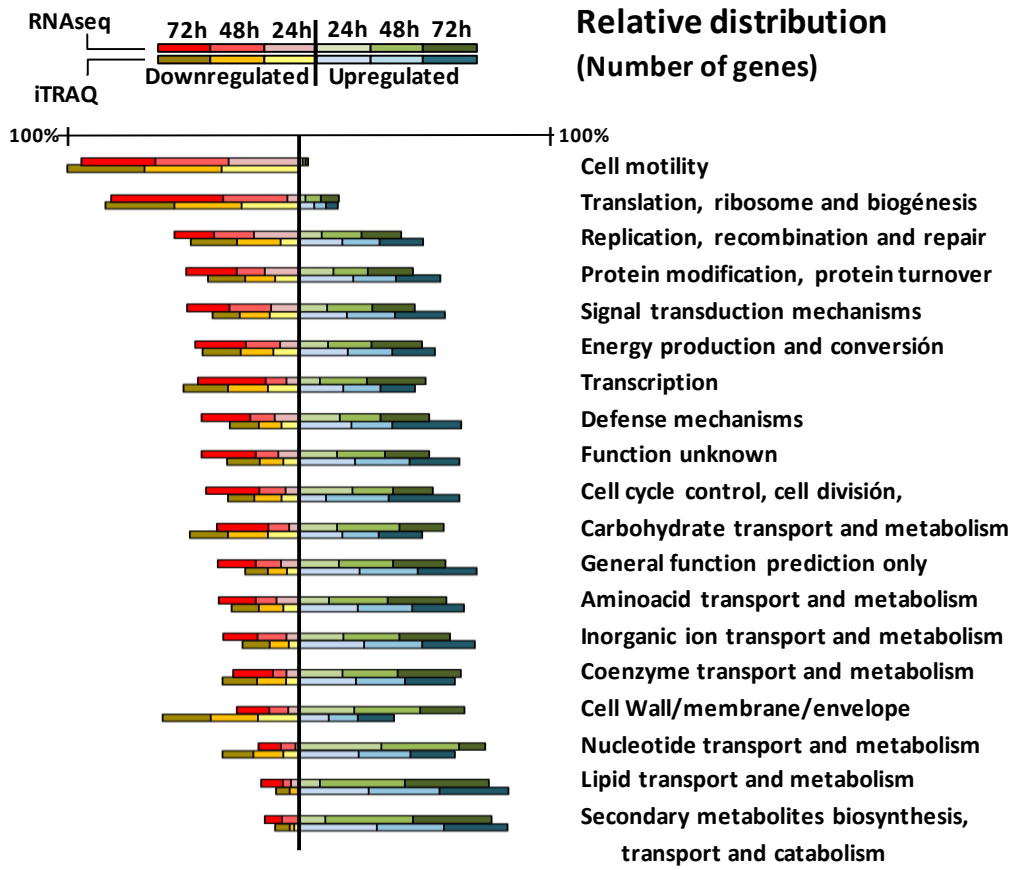

Figure 3. Relative comparison of COG categories of genes and proteins. Total number of elements of each category were relativized to a percentage and distributed as down- or upregulated. This graph shows that the ratio of elements that are up- or downregulated within each COG category is conserved, revealing similar results in terms of functional categories among RNAseq and iTRAQ techniques.

group, as it is linked to biofilm formation. In addition, some known regulators, such as the positive biofilm regulator SinI, are upregulated,

and the negative biofilm regulator PlcR is downregulated (Hsueh et al., 2006).

Commonly, changes in gene expression in cells associated with biofilms were more pronounced over time, with only subtle fluctuations but maintaining the up or down- regulated state in comparison to planktonic cells. However, we looked for the existence of groups of genes that specifically changed their expression in any of the sampling times and not in other stages. Many genes belonging to several functional categories showed time-specific variations, with an enrichment of functions at 48 h (Fig. S2). These variations can be explained as i) proteins involved in the punctual fine tuning of cell homeostasis, which would reflect the necessity of cell adaptation to the new lifestyle; ii) proteins that play a role in regulating bottlenecks of metabolic pathways; or iii) noise oscillations in the regulation of gene expression (Eldar and Elowitz, 2010). Considering the difficulty to discern specific reasons and confirm the expression levels of these genes, we will only focus on groups of genes belonging to the same functional category that show a clear and complete response. At 24 h, genes of pyrimidine metabolism are specifically upregulated in biofilm cells, which will be discussed later in this paper. Time-specific functions also affect sporulation. Clustering of the 124 sporulation-related genes by expression pattern using the Short Time-series Expression Miner (STEM) showed an increase of expression at 24 and 48 h and repression at 72 h of biofilm formation (Fig. S3A). Cluster 6 of the STEM clustering results (Fig. S3B) showed a small group of genes with an overexpression pattern at 72 h compared to previous stages. Contrary to our expectations, we found a sharp

decrease in the level of Spo0A in biofilm cells at 72 h compared to 24 h, along with a 60% reduction in the amount of the pre-spore specific transcriptional activator RsfA; the continuous upregulation of the phosphatase of Spo0A, Spo0E (*BC2353)* and upregulation of the sporulation control factor Spo0M (*BC2259*)* led us to think of at least two pathways to trigger sporulation: one that associated with starvation that may occur in both biofilm and floating cells and another that is independent of the nutritional state and associated with biofilm development.

These time-resolved analyses show that most of the biofilm functions are intrinsically associated with the biofilm state, with only some exceptions of processes only required in specific developmental stages.

2. Floating and biofilm cells are metabolically specialized

In our experimental setup, biofilm and floating cells coexisted, which let us explore the existence of metabolic specialization and possible cooperation between these two populations of cells at 24 h, when each population initiates the differentiation process. To do so, we looked for metabolic pathways developed in stages performed by biofilm or planktonic cells, completing the pathway by cooperation. With this aim, we did a bioinformatic analysis. Among the genes showing differential expression between floating and biofilm cells, 862 showed predicted associations in the STRING database with a confidence threshold > 500, which were used to build a primary network (Fig. 4). Using the

Betweenness algorithm (Newman and Girvan), we found 16 subnetworks with a minimum of ten genes. We observed that the majority of modules contain genes either more highly expressed in the biofilm (red nodes) or in floating cells (blue nodes), corresponding to specific functions described previously, which clearly belong to biofilm or planktonic cells. Two examples of clusters supported the validity of our analysis, showing enrichment of expected functions for biofilm or floating cells, respectively: Cluster 2 contains genes associated with sporulation, a developmental process that is upregulated in biofilms (Cluster 2: Fig. 4 and Supplemental Table S4). Cluster 3 is involved in the bacterial flagella assembly and chemotaxis, a function that is predominantly activated in floating cells (Cluster 3: Fig. 3 and Supplemental Table S5).

Clusters containing mixed elements (red for biofilm and blue for floating cells) were ranked by size and functionally analyzed to identify pathways that could be performed in cooperation by both cell populations. The mixed Cluster 1 is composed of 83 genes (52 planktonic and 32 biofilm) (Figure S3-S8, Supplemental Table S1). A total of 9 KEGG pathways are included in this cluster (Supplemental Table S2). Within these global metabolic groups, six were more specifically enriched: the citrate cycle (TCA cycle); 2-oxocarboxylic acid metabolism, glyoxylate and dicarboxylate metabolism; pyruvate metabolism; propanoate metabolism; and butanoate metabolism (Supplemental Table S2). The integration of genes from each population is specifically outstanding in i) the TCA cycle and 2-

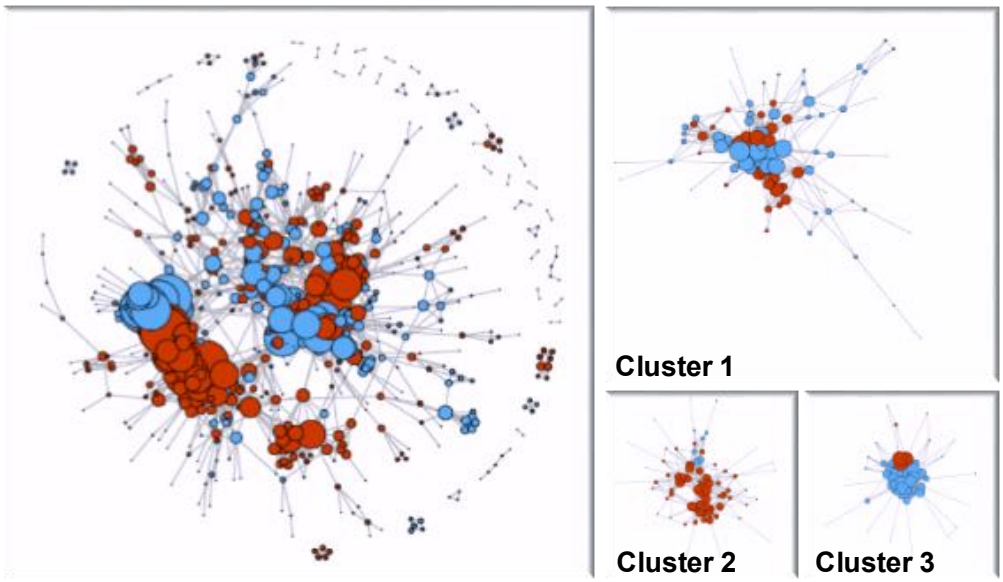

Fig 4. Specialization of biofilm and floating cells in distinct but coordinated metabolic activity. Networks formed by the differentially expressed (DE) genes and the functional associations between them. Each node represents a gene significantly DE between planktonic and biofilm samples at 24 hours; each edge represents an association between two genes according to the STRING database, as described in the Methods. Red nodes represent genes more highly expressed in the biofilm samples; blue genes represent genes more highly expressed in the planktonic samples. To the left is the global network formed by all DE genes. To the right, Clusters 1-3 represent subsets of the global network, obtained using the module detection method. Cluster 1 contains genes related to sporulation and are mostly from biofilm cells. Cluster 2 contains genes dedicated to flagellum assembly and chemotaxis and are mostly from floating cells. Cluster 3, contains a mix of genes from both populations (floating and biofilm cells) and are dedicated to global metabolic pathways.

oxocarboxylic acid metabolism, with the floating and biofilm genes clearly divided into different subroutes within the same metabolic pathways and ii) three metabolic KEGG pathways containing genes prominently dedicated to secondary metabolism and antibiotic biosynthesis (Cluster 1 Fig. 4 and Supplemental Table S3).

These results confirm that floating and biofilm cells specialize in different metabolic functions. Some are specific for either biofilm or planktonic cells, which will be explained in more detail in the next sections. Other routes are integrated by both populations, suggesting a possible metabolic collaboration that would ideally be energetically more favorable or play any role in communication, opening a new focus for the study of these bacterial populations that are actually considered independent groups of cells but will stablish a new paradigm if this hypothesis is confirmed.

3. Synthesis of the extracellular matrix

It appears that cells committed to the biofilm lifestyle have specialized in certain metabolic pathways most likely directed to the synthesis of proteins, polysaccharides or eDNA, all part of the extracellular matrix and necessary to cover a range of functions from adhesion to surfaces or other cells, structural support to the final architecture of the biofilm or protection (Fig. 5A).

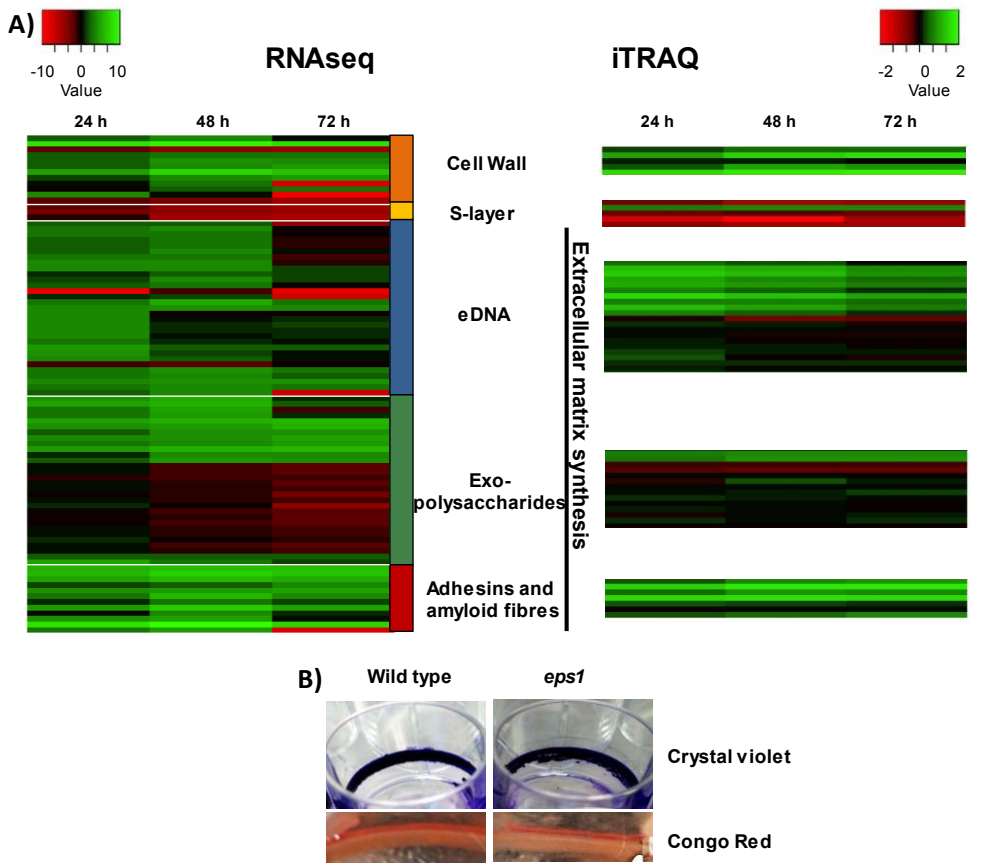

Figure 5. Expression dynamics of external elements and extracellular matrix components during biofilm formation. **A)** Comparison of heat maps from RNA-seq (left) and iTRAQ (right) results at 24, 48 and 72 h, over a selection of elements of the outer layers of *B. cereus* cells and components of the extracellular-matrix shows the following: i) The low expression levels of S-layer components, the major relevance of eDNA at 24 h-48 h, and the continuous overexpression of factors related to cell wall synthesis, some exopolysaccharides and other adhesins. **B)** Crystal violet and Congo Red biofilm staining showing no difference between the *B. cereus* ATCC14579 wild type and the *eps1* mutant.

In addition, we observed notable differences in the levels of transcripts of a number of genes encoding new elements involved in biofilm formation in *B. cereus.* We found in biofilm cells the overexpression of triple helix repeat-containing collagen proteins. In the closely related *Bacillus amyloliquefaciens,* a bacterial species that lives in association with the plant rhizosphere, the collagen-like proteins ClpA-D were demonstrated as being required for adhesion and biofilm formation (Zhao et al., 2015). No orthologues to ClpA are present in the genome of *B. cereus*, but several proteins with high similarity to ClpB-D (*BC2569, BC2570, BC3712, BC4527, BC4725*) are upregulated in biofilm-associated cells, making it tempting to speculate on the involvement of these proteins in the formation of biofilms of *B. cereus*. There is another group of proteins with very similar functions, termed collagen adhesion proteins (Cap), the expression of which has been described to be dependent on c-di-GMP through a riboswitch, thus showing strong translational regulation. The genome of *B. cereus* ATCC14579 harbors eight genes annotated as collagen adhesion proteins, and four of them (*BC1060, BC5056*, *BC0087* and *BC5357)* are highly expressed either at 24 or 48 h. These data pinpoint to a putative important role of these proteins in the early stages of biofilm formation during the process of adhesion to surfaces (Abranches et al., 2011; Miller et al., 2015; Tang et al., 2016; Zhao et al., 2015).

Lysis-independent eDNA release has been reported for *B. subtilis*; however, the lack of a definitive implication in biofilm formation led authors to propose a role in competence and horizontal gene transfer (Zafra et al., 2012). Contrary to this finding, extracellular DNA is an

essential element in biofilm formation by *B. cereus* (Vilain et al., 2009a) and is a major factor in the protection against the activity of aminoglycosides, fluoroquinolones and antimicrobial peptides (Chiang et al., 2013; Johnson et al., 2013; Lewenza, 2013; Tetz et al., 2009). Our data support the model of active synthesis of DNA as an adhesin rather than passive release by cell death. Indeed, phosphate, ribose and nucleosides, all molecules required for DNA synthesis, and similarly, the nucleoside transporters (*BC2973, BC0363*) and specific phosphate transporters (*BC4265-68* and *BC0711*) are upregulated in biofilm-associated cells at 24 h. Accordingly, the complete gene cassette for pyrimidine synthesis (*BC3883-89**) is specifically overexpressed only at 24 h, a finding that highlights the relevant contribution of eDNA in earlier stages of biofilm formation. In a previous work, the genes *purA* (*BC5468*), *purC* (*BC0326*) and *purI* (*BC0327*), which are implicated in purine biosynthesis, were demonstrated to be indispensable for biofilm formation in *B. cereus* (Vilain et al., 2009b). The synthesis of purine nitrogen bases requires glycine, aspartic acid and glutamine, and accordingly, the transporters for these amino acids are upregulated (Table 1). Formate is another substrate for purine biosynthesis, and two processes would apparently satisfy the demand for this organic acid in biofilm- associated cells: i) the upregulation of the biosynthetic enzymes oxalate decarboxylase (*BC2383*) and formamidase (BC3939*) and ii) the downregulation of the oxalate/formate antiporter (*BC2300*) that extrudes formate. Thus, pyrimidine synthesis is upregulated at 24 h, while purine synthesis remains active at all stages of biofilm formation. A close examination of

iTRAQ data provides purines with an additional demanding pathway besides the formation of eDNA: the synthesis of c-di-GMP, c-GMP-AMP and ppGpp, all secondary messengers important in shaping multicellularity and in bacteria-host cell interactions (Jenal et al., 2017). High levels of c-di-GMP induce adhesion and biofilm formation, concomitantly with the blocking of flagellum mobility (Purcell et al., 2012). According to our hypothesis, a diguanylate cyclase (*BC3989*) is overrepresented in our iTRAQ analysis.

Table 1. Differential expression (Log2 (fold change)) of genes implicated in the synthesis of secondary metabolites. Stars indicate up/down regulation behaviour confirmed by proteomic results.

	Log_2 (fold change)				
Gene ID	**24 h**	**48 h**	**72 h**	**Molecule**	**iTRAQ**
BC1201	2,87	5,63	1,75	Tylosin	
BC1204	8,07	9,53	5,09	Tylosin	
BC1206	7,01	8,13	2,73	Tylosin	*
BC1208	5,00	6,74	1,04	Streptomycin like	
BC1209	5,95	7,91	2,46	Streptomycin like	*
BC1210	3,47	4,24	-0,52	Streptomycin like	
BC1211	3,78	6,19	2,59	Streptomycin like	
BC1212	4,36	6,94	0,28	Streptomycin like	*
BC1213	3,38	5,85	-1,63	Streptomycin like	
BC1214	3,10	5,17	0,92	Streptomycin like	*
BC1248	3,77	5,88	2,80	Bacteriocin	

BC1249	4,28	5,43	3,24	Bacteriocin	
BC1250	4,31	5,00	1,78	Bacteriocin	
BC2452	0,24	3,00	4,99	Bacitracin	
BC2966	16,71	17,72	10,24	Polyketide synthase	
BC5079	-1,90	3,60	4,62	Thiocillin	*
BC5080	-1,58	3,00	3,75	Thiocillin	*
BC5081	-0,86	3,27	4,33	Thiocillin	*
BC5082	-2,43	3,20	4,32	Thiocillin	*
BC5083	-2,33	2,06	3,34	Thiocillin	*
BC5084	-1,76	2,48	3,69	Thiocillin	*
BC5085	-0,77	3,52	3,36	Thiocillin	*
BC5086	-1,76	2,83	4,04	Thiocillin	*
BC5087	2,85	3,61	3,02	Thiocillin	
BC5088	2,81	3,74	3,14	Thiocillin	
BC5089	2,61	3,65	2,90	Thiocillin	
BC5090	2,61	2,87	3,13	Thiocillin	
BC3021	0,48	2,21	2,78	Colicin	*
BC1426	2,01	8,10	8,50	Porphirin	
BC1427	1,46	5,19	4,77	Porphirin	
BC1428	3,04	6,66	6,96	Porphirin	*
BC2133	-2,57	-4,22	-11,87	Porphirin	
BC2134	-2,99	-4,05	-6,25	Porphirin	
BC4468	2,84	3,27	3,62	Porphirin	

Besides proteins and eDNA, exopolysaccharides (EPSs) constitute an integral component of the extracellular matrix of the majority of bacterial biofilms. Importantly, our data indicate noticeable differences in the well-defined role of EPS in *B. subtilis*. First, the putative EPS gene cluster

*BC5263-BC5279**, homologous to the *eps* operon of *B. subtilis*, showed a similar expression pattern to that of floating cells. Indeed, knockout mutants in this genetic region (called *eps1)* were not arrested in biofilm formation in comparison to the wild type strain ATCC14579, based on the crystal violet staining of the adhered biomass or staining with Congo Red, a dye used to show the presence of certain exopolysaccharides (Fig. 5B). This finding is in agreement with previous studies showing that mutants in this gene cluster in *B. cereus* 905 were not arrested in biofilm formation (Gao et al., 2015). Second, the recently reported four-gene-operon *BC3358-61*, which is dedicated to the production of two spore-decorating sugars (Li et al., 2017), is upregulated in the biofilm-forming subpopulation, in parallel to the increased rate of sporulation at this stage. Third, we identified an additional gene cluster, putatively dedicated to the synthesis of a capsular EPS, which was overexpressed in biofilm-associated cells (*BC1583-BC1590*). In agreement with a previous report (Sue et al., 2006), we could not microscopically visualize a capsule in this strain of *B. cereus*, which led us to propose a role of this new gene cluster in biofilm formation which is studied in the chapter VI of this thesis. All these observations are thus suggestive of the heterogeneity of the EPS arsenal employed by this bacterial species not only to form biofilms but also to adapt to diverse environmental conditions.

The biofilm architecture is a complex challenge for bacteria that involves many changes and many elements. The requirements for huge amounts of resources should be achieved by a coupling metabolism with the machinery dedicated to the assimilation of nutrients. Consistent

with this idea, our results show a strong response of biofilm cells to seize and synthetize amino acids, nucleotides and sugars, revealing biofilms as a very resource-consuming state. The supply of amino acids might come from protein recycling or be compensated by downregulation of the synthesis of other polymers such as flagellum assembly, but this supply seems to be insufficient, according to our results. We found a noticeable upregulation of genes encoding transporters of specific amino acids (Supplemental Table S6), especially those genes encoding a glutamine transporter and a glutamine-binding protein, which were significantly upregulated in comparison to other specific amino acid transporters. Glutamine is an important amino acid in bacterial physiology, and beyond the well-known involvement in the synthesis of proteins, this amino acid serves additional functions as a growth control signal. In *B. subtilis,* glutamine plays a determinant role in the internal metabolite gradient inside biofilms, in which external biofilm cells periodically alter the growth in a culture on an agar plate (Liu et al., 2015). Apart from signaling, the glutamine supply is consumed for important functions, such as the synthesis of the protein component of the extracellular matrix or cell wall polylinking. Remarkably, L-glutamine was recently reported as a signal that activates the expression of virulence factors in *Listeria monocytogenes*. As human serum is rich in this amino acid, high levels of L-glutamine serve in this bacteria as a signal of living inside a host, switching to an aggressive disposition (Haber et al., 2017). According to our results, this mechanism can also be foreseen as a sensor of *B. cereus* in niches such as living in association with growing plant roots, which secrete exudates rich in

amino acids, or accessing a skin wound in a mammal with leakage of blood or serum. More research would help clarifying the specific response of a biofilm when levels of L-glutamine rise.

Two lines of evidence indicate that amino acid intake is apparently insufficient to fulfill the community requirements. First, several gene clusters (*BC1779*-BC1780*-BC1781*, BC1396*-BC1397*-BC1398*, and BC1399*, BC1400*, BC1401*, BC1402*, *BC1403*) implicated in the biosynthesis of valine, leucine and isoleucine are upregulated; second, there is upregulation of the aminotransferase *BC1610**, which uses pyridoxamine and alpha-ketoglutarate, pyruvate or oxaloacetate to synthesize glutamine, alanine and aspartic acid, respectively. The glyoxylate shunt bypasses the TCA cycle from isocitrate to malate. Although the expression of TCA cycle genes is generally downregulated, the next step, which converts isocitrate to alpha-ketoglutarate, is specifically upregulated in biofilm-associated cells, feeding the pathway for amino acid synthesis. Sulfur is another essential element for metabolic pathways leading progressively to sulfite, sulfide and, finally, the synthesis of cysteine and methionine. The genes encoding transporters of sulfate (*BC1092*) and alkane sulfonate (*BC2909*, BC010, BC011, BC2912**) are also overexpressed at all stages of biofilm development. We anticipate that this is especially important during biofilm formation in soils, where 95% of available sulfur is present in the form of sulfonate and sulfate esters (Kertesz and Mirleau, 2004). Sulfur is an essential element in additional processes: i) biosynthesis of lipoproteins, which are scarce in *B. cereus*, but contributors to biofilm formation in other bacteria species (Banse et al.,

2011; Nakayama et al., 2012; Xie et al., 2016); ii) synthesis of glutathione, which protects cells from osmotic, redox and low pH stresses (Masip et al., 2006); and iii) synthesis of coenzyme A, important for the metabolism of fatty acids, which is upregulated in biofilms (Smirnova and Oktyabrsky, 2005; Tófoli de Araújo et al., 2013). Sulfur mobilization is one of the benefits obtained by plants from the symbiotic interaction with microbes in the rhizosphere (Alhendawi et al., 2005). In this way, *B. cereus* living as a symbiotic member of the rhizosphere may use this sulfur as a currency to deal the symbiosis with plants, that provide exudates in exchanges as nutrient to ensure bacterial survival.

The synthesis of amino acids is under the control of DnaK (*BC4858*), a suppressor protein homologous to DksA in *E. coli*, which is a negative regulator of rRNA general expression during starvation and a positive regulator of several amino acid biosynthesis, amplifying the effects of the secondary messenger ppGpp (Paul et al., 2005). In *E.coli*, DksA is present at similar concentrations at mid-log phase and in late stationary phase with unchangeable levels; however, the levels during biofilm formation were not explored (Paul et al., 2004). In a biofilm of *B. cereus*, levels of DnaK change remarkably compared with that of floating cells, with a visible rise at 24 h and 48 h. This led us to speculate that DnaK is a specific biofilm regulator that participates in the coordination and synchronization of the machinery of biofilm formation in *B. cereus* and explains the enhancement of the machinery of amino acid synthesis found and discussed above.

4. Biofilm-associated cells prepare their cell walls and membranes for the new mega-architecture

In addition to the collective protection to antimicrobials provided by the extracellular matrix, our data show that individual cells develop protection against external aggressors by enhancing the physical barrier represented by the cell wall. Lipoteichoic acid (LTA) is a major component of the cell wall in gram-positive bacteria, and the LTA synthase (*BC3765*) is upregulated in 48- and 72-hour aged biofilms. Peptidoglycan (PG), the other main component of the cell wall, is composed of units of N-acetylglucosaminic acid and N-acetylmuramic acid. In our experiments, we found that cell wall degradation enzymes are downregulated (*BC0888*, BC5237, BC3257, BC1660, BC3677*), with the exception of the N-acetylmuramoyl-L-alanine amidase (*BC2823**) that is specifically upregulated in biofilm cells. In addition, several penicillin-binding proteins (*BC1469, BC2190*, BC2448, BC2688, BC4075*), which are involved in the final stages of PG synthesis, are upregulated in biofilms with a maximum expression level at 48 h, as well as three transpeptidases (*BC2468*, BC5027, BC0771*) that catalyze the PG cross-linking (Fig. 6). D-alanine is another important component of the cell wall that is implicated not only in the peptide cross-liking but also in the D-alanylation of teichoic acid, a modification reported to contribute to the resistance to several antimicrobials, biofilm formation, host defense or mouse intestinal tract colonization in other gram-positive bacteria (Gross et al., 2001; Kristian et al., 2005; Peschel et al., 1999; Walter et al., 2007). The bidirectional

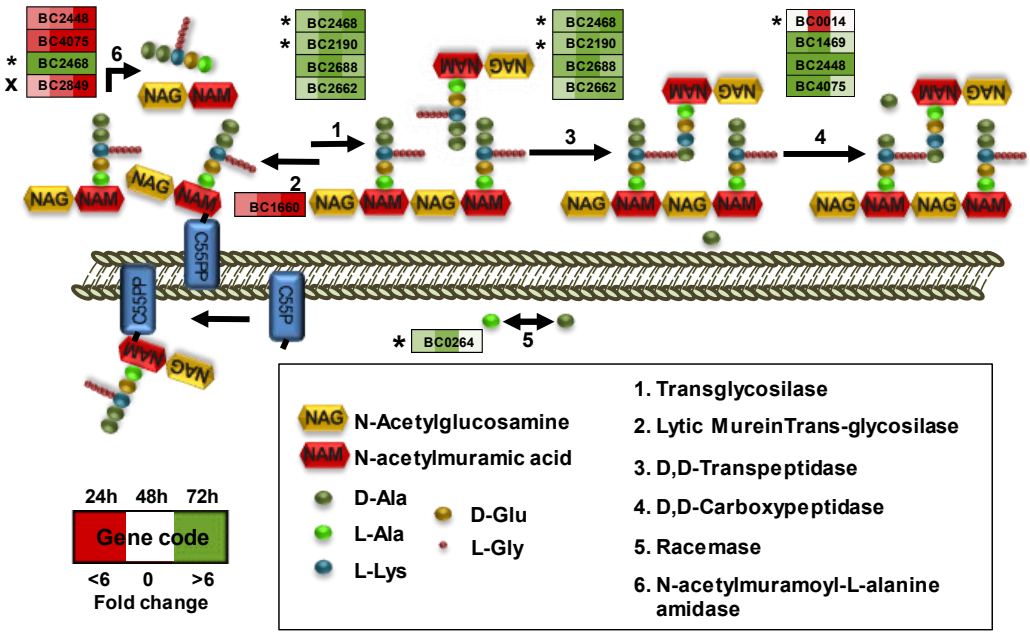

Figure 6. Scheme of the cell wall synthesis pathway. Each step is performed by several genes represented in boxes. Colored squares inside boxes represent 24, 48 and 72 h sampling times, and the intensity of color shows the level of upregulation (green) or downregulation (red). Stars indicate confirmation of the behavior by iTRAQ results and cross indicate conflicting results.

conversion of L-alanine into D-alanine is catalyzed by alanine racemases, and out of the two paralogs found in *B. cereus* (*BC0263, BC0264*), only *BC0264* is upregulated at 24 h and 48 h. Interestingly, this locus is orthologous to *Dal-1* in *B. anthracis*, which is known to rescue the phenotype of a D-ala auxotrophic strain of *E. coli*. In addition, Ala racemases have been associated with the outermost layer of

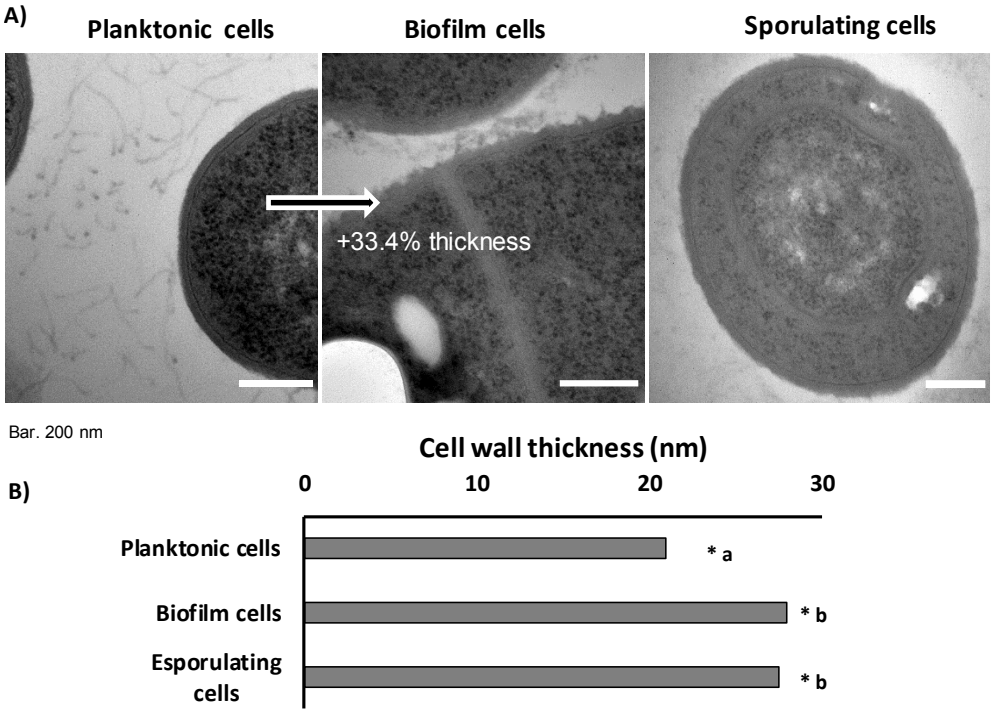

Figure 7. Cells in a biofilm increase the thickness of the cell wall. A) Transmission electron micrographs of floating cells, biofilm cells and sporulating cells inside the biofilm structure. **B)** Measurements of the cell wall thickness was done with ImageJ Fiji software over 40 images and 300 measures around the edges of each cell, showing an increase of 33.4% in the thickness of biofilm and sporulating cells. Standard deviation SC<0.01.

Bacillus sp. spores driving the suppression of germination (Chesnokova et al., 2009; Yasuda et al., 1993). These findings on the upregulation of the enzymatic machinery involved in PG, LTA and D-alanine synthesis in conjunction with the downregulation of enzymes implicated in cell wall degradation in biofilm cells, raised the question of whether there is an

alteration in the cell wall thickness of biofilm-associated cells compared to floating cells. Examination of cell sections of 48-h biofilm and floating cells by electron microscopy revealed a 33.4% increase in the cell wall thickness of biofilm cells, a structural change that was also observed in sporulating cells (Fig. 7).

According to our results, changes in the cell wall might also reflect chemical changes in the cell membrane. The lipid cardiolipin constitutes approximately 20% of the total lipid components of bacterial membranes. Our results show that biofilm cells overexpress the cardiolipin synthase (*BC2039*) and the previous step, the synthesis of diacylglycerol (*BC3765*), and downregulates the alternative pathway that converts CDP-diacylglycerol to phosphatidylcholine (*BC0976*) (Vences-Guzmán et al., 2008). In *B. subtilis*, cardiolipin has been proposed to rigidize the cell membrane, contributing partially to self-resistance to the lipopeptide surfactin, which produce the opposite effect (Seydlová et al., 2013). Biofilm cells of other gram-positive bacteria reduce the membrane fluidity with saturated fatty acids (Dubois-Brissonnet et al., 2016), an effect that can be achieved by the increase of cardiolipin in membranes of *B. cereus* biofilm cells, which might also confer resistance against surfactin in multispecies biofilms in the soil or plant rhizosphere, where *B. subtilis* is also commonly present. On the other hand, the fatty acid degradation region *BC2484-89** is upregulated in biofilm cells, as well as *BC0890*, which is implicated in the breakdown of complex fatty acids. In this way, membranes may

undergo the replacement of phospholipids to produce a strong membrane rich in cardiolipin.

The S-layer is an outer layer of proteins, and based on a previous study with 102 *B. cereus* strains, it seems to be negatively correlated with the ability to form biofilms (Auger et al., 2009). However, differences between the floating and biofilm populations of cells were not evaluated. *B. cereus* ATCC14579 only possesses five genes (*BC0896*, BC0902*, BC0991, BC1125-26*) with canonical S-layer domains, lacking the complete set of genes reported for effective assembly of the S-layer. Our results are in agreement with that study, given that the genes *BC0896*, BC0902*,* and *BC0991**, which encode S-layer components, are mainly expressed in floating cells and downregulated in biofilm cells. This indeed underlines that strains lacking extensive S-layer synthesis are more prone to biofilm formation. Pioneer studies proved that cells of *B. thuringiensis* slough off fragments of the S-layer when entering the stationary phase of growth, which was proposed to be the result of the cell wall turnover (Luckevich and Beveridge, 1989). Even lacking the most important genes for S-layer assembly, *B. cereus* ATCC14579 still maintains some genes and presumably the regulatory cascade for the S-layer assembly; thus, it is tentative to think of a role of the S-layer as a physical regulator of biofilm formation and recruitment of planktonic cells.

5. Biofilm-associated cells are prepared for a hostile competitive environment

Living encased within a shell represented by the extracellular matrix confers to sessile bacterial cells the inability to flee and overcome the hostilities. Physical stresses are mainly reduced by the extracellular matrix, but how can bacteria defend themselves from attacks from other bacteria in the competition for space in the soil, plant rhizosphere or human gut? One way in which sessile bacterial cells may efficiently fight competitors regards the offense inflicted by antimicrobials. *B. cereus* possesses several genomic regions dedicated to the production of secondary metabolites with antimicrobial activity. In addition to these, we found genes with unknown functions that after *in silico* analysis (see the materials and methods) appeared to be hypothetically involved in the production of putative secondary metabolites. Interestingly, all of them are upregulated in biofilm-associated cells (Supplemental Table S7). Among those regions there are genes encoding NRPS/PKS or putative bacteriocin-synthesizing proteins such as i) thiocillin, ii) tylosin-like, iii) bacitracin, iv) porphyrins, v) a putative member of the heterocycloanthracin/sonorensin family of bacteriocins; vi) other putative bacteriocin (*BC1248-50)* vii) the cluster *BC1210-BC1212* orthologous to a streptomycin synthesis gene cluster in *B. subtilis*; and viii) a colicin-like toxin. Colicin is a bacteriocin proposed to play an important role in microbial competition in the gut and to facilitate intestinal colonization (Bosák et al., 2016). There is a gap in the study of secondary metabolites in *B. cereus* to confirm that these genomic regions are responsible for the synthesis of active compounds. Although

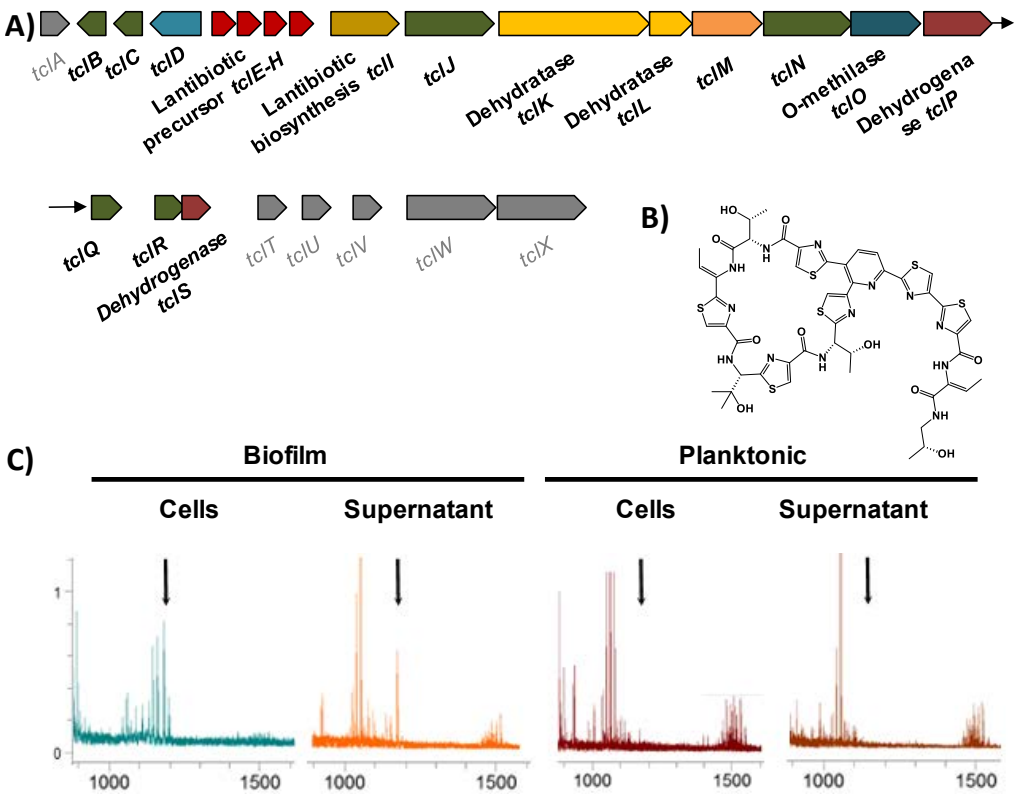

Figure 8. Cells in a biofilm produce more antimicrobials. A) Scheme of the genes for the biosynthesis of thiocillin are overexpressed in biofilm cells (*BC5094-BC5070)*. Genes with no variation in expression level are shown in gray color. **B)** 3D structure of the thiocillin molecule. **C)** Detail of the traces from HPLC-MS-MS (TOF-TOF) of cells and supernatants of 48h cultures. Biofilms were collected and suspended in PBS, separating cells from the supernatant after centrifugation. Culture medium was centrifuged to separate floating cells from supernatant. Samples were purified with C8 ZipTip® (Merck) previous to analysis. Black arrows indicate the positions of the thiocillin peaks. See the supplemental material for the complete spectra (Fig. S10).

all these putative antimicrobial molecules are upregulated in biofilm-associated cells, only thiocillin has been studied in detail and has been proven to produce an active peptide (Bowers et al., 2010). As the iTRAQ method is unable to detect these peptides and given that this antimicrobial is presumably produced in higher amounts by biofilm cells, we analyzed the presence of this metabolite in the two fractions (floating and biofilm cells) using mass spectrometry. This analysis confirmed that thiocillin was present in the pellet and supernatant of biofilm cells, but below detectable levels both in the pellets of floating cells and in the spent medium (Fig. 8 and supplemental Fig. S10).

Based on this observation, one might speculate that the production of these antimicrobials is used to colonize a niche and to protect it from competitors that are in close contact in the direct surroundings. In addition, biofilm cells also express several putative antimicrobial resistance genes that presumably help to overcome the attack from other competitors within the biofilm (Supplemental Table S8).

Reactive oxygen species (ROS) are well-known factors that elicit antimicrobial-mediated killing and are discussed to be the final cause of bacterial cell death instead of the direct effect of antimicrobials (Van Acker and Coenye, 2017). ROS production has also been described to be part of the defense arsenal of plants and mammals to fight against pathogen invasions (Vatansever et al., 2013). Bacteria produce several enzymes that neutralize ROS, either preventing or reducing cell damage as well as other repairing enzymes. According to the protective mode that characterizes the lifestyle of biofilm cells, our analyses

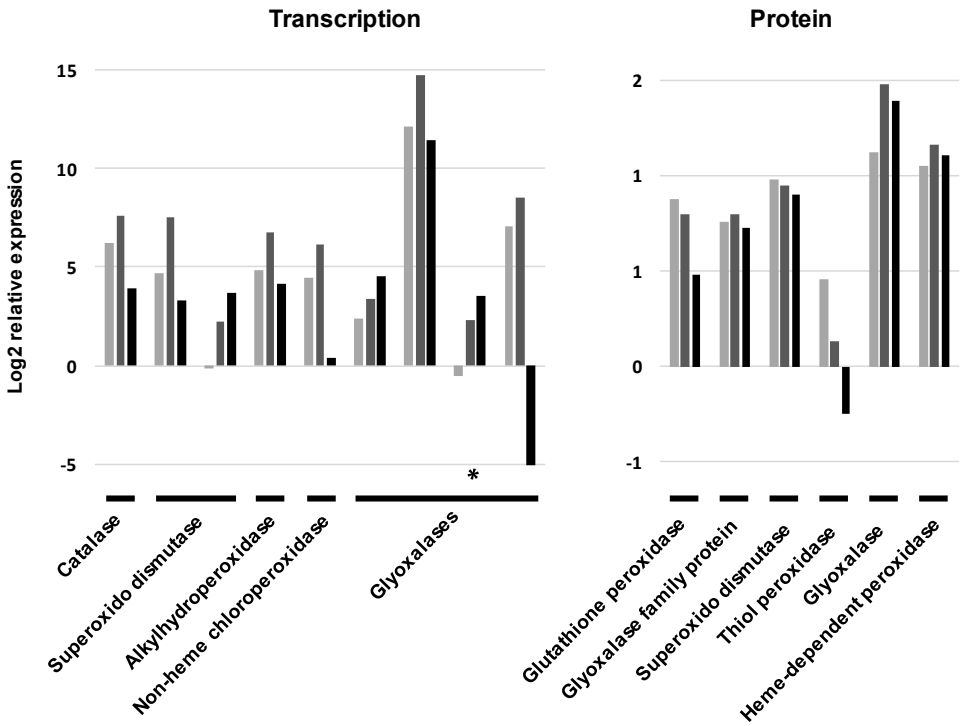

Figure 9. Cells in a biofilm trigger the machinery to scavenge reactive oxygen species. Expression pattern of ROS detoxification enzymes in biofilm compared to floating cells at 24 h (light gray), 48 h (gray) and 72 h (black) based on RNAseq (left) or iTRAQ (right) analysis.

revealed the overexpression of a battery of enzymes dedicated to scavenge diverse ROS: a catalase (BC3008), superoxide dismutases (*BC1468, BC4907*), chloroperoxidase (*BC4774*), alkylhydroperoxidase (*BC2830*) and glyoxalases (*BC5092*, BC3178, BC0824*). Additionally, iTRAQ analysis showed higher amounts of glutathione peroxidase (*BC2114*), glyoxalases (*BC5092, BC3532*), superoxide dismutase (*BC4272*), thioredoxin-dependent thiol peroxidase (*BC0517*), thiol peroxidase (*BC4639*) and heme-dependent peroxidase (*BC5388*) in

biofilm-associated cells (Fig. 9). To maintain a reducing environment and to repair protein damage caused by oxidative stress, biofilm cells also increase the amount of thioredoxins (*BC0778, BC1385, BC4521, BC4691,* iTRAQ data) and the bifunctional methionine sulfoxide reductase A/B proteins (*BC5436*, BC1774**).

Interestingly, biofilm cells form a complex rearrangement of the machinery for metabolic energy generation to prevent ROS production (Fig. 10). Complex I of the electron transport chain is the major component responsible for electron leakage (Jastroch et al., 2010a)., However, as a result of the leakage, these electrons react with O_2 and produce ROS that can damage proteins and DNA (Jastroch et al., 2010b). We stated above that biofilm and planktonic cells undergo metabolic specialization (Fig. 3, Fig. S4-9). One of the differences shown in the analysis of Cluster 1 is the downregulation of the TCA cycle in biofilm cells (*BC1251*, BC3833*, BC3834*, BC1790*, BC0466*, BC1712*, BC0466**), including Complex II of the electron transport chain (BC4516*, BC4517*), which supplies two electrons to ubiquinone (Fig. S11). In addition, biofilm cells overexpress Complex I of the electron transport chain, increasing the total amount of the FMN (flavin mononucleotide) component of Complex I, which receives the electron from NADH. As a result, the amount of NADH required to saturate the pull of FMN is higher, preventing a fully reduced state of the FMN, which is prone to leak electrons, and subsequent production of $O_2^{\bullet -}$ (Hirst et al., 2008). We also found that biofilm cells activate the glyoxylate shunt (isocitrate lyase *BC1128**, malate synthase *BC1127**), which is a bypass of the TCA that converts isocitrate to glyoxylate and

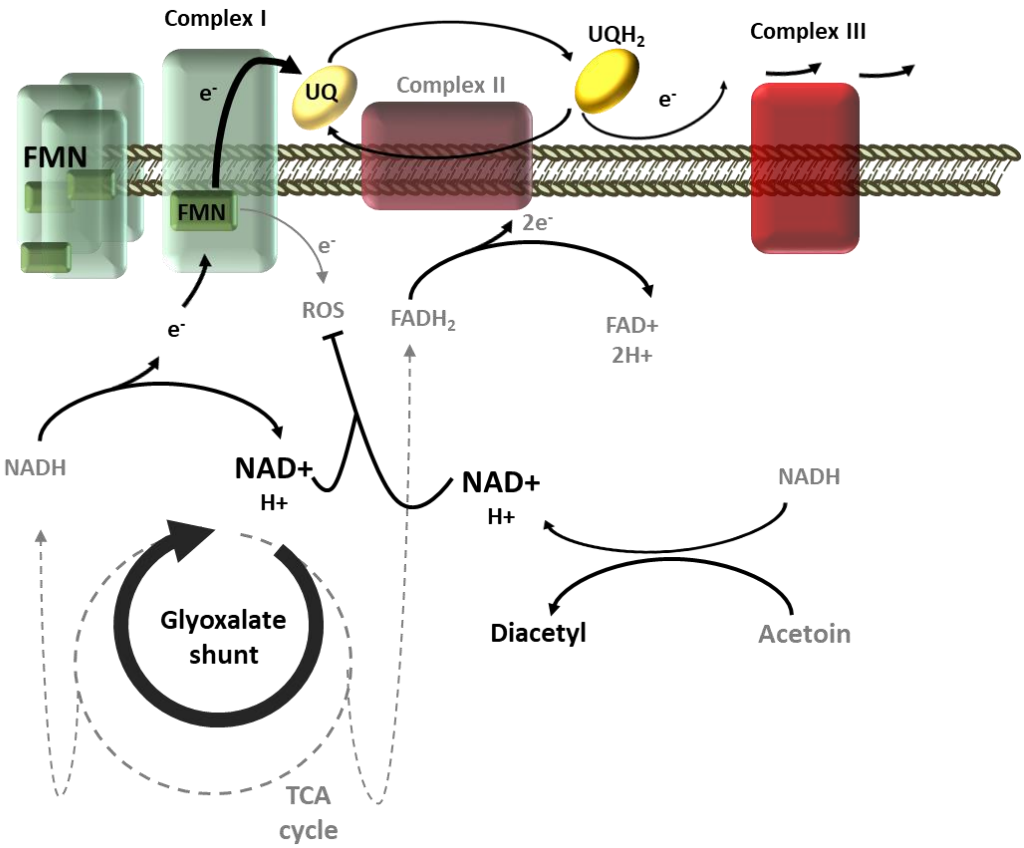

Figure 10. Biofilm cells rearrange their metabolism to prevent ROS production with an origin in the electron leakage of the flavin mononucleotide (FMN). Overexpression of the complex I and FMN, reduction of the NADH/NAD^+ ratio degrading acetoin, activation of the glyoxylate shunt, and reduction of the ubiquinone (UQ) saturation lead to release the fully reduced state of the FMN, preventing electron leakage.

succinate and then converts glyoxylate to malate. This shunt yields less reducing power given that one NADH and one $FADH_2$ are not produced, which indirectly increases the concentration of NAD+ and contributes to arrest superoxide production by Complex I (Kussmaul and Hirst, 2006).

Reduction of $FADH_2$ results in a reduced ubiquinone reduction state, which also facilitates electron transport from Complex I to Complex III, preventing the accumulation of electrons in the FMN and its fully reduction state. This bypass has been demonstrated to reduce ROS production (Ahn et al., 2016) and has been found to be upregulated in *Mycobacterium tuberculosis* after exposure to antibiotics (Nandakumar et al., 2014). Studies of *Staphylococcus epidermidis* revealed a tendency in clinical isolates to accumulate mutations in the TCA cycle that increase their tolerance to β-lactam stress, a confirmation of the contribution of TCA-dependent ROS in enhancing antibiotic susceptibility (Chittezham Thomas et al., 2013). Complementary to this detoxifying strategy, there is an extra input of succinate stemming from the shunt and the activity of the succinate-semialdehyde dehydrogenase (*BC0357**), which is also overexpressed in biofilm cells. Succinate is an intermediate of the TCA that is primary used for energy production but is also connected with alternative pathways, including the synthesis of secondary metabolites and antibiotics which, as explained above, are upregulated in biofilm-associated cells, working as a sink of succinate.

These changes in the central metabolism aimed at reducing ROS production are accompanied by a downregulation of the following fermentative metabolism pathways in biofilm-associated cells: lactate dehydrogenase (*BC4870*, BC4996**), formate acetyl-transferase and its regulator (*BC0491*-92**), alcohol dehydrogenase (*BC2220**), and butanediol fermentation (*BC0668**) (Fig. S12A). A reduction in fermentative metabolism prevents local acidification within the biofilm

environment, which is associated with damaging effects on *B. cereus* (Mols and Abee, 2011). Studies on *B. cereus* ATCC14579 have shown that glutamate, arginine and lysine enhance the adaptation to an acidic pH (Senouci-Rezkallah et al., 2011), which connects with the enhanced amino acid synthesis of biofilm cells, as described above. Furthermore, the synthesis of acetoin is downregulated (Fig. S12B). Acetoin is a carbon storage molecule during exponential growth that prevents acidification and yields a NADH molecule for the synthesis and requires the consumption of NADH for the inverted reaction, which is proposed as a regulatory mechanism of the NAD/NADH ratio (Xiao and Xu, 2007). In accordance with the role of this ratio in ROS production, this metabolic pathway serves as an extra tool to reduce the levels of NADH and prevent the saturation of the Complex I.

These results suggest that *B. cereus* has the ability to specifically redirect the metabolism grid to succeed in a wide variety of competitive and stressful situations that stem from conversion to a sessile lifestyle or from the threats of a specific niche. Secondary metabolite synthesis is metabolically costly and must be fine-tuned, which is becoming especially important when individuals are attached. These changes are also focused towards the defense against attacks inflicted from other bacteria, especially when escape is difficulty due to the sessile lifestyle, switching the metabolism to an ROS production preventive state together with the expression of ROS detoxification enzymes, pumps and antimicrobial resistance enzymes. Such a number of strategies oriented to ROS damage prevention provides a valuable clue of the weakness of bacterial biofilms, which may be a new, important target to

fight against bacteria as a unique strategy or in combination with other chemotherapies, which probably will enhance their effectiveness. In line with this ROS damage-preventive state, an increase in the cell wall thickness provides an advantage against the effect of antimicrobials oriented to cell wall disruption. As noted above, exopolysaccharides and eDNA also confer protection against different antimicrobials, completing a whole strategy to survive the hostility of competition.

6. Planktonic cells are prone to attack the host

In the interaction with hosts, bacterial cells must overcome their diversified immune response, and this is achievable with the gain of so-called virulence factors. Cells within biofilms are globally protected by the extracellular matrix, and we have also shown that single cells within the biofilm are anatomically prepared to resist external aggressions. In addition to these physical barriers in the bacterial community, we have found two factors that might complementarily contribute to the survival of bacterial cells despite the host immune system. One factor is a specific beta-lysine acetyltransferase (*BC2249**), which may confer resistance to beta-lysine, an antibacterial compound produced by platelets during coagulation, and is responsible for lysing many gram-positive bacteria (Hamzeh-Cognasse et al., 2015). The other factor is the immune Inhibitor A (InhA) precursor, which is a bacterial enzyme able to i) digest attacins and cecropins, two classes of antibacterial humoral factors in insects, and ii) cleave hemoglobin and serum albumin, two natural sources of amino acids that are thus relevant for

bacteremia (Terwilliger et al., 2015). Consistent with the biofilm resilience, the three InhA paralogues (*BC0666[x], BC1284*, BC2984**) found in the genome of *B. cereus* are upregulated within the biofilm.

Some strains of *B. cereus* have been described to be internalized into host cells (Minnaard et al., 2004). We found the following proteins that are upregulated in planktonic cells and might mediate a putative internalization: i) A sphingomyelin phosphodiesterase (*BC0671*), an enzyme that produces ceramide and is known to be implicated in the liberation of cells of *Neisseria gonorrhoeae* from endosomes or the release of viruses into the host cell cytosol as a result of vacuole disruption (Faulstich et al., 2015; Shivanna et al., 2015). In addition, this protein and ceramide have been proposed to be essential for the hydrolysis of sphingomyelin in membranes, leading to a reduction in phagocytosis (Oda et al., 2010). ii) The 1-phosphatidylinositol phosphodiesterase precursor (*BC3761*), which is essential in the pathogenesis of *Listeria* and speculated to participate in the lysis of the phagolysosome membrane (Wei et al., 2005). Contrary to this observation, in biofilm cells, we found upregulation of the genes *BC1592, BC2639, BC3546* and *BC3547,* annotated as cell surface proteins and orthologues to internalins of *Listeria monocytogenes,* which are implicated in the internalization inside host cells via cadherins and are demonstrated to be implicated in oral infection of *Galleria mellonella* (Fedhila et al., 2006). The genes *esxA/B* are overexpressed in biofilm cells, and these are orthologous to the EsxA and EsxB proteins of the type VIIb secretion system, an important virulence factor responsible for translocation from the phagolysosome to the cytosol

(Warne et al., 2016). These data are contradictory at first and might correspond to different invasion strategies of cells in a planktonic or in biofilm state. We speculate that *B. cereus* internalins might have evolved for an incomplete internalization, working as specific adhesins to cadherins that do not induce phagosome formation or prevented by the injection of any effector by the type VIIb secretion system (Cossart and Lecuit, 1998).

In addition to these changes in gene expression leading to resilience of *B. cereus* biofilms against the host immune system, bacterial cells possess a complete arsenal of toxins and proteases, which may promote bacterial cell survival in two complementary ways: i) reducing the defensive ability of the host to attack the pathogen and ii) seizing host nutrients. *B. cereus* possesses a wide variety of these virulence factors with different targets: cytotoxic K (cytK), nonhemolytic enterotoxin (NHE), enterotoxin C (EntC), hemolysin III, hemolysin BL (HBL) and hemolysin XhlA. *B. cereus* also expresses three collagenases and a phospholipase C as invasins. Perfringolysin O is a sulfhydryl-activated toxin that causes cytolysis by forming pores in cholesterol-containing host membranes (Heuck et al., 2007). These toxins, except hemolysin III, are strongly downregulated in biofilm-associated cells at any stage (Fig. 11), which is in agreement with the downregulation of PlcR, the master regulator that controls the expression of these toxins (Gohar et al., 2008). The expression of hemolysin III is, however, independent of PlcR, which would be the reason for the divergent result with the remaining toxins (Ramarao and Sanchis, 2013). To demonstrate that floating cells are more prone than

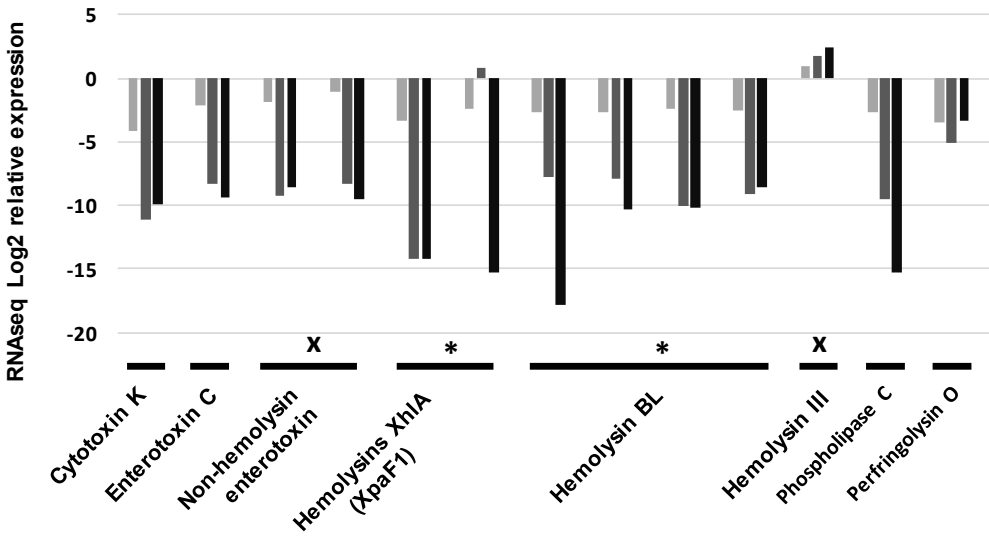

Figure 11. Biofilm cells reduce toxin synthesis. Expression pattern of toxins in a biofilm compared to floating cells at 24 (light gray), 48 (gray) and 72 h (black) (RNAseq data). Data confirmed by iTRAQ results are marked with a star. Data in conflict with iTRAQ data are marked with a cross.

biofilm-associated cells to attack the hosts, both bacterial cell types were isolated and tested for their toxicity potential toward human HELA and MDA cell lines in toxicity assays (Fig. 12). As expected from our analysis, floating cells, which possess an enhanced machinery for toxin production, killed human cells much faster than biofilm-associated cells did, an effect that was seen using different bacteria:cell ratios and was more evident using 10^{-2} and 10^{-4} CFU/ml. These enterotoxins are heat-labile and do not survive gastrointestinal passage, injuring the hosts only when they are produced within the GI tract. Thus, it might be

reasonably suggested that germination of *B. cereus* spores lead to cells with a physiological state that is prone to produce toxins, a situation mimicked by the physiological stage of floating cells in our model. All these findings are indicative of the tendency of *B. cereus* to maintain a floating metabolic state when living in association with the human host, as supported by the fact that GI tract illnesses generally decline within 24 h. However, the fact that *B. cereus* can be collected over 18 days after the initial administration to mice (Duc et al., 2004), indicates that a sparse colonization of the gut takes place. Colonization is similar to a biofilm state, which requires that the defense against the host immune system is upregulated. The strategy used by floating cells is less oriented to survive the host attack, redirecting all the efforts to produce the arsenal of toxins and other virulence factors oriented to fast, aggressive and effective invasion of the host. This strategy is not usually victorious for *B. cereus* against humans, but some cases of "successful" invasion are periodically reported, as happened in a severe infection with fatal result that occurred 13 h after ingestion of a pasta dish contaminated with *B. cereus* (Dierick et al., 2005). Nevertheless, this strategy can be very advantageous against other hosts.

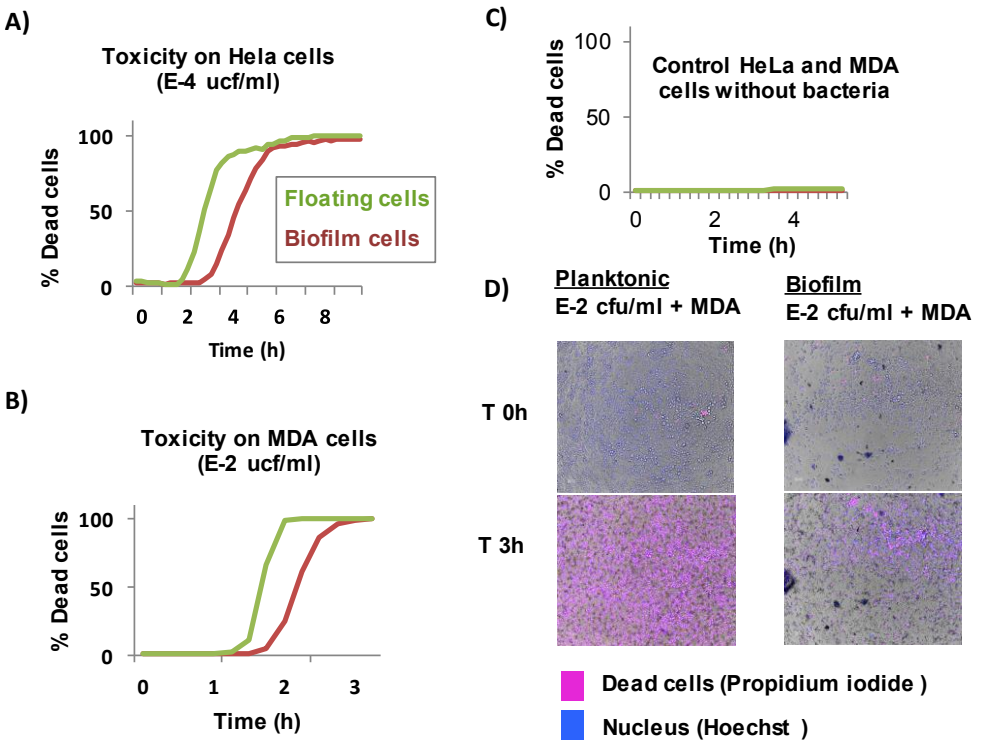

Figure 12. Cells in a biofilm are less aggressive to the host than floating cells are. A-B) Toxicity assay of floating (green line) or biofilm (red line) cells of 48 h cultures against HeLa and MDA cell lines culture without addition of antibiotics. **C)** Negative control of the toxicity assay. **E)** Micrographs of the toxicity assay after 3 h of incubation. Dead cells (pink) are stained with propidium iodide. Nuclei are stained with Hoechst (blue).

7. Proteins with unknown functions but associated with biofilm formation

The lack of information about hypothetical proteins often leads to their exclusion from deeper analyses in -omics studies. Hypothetical proteins (HPs) and genes of unknown function represent more than one-third of

the total molecules differentially expressed within this study. We wondered if gathering cross information from diverse databases and our RNA sequencing results might set a starting point to furthering functionality. All these HPs showed differential expression in our analysis, and thus, many of them probably participate in some of the described functions of biofilm or planktonic cells. As in this work, we characterized biofilm and planktonic functional patterns, we can use bioinformatic analysis for function prediction and determine if the expression behavior pattern of these proteins is the same shown by the genes implicated in the predicted function. An interaction network analysis using the STRING database for each HP yielded interaction maps with other already functionally characterized proteins and more than five connections that suggest a function for the proteins. By doing so, we propose a function for 37 HPs (Fig. 13 and Supplemental Table S9). We found 23 sporulation proteins, 6 genes implicated in secondary metabolites, 3 flagellum proteins and one protein involved in exopolysaccharide production. As a confirmation, all 23 sporulation proteins showed the spore protein patterns exposed above with the expression at 72 h decay after their overexpression at 24 and 48 h. All three flagellum-predicted proteins showed downregulation at all three stages, as happens with most of the known flagellum proteins. Especially interesting are the six genes implicated in antibiotic biosynthesis. One of them belongs to the known region in charge of thiocillin biosynthesis. The other five genes belong to a region (*BC5115-BC5125)* within the gene *BC5123,* which possesses a thiopeptide-type

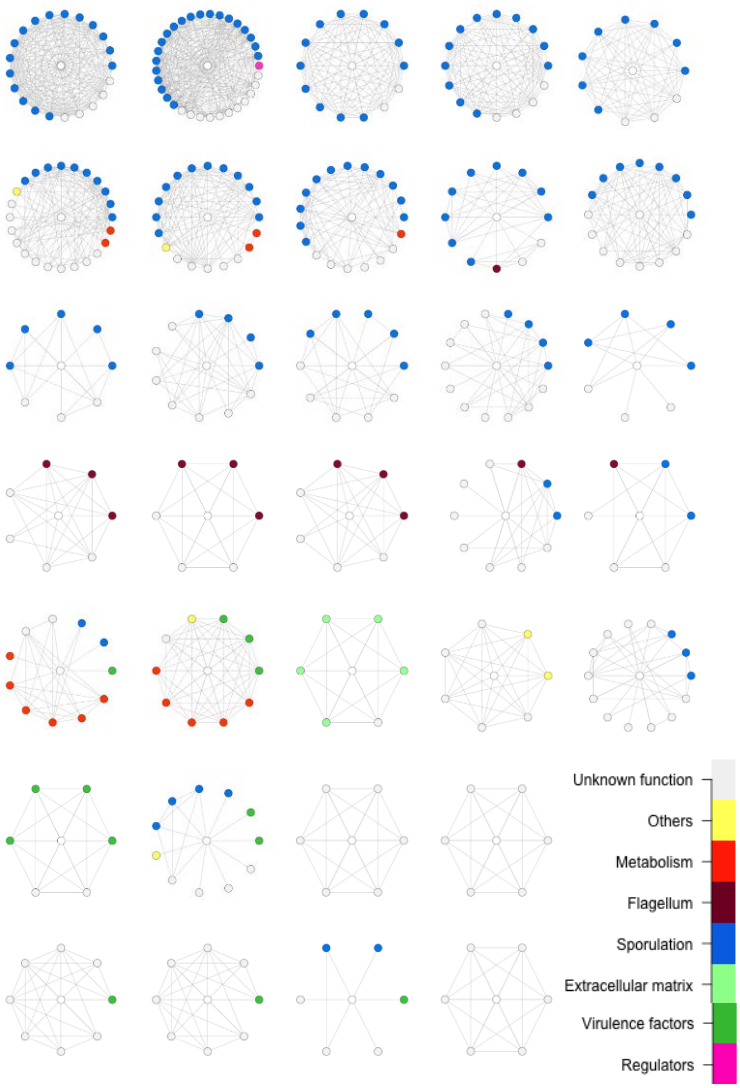

Figure 13. Hypothetical protein function prediction. Nodes represent proteins, and edges represent the functional association obtained from the STRING database. Each network comprises a hypothetical protein (center) whose encoding mRNA changes in expression at one of the three time points, surrounded by its first-degree associations. The colors of the nodes represent different functional annotations for the different proteins, obtained as described in the Methods.

bacteriocin biosynthesis domain, the same domain of protein *BC5083* that is implicated in the thiocillin biosynthesis.

8. The final model: Subpopulations of planktonic and sessile cells act coordinately to attack and defend

All the information obtained from our studies have been integrated into a model that collects the most distinctive features characterizing floating or biofilm-associated cells (Fig. 14). The fact that these two populations coexist are suggestive of coordination to accomplish different functions, which require a complete redistribution of energy and nutrients. This specialization at the metabolic level is oriented to a protective mode of biofilm-associated cells reached by the synthesis of the extracellular matrix and anatomical changes conducive to individual resilience to external aggressions. This specialization is complemented by the deviation of the metabolism to the synthesis of secondary metabolites, some of which appear to mediate the interaction with competitors at short distances from or even in close contact with the biofilm. However, floating cells are metabolically predisposed to colonize new niches and are also more aggressive in terms of pathogenicity, showing an increased production of toxin, which lead to the acquisition of more nutrients. In summary, this study redefines our view of *B. cereus* biofilm versus floating cells and goes further, mapping how deep the physiological and functional changes are in the switch from one lifestyle to the other. The great effort made by biofilm-forming bacteria, oriented

to prevent ROS damage, highlights the weakness of this cell population, pointing to new targets in the fight against resilient biofilms.

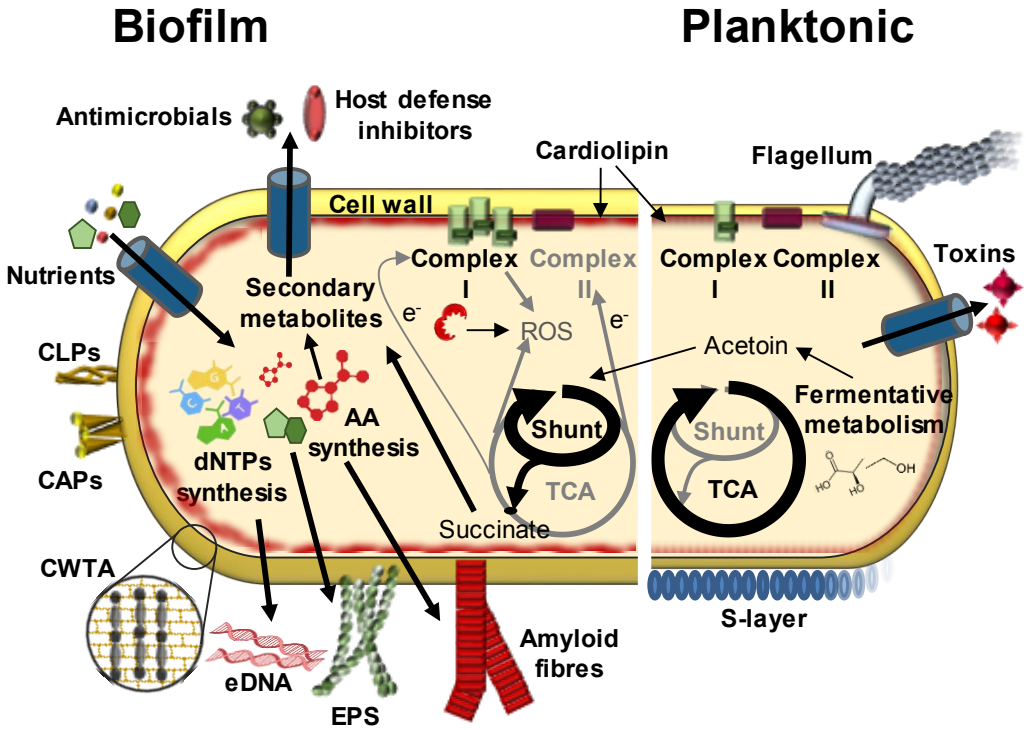

Figure 14. Model of offence and defense of floating cells and cells in the air-liquid interphase biofilm. Major changes differentiate the biofilm from floating cells. Biofilm cells manifest a collection of physiological and morphological changes leading to protection mediated by the increase in the cell wall thickness, the expression of inhibitors of the host defense and antimicrobial resistance genes, or the triggering of sporulation and enhancing of the ROS detoxification system. These changes coordinate with an offensive action against competitors driven by the production of antimicrobials. In contrast, floating cells tend to be more active metabolically and more aggressive in the interaction with hosts, overexpressing, among other compounds, a battery of toxins. CWTA, cell wall teichoic acids; CLPs, collagen-like proteins; CAPs, collagen adhesion proteins; EPS, exopolysaccharides.

3. METHODS AND MATERIAL

Bacterial Strains and Culture Conditions

The bacteria used in this study was *B. cereus* ATCC14579. The mediums used to culture bacteria were LB agar and liquid Ty broth [(1% tryptone, OXOID), 0.5% yeast extract (OXOID), 0.5% NaCl, 10 mM $MgSO_4$, and 0.1 mM $MnSO_4$] were used for bacterial cultures. Bacteria were routinely streaked from -80°C stocks onto LB agar and incubated at 24 h at 30°C before each experiment. For biofilm experiments, one colony was suspended in 1 ml of Ty broth, and the final OD600 was adjusted to one. One milliliter of Ty in 24-well plates was inoculated with 10 µl of the bacterial cell suspension. Only central lines of the wells in the plates where used for culture. Plates were incubated at 30°C for 24, 48 and 72 h.

Cell sampling, RNA isolation and whole transcriptome sequencing

Biofilm, a bacterial biomass adhered to the walls of the wells, was collected with sterile cotton swabs, suspended in 1 ml of Ty, and centrifuged at 12000 g for 10 seconds; the pellet was immediately frozen in liquid nitrogen after discarding the supernatant. As the amount of biofilm formed change over time, collections from 2-8 wells were merged to reach a feasible number of cells for further RNA isolation. For floating cell sampling, 250-500 µl of culture was collected from several wells without disturbing the submerged biofilm, mixed in a 2 ml tube, and centrifuged at 12000 g for 10 seconds; the pellet was immediately frozen in liquid nitrogen after discarding the supernatant. Samples were

stored at -80°C. Samples were recovered from -80ºC, and cold beads were added to each tube and 900 µl of TRI-reagent (Invitrogen), followed by bead beating in a tissue lyser immediately for 1 min. The samples were placed 3 minutes at 55°C. After addition of 200 µl chloroform, tubes were vortexed for 10 seconds, incubated 2-3 min at room temperature and centrifuged at 12,000 g for 10 minutes at 4ºC. The upper phase was mixed with 500 µl ice-cold isopropanol for RNA precipitation, incubated for 10 minutes at RT, and centrifuged at 12,000 g for 10 minutes at 4ºC. The pellet was washed with 75% ethanol, centrifuged twice to remove all supernatant and air-dried for 5 minutes. The pellet was suspended in 20 µl DEPC water (Carl Roth GmbH). DNA was removed using RQ1 DNase treatment (Promega) with a RiboLock RNase inhibitor (Thermo) following the product instructions. After digestion, 400 µl DEPC-MQ water, 250 µl phenol and 250 µl chloroform were added to the samples, vortexed for 5 seconds and centrifuged at 15000 g for 15 minutes at 4ºC. The supernatant was mixed with 1 ml ice-cold 10% ethanol and 50 µl 3 M sodium acetate pH 5.2. The mixture was incubated at least 30 minutes at -20°C and then centrifuged at 15000 g for 15 minutes at 4°C. The pellets were washed twice with 75% ethanol and centrifuged at 15000 g for 5 minutes at 4°C. After spinning the tubes to retire as much of the supernatant as possible, pellets were air-dried at RT for 5 minutes and suspended in 20 µl DEPC water (Carl Roth GmbH). Samples were sent as two biological replicates to the PrimBio Research Institute (Exton, PA, USA), at which the 16S/23S rRNA removal with the Ribo-Zero kit, mRNA quality control (QC), cDNA

library preparation, library QC, template preparation, template QC, and RNA-sequencing on an Illumina platform was performed.

Data analysis of the whole transcriptomes

After trimming the raw RNA-seq reads from the adapter sequences, reads were mapped against the *B. cereus* ATCC 14579 genome sequence. The RPKM (reads per kilo base per million mapped reads) table was generated, and differential gene expression analyses were carried out with the webserver pipeline T-Rex (de Jong et al., 2015) on the Genome2D webserver (http://genome2d.molgenrug.nl/). The significance threshold was defined by a p-value of < 0.05 and a fold-change of >2 ("TopHits" in T-REx). Cluster of orthologous groups (COG) analysis was performed using the Functional Analysis Tools of the T-REx pipeline. The RNA-seq data from this study have been submitted to the NCBI Gene Expression Omnibus (GEO; https://www.ncbi.nlm.nih.gov/geo/query/acc.cgi?acc=GSE115528).

BAGEL3 (Heel et al., 2013) and antiSMASH (Blin et al., 2017) were used to identify secondary metabolite synthesis regions in the genome of *B. cereus* ATCC 14579. To compare the behavior of sporulation genes across the maturation progress of the biofilm, we used *k*-means clustering with the STEM (Short Time-series Expression Miner) software package.

Proteomic analysis

Biofilm and floating cells were separated following the method described above. Samples were sent in triplicate to the Proteomic Facility of the Centro Nacional de Biotecnología CSIC (Spain) for Isobaric Tags for Relative and Absolute Quantitation (iTRAQ). Protein digestion and tagging with a TMTsixplex™ reagent was performed as follows: The total protein concentration was determined using a Pierce 660 nm protein assay (Thermo). For digestion, 40 µg of protein from each condition was precipitated by the methanol/chloroform method. Protein pellets were suspended and denatured in 20 µl 7 M urea/2 M thiourea/100 mM TEAB, pH 7.5, reduced with 2 µL of 50 mM Tris (2-carboxyethyl) phosphine (TCEP, SCIEX), pH 8.0, at 37°C for 60 min and followed by 1 µL of 200 mM cysteine-blocking reagent (methyl methanethiosulfonate (MMTS, Pierce) for 10 min at room temperature. Samples were diluted up to 140 µL to reduce the urea concentration with 25 mM TEAB. Digestions were initiated by adding 2 µg of sequence grade-modified trypsin (Sigma-Aldrich) to each sample at a ratio of 1:20 (w/w); the samples were then incubated at 37°C overnight on a shaker. Sample digestions were evaporated to dryness in a vacuum concentrator. The resulting peptides were subsequently labeled using a TMT-sixplex Isobaric Mass Tagging Kit (Thermo Scientific, Rockford, IL, USA) according to the manufacturer's instructions, as follows: 126: 1B-24 h; 127: 1B-48 h; 128: 1B-72 h; 129: 1P-24 h; 130: 11B-24 h; 131: 13B-72 h. After labeling, the samples were pooled, evaporated to dryness and stored at -20°C until the LC−MS analysis.

For liquid chromatography and mass spectrometry analysis, 1 µg of the labeled protein mixture was subjected to 1D-nano LC ESI-MS/MS analysis using a nanoliquid chromatography system (Eksigent Technologies NanoLC Ultra 1D plus, SCIEX, Foster City, CA) coupled to a high-speed Triple TOF 5600 mass spectrometer (SCIEX, Foster City, CA) with a Nanospray III source. The analytical column used was a silica-based reversed-phase ACQUITY UPLC-Class Peptide BEH C18 Column, 75 µm × 150 mm, 1.7 µm particle size and 130 Å pore size (Waters). The trap column was C18 Acclaim PepMap™ 100 (Thermo Scientific), 100 µm × 2 cm, 5 µm particle diameter, 100 Å pore size, switched on-line with the analytical column. The loading pump delivered a solution of 0.1% formic acid in water at 2 µl/min. The nanopump provided a flow-rate of 250 nl/min and was operated under gradient elution conditions. Peptides were separated using a gradient of 250 minutes ranging from 2% to 90% mobile phase B (mobile phase A: 2% acetonitrile, 0.1% formic acid; mobile phase B: 100% acetonitrile, 0.1% formic acid). The injection volume was 5 µl.

Data acquisition was performed with a TripleTOF 5600 System (SCIEX, Foster City, CA). Data were acquired using an ionspray voltage floating (ISVF) 2300 V, curtain gas (CUR) 35, interface heater temperature (IHT) 150, ion source gas 1 (GS1) 25, declustering potential (DP) 150 V. All data was acquired using information-dependent acquisition (IDA) mode with Analyst TF 1.7 software (SCIEX, Foster City, CA). For IDA parameters, a 0.25 s MS survey scan in the mass range of 350–1250 Da were followed by 30 MS/MS scans of 150 ms in the mass range of 100–1800. Switching criteria were set to ions greater than a mass-to-

charge ratio (m/z) of 350 and smaller than m/z 1250 with a charge state of 2–5 and an abundance threshold of more than 90 counts (cps). Former target ions were excluded for 20 s. An IDA rolling collision energy (CE) parameters script was used for automatically controlling the CE.

For data analysis and protein identification, the mass spectrometry data obtained were processed using PeakView® 2.2 software (SCIEX, Foster City, CA). Raw data file conversion tools generated mgf files, which were also searched against the *B. cereus* protein database from Uniprot (database state June-August 2016), containing 40530 protein-coding genes that included their corresponding reversed entries using four different search engines (Mascot, OMSSA, X!TANDEM and MyriMatch). Search parameters were set as follows: enzyme, trypsin; allowed missed cleavages, 2; methylthio (C) as a fixed modification and TMT-6plex (N-term, K, Y), acetyl (protein N-term), oxidation (M), Gln->pyro-Glu (N-term Q) and Glu->pyro-Glu (N-term E) as variable modifications. The peptide mass tolerance was set to ± 25 ppm for precursors and 0.02 Da for fragment masses. The confidence interval for protein identification was set to ≥ 95% ($p<0.05$), and only peptides with an individual ion score above the 1% false discovery rates (FDR) threshold were considered correctly identified. A 5% quantitation FDR threshold was estimated to consider the significant differentially expressed proteins.

The RNA-seq data from this study have been submitted to the database http://www.proteomexchange.org.

Network creation, clustering and functional analysis

Data on potential pairwise associations between *Bacillus cereus* genes were downloaded from the STRING database (Szklarczyk et al., 2017) using the STRINGdb Bioconductor package for R. This resource comprises data from multiple sources related to direct interactions, both direct and inferred through homology, and predicted associations, made through a variety of algorithms using different data sources. These pairwise associations were then used to build a network between all genes that showed differential expression between biofilm and floating samples, using igraph (Csardi and Nepusz, 2006), visualized using Cytoscape (Shannon et al., 2003). This network was then clustered using the edge betweenness algorithm (Newman and M Girvan, 2004) to find modules of genes with a high degree of connectivity between them, compared to connections to genes outside the module. The DAVID tool was employed for the genes' functional annotation and to look for enrichment of specific biological processes in the GO and KEGG databases within the cluster (Huang et al., 2009). When GO and KEGG enrichment analyses showed the same pathways, the results of one of these two database sources were selected to avoid functional annotation redundancy of clusters.

Mass spectrometry analysis for thiocillin detection

Thiocillin detection was analyzed using HPLC-MS-MS (Ultraflex TOF-TOF, Bruker) of cells and supernatants of 48 h cultures of *B. cereus* in TY medium incubated at 28ºC without shaking. The biofilm was

collected and thoroughly suspended in PBS and then centrifuged at 12000 g to separate cells from the supernatant. Culture medium was centrifuged to separate floating cells from the supernatant. Previous to analysis, the samples were purified with C8 ZipTip® (Merck) to discard salts. To perform MS-MS, a low molecular weight matrix was used.

B. cereus eps1 region mutant

B. cereus eps1 mutant was obtained by electroporation using the plasmid pMAD (Arnaud et al., 2004), harboring a fragment to delete the genes *BC5279-BC5274* by double recombination. The construct was created by joining PCR. In the first step, regions flanking the target genes were amplified separately, purified, and used for the joining PCRs. These PCR products were digested and cloned into the pMAD vector digested with the same enzymes. The resulting suicide plasmids were used to transform *B. cereus* electrocompetent cells as described previously (Kahrs, 1977) with some modifications. Electroporation was performed with 10 µg of plasmids in 100 µL of electrocompetent *B. cereus* in 0.2-cm cuvettes using the following electroporation parameters: voltage 1400 kV, capacitance 25µF, resistance 400 Ω. After electroporation, cells were incubated in LB for 5 hours, and then seeded in LB medium supplemented with X-Gal and erythromycin for 72 h at 30°C. Blue colonies were selected and streaked to trigger allele replacement. Finally, white colonies that were sensitive to MLS were selected, and deletion of the target gene was verified by colony PCR analysis and sequencing of the amplicons.

Evaluation of bacterial cell wall thickness

Biofilm and floating cells were separated following the method described above and fixed in 2% glutardialdehyde. Postfixation was performed with 1% osmium tetroxide in 0.1 M, pH 7.4 phosphate buffer, following dehydration in an acetone gradient at 4 ºC: 30%, 50%, 70% and 90%. A step for in bloc staining with 1% uranyl acetate in 50% cold acetone was included after the 50% step, leaving the samples overnight at 4 ºC. Dehydration was continued with serial incubations in absolute acetone and propylene oxide at room temperature. The embedding in Spurr's resin was made following different steps that combined Spurr's resin:propylene oxide at 1:1, 3:1 (overnight) and two changes in pure resin (the second one, overnight). Finally, samples were embedded in pure resin at 70 ºC for 3 days. Ultrathin sections were visualized in a JEOL JEM-1400 transmission electron microscope with a high-resolution camera (Gatan ES1000 W). The analysis was done using ImageJ-Fiji software over 40 images of each sample and 6-10 measurements over each picture using only circular cell sections to avoid the effect of a tilted sectioning.

Human cell toxicity assay

MDA-MB-231 breast adenocarcinoma and HeLa cervical cancer cell lines were obtained from the American Type Culture Collection (ATCC) and were grown in RPMI 1640 and DEMEM glucose (4.5 g/L) medium cultures respectively, supplemented with glutamine (2 mM), penicillin (50 IU/mL), streptomycin (50 mg/L), amphotericin (1.25 mg/L), and 10%

FBS, at 37°C with 5% CO_2 in air. Cells were seeded at 2000 and 1500 cells/well in a 96-well plate and incubated for 72 h at 37ºC and 5% CO_2 to achieve confluence and a cell density of $1 \cdot 10^4$ cells/well. HeLa and MDA cell medium culture was replaced with 'assay culture' (supplemented with glutamine and FBS, without antibiotics), the cells were incubated for two hours, and then the culture medium was replaced again with assay culture.

B. cereus ATCC14579 was streaked onto an LB agar plate and incubated for 24 h at 28 ºC. The *B. cereus* biomass was suspended in LB and seeded into a 24-well plate with 1 ml of TY and incubated for 48 h. Biofilm and floating cells were separated following the method described above. Both cell fractions of *B. cereus* were washed twice with sterile PBS, and the OD600 was adjusted to 1 (approx. 10^7 cfu/ml). These bacterial fractions were serially diluted 2-10 times, inoculated into 96-well cell culture plates and centrifuged 5 minutes at 2000 g to force the bacteria to make contact with human cell cultures. Propidium iodide and DAPI were added to wells to check the viability state of the eukaryotic cells. The plate was incubated in an Operreta photometer for time-lapse counting of live and dead cells every 15 minutes.

Congo Red and Crystal violet assay

For the Congo Red assay, a *B. cereus* biofilm grown in 4.5 mm diameter plates was analyzed using Ty medium supplemented with Congo Red and Coomassie Brilliant Blue G at final concentrations of 20 µg/ml and 10 µg/ml, respectively; the dyes were filtered and added to autoclaved

Ty medium. *B. cereus* was grown in 1 ml of Ty medium in 4.5 mm diameter plates. Biofilms were stained by removing the spent medium and filling the well with 2 ml of 1% crystal violet for 5 minutes, followed by three washing steps with deionized water (Caro-Astorga et al., 2015).

4. SUPPLEMENTAL TABLES

Table S1. Specialization of biofilm and floating cells in distinct but coordinated metabolic activity. Genes belonging the cluster 1.

GeneIDs	Planktonic(blue)/Biofilm(red)	DAVID Functional annotation
BC0344	blue	1-pyrroline-5-carboxylate dehydrogenase
BC0410	blue	Crp family transcriptional regulator
BC0411	blue	hypothetical protein
BC0466	blue	fumarate hydratase
BC0491	blue	formate acetyltransferase
BC0492	blue	pyruvate formate-lyase activating enzyme
BC0589	blue	formate dehydrogenase alpha chain
BC0590	blue	hypothetical protein
BC0611	blue	aspartate ammonia-lyase
BC0612	blue	L-lactate permease
BC0621	blue	2-amino-3-ketobutyrate CoA ligase
BC0849	blue	acetyltransferase
BC0898	blue	enoyl-CoA hydratase
BC1149	blue	ornithine--oxo-acid transaminase
BC1231	blue	sodium/proline symporter
BC1252	blue	2-oxoglutarate dehydrogenase subunit E1
BC1746	blue	asparagine synthetase AsnA
BC2220	blue	alcohol dehydrogenase
BC2758	blue	metal-dependent hydrolase
BC2896	blue	aspartate aminotransferase
BC2959	blue	malate:quinone oxidoreductase
BC3616	blue	aconitate hydratase
BC3650	blue	imidazolonepropionase
BC3651	blue	urocanate hydratase
BC3652	blue	histidine ammonia-lyase
BC3653	blue	anti-terminator HutP
BC3833	blue	succinyl-CoA synthetase subunit alpha
BC3834	blue	succinyl-CoA synthetase subunit beta

BC4023	blue	acetyl-CoA acetyltransferase
BC4224	blue	glycine dehydrogenase subunit 2
BC4225	blue	glycine dehydrogenase subunit 1
BC4226	blue	glycine cleavage system aminomethyltransferase T
BC4365	blue	bifunctional acetaldehyde-CoA/alcohol dehydrogenase
BC4516	blue	succinate dehydrogenase iron-sulfur subunit
BC4517	blue	succinate dehydrogenase flavoprotein subunit
BC4592	blue	malate dehydrogenase
BC4593	blue	isocitrate dehydrogenase
BC4594	blue	citrate synthase
BC4870	blue	L-lactate dehydrogenase
BC4995	blue	regulatory protein
BC4996	blue	L-lactate dehydrogenase
BC5002	blue	acyl-CoA dehydrogenase
BC5003	blue	acetyl-CoA acetyltransferase
BC5004	blue	enoyl-CoA hydratase
BC5006	blue	Prolyne dehydrogenase
BC5228	blue	L-lactate permease
BC5342	blue	acyl-CoA dehydrogenase
BC5344	blue	acetyl-CoA acetyltransferase
BC5345	blue	Iron-sulphur-binding reductase
BC5438	blue	antiholin-like protein LrgB
BC5439	blue	murein hydrolase regulator LrgA
BC0355	red	4-aminobutyrate--2-oxoglutarate transaminase
BC0356	red	sigma-54-dependent transcriptional activator
BC0357	red	succinate-semialdehyde dehydrogenase [NADP+]
BC1036	red	glycerol-3-phosphate dehydrogenase
BC1301	red	two component system histidine kinase
BC1396	red	branched-chain amino acid aminotransferase
BC1398	red	acetolactate synthase small subunit
BC1399	red	ketol-acid reductoisomerase
BC1400	red	2-isopropylmalate synthase
BC1401	red	3-isopropylmalate dehydrogenase
BC1402	red	3-isopropylmalate dehydratase large subunit
BC1610	red	aminotransferase
BC1611	red	hypothetical protein

BC1776	red	branched-chain amino acid aminotransferase
BC1777	red	acetolactate synthase 3 catalytic subunit
BC2285	red	citrate synthase 3
BC2286	red	2-methylcitrate dehydratase
BC2287	red	methylisocitrate lyase
BC2288	red	acyl-CoA dehydrogenase
BC2289	red	3-hydroxyisobutyrate dehydrogenase
BC2290	red	methylmalonate-semialdehyde dehydrogenase
BC2292	red	3-hydroxyisobutyryl-CoA hydrolase
BC2776	red	dihydrolipoamide dehydrogenase
BC2778	red	acetoin dehydrogenase E1 component beta-subunit
BC3555	red	aldehyde dehydrogenase
BC3939	red	formamidase
BC4325	red	late competence protein ComER
BC4595	red	hypothetical protein
BC4644	red	PhnB protein
BC4645	red	acetyl-coenzyme A synthetase
BC4762	red	phosphoenolpyruvate carboxykinase
BC5133	red	holin-like protein

Table S2. KEGG pathways enrichment data for ALL, blue (planktonic), and red (biofilm) genes in cluster 1. Significance tests p-value and Benjamin are shown, and the number and percentage of gene over the total genes in Cluster 1 is also shown for each KEGG pathway.

KEGG: Metabolic pathways	P-Value	Benjamini	#genes	%genes
ALL	8.00E-10	6.80E-09	52	62.7
BLUE (Planktonic)	3.50E-07	2.10E-06	34	66.7
RED (Biofilm)	1.70E-03	6.10E-03	18	56.2

KEGG: Biosynthesis of antibiotics	P-Value	Benjamini	#genes	%genes
ALL	5.80E-14	2.90E-12	35	42.2
BLUE (Planktonic)	1.60E-10	6.60E-09	24	47.1
RED (Biofilm)	5.00E-04	2.30E-03	11	34.4

KEGG: Biosynthesis of secondary metabolites	P-Value	Benjamini	#genes	%genes
ALL	8.90E-13	2.30E-11	40	48.2
BLUE (Planktonic)	7.10E-08	5.90E-07	25	49
RED (Biofilm)	1.90E-05	1.70E-04	15	46.9

KEGG: Citrate cycle (TCA cycle)	P-Value	Benjamini	#genes	%genes
ALL	9.00E-13	1.50E-11	15	18.1
BLUE (Planktonic)	1.00E-09	1.40E-08	11	21.6
RED (Biofilm)	8.70E-03	2.10E-02	4	12.5

KEGG: 2-Oxocarboxylic acid metabolism	P-Value	Benjamini	#genes	%genes
ALL	2.80E-10	2.80E-09	13	15.7
BLUE (Planktonic)	4.00E-02	1.00E-01	4	7.8

RED (Biofilm)	1.70E-09	3.20E-08	9	28.1

KEGG: Glyoxylate and dicarboxylate metabolism	P-Value	Benjamini	#genes	%genes
ALL	4.10E-09	2.60E-08	13	15.7
BLUE (Planktonic)	1.10E-07	7.60E-07	10	19.6
RED (Biofilm)	9.30E-02	1.90E-01	3	9.4

KEGG: Pyruvate metabolism	P-Value	Benjamini	#genes	%genes
ALL	2.20E-08	1.20E-07	15	18.1
BLUE (Planktonic)	7.50E-05	3.40E-04	9	17.6
RED (Biofilm)	1.10E-03	4.40E-03	6	18.8

KEGG: Propanoate metabolism	P-Value	Benjamini	#genes	%genes
ALL	5.50E-08	2.80E-07	11	13.3
BLUE (Planktonic)	5.70E-05	2.90E-04	7	13.7
RED (Biofilm)	7.10E-03	2.00E-02	4	12.5

KEGG: Butanoate metabolism	P-Value	Benjamini	#genes	%genes
ALL	1.20E-07	5.20E-07	11	13.3
BLUE (Planktonic)	8.90E-05	3.60E-04	7	13.7
RED (Biofilm)	8.70E-03	2.10E-02	4	12.5

Table S3. Gene composition of three general enriched KEGG pathways in Cluster 1 is indicated by "x" symbol.

KEGG: Metabolic pathways	KEGG: synthesis of secondary metabolites	KEGG: synthesis of antibiotics	Functional annotation	Gene
x			1-Pyrroline-5-Carboxylate dehydrogenase	BC0344
x			4-Aminobutyrate--2-Oxoglutarate transaminase	BC0355
	x		Glycerol-3-Phosphate dehydrogenase	BC1036
x			Succinate-Semialdehyde dehydrogenase [NADP+]	BC0357
x	x	x	Fumarate hydratase	BC0466
x			Formate acetyltransferase	BC0491
x			formate dehydrogenasealpha chain	BC0589
x			aspartate ammonia-lyase	aspA
x	x	x	acetyltransferase	BC0849
x	x	x	ornithine--oxo-acid transaminase	rocD
x	x	x	2-oxoglutarate dehydrogenasesubunit E1	sucA
x	x	x	branched-chain aminoacid aminotransferase	BC1396
x	x	x	acetolactate synthasesmall subunit	ilvH
x	x	x	ketol-acid reductoisomerase	BC1399
x	x		2-isopropylmalate synthase	BC1400
x	x		3-isopropylmalate dehydrogenase	BC1401
x	x		3-isopropylmalate dehydrataselarge subunit	BC1402
x	x		asparagine synthetaseAsnA	BC1746
x	x	x	branched-chain aminoacid aminotransferase	BC1776
x	x	x	acetolactate synthase small subunit	BC1777
x	x	x	alcohol dehydrogenase	BC2220
x	x	x	citrate synthase3	BC2285
x			3-hydroxyisobutyrate dehydrogenase	BC2289
x			methylmalonate-semialdehyde dehydrogenase	acylating
x	x		metal-dependent hydrolase	BC2758
x	x	x	dihydrolipoamide dehydrogenase	acoL

x	x	x	acetoin dehydrogenase E1 component beta-subunit	BC2778
x	x	x	malate:quinone oxidoreductase	BC2959
x	x	x	aldehyde dehydrogenase	BC3555
x	x	x	aconitate hydratase	BC3616
x	x		imidazolonepropionase	BC3650
x	x		urocanate hydratase	BC3651
x	x		histidine ammonia-lyase	hutH
x	x	x	succinyl-CoA synthetasesubunit alpha	BC3833
x		x	succinyl-CoA synthetasesubunit beta	sucC
x		x	acetyl-CoA acetyltransferase	BC4023
x		x	glycine dehydrogenasesubunit 2	BC4224
x	x	x	glycine dehydrogenasesubunit 1	BC4225
x	x	x	glycine cleavage system aminomethyltransferase T	gcvT
x	x	x	bifunctional acetaldehyde-CoA/alcoholdehydrogenase	BC4365
x	x	x	succinate dehydrogenaseiron-sulfur subunit	sdhB
x	x	x	succinate dehydrogenaseflavoprotein subunit	sdhA
x	x	x	malate dehydrogenase	BC4592
x	x	x	isocitrate dehydrogenase	BC4593
x	x	x	citrate synthase	BC4594
x	x	x	acetyl-coenzyme Asynthetase	BC4645
x	x	x	phosphoenolpyruvate carboxykinase	BC4762
x	x	x	L-lactate dehydrogenase	ldh
x	x	x	L-lactate dehydrogenase	ldh
x		x	acetyl-CoA acetyltransferase	BC5003
x	x		enoyl-CoA hydratase	BC5004
x	x	x	Prolyne dehydrogenase	BC5006
x		x	acetyl-CoA acetyltransferase	BC5344

Table S4. Specialization of biofilm and floating cells in distinct but coordinated metabolic activity. Genes belonging the cluster 2.

GeneIDs	Planktonic(blue)/Biofilm(red)	DAVID functional annotation
BC0049	red	SspF protein
BC0069	red	stage II sporulation protein E
BC0169	red	spore germination protein GerD
BC0170	blue	#N/A
BC0263	red	#N/A
BC0520	blue	#N/A
BC0603	red	hypothetical protein
BC0875	red	small acid-soluble spore protein
BC0877	red	hypothetical protein
BC1012	blue	#N/A
BC1225	blue	#N/A
BC1500	red	hypothetical protein
BC1501	red	hypothetical protein
BC1502	red	hypothetical protein
BC1509	red	stage IV sporulation protein A
BC1520	red	#N/A
BC1984	red	small acid-soluble spore protein
BC1994	blue	#N/A
BC2010	red	#N/A
BC2050	red	#N/A
BC2095	red	hypothetical protein
BC2536	red	cell wall hydrolase cwlJ
BC3106	red	small acid-soluble spore protein
BC3605	red	#N/A
BC3770	red	spore coat protein E
BC3783	red	#N/A
BC3800	red	dipicolinate synthase subunit B
BC3801	red	dipicolinate synthase subunit A
BC3802	red	hypothetical protein
BC3902	red	hypothetical protein
BC3905	red	sporulation sigma-E factor processing peptidase
BC3922	red	prespore specific transcriptional activator rsfA
BC4067	red	stage V sporulation protein AD

BC4073	red	anti-sigma F factor
BC4088	red	hypothetical protein
BC4186	red	stage III sporulation protein AH
BC4187	red	stage III sporulation protein AG
BC4188	red	stage III sporulation protein AF
BC4191	red	stage III sporulation protein AC
BC4192	red	stage III sporulation protein SpoAB
BC4193	red	#N/A
BC4194	red	hypothetical protein
BC4288	blue	membrane-attached cytochrome c550
BC4440	red	#N/A
BC4466	red	CotS-related protein
BC4467	red	stage VI sporulation protein D
BC4495	red	germination protein germ
BC4563	red	small acid-soluble spore protein SspI
BC4577	red	hypothetical protein
BC4606	red	hypothetical protein
BC4640	red	hypothetical protein
BC4641	red	hypothetical protein
BC4642	blue	inorganic polyphosphate/ATP-NAD kinase
BC4660	blue	#N/A
BC4662	blue	#N/A
BC4899	red	hypothetical protein
BC4923	blue	#N/A
BC4924	blue	#N/A
BC5145	red	hypothetical protein
BC5147	red	stage V sporulation protein AC
BC5148	red	stage V sporulation protein AD
BC5149	red	stage V sporulation protein AE
BC5282	red	stage III sporulation protein D
BC5283	red	stage II sporulation protein Q
BC5287	red	stage II sporulation protein D
BC5289	red	#N/A
BC5385	red	prespore specific transcriptional activator rsfA
BC5390	red	cell wall hydrolase cwlJ
BC5480	red	hypothetical protein

BC5391	red	hypothetical protein
BC4607	red	hypothetical protein

Table S5. Specialization of biofilm and floating cells in distinct but coordinated metabolic activity. Genes belonging the cluster 3.

GeneIDs	Planktonic(blue)/Biofilm(red)	DAVID functional annotation
BC0114	blue	RNA polymerase factor sigma-70
BC0404	blue	methyl-accepting chemotaxis protein
BC0405	blue	#N/A
BC0422	blue	methyl-accepting chemotaxis protein
BC0559	blue	methyl-accepting chemotaxis protein
BC0576	blue	methyl-accepting chemotaxis protein
BC0678	blue	methyl-accepting chemotaxis protein
BC0679	red	#N/A
BC1625	blue	flagellar motor protein MotP
BC1626	blue	#N/A
BC1627	blue	chemotaxis protein CheY
BC1628	blue	chemotaxis protein CheA
BC1629	blue	flagellar motor switch protein
BC1630	blue	hypothetical protein
BC1636	blue	flagellar hook-associated protein FlgK
BC1637	blue	flagellar hook-associated protein FlgL
BC1638	blue	flagellar capping protein
BC1639	blue	flagellar protein fliS
BC1643	blue	flagellar hook-basal body protein FliE
BC1644	blue	flagellar MS-ring protein
BC1645	blue	flagellar motor switch protein G
BC1646	blue	flagellar assembly protein H
BC1647	blue	flagellum-specific ATP synthase
BC1651	blue	flagellar hook protein FlgE
BC1653	blue	hypothetical protein
BC1654	blue	chemotaxis protein CheV
BC1657	blue	flagellin
BC1658	blue	flagellin
BC1659	blue	flagellin
BC1660	blue	soluble lytic murein transglycosylase
BC1662	blue	flagellar motor switch protein FliM
BC1664	blue	flagellar motor switch protein fliN

BC1671	blue	flagellar basal body rod protein FlgG
BC1672	blue	metal-dependent hydrolase related to alanyl-tRNA synthetase
BC2006	blue	methyl-accepting chemotaxis protein
BC2766	blue	#N/A
BC3903	red	sporulation sigma factor SigG
BC3904	red	sporulation sigma factor SigE
BC4071	red	Sodium/proline symporter
BC4072	red	sporulation sigma factor SigF
BC4074	red	anti-sigma F factor antagonist
BC4512	blue	flagellar motor protein MotB
BC4513	blue	flagellar motor protein MotA
BC5009	blue	methyl-accepting chemotaxis protein
BC5034	blue	methyl-accepting chemotaxis protein
BC5065	blue	#N/A
BC5143	blue	#N/A
BC1631	blue	hypothetical protein
BC1640	blue	hypothetical protein
BC1648	blue	cytoplasmic protein
BC1652	blue	hypothetical protein
BC5035	red	#N/A
BC5066	blue	endonuclease/exonuclease/phosphatase family protein

Table S6. Expression pattern of genes involved in amino acid transport. Asterisk indicate confirmed behavior in protein levels.

		Log2 (fold change)			
Gene ID	**24 h**	**48 h**	**72 h**	**Gene name**	**iTRAQ**
BC0401	1.38	4.05	4.71	cystine transport system permease	*
BC0402	2.46	4.30	5.42	cystine-binding protein	*
BC0403	1.24	4.12	4.70	glutamine transport ATP-binding protein glnQ	*
BC0638	1.44	4.50	5.10	Sodium/proton-dependent alanine carrier protein	*
BC0639	8.70	8.82	1.78	glutamine transport ATP-binding protein glnQ	
BC0640	15.73	17.36	7.72	glutamine-binding protein	*
BC0703	1.23	3.41	3.47	Sodium/proline symporter	
BC0865	0.02	-0.51	-3.69	arginine/ornithine antiporter	
BC1231	-3.21	-1.45	-0.07	Sodium/proline symporter	
BC1432	-1.59	-1.90	-3.18	proton/sodium-glutamate symport protein	*
BC1609	1.55	4.17	5.94	Sodium/proline symporter	*
BC1927	2.11	5.79	6.66	leu-, iso-, val-, trn-, ala-binding protein	*
BC2790	5.31	7.63	5.29	glycine betaine transport system permease	
BC2980	-0.14	-0.53	-4.31	arginine permease	
BC3398	0.01	-2.47	-5.75	Serine transporter	*
BC4071	2.82	5.62	6.82	Sodium/proline symporter	*
BC4149	-2.26	-3.48	-1.42	arginine ABC transporter permease	*
BC4150	-2.13	-2.90	-0.30	arginine-binding protein	*
BC4242	1.12	2.20	4.00	proton/sodium-glutamate symport protein	
BC5043	-1.63	-3.20	-4.10	Sodium/proton-dependent alanine carrier protein	
BC5051	-3.53	-1.60	-3.76	Sodium/proton-dependent alanine carrier protein	
BC5218	-0.03	-3.89	-16.49	proton/sodium-glutamate symport protein	

Table S7. Expression pattern of genes involved in antimicrobial biosynthesis. Asterisk indicate confirmed behavior in protein levels.

	Log2 (fold change)				
Gene ID	**24 h**	**48 h**	**72 h**	**Molecule**	**iTRAQ**
BC1201	2.87	5.63	1.75	Tylosin	
BC1204	8.07	9.53	5.09	Tylosin	
BC1206	7.01	8.13	2.73	Tylosin	*
BC1208	5.00	6.74	1.04	Streptomycin like	
BC1209	5.95	7.91	2.46	Streptomycin like	*
BC1210	3.47	4.24	-0.52	Streptomycin like	
BC1211	3.78	6.19	2.59	Streptomycin like	
BC1212	4.36	6.94	0.28	Streptomycin like	*
BC1213	3.38	5.85	-1.63	Streptomycin like	
BC1214	3.10	5.17	0.92	Streptomycin like	*
BC1248	3.77	5.88	2.80	Bacteriocin	
BC1249	4.28	5.43	3.24	Bacteriocin	
BC1250	4.31	5.00	1.78	Bacteriocin	
BC2452	0.24	3.00	4.99	Bacitracin	
BC2966	16.71	17.72	10.24	Polyketide synthase	
BC5079	-1.90	3.60	4.62	Thiocillin	*
BC5080	-1.58	3.00	3.75	Thiocillin	*
BC5081	-0.86	3.27	4.33	Thiocillin	*
BC5082	-2.43	3.20	4.32	Thiocillin	*
BC5083	-2.33	2.06	3.34	Thiocillin	*
BC5084	-1.76	2.48	3.69	Thiocillin	*
BC5085	-0.77	3.52	3.36	Thiocillin	*
BC5086	-1.76	2.83	4.04	Thiocillin	*
BC5087	2.85	3.61	3.02	Thiocillin	
BC5088	2.81	3.74	3.14	Thiocillin	
BC5089	2.61	3.65	2.90	Thiocillin	
BC5090	2.61	2.87	3.13	Thiocillin	
BC3021	0.48	2.21	2.78	Colicin	*
BC1426	2.01	8.10	8.50	Porphirin	

BC1427	1.46	5.19	4.77	Porphirin	
BC1428	3.04	6.66	6.96	Porphirin	*
BC2133	-2.57	-4.22	-11.87	Porphirin	
BC2134	-2.99	-4.05	-6.25	Porphirin	
BC4468	2.84	3.27	3.62	Porphirin	

Table S8. Expression pattern of genes involved in antimicrobial resistances. Asterisk indicate confirmed behavior in protein levels. Cross indicate conflicting result.

	Log_2 (fold change)				
	24 h	**48 h**	**72 h**	**Gene**	**iTRAQ**
BC1379	0.89	2.26	4.06	Gentamycin	
BC3197	1.41	4.83	5.44	Tetracyclin	
BC5068	2.11	1.81	-14.51	Camphor	
BC3231	2.21	4.11	3.90	Microcin	*
BC3533	2.47	2.96	2.73	Vancomycin	x
BC3545	3.18	6.07	3.87	Chloranphenicol	
BC2673	11.25	11.55	9.13	Tetracyclin	
BC4207	-0.85	-0.01	-4.05	Bacteriocina AS-48	

Table S9. Hypothetical protein function prediction.

			Differential expression		
Gene	Num. Genes functionally associated	Prediction	24h	48h	72h
BC5123	6	Secondary metabolites	-3.77	-5.02	-8.29
BC5124	6	Secondary metabolites	-3.60	-3.72	-4.70
BC5125	6	Secondary metabolites	-3.07	-3.08	-4.42
BC1640	6	Flagellum	-2.88	-4.76	-7.02
BC5082	6	Secondary metabolites	-2.43	3.20	4.32
BC2138	6	Sporulation	2.13	5.75	3.28
BC1219	6	Sporulation	2.89	3.43	-12.08
BC1591	6	Secondary metabolites	4.33	7.08	5.00
BC2893	6	Sporulation	9.36	13.60	8.43
BC1853	7	None	-4.33	-16.56	-16.56
BC1635	7	Flagellum	-3.21	-5.14	-6.07
BC1634	7	Flagellum	-2.86	-6.59	-5.47
BC4388	7	Sporulation	-0.36	3.13	0.77
BC1221	7	Sporulation	4.29	9.14	5.99
BC0877	7	Sporulation	7.50	8.63	5.66
BC5121	8	Secondary metabolites	-3.94	-5.63	-8.69
BC5119	8	Secondary metabolites	-3.93	-4.79	-6.01
BC3784	8	Sporulation	1.15	5.57	0.58
BC5150	10	Sporulation	1.12	5.24	-11.30
BC5145	10	Sporulation	10.35	13.20	7.98
BC1425	10	Metabolism	12.74	18.06	17.30
BC0825	11	Sporulation	2.83	4.79	1.50
BC4088	11	Metabolism	3.66	2.32	0.59
BC3802	11	Sporulation	12.64	15.00	14.74
BC2095	11	Sporulation	14.89	16.42	10.17
BC5391	12	Sporulation	6.30	6.76	-0.92
BC1502	14	Sporulation	5.92	8.16	5.30
BC4606	14	Sporulation	14.35	14.18	0.00

BC5480	14	Sporulation	17.77	18.53	15.09
BC1392	16	Sporulation	2.70	7.01	-0.87
BC4577	16	Sporulation	3.75	4.28	-11.36
BC2752	19	Sporulation	2.53	5.43	-10.54
BC4640	20	Sporulation	6.01	7.30	4.17
BC3902	21	Sporulation	14.32	16.72	11.34
BC4641	24	Sporulation	6.78	8.60	-9.69
BC3928	33	Sporulation	3.83	4.68	-10.58

5. SUPPLEMENTAL FIGURES

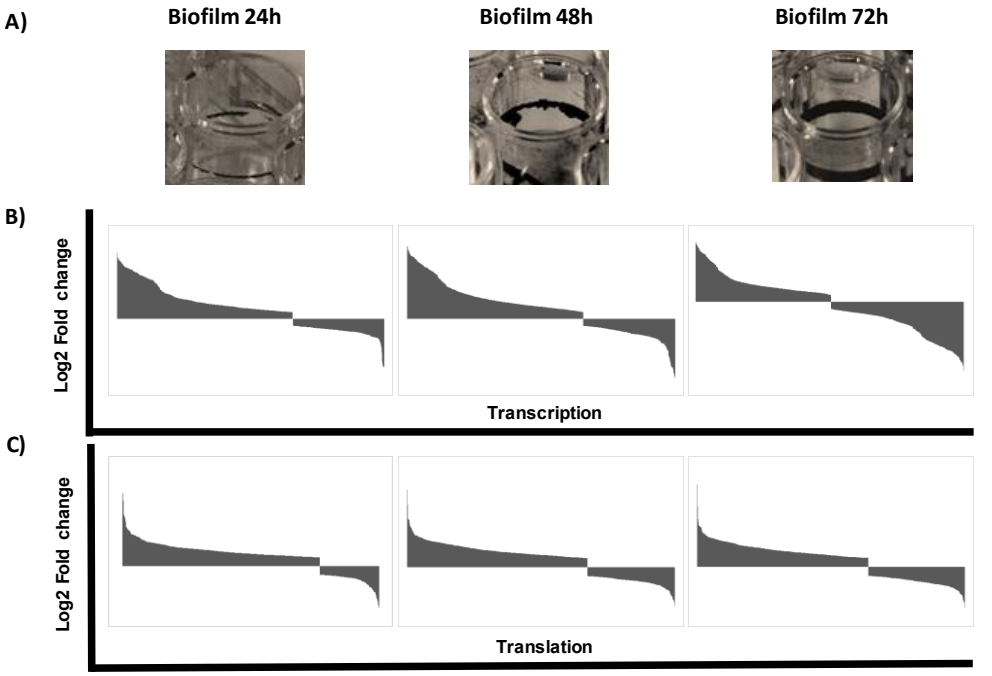

Figure S1. A) Pictures of biofilm stained with crystal violet at 24, 48 and 72 h. **B)** Graph Log_2 Fold Change of genes transcription levels at 24, 48 and 72 h. Showed only statistically significant changes ($Log_2 > 2$ and p-value < 0.05). **C)** Graph Log_2 (Fold Change) of protein levels at 24, 48 and 72 h. Showed only statistically significant changes ($Log_2 > 0.7$ and q-value < 0.05).

A)

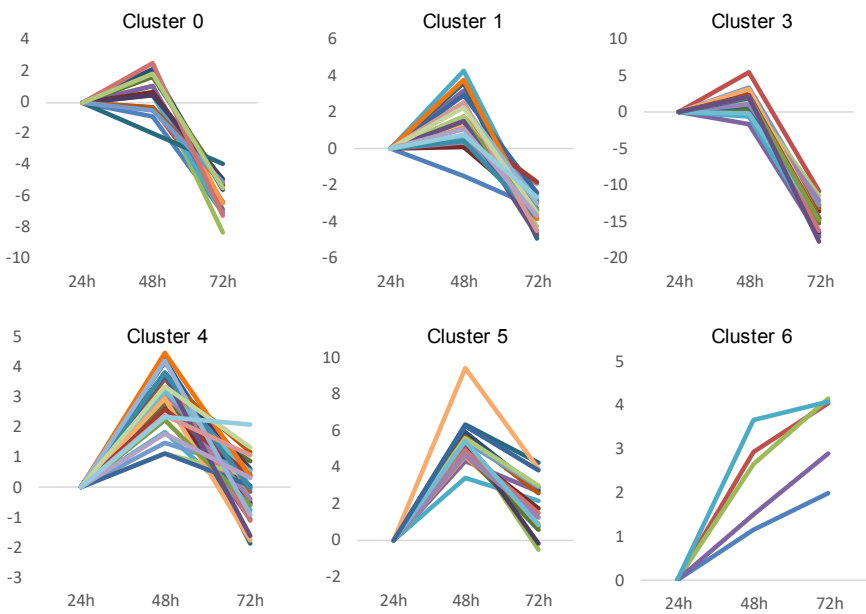

B) **Cluster 6**

Gene ID	24h	48h	72h	Gen name
BC2353	1.47	2.61	3.46	Spo0A-P phosphatase
BC2142	-0.32	2.59	3.71	stage V sporulation protein S
BC1340	-0.45	2.19	3.71	Sporulation kinase KinE
BC2259	3.21	3.81	3.80	Sporulation-control protein Spo0M
BC5482	-3.31	0.36	0.77	Sporulation initiation inhibitor protein soj

Figure S2. A) Clustering of sporulation genes with STEM. Clusters 1-5 show sharp downregulation of most of sporulation genes. Cluster 6 contain five genes with an expression pattern of higher expression at 72 h than in previous stages. **B)** List of genes included in cluster 6 showing that three out of five genes are involved in negative regulation of sporulation and one gene involved in the last stage of spore maturation, proposed to play a role in the coat assembly. KinE, has been demonstrated low phosphorylation activity to the sporulation phosphorelay (Fujita and Losick, 2005).

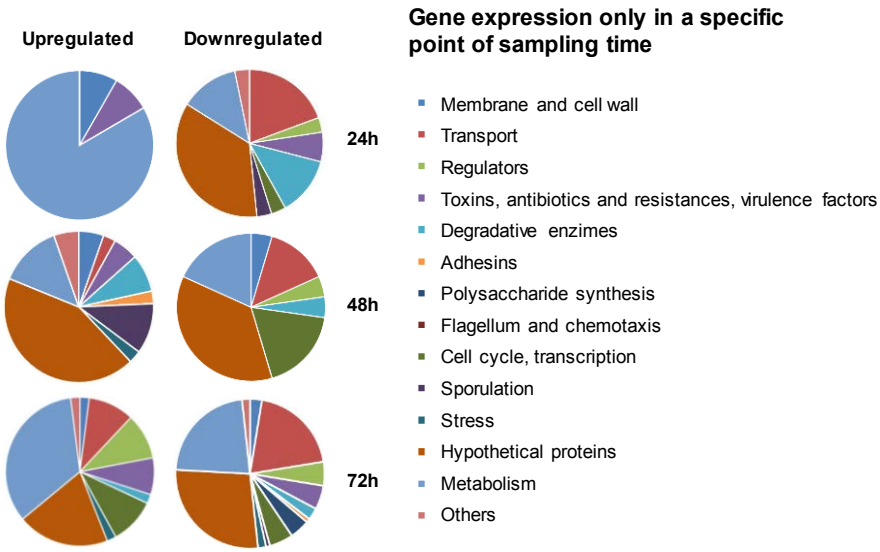

Figure S3. Circle charts of genes with an expression pattern change statistically significant (Log2 (Fold change) > |2|) up or down regulated in a specific sampling time 24, 48 and 72 h and no significant change at other stage. Specific stage genes increase their diversity especially at 48 and 72 h biofilms.

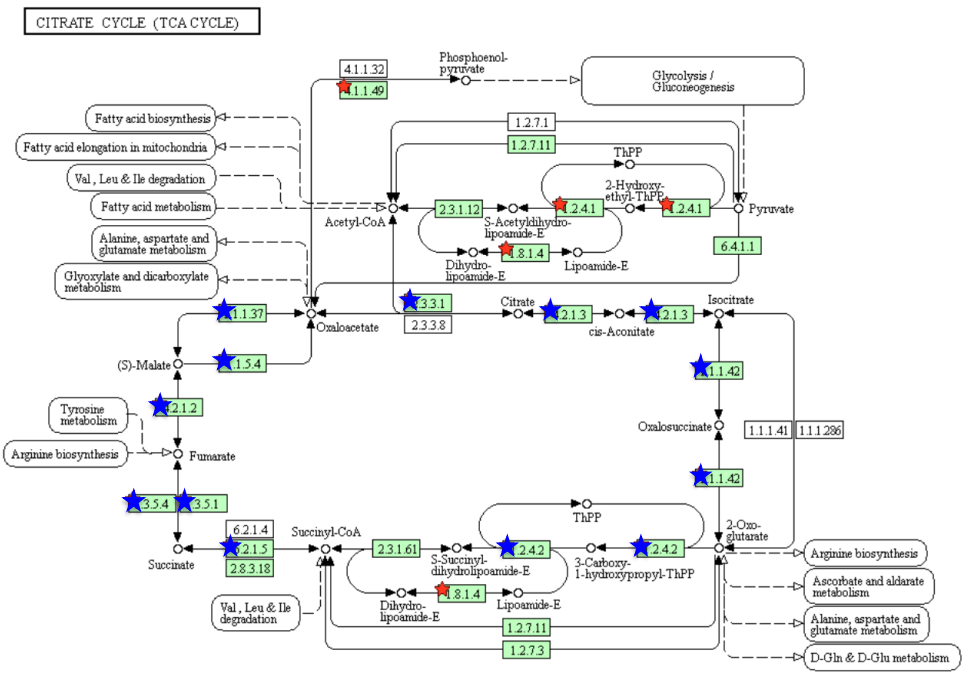

Figure S4. Canonical scheme of Tricarboxilic Acid Cycle (TCA) (KEGG Database). Squares indicate enzymatic process. Green squares indicate process able to be accomplished by *B. cereus*. Stars indicate enhanced expression in planktonic cells (blue) or biofilm cells (red).

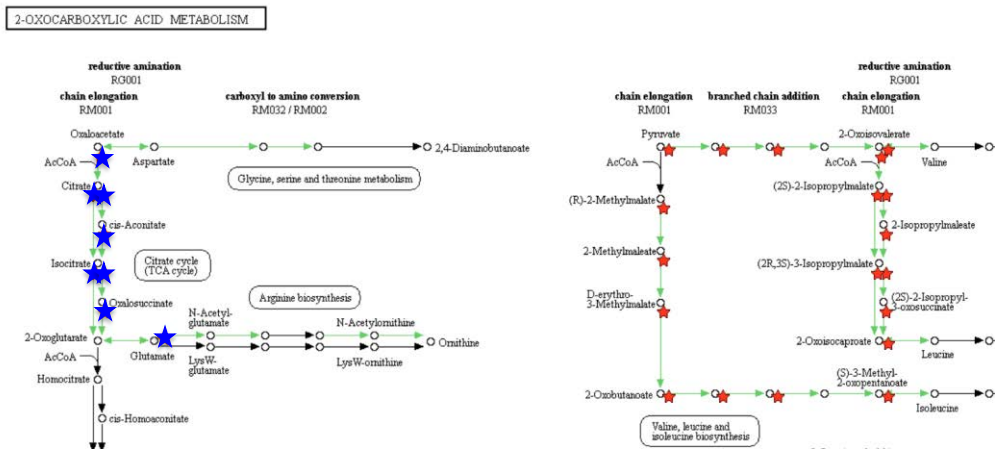

Figure S5. Canonical scheme of 2-Oxocarboxylic Acid metabolism (KEGG Database). Arrows indicate enzymatic process. Green arrows indicate process able to be accomplished by *B. cereus*. Stars indicate enhanced expression in planktonic cells (blue) or biofilm cells (red).

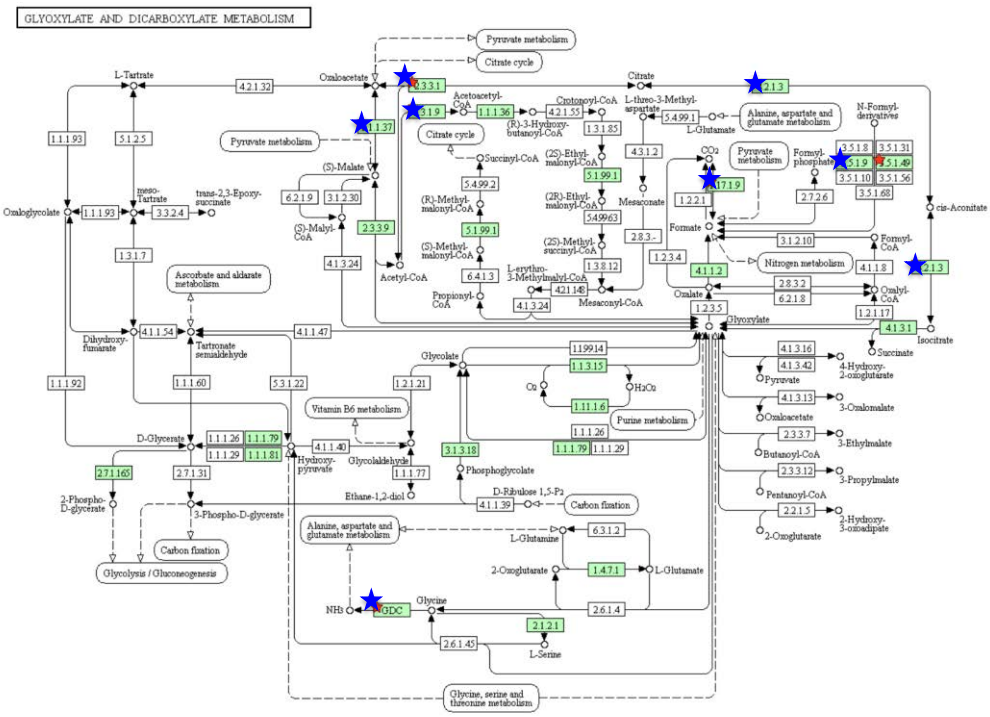

Figure S6. Canonical scheme of Glyoxilate and Dicarboxylate metabolism (KEGG Database). Squares indicate enzymatic process. Green squares indicate process able to be accomplish by *B. cereus*. Stars indicate enhanced expression in planktonic cells (blue) or biofilm cells (red).

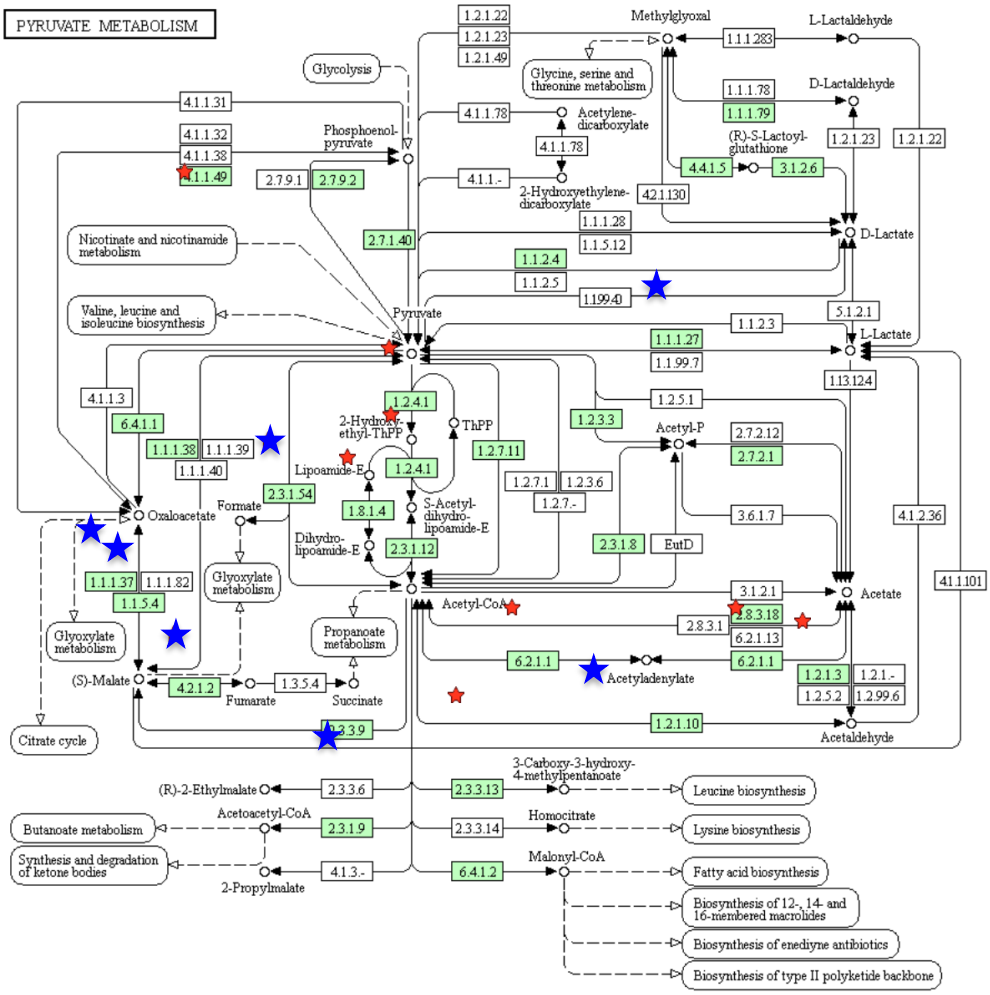

Figure S7. Canonical scheme of Pyruvate metabolism (KEGG Database). Squares indicate enzymatic process. Green squares indicate process able to be accomplish by *B. cereus*. Stars indicate enhanced expression in planktonic cells (blue) or biofilm cells (red).

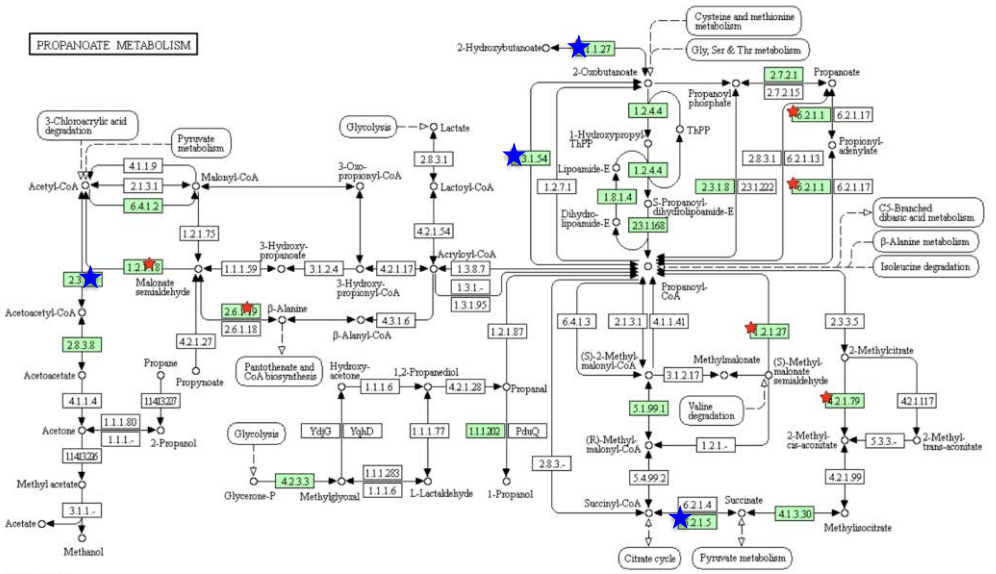

Figure S8. Canonical scheme of Propanoate metabolism (KEGG Database). Squares indicate enzymatic process. Green squares indicate process able to be accomplish by *B. cereus*. Stars indicate enhanced expression in planktonic cells (blue) or biofilm cells (red).

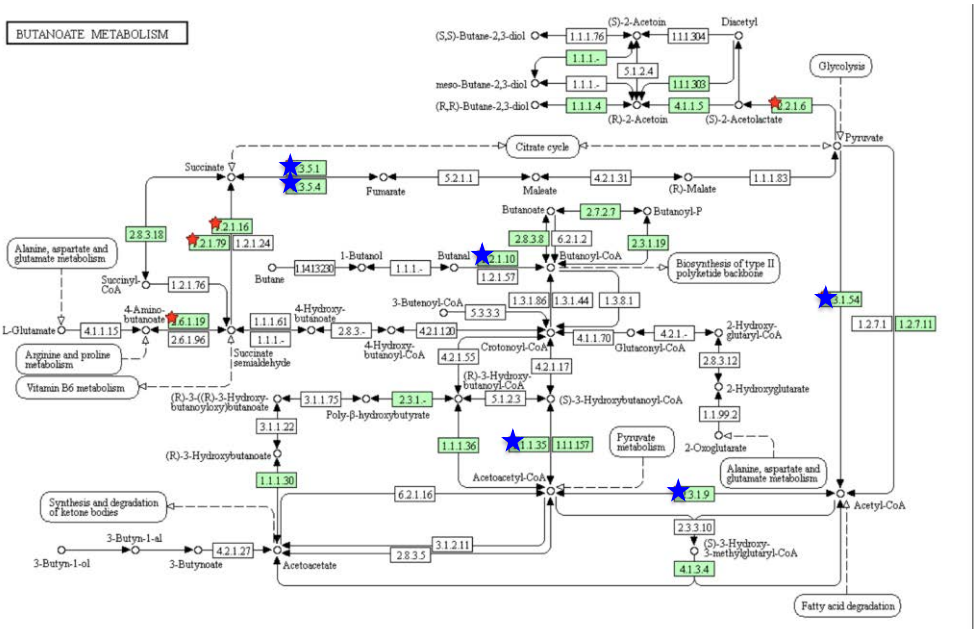

Figure S9. Canonical scheme of Butanoate metabolism (KEGG Database). Squares indicate enzymatic processes. Green squares indicate process able to be accomplish by *B. cereus*. Stars indicate enhanced expression in planktonic cells (blue) or biofilm cells (red).

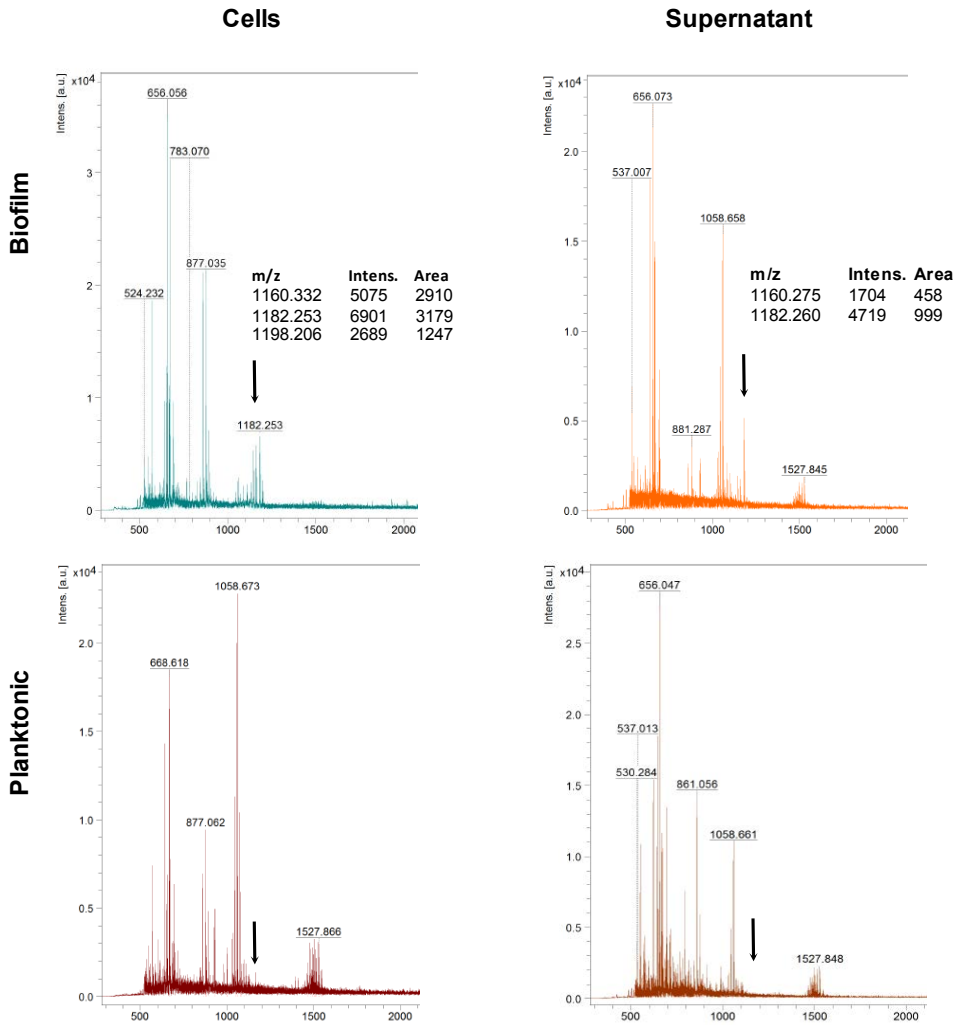

Figure S10. Complete spectrums from Mass-spectrometry HPLC-MS-MS (Tof-Tof) of cells and supernatants of 48 h cultures. Biofilm was collected and suspended in PBS, separating cells from supernatant with centrifugation. Culture medium was centrifuged to separate floating cells from supernatant. Samples were purified with C8 ZipTip® (Merk) previous to MS analysis. Tables resume the m/z found corresponding to Thiocillin (m/z=1160) and sodium (m/z=1182) and potassium aducts (m/z=1198). Black arrows indicate approximate positions of Thiocillin peaks.

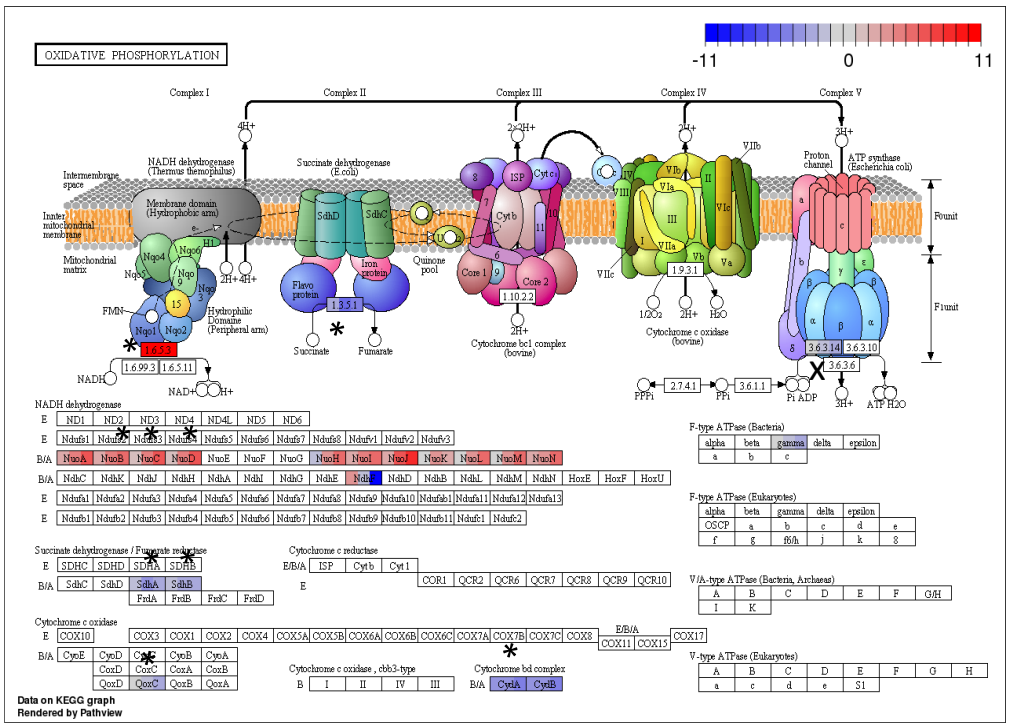

Figure S11. Oxidative phosphorylation pathway scheme showing the overexpression of the Complex I in biofilm cells and downregulation of complex II. Stars indicate confirmation of the behavior by iTRAQ results and cross indicate conflicting results. Cross indicate discordant result with proteomic results.

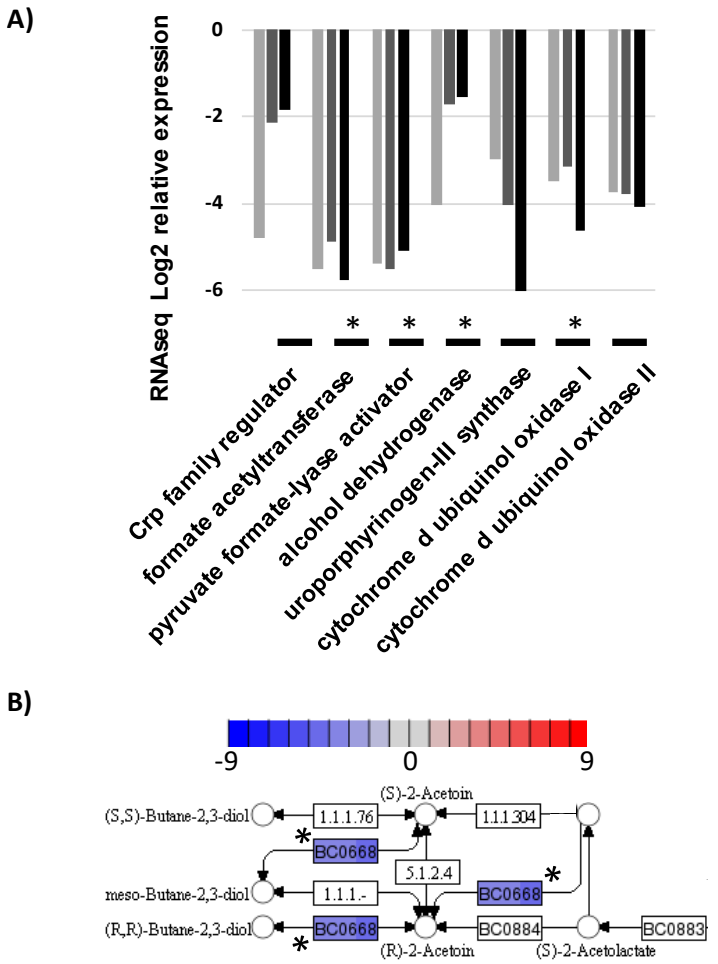

Figure S12. A) Expression pattern of genes implicated in fermentative metabolism in biofilm compared to floating cells 24 (light grey), 48 (grey) and 72 h (black) (RNAseq data). Data confirmed by iTRAQ results are marked with a star. Data in conflict with iTRAQ data are marked with a cross. B) Metabolic Pathway of synthesis of the carbon and energy accumulation polymer of acetoine. Boxes indicate the gene that code for the protein that perform the enzymatic reaction, squares inside boxes represent 24, 48 and 72 h sampling time and intensity of color show level of upregulation (red) or downregulation (blue). Stars indicate confirmation of the expression pattern by iTRAQ results and cross indicate conflicting results.

6. REFERENCES

Abranches, J., Miller, J.H., Martinez, A.R., Simpson-Haidaris, P.J., Burne, R.A., and Lemos, J.A. (2011). The Collagen-Binding Protein Cnm Is Required for Streptococcus mutans Adherence to and Intracellular Invasion of Human Coronary Artery Endothelial Cells. Infect. Immun. *79*, 2277–2284.

Ahn, S., Jung, J., Jang, I.-A., Madsen, E.L., and Park, W. (2016). Role of Glyoxylate Shunt in Oxidative Stress Response. J. Biol. Chem. *291*, 11928–11938.

Alhendawi, R.A., Kirkby, E.A., and Pilbeam, D.J. (2005). Evidence That Sulfur Deficiency Enhances Molybdenum Transport in Xylem Sap of Tomato Plants. J. Plant Nutr. *28*, 1347–1353.

Arnaud, M., Chastanet, A., and Débarbouillé, M. (2004). New Vector for Efficient Allelic Replacement in Naturally Nontransformable, Low-GC-Content, Gram-Positive Bacteria. Appl. Environ. Microbiol. *70*, 6887–6891.

Auger, S., Ramarao, N., Faille, C., Fouet, A., Aymerich, S., and Gohar, M. (2009). Biofilm Formation and Cell Surface Properties among Pathogenic and Nonpathogenic Strains of the Bacillus cereus Group. Appl. Environ. Microbiol. *75*, 6616–6618.

Banse, A.V., Hobbs, E.C., and Losick, R. (2011). Phosphorylation of Spo0A by the Histidine Kinase KinD Requires the Lipoprotein Med in Bacillus subtilis ▿. J. Bacteriol. *193*, 3949–3955.

Blin, K., Wolf, T., Chevrette, M.G., Lu, X., Schwalen, C.J., Kautsar, S.A., Suarez Duran, H.G., de los Santos, E.L.C., Kim, H.U., Nave, M., et al. (2017). antiSMASH 4.0—improvements in chemistry prediction and gene cluster boundary identification. Nucleic Acids Res. *45*, W36–W41.

Bosák, J., Micenková, L., Doležalová, M., and Šmajs, D. (2016). Colicins U and Y inhibit growth of Escherichia coli strains via recognition of conserved OmpA extracellular loop 1. Int. J. Med. Microbiol.

Bowers, A.A., Acker, M.G., Koglin, A., and Walsh, C.T. (2010). Manipulation of Thiocillin Variants by Prepeptide Gene Replacement: Structure, Conformation, and Activity of Heterocycle Substitution Mutants. J. Am. Chem. Soc. *132*, 7519–7527.

Caro-Astorga, J., Pérez-García, A., de Vicente, A., and Romero, D. (2015). A genomic region involved in the formation of adhesin fibers in Bacillus cereus biofilms. Front. Microbiol. *5*.

Chaloupka, J., Strnadová, M., and Moravcová, J. (1981). Protein turnover in growing cultures of Bacillus megaterium. Acta Biol. Med. Ger. *40*, 1227–1234.

Chesnokova, O.N., McPherson, S.A., Steichen, C.T., and Turnbough, C.L. (2009). The Spore-Specific Alanine Racemase of Bacillus anthracis and Its Role in Suppressing Germination during Spore Development. J. Bacteriol. *191*, 1303–1310.

Chiang, W.-C., Nilsson, M., Jensen, P.O., Hoiby, N., Nielsen, T.E., Givskov, M., and Tolker-Nielsen, T. (2013). Extracellular DNA Shields against Aminoglycosides in Pseudomonas aeruginosa Biofilms. Antimicrob. Agents Chemother. *57*, 2352–2361.

Chittezham Thomas, V., Kinkead, L.C., Janssen, A., Schaeffer, C.R., Woods, K.M., Lindgren, J.K., Peaster, J.M., Chaudhari, S.S., Sadykov, M., Jones, J., et al. (2013). A Dysfunctional Tricarboxylic Acid Cycle Enhances Fitness of Staphylococcus epidermidis During -Lactam Stress. MBio *4*, e00437-13-e00437-13.

Cossart, P., and Lecuit, M. (1998). Interactions of Listeria monocytogenes with mammalian cells during entry and actin-based movement: bacterial factors, cellular ligands and signaling. EMBO J. *17*, 3797–3806.

Dierick, K., Van Coillie, E., Swiecicka, I., Meyfroidt, G., Devlieger, H., Meulemans, A., Hoedemaekers, G., Fourie, L., Heyndrickx, M., and Mahillon, J. (2005). Fatal Family Outbreak of Bacillus cereus-Associated Food Poisoning. J. Clin. Microbiol. *43*, 4277–4279.

Dubois-Brissonnet, F., Trotier, E., and Briandet, R. (2016). The Biofilm Lifestyle Involves an Increase in Bacterial Membrane Saturated Fatty Acids. Front. Microbiol. *7*.

Duc, L.H., Hong, H.A., Barbosa, T.M., Henriques, A.O., and Cutting, S.M. (2004). Characterization of Bacillus Probiotics Available for Human Use. Appl. Environ. Microbiol. *70*, 2161–2171.

Eldar, A., and Elowitz, M.B. (2010). Functional roles for noise in genetic circuits. Nature *467*, 167–173.

Faulstich, M., Hagen, F., Avota, E., Kozjak-Pavlovic, V., Winkler, A.-C., Xian, Y., Schneider-Schaulies, S., and Rudel, T. (2015). Neutral sphingomyelinase 2 is a key factor for PorB-dependent invasion of Neisseria gonorrhoeae. Cell. Microbiol. *17*, 241–253.

Fedhila, S., Daou, N., Lereclus, D., and Nielsen-LeRoux, C. (2006). Identification of *Bacillus cereus* internalin and other candidate virulence genes specifically induced during oral infection in insects: *Bacillus cereus* internalin. Mol. Microbiol. *62*, 339–355.

Gao, T., Foulston, L., Chai, Y., Wang, Q., and Losick, R. (2015). Alternative modes of biofilm formation by plant-associated *Bacillus cereus*. MicrobiologyOpen *4*, 452–464.

Gohar, M., Faegri, K., Perchat, S., Ravnum, S., Økstad, O.A., Gominet, M., Kolstø, A.-B., and Lereclus, D. (2008). The PlcR Virulence Regulon of Bacillus cereus. PLoS ONE *3*, e2793.

Gowrishankar, J., and Harinarayanan, R. (2004). Why is transcription coupled to translation in bacteria? Mol. Microbiol. *54*, 598–603.

Gross, M., Cramton, S.E., Gotz, F., and Peschel, A. (2001). Key Role of Teichoic Acid Net Charge in Staphylococcus aureus Colonization of Artificial Surfaces. Infect. Immun. *69*, 3423–3426.

Gurler, N., Oksuz, L., Muftuoglu, M., Sargin, F., and Besisik, S. (2012). Bacillus Cereus Catheter Related Bloodstream Infection in a Patient with Acute Lymphoblastic Leukemia. Mediterr. J. Hematol. Infect. Dis. *4*.

Haber, A., Friedman, S., Lobel, L., Burg-Golani, T., Sigal, N., Rose, J., Livnat-Levanon, N., Lewinson, O., and Herskovits, A.A. (2017). L-glutamine Induces Expression of Listeria monocytogenes Virulence Genes. PLoS Pathog. *13*, e1006161.

Hamzeh-Cognasse, H., Damien, P., Chabert, A., Pozzetto, B., Cognasse, F., and Garraud, O. (2015). Platelets and Infections – Complex Interactions with Bacteria. Front. Immunol. *6*.

Heel, V., J, A., de Jong, A., Montalbán-López, M., Kok, J., and Kuipers, O.P. (2013). BAGEL3: automated identification of genes encoding bacteriocins and (non-)bactericidal posttranslationally modified peptides. Nucleic Acids Res. *41*, W448–W453.

Helgason, E., Okstad, O.A., Caugant, D.A., Johansen, H.A., Fouet, A., Mock, M., Hegna, I., and Kolstø, A.B. (2000). Bacillus anthracis, Bacillus cereus, and Bacillus thuringiensis--one species on the basis of genetic evidence. Appl. Environ. Microbiol. *66*, 2627–2630.

Hirst, J., King, M.S., and Pryde, K.R. (2008). The production of reactive oxygen species by complex I. Biochem. Soc. Trans. *36*, 976–980.

Hobley, L., Ostrowski, A., Rao, F.V., Bromley, K.M., Porter, M., Prescott, A.R., MacPhee, C.E., van Aalten, D.M.F., and Stanley-Wall, N.R. (2013). BslA is a self-assembling bacterial hydrophobin that coats the Bacillus subtilis biofilm. Proc. Natl. Acad. Sci. U. S. A. *110*, 13600–13605.

Hsueh, Y.-H., Somers, E.B., Lereclus, D., and Wong, A.C.L. (2006). Biofilm Formation by Bacillus cereus Is Influenced by PlcR, a Pleiotropic Regulator. Appl. Environ. Microbiol. *72*, 5089–5092.

Hu, H.-J., Chen, Y.-L., Wang, Y.-F., Tang, Y.-Y., Chen, S.-L., and Yan, S.-Z. (2017). Endophytic *Bacillus cereus* Effectively Controls *Meloidogyne incognita* on Tomato Plants Through Rapid Rhizosphere Occupation and Repellent Action. Plant Dis. *101*, 448–455.

Huang, D.W., Sherman, B.T., and Lempicki, R.A. (2009). Systematic and integrative analysis of large gene lists using DAVID bioinformatics resources. Nat. Protoc. *4*, 44–57.

Jastroch, M., Divakaruni, A.S., Mookerjee, S., Treberg, J.R., and Brand, M.D. (2010a). Mitochondrial proton and electron leaks. Essays Biochem. *47*, 53–67.

Jastroch, M., Divakaruni, A.S., Mookerjee, S., Treberg, J.R., and Brand, M.D. (2010b). Mitochondrial proton and electron leaks. Essays Biochem. *47*, 53–67.

Jenal, U., Reinders, A., and Lori, C. (2017). Cyclic di-GMP: second messenger extraordinaire. Nat. Rev. Microbiol. *15*, 271–284.

Johnson, L., Horsman, S.R., Charron-Mazenod, L., Turnbull, A.L., Mulcahy, H., Surette, M.G., and Lewenza, S. (2013). Extracellular DNA-induced antimicrobial peptide resistance in Salmonella enterica serovar Typhimurium. BMC Microbiol. *13*, 115.

de Jong, A., van der Meulen, S., Kuipers, O.P., and Kok, J. (2015). T-REx: Transcriptome analysis webserver for RNA-seq Expression data. BMC Genomics *16*.

Kertesz, M.A., and Mirleau, P. (2004). The role of soil microbes in plant sulphur nutrition. J. Exp. Bot. *55*, 1939–1945.

Kristian, S.A., Datta, V., Weidenmaier, C., Kansal, R., Fedtke, I., Peschel, A., Gallo, R.L., and Nizet, V. (2005). D-alanylation of teichoic acids promotes group a streptococcus antimicrobial peptide resistance, neutrophil survival, and epithelial cell invasion. J. Bacteriol. *187*, 6719–6725.

Kristoffersen, S.M., Haase, C., Weil, M.R., Passalacqua, K.D., Niazi, F., Hutchison, S.K., Desany, B., Kolstø, A.-B., Tourasse, N.J., Read, T.D., et al. (2012). Global mRNA decay analysis at single nucleotide resolution reveals segmental and positional degradation patterns in a Gram-positive bacterium. Genome Biol. *13*, R30.

Kusama, Y., Honma, I., Masuda, M., Goto, H., and Onodera, S. (2015). *Bacillus cereus* Outbreak in Normal Neonates at Our Hospital. Jpn. J. Infect. Prev. Control *30*, 385–390.

Kussmaul, L., and Hirst, J. (2006). The mechanism of superoxide production by NADH:ubiquinone oxidoreductase (complex I) from bovine heart mitochondria. Proc. Natl. Acad. Sci. *103*, 7607–7612.

Lewenza, S. (2013). Extracellular DNA-induced antimicrobial peptide resistance mechanisms in Pseudomonas aeruginosa. Front. Microbiol. *4*.

Li, Z., Mukherjee, T., Bowler, K., Namdari, S., Snow, Z., Prestridge, S., Carlton, A., and Bar-Peled, M. (2017). A Four-gene Operon in Bacillus cereus Produces Two Rare Spore-decorating Sugars. J. Biol. Chem. jbc.M117.777417.

Liu, J., Prindle, A., Humphries, J., Gabalda-Sagarra, M., Asally, M., Lee, D.D., Ly, S., Garcia-Ojalvo, J., and Süel, G.M. (2015). Metabolic co-dependence gives rise to collective oscillations within biofilms. Nature *523*, 550–554.

Luckevich, M.D., and Beveridge, T.J. (1989). Characterization of a dynamic S layer on Bacillus thuringiensis. J. Bacteriol. *171*, 6656–6667.

Masip, L., Veeravalli, K., and Georgiou, G. (2006). The many faces of glutathione in bacteria. Antioxid. Redox Signal. *8*, 753–762.

Miller, J.H., Avilés-Reyes, A., Scott-Anne, K., Gregoire, S., Watson, G.E., Sampson, E., Progulske-Fox, A., Koo, H., Bowen, W.H., Lemos, J.A., et al. (2015). The Collagen Binding Protein Cnm Contributes to Oral Colonization and Cariogenicity of Streptococcus mutans OMZ175. Infect. Immun. *83*, 2001–2010.

Minnaard, J., Lievin-Le Moal, V., Coconnier, M.-H., Servin, A.L., and Perez, P.F. (2004). Disassembly of F-Actin Cytoskeleton after Interaction of Bacillus cereus with Fully Differentiated Human Intestinal Caco-2 Cells. Infect. Immun. *72*, 3106–3112.

Mols, M., and Abee, T. (2011). Bacillus cereus responses to acid stress. Environ. Microbiol. *13*, 2835–2843.

Nakayama, H., Kurokawa, K., and Lee, B.L. (2012). Lipoproteins in bacteria: structures and biosynthetic pathways. FEBS J. *279*, 4247–4268.

Nandakumar, M., Nathan, C., and Rhee, K.Y. (2014). Isocitrate lyase mediates broad antibiotic tolerance in Mycobacterium tuberculosis. Nat. Commun. *5*.

Oda, M., Takahashi, M., Matsuno, T., Uoo, K., Nagahama, M., and Sakurai, J. (2010). Hemolysis induced by Bacillus cereus sphingomyelinase. Biochim. Biophys. Acta BBA - Biomembr. *1798*, 1073–1080.

Paul, B.J., Barker, M.M., Ross, W., Schneider, D.A., Webb, C., Foster, J.W., and Gourse, R.L. (2004). DksA: a critical component of the transcription initiation machinery that potentiates the regulation of rRNA promoters by ppGpp and the initiating NTP. Cell *118*, 311–322.

Paul, B.J., Berkmen, M.B., and Gourse, R.L. (2005). DksA potentiates direct activation of amino acid promoters by ppGpp. Proc. Natl. Acad. Sci. *102*, 7823–7828.

Peschel, A., Otto, M., Jack, R.W., Kalbacher, H., Jung, G., and Götz, F. (1999). Inactivation of the dlt operon in Staphylococcus aureus confers sensitivity to defensins, protegrins, and other antimicrobial peptides. J. Biol. Chem. *274*, 8405–8410.

Potera, C. (1999). Forging a Link Between Biofilms and Disease. Science *283*, 1837–1839.

Purcell, E.B., McKee, R.W., McBride, S.M., Waters, C.M., and Tamayo, R. (2012). Cyclic Diguanylate Inversely Regulates Motility and Aggregation in Clostridium difficile. J. Bacteriol. *194*, 3307–3316.

Rajasekar, A., and Ting, Y.-P. (2010). Microbial Corrosion of Aluminum 2024 Aeronautical Alloy by Hydrocarbon Degrading Bacteria *Bacillus cereus* ACE4 and *Serratia marcescens* ACE2. Ind. Eng. Chem. Res. *49*, 6054–6061.

Rajasekar, A., Ganesh Babu, T., Karutha Pandian, S., Maruthamuthu, S., Palaniswamy, N., and Rajendran, A. (2007). Biodegradation and corrosion behavior of manganese oxidizer Bacillus cereus ACE4 in diesel transporting pipeline. Corros. Sci. *49*, 2694–2710.

Ramarao, N., and Sanchis, V. (2013). The Pore-Forming Haemolysins of Bacillus Cereus: A Review. Toxins *5*, 1119–1139.

Schultz, M.P., Bendick, J.A., Holm, E.R., and Hertel, W.M. (2011). Economic impact of biofouling on a naval surface ship. Biofouling *27*, 87–98.

Senouci-Rezkallah, K., Schmitt, P., and Jobin, M.P. (2011). Amino acids improve acid tolerance and internal pH maintenance in Bacillus cereus ATCC14579 strain. Food Microbiol. *28*, 364–372.

Seydlová, G., Fišer, R., Čabala, R., Kozlík, P., Svobodová, J., and Pátek, M. (2013). Surfactin production enhances the level of cardiolipin in the cytoplasmic membrane of Bacillus subtilis. Biochim. Biophys. Acta BBA - Biomembr. *1828*, 2370–2378.

Shannon, P., Markiel, A., Ozier, O., Baliga, N.S., Wang, J.T., Ramage, D., Amin, N., Schwikowski, B., and Ideker, T. (2003). Cytoscape: a software environment for integrated models of biomolecular interaction networks. Genome Res. *13*, 2498–2504.

Shivanna, V., Kim, Y., and Chang, K.-O. (2015). Ceramide formation mediated by acid sphingomyelinase facilitates endosomal escape of caliciviruses. Virology *483*, 218–228.

Smirnova, G.V., and Oktyabrsky, O.N. (2005). Glutathione in bacteria. Biochem. Biokhimiiâ`*70*, 1199–1211.

von Stetten, F., Mayr, R., and Scherer, S. (1999). Climatic influence on mesophilic Bacillus cereus and psychrotolerant Bacillus weihenstephanensis populations in tropical, temperate and alpine soil. Environ. Microbiol. *1*, 503–515.

Sue, D., Hoffmaster, A.R., Popovic, T., and Wilkins, P.P. (2006). Capsule Production in Bacillus cereus Strains Associated with Severe Pneumonia. J. Clin. Microbiol. *44*, 3426–3428.

Swiecicka, I., and Mahillon, J. (2006). Diversity of commensal Bacillus cereus sensu lato isolated from the common sow bug (Porcellio scaber, Isopoda): Diversity of commensal Bacillus cereus isolated from the sow bug. FEMS Microbiol. Ecol. *56*, 132–140.

Szklarczyk, D., Morris, J.H., Cook, H., Kuhn, M., Wyder, S., Simonovic, M., Santos, A., Doncheva, N.T., Roth, A., Bork, P., et al. (2017). The STRING database in 2017: quality-controlled protein-protein association networks, made broadly accessible. Nucleic Acids Res. *45*, D362–D368.

Tang, Q., Yin, K., Qian, H., Zhao, Y., Wang, W., Chou, S.-H., Fu, Y., and He, J. (2016). Cyclic di-GMP contributes to adaption and virulence of Bacillus thuringiensis through a riboswitch-regulated collagen adhesion protein. Sci. Rep. *6*, 28807.

Terwilliger, A., Swick, M.C., Pflughoeft, K.J., Pomerantsev, A., Lyons, C.R., Koehler, T.M., and Maresso, A. (2015). Bacillus anthracis Overcomes an Amino Acid Auxotrophy by Cleaving Host Serum Proteins. J. Bacteriol. *197*, 2400–2411.

Tetz, G.V., Artemenko, N.K., and Tetz, V.V. (2009). Effect of DNase and Antibiotics on Biofilm Characteristics. Antimicrob. Agents Chemother. *53*, 1204–1209.

Tófoli de Araújo, F., Bolanos-Garcia, V.M., Pereira, C.T., Sanches, M., Oshiro, E.E., Ferreira, R.C.C., Chigardze, D.Y., Barbosa, J.A.G., de Souza Ferreira, L.C., Benedetti, C.E., et al. (2013). Structural and Physiological Analyses of the Alkanesulphonate-Binding Protein (SsuA) of the Citrus Pathogen Xanthomonas citri. PLoS ONE *8*, e80083.

Van Acker, H., and Coenye, T. (2017). The Role of Reactive Oxygen Species in Antibiotic-Mediated Killing of Bacteria. Trends Microbiol. *25*, 456–466.

Vatansever, F., de Melo, W.C.M.A., Avci, P., Vecchio, D., Sadasivam, M., Gupta, A., Chandran, R., Karimi, M., Parizotto, N.A., Yin, R., et al. (2013). Antimicrobial strategies centered around reactive oxygen species – bactericidal antibiotics, photodynamic therapy, and beyond. FEMS Microbiol. Rev. *37*, 955–989.

Vences-Guzmán, M.A., Geiger, O., and Sohlenkamp, C. (2008). Sinorhizobium meliloti mutants deficient in phosphatidylserine decarboxylase accumulate phosphatidylserine and are strongly affected during symbiosis with alfalfa. J. Bacteriol. *190*, 6846–6856.

Vilain, S., Pretorius, J.M., Theron, J., and Brozel, V.S. (2009a). DNA as an Adhesin: Bacillus cereus Requires Extracellular DNA To Form Biofilms. Appl. Environ. Microbiol. *75*, 2861–2868.

Vilain, S., Pretorius, J.M., Theron, J., and Brözel, V.S. (2009b). DNA as an adhesin: Bacillus cereus requires extracellular DNA to form biofilms. Appl. Environ. Microbiol. *75*, 2861–2868.

Vlamakis, H., Chai, Y., Beauregard, P., Losick, R., and Kolter, R. (2013). Sticking together: building a biofilm the Bacillus subtilis way. Nat. Rev. Microbiol. *11*, 157–168.

Walter, J., Loach, D.M., Alqumber, M., Rockel, C., Hermann, C., Pfitzenmaier, M., and Tannock, G.W. (2007). D-alanyl ester depletion of teichoic acids in Lactobacillus reuteri 100-23 results in impaired colonization of the mouse gastrointestinal tract. Environ. Microbiol. *9*, 1750–1760.

Wan, H., Song, D., Zhang, D., Du, C., Xu, D., Liu, Z., Ding, D., and Li, X. (2018). Corrosion effect of Bacillus cereus on X80 pipeline steel in a Beijing soil environment. Bioelectrochemistry *121*, 18–26.

Warne, B., Harkins, C.P., Harris, S.R., Vatsiou, A., Stanley-Wall, N., Parkhill, J., Peacock, S.J., Palmer, T., and Holden, M.T.G. (2016). The Ess/Type VII secretion system of Staphylococcus aureus shows unexpected genetic diversity. BMC Genomics *17*.

Wei, Z., Zenewicz, L.A., and Goldfine, H. (2005). Listeria monocytogenes phosphatidylinositol-specific phospholipase C has evolved for virulence by greatly reduced activity on GPI anchors. Proc. Natl. Acad. Sci. *102*, 12927–12931.

Xiao, Z., and Xu, P. (2007). Acetoin Metabolism in Bacteria. Crit. Rev. Microbiol. *33*, 127–140.

Xie, F., Li, G., Zhang, W., Zhang, Y., Zhou, L., Liu, S., Liu, S., and Wang, C. (2016). Outer membrane lipoprotein VacJ is required for the membrane integrity, serum resistance and biofilm formation of Actinobacillus pleuropneumoniae. Vet. Microbiol. *183*, 1–8.

Yasuda, Y., Kanda, K., Nishioka, S., Tanimoto, Y., Kato, C., Saito, A., Fukuchi, S., Nakanishi, Y., and Tochikubo, K. (1993). Regulation of L-alanine-initiated germination ofBacillus subtilis spores by alanine racemase. Amino Acids *4*, 89–99.

Zafra, O., Lamprecht-Grandío, M., de Figueras, C.G., and González-Pastor, J.E. (2012). Extracellular DNA Release by Undomesticated Bacillus subtilis Is Regulated by Early Competence. PLoS ONE *7*, e48716.

Zhao, X., Wang, Y., Shang, Q., Li, Y., Hao, H., Zhang, Y., Guo, Z., Yang, G., Xie, Z., and Wang, R. (2015). Collagen-Like Proteins (ClpA, ClpB, ClpC, and ClpD) Are Required for Biofilm Formation and Adhesion to Plant Roots by Bacillus amyloliquefaciens FZB42. PLOS ONE *10*, e0117414.

CHAPTER V

DEVELOPMENTAL PROGRAM OF *B. cereus* BIOFILM AND THE REGULATORY ROLE OF TasA

1. INTRODUCTION

Biofilms are complex structured bacterial communities formed on any virtual surfaces, starting with the adhesion of individual cells, and followed by the synthesis and assembly of the extracellular matrix, the structure that protects the community (Branda et al., 2001; Gil et al., 2014; Nadell et al., 2015). As exposed in previous chapters, this process involves a complex molecular machinery affecting multiple physiological functions oriented to the synthesis of the extracellular DNA, protein amyloid fibres, exopolysaccharides and other adhesins as structural components of the biofilm.

The structural events that comprise the scheduled steps of biofilm formation have been described in the model organism *B. subtilis* (Kobayashi, 2007; Lemon et al., 2008; Vlamakis et al., 2013). Studies in this bacterial species have demonstrated a cell differentiation within the biofilm population, meaning sub-populations of cells taking different tasks: matrix producers, surfactin producers, van Gogh bundle formers, cannibal cells, sporulating cells, miners, motile cells or competent cells (Fig. 1) (van Gestel et al., 2015; Iber et al., 2006; López et al., 2010). Cell differentiation has also been described in the close related specie *B. thuringiensis*. It has been described four cell types including virulent and necrotrophic cells, which can differentiate from undefined cells; and sporulating cells, which differentiate from virulent or necrotrophic individuals (Verplaetse et al., 2015).

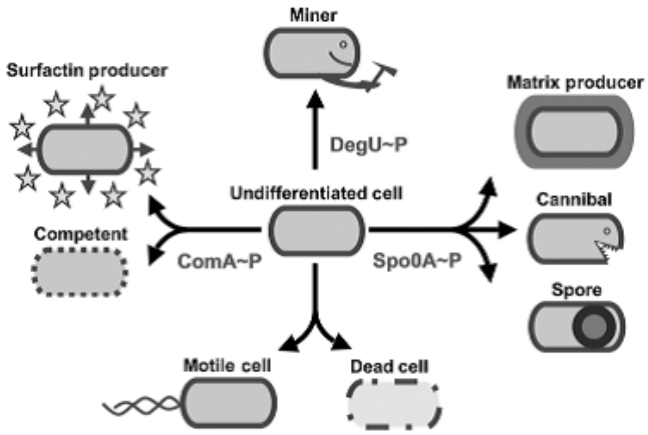

Figure 1. *B.* subtilis biofilm. Scheme of *B. subtilis* cell differentiation into different types that co-exist within a biofilm. Image taken from (López et al., 2010).

The equilibrium among the cell types and their function is tightly regulated and can be dramatically altered under the lack of one of the elements involved in the regulation networks, resulting in different biofilm formation phenotypes (Gundlach et al., 2016; Lemon et al., 2008). As an example, deletion of a gene involved in competence, results in biofilm formation altered phenotype in *B. cereus* and *B. subtilis* (Yan et al., 2016).

In *B. subtilis,* the growing process has been described as filament formed in the air-liquid interface forming a wrinkled floating pellicle, occurring the sporulation process at the top of those wrinkles, where fruiting bodies emerge (Branda et al., 2001; Kobayashi, 2007). The growing process of biofilm in *B. cereus* leading the ring-shape biofilm has never been described microscopically (Fig. 2), what led us to

explore and define it in order to have a better understanding of biofilm formation, filling the gap between the molecular and the macroscopic characteristics of *B. cereus* biofilm described in the previous chapters.

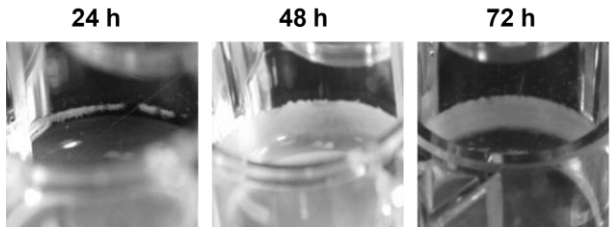

Figure 2. *B. cereus* biofilm. Biofilm developmental progression of *B. cereus* in polystyrene plate and Ty medium culture without shaking.

In chapter I, it was evidenced that a single *tasA* mutant of *B. cereus* shows an altered biofilm dynamic pattern: a bigger cell biomass loosely adhered to the wells of the plates observed at earlier stages of the biofilm cycle (24 h) compared to wild type. This observation led us to suggest a deregulation of other factors implicated in biofilm formation. The analysis of the whole transcriptome of *tasA* mutant at 24 h along with a quantitative high-throughput analysis of the proteome (iTRAQ) revealed the existence of deregulation that might reflect the deviated pattern of biofilm formation of a *tasA* mutant strain. Further analysis of promoters led us to define the expression pattern of TasA along the biofilm developmental process.

2. RESULTS

1. Microscopic development of the air-liquid interface biofilm of *B. cereus*

To define microscopically the stages of the biofilm life cycle, a piece of a cover slide was introduced in TY medium inoculated with *B. cereus*. During the first four hours, planktonic motile cells might be observed at the microscope from the cell suspension. The observations of the cover slides were done over the area of the air-liquid interface where a number of isolated bacteria get adhered. During the analysis, it was observed how some motile bacteria attached reversibly to the glass, doing it vertically, adhering a pole of the bacteria at the same time that continuous movement was evident. After this initial vertical attach, bacteria lay horizontally on the surface, getting in contact with the glass laterally (Fig. 3A).

At four hours, small clumps of motile bacteria were seen in the liquid culture (Fig.3A-B), and also could be seen groups of individual bacteria adhered to the glass. After six hours, clumps in the medium became bigger, and two forms of bacterial aggregates were observed over the glass: one composed of loosely organized cells and other composed of a monolayer of organized bacteria (Fig. 3C-D). At twelve hours, biofilm appeared uniformly formed in all the air-liquid interface area, indicating that both initial aggregates in the air-liquid interface evolved to the same biofilm structure.

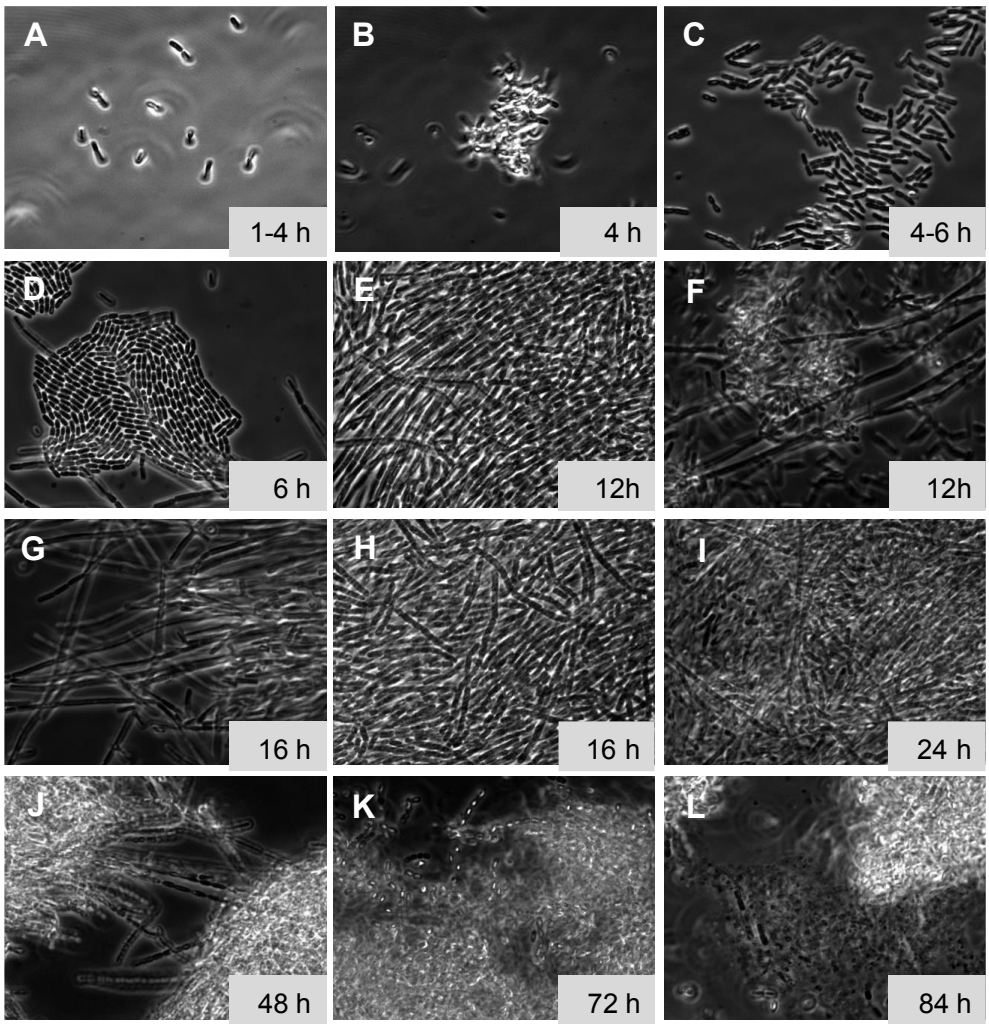

Figure 3. *B. cereus* developmental program. Bright-field micrographs of the stages of biofilm formation over pieces of glass cover slides (Objective 100x). A) Vertical reversible attachment and horizontal (white arrow) reversible attachment. B) Floating planktonic cells clumps. C) Disorganized micro colony. D) Organized micro colony. E) Biofilm from which initial bunch of cell chains originate. F) Small clumps adhered to biofilm chains. G) Bunch of biofilm chains. H-I) Biofilm chains with clumps fully recruited into the biofilm and lateral chaining weaving the biofilm structure. J) Smashed biofilm were tightening inner cell chains are visible (white arrow). K) Upper part of a biofilm with visible high sporulation rate. L) Smashed 84 h aged biofilm with a visible cell death bacteria mass (white arrow).

In these early stages, a subpopulation of cells grew in chains with one end anchored to the biofilm and the other floating in the medium to which clumps of planktonic motile bacteria adhered (Fig. 3F). From this time on, the clumps consolidated and cells acquire a compact organization within the biofilm. An interesting observation was the appearance of a compact grid of chains on partially smashed biofilm (Fig. 3H-J). At 72 h, the upper part of the community and closer to the air showed a high cell differentiation into spores (refringent cells) (Fig. 3K), while localized death of cells appeared, observed as a mucous mass of lysed cells in the inner part of the biofilm. It is noteworthy the characteristic absence of spores in the inner part of the biofilm (Fig. 3L).

All these stages and changes have been organized in a model of the biofilm developmental process of the ring-shape biofilm formation in the air-liquid interface of *B. cereus* (Fig. 4).

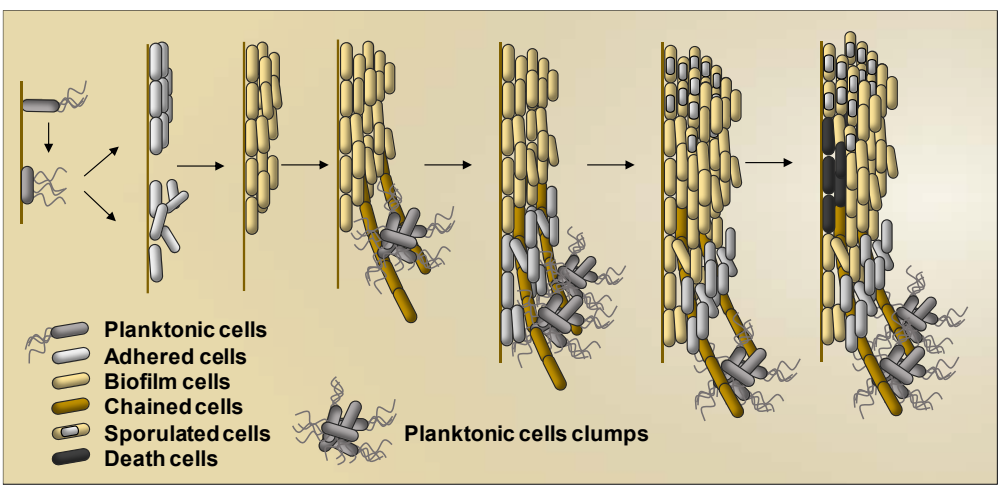

Figure 4. **Scheme of the developmental program of *B. cereus* biofilm in the air-liquid interface.** Time course microscopic analysis over 96 h of biofilm formation over glass slides.

2. Exploring the differences in the developmental progression of biofilm formation in the *tasA* mutant

Once described the microscopic developmental progression of the biofilm formation in *B. cereus*, we wondered if the phenotype of the single *tasA* mutant had any relation with the alteration of any of these developmental stages. In the first stages of biofilm formation, *tasA* and wild type strains showed a similar adhesion and micro colonies formation. However, at later stages (12-16h) most of the *tasA* population appeared forming large bundles of chained cells along all the biofilm biomass (Fig. 5).

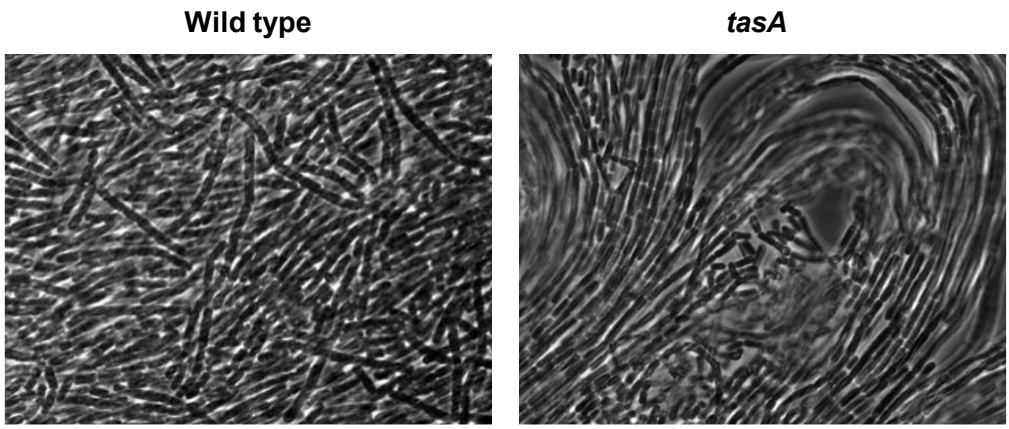

Figure 5. Developmental program differences in *tasA* mutant strain. Bright-field micrographs of 16h-old biofilms of wild type (left) and *tasA* mutant showing a hyper cell chaining phenotype (right).

3. TasA is not relevant for initial stages of biofilm formation

Although visual observation of adhesion and micro colony formation were not altered, and given the important role of TasA in biofilm formation and biofilm regulation, we wondered if TasA is involved in the initial stages of biofilm formation and if it starts to be expressed in planktonic cells or the expression is triggered once bacteria are incorporated into the biofilm. In order to assess the timing of the expression pattern of TasA in biofilm and planktonic cells we made a transcriptional fusion of the *tasA* promoter to the fluorescent protein gene *yfp* and it was integrated in the chromosome locus *pyrD*. Fluorescence microscopy analysis showed that planktonic cells or cells initially adhered to the glass slide (4 hours) did not actively express *tasA* at detectable levels (Fig. 6A-B). After six hours, disorganized group of cells failed in expressing *tasA*, (Fig. 6C) and only some cells or organized bacterial clumps started showing signal (Fig. 6D). Interestingly, visible floating clumps of planktonic cells did not emit any signal, indicating that this is probably independent on TasA expression. The number of cells expressing *tasA* increased in the bacterial micro colonies at 8 hours, and after twelve hours of incubation, it was visible a continuous mass of bacteria adhered to the glass following the line of the air-liquid interface, with intense fluorescence signal in almost all cells (Fig. 6F-G). Floating clumps of cells did not glow, a situation that remains until the end of the experiment. In the next stages, the filaments of cells emerging from the biofilm showed high expression levels of *tasA* over which lighted-off clumps were adhered (Fig. 6H-I). The *tasA*

promoter remained active until later stages (72h), when sporulating cells started to be clearly differentiated (Fig. 6J).

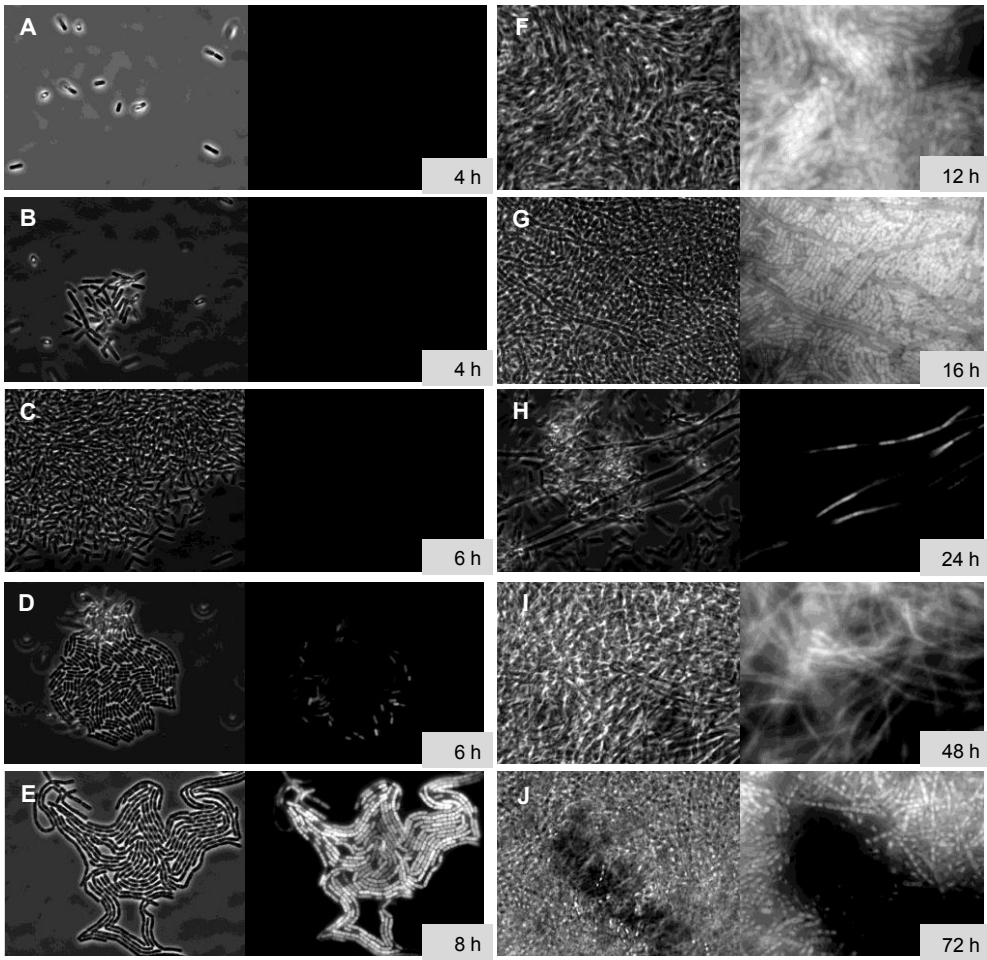

Figure 6. *tasA* expression pattern during biofilm formation. Phase-contrast micrographs (left) (objective 100x) and fluorescence micrographs (right) of the different events of the developmental program of *B. cereus* biofilm. Grey squares indicate the time the picture was taken after inoculation. A) Isolated adhered cells. B) Small floating clumps. C) Disorganized groups of adhered cells. D-E) Organized groups of adhered cells. F-G) Consolidated biofilm. H) Clumps adhered to cell chains. I) Fully-recruited clumps into biofilm. J) Matured upper part of the biofilm.

4. The absence of TasA triggers cell chaining and enhances recruitment of cells to the biofilm

The microscopic observation depicted in Fig. 5 is the result of a complex regulatory program that induced relevant changes in the physiology of cells (Chapter III). Thus, we reasoned that the deviation in the developmental program experienced by a *tasA* mutant should be reflective of deviations in this physiological switch compared to the wild type. To explore this, we sequenced total mRNA and quantified total protein content as previously done and analysis for the wild type.

Transcriptomic comparison of tasA mutant biofilm - wild type biofilm

The analysis of the differential gene expression of *tasA* compared with the wild type revealed 66 genes differentially expressed. After a detailed analysis, we found that the gene encoding the cell division protein *ftsH* was clearly downregulated. Interestingly, in other work it was studied a knock out mutant of this gene in the closely related *B. subtilis,* which causes filamentous growth (Deuerling et al., 1997; Wehrl et al., 2000). In the previous section, we have described cell chains as one of the elements in biofilm formation and growth. Besides, the *tasA* mutant showed an enhanced filament phenotype (Fig. 5). Thus, an increase in chaining inside the biofilm might explain, at least in part, the enhanced biofilm formation given that, as reported in the previous section, these structures might be in charge of recruiting planktonic clumps of cells.

Transcriptomic comparison of tasA mutant biofilm - wild type planktonic

Previous results show that transcriptomic data from biofilms cells of wild type and mutant are very similar, so that, *tasA* biofilm cells should show differences in comparison to wild-type planktonic cells. Biosynthesis of purines, cardiolipin synthase, thiocillin biosynthesis, and vancomycin resistance showed the same expression differences as in the wild type. Although, the comparison *tasA* biofilm with wild type planktonic cells analysis yielded several differences: i) the expression levels of *ftsH* appeared downregulated in *tasA* mutant, in accordance with the results of the previous contrast; ii) sporulation is downregulated in *tasA* biofilm. Although, we found a relevant difference in this contrast. It was not found statistical significant overexpression of most of the genes involved in cell wall synthesis, pyrimidine synthesis, the TCA cycle shunt, ROS detoxification genes, collagen like proteins, collagen adhesion proteins, invasins and overexpression of the *eps2* region, all of them groups of genes which showed a different pattern among biofilm and planktonic cells in the wild type. In the same way, downregulation of toxins, flagellum and chemotaxis found in biofilm cells of the wild type was not observed in the comparison of *tasA* biofilm with wild-type planktonic cells. The fact that neither of the *tasA* comparisons (*tasA* biofilm- WT biofilm and *tasA* biofilm- WT planktonic) revealed those changes was contradictory, although it has a statistical explanation.

The selection of RNAseq analysis threshold is arbitrary and it usually ranges between |0.3| and |5| (Han et al., 2017; Hart et al., 2013; Magee et al., 2017). The statistical treatment used in our experiment was a Log_2

(fold change) > |2|, what means four times of difference in transcripts readings what is a quite conservative threshold.

The fact that no changes were found comparing the *tasA* mutant against biofilm and planktonic cells of the wild type indicates that the levels of transcripts are in an intermediate range between both samples. Even showing changes in the expression pattern, they are hidden because of the statistical threshold, therefore it can be reasoned that all these functions may be indirectly controlled by TasA given that they are not fully up or downregulated when TasA is absent.

Comparisons at protein levels

In order to confirm the explanation of the initial contradictory findings among both transcriptomic contrasts which we reasoned to be due to the statistical threshold, we performed a proteomic analysis. The quantitative proteomic iTRAQ technique is very sensitive, what is translated into a statistical analysis with reduced thresholds. We used for our analysis a Log_2 (fold change) > |0.7|. Apart from the statistical parameters, results can be also influenced by other factors, like translation rate or protease activity. The comparison between both biofilm stages, wild type and of *tasA* mutant, revealed 211 proteins differentially represented. We did not find differences in structural elements such as CalY, exopolysaccharides biosynthesis proteins or eDNA biosynthesis proteins. Among the proteins with differential quantities, we found in *tasA* lower quantities of 22 proteins associated

to sporulation and higher quantities of flagellin, other proteins of flagellum and some toxins.

Most of the changes found comparing biofilms of the wild type and *tasA* were in the opposite direction to the biofilm program. To visualize this contrary behaviour, we represented the changes between planktonic and biofilm cells in the wild type in contrast to the changes between both biofilms using the 178 proteins which were common to both analyses. A perfect contrary behaviour is evident for those 178 proteins, although it is important to note that for the same protein, the values are not equal, remaining in intermediate numbers among planktonic and biofilm cells (Fig. 7). These results also confirm the statistical explanation of the initial contradictory data of RNAseq contrasts.

In alignment to the results showed by the transcriptomic analysis, these findings confirm that *tasA* mutant biofilm shows an altered regulation for some of the functions implicated in biofilm formation. Protein comparison of wild type and *tasA* biofilms revealed that proteins involved in exopolysaccharide biosynthesis, cell wall biosynthesis, TCA cycle rearrangement, ROS detoxification machinery or CalY did not show variations, as was found in RNAseq data.

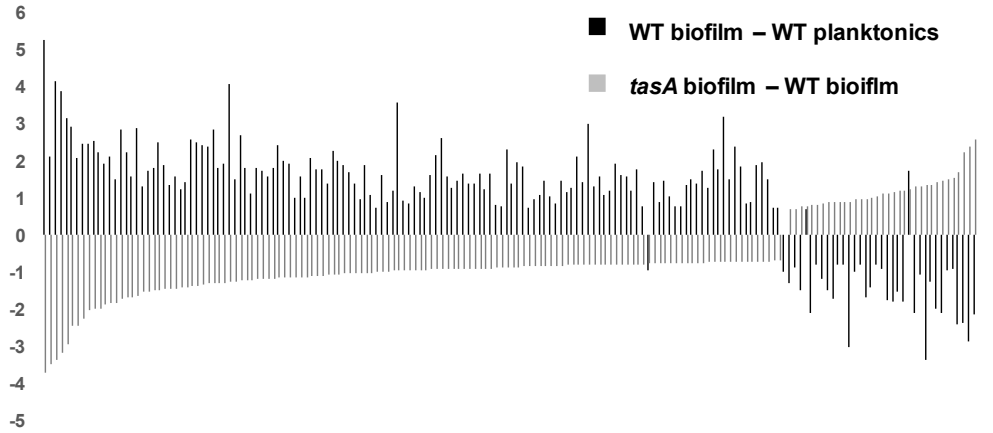

Figure 6. Relative quantities of proteins derived from comparisons of biofilms of *tasA*-WT strains (black) and biofilm -planktonic cells (grey). The opposite value of the bars indicates *tasA* biofilm levels share the same tendency as WT planktonic cells.

There is a group of proteins which are highly present and might explain the enhanced biofilm formation by *tasA* mutant strain in combination with the enhanced chaining of cells in biofilm found microscopically and explained by the upregulation of the gene *ftsH*. Among the functions deregulated, the quantity of flagellum proteins was higher in biofilm cells of the *tasA* mutant strain. Flagellum was described in *B. cereus* to be involved in the biofilm growth through bacteria recruitment (Houry et al., 2010). An increase in the amount of flagellum in the biofilm cells combined with the enhanced cell chaining (also involved in the recruitment of clumps of planktonic cells), would contribute to the higher growth of biofilm in *tasA* mutant.

To verify the hypothesis of the enhanced recruitment in *tasA* mutant, we compared the optical densities (OD) of the spent medium on a static

culture in 24 well-plates. This experiment confirmed that the total planktonic cells in the liquid culture was clearly reduced in the *tasA* mutant, even when this strain has a higher tendency to retain the flagellum. As seen in the chapter III of this thesis, external complementation of cultures with purified TasA restored the phenotype and normal recruitment rates (Fig. 8).

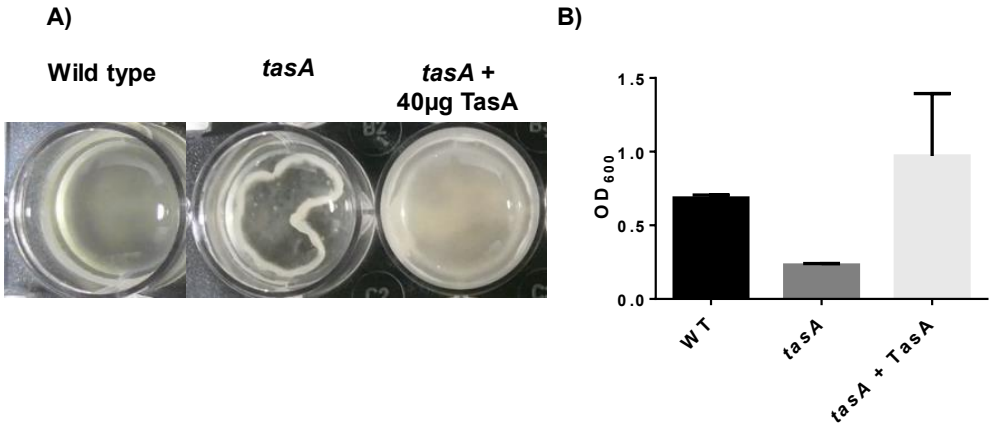

Figure 8. A) Static liquid culture of *B. cereus* wild type or *tasA* mutant in TY medium in 24-well plates for 24 h at 28ºC. External supplementation with purified TasA restores the wild type phenotype. **B)** Optical density of the liquid spent medium of a 24 h culture of wild type, mutant in *tasA* and *tasA* mutant externally supplemented with purified TasA.

3. DISCUSSION

Bacterial contamination of processed or natural products is one of the main concerns of the food industry (Hussain, 2016). One of the most recurrent contaminant of these environments is *B. cereus*, either in the form of biofilms or spores (Eneroth et al., 2001; Magnusson et al., 2007). Many studies on biofilm development have been done in *B. subtilis* (Lemon et al., 2008; López et al., 2010; Vlamakis et al., 2013), but comparatively little is known on *B. cereus* biofilms. In this study we do provide an overview on the general developmental program driving the formation of biofilm of *B. cereus* as cellular biomass adhered to surfaces in the air-liquid interface.

Initial stages are apparently dominated by two micro colonies distributions, organized and disorganized, with differences in the pattern of expression of the matrix protein TasA. Over time, both merge in a uniform bacterial mass formed immediately under the air-liquid interface. In this stage, a new cell typology is clearly differentiated as long chains apparently emerging from the biofilm and growing in the extreme suspended into the medium culture. These chains appear to be involved in the recruitment of planktonic cells clumps. In *B. subtilis,* all the cells within the floating pellicle form long chains, which also are the origin of the air-liquid interface biofilm and the pellicle is not adhered to the well, revealing how different is the biofilm phenotype (Kobayashi, 2007; Vlamakis et al., 2013). Interestingly, the transcriptional fusion of the *tasA* promoter to the *yfp* fluorescent protein led us to state that TasA is not important in the first stages of biofilm formation. This hypothesis

is also supported by the fact that time course of biofilm development in *tasA* mutant did not evidence any difference with the wild type. It could then be speculated that first stages of biofilm associated functions (adhesion and micro colony formation) are triggered normally.

Maturation of the biofilm structure show that differentiation into sporulating cells occurs in the upper part of the biofilm at 72 h. This finding would be reminiscent of fruiting bodies of *B. subtilis* that develops in the air-contact part of the pellicle that harbours the spores (Branda et al., 2001). Our results show that cell death appears to happen in this stage in the inner part of the biofilm. This event also reported in gram-positive and gram-negative bacteria has been proposed to be involved in the rising of wrinkles in *B. subtilis* (Asally et al., 2012; Webb et al., 2003). As previously reported for other bacterial species, this programmed cell death would be conceived as a strategy to eliminate inviable siblings and ensure the viability of the biofilm and as a supply of nutrients for sporulation (Allocati et al., 2015; Asally et al., 2012; Engelberg-Kulka et al., 2006).

Contrary to the role of TasA as an adhesin protein, a mutant in *tasA* shows higher biomass adhered to the wells. The fact that both *eps* and other putative adhesins are equally expressed than in the wild type, rest relevance to the major production of the extracellular matrix as the causative of this phenotype. An alternative explanation would be the major recruitment of cells from the spent medium, which is supported by diverse evidences. First, cell chaining is predominantly evidenced as a differentiated cell organization in stages of biofilm maturation, and

interestingly, these cells are actively expressing *tasA*. Second, in a tasA mutant bacterial counts in spent medium of tasA is outstandingly lower than in wild type. Responsible for these events are suggested to be at least two convergent factors, the downregulation of *ftsH* and the enhanced presence of flagella proteins in biofilm cells, both contributing positively to cell recruitment (Houry et al., 2010). These findings suggest that TasA would not be directly implicated in cell recruitment as we hypothesized first, and led us to propose a regulatory role of TasA which affects most of the biofilm associated functions explained in the chapter III of this thesis (exopolysaccharide synthesis, cell wall synthesis, pyrimidine synthesis, the TCA cycle shunt, ROS detoxification genes, collagen like proteins, collagen adhesion proteins, toxins, flagellum and chemotaxis).

4. METHODS AND MATERIAL

Strains and growth conditions

The strain used in this study was *B. cereus* ATCC14579. Bacteria were grown in 24-wells plates with 1 ml of Ty broth: 1% tryptone, (OXOID), 0.5% yeast extract (OXOID), 0.5% NaCl, 10 mM $MgSO_4$, and 0.1 mM $MnSO_4$. To obtain biofilm samples, pieces of cover slides were introduced into wells in a position in which the medium culture cover only a portion of the glass.

Construction of B. cereus strain expressing the transcriptional fusion tasA promoter-yfp

The strain was obtained by double recombination using a derive of the plasmid pMAD (Arnaud et al., 2004) harboring flanking regions for recombination within *pyrD* and the genetic fusion *tasA*-promoter – *yfp* – *tetracycline cassette*, which was constructed using the primers listed in Table 1. The construct were created by joining PCR, as previously described (López et al., 2009). In the first step, regions flanking the target genes and tetracycline resistance cassette were amplified separately, purified, and used for the joining PCRs. These PCR products were digested with enzymes BamHI and NcoI and cloned into the pMAD vector digested with the same. The resulting suicide plasmid were used to transform *B. cereus* electrocompetent cells as described previously (Pflughoeft et al., 2011). Electroporation was performed with 4 µg of plasmids and 100 µL of electrocompetent *B. cereus* in 0.2-mm cuvettes using the following electroporation parameters: voltage 2500

kV, capacitance 25 μF, resistance 350 Ω. The electropored cells were seeded in LB plates supplemented with X-Gal and erythromycin for 72 h at 30°C. Blue colonies were selected and restreaked as previously described to trigger allele replacement (Arnaud et al., 2004). Finally, white colonies sensitive to MLS were selected, and deletion of the target gene was verified by colony-PCR and sequencing of the amplicons.

Microscopy analysis and *image capture*

Biofilms were examined with a Nikon Eclipse TE2000-U microscope equipped with a Plan Apo oil objective 100x, and pictures were taken with a Hamamatsu digital camera model ORCA-ER. Fluorescence signal was detected using a CFP/YFP dual-band filter set (Chroma #52017). All images were taken at the same exposure time, processed identically for compared image sets.

Whole transcriptome analysis and iTRAQ analysis

The mRNA isolation, RNAseq analysis and proteomics were done following the same procedures described in Methods and Material in Chapter III.

5. ANNEX

Table 1. Primers for joining PCR to obtain the construction *pyrD* :: *tasA*-promoter – *yfp* – *tetracycline cassette*.

	Sequence
ApaI P-TasA Fw	TTTTGGGCCCGCGTAGTAATGGCTT
ClaI P-TasA yfp Rv	TTCTCCTTTACTCATATCGATATGAGATCGCGTTGCT
yfp Fw	ATGAGTAAAGGAGAACTTTTCACT
yfp Rv	TTATTTGTATAGTTCATCCATGCC
Tc yfp Fw	GGCATGGATGAACTATACAAATAAGTATACGCTTATCAACGTAGTAAGCGTGG
Tc Rv	TATATCTCGAGGAACTCTCTCCCAAAGTTGATCCC

6. REFERENCES

Allocati, N., Masulli, M., Ilio, C.D., and Laurenzi, V.D. (2015). Die for the community: an overview of programmed cell death in bacteria. Cell Death Dis. *6*, e1609.

Asally, M., Kittisopikul, M., Rué, P., Du, Y., Hu, Z., Çağatay, T., Robinson, A.B., Lu, H., Garcia-Ojalvo, J., and Süel, G.M. (2012). Localized cell death focuses mechanical forces during 3D patterning in a biofilm. Proc. Natl. Acad. Sci. *109*, 18891–18896.

Branda, S.S., Gonzalez-Pastor, J.E., Ben-Yehuda, S., Losick, R., and Kolter, R. (2001). Fruiting body formation by Bacillus subtilis. Proc. Natl. Acad. Sci. *98*, 11621–11626.

Deuerling, E., Mogk, A., Richter, C., Purucker, M., and Schumann, W. (1997). The ftsH gene of *Bacillus subtilis* is involved in major cellular processes such as sporulation, stress adaptation and secretion. Mol. Microbiol. *23*, 921–933.

Eneroth, A., Svensson, B., Molin, G., and Christiansson, A. (2001). Contamination of pasteurized milk by *Bacillus cereus* in the filling machine. J. Dairy Res. *68*, 189–196.

Engelberg-Kulka, H., Amitai, S., Kolodkin-Gal, I., and Hazan, R. (2006). Bacterial programmed cell death and multicellular behavior in bacteria. PLoS Genet. *2*, e135.

van Gestel, J., Vlamakis, H., and Kolter, R. (2015). From cell differentiation to cell collectives: *Bacillus subtilis* uses division of labor to migrate. PLoS Biol. *13*, e1002141.

Gil, C., Solano, C., Burgui, S., Latasa, C., García, B., Toledo-Arana, A., Lasa, I., and Valle, J. (2014). Biofilm Matrix Exoproteins Induce a Protective Immune Response against *Staphylococcus aureus* Biofilm Infection. Infect. Immun. *82*, 1017–1029.

Gundlach, J., Rath, H., Herzberg, C., Mäder, U., and Stülke, J. (2016). Second Messenger Signaling in Bacillus subtilis: Accumulation of Cyclic di-AMP Inhibits Biofilm Formation. Front. Microbiol. *7*, 804.

Han, Y., Wan, H., Cheng, T., Wang, J., Yang, W., Pan, H., and Zhang, Q. (2017). Comparative RNA-seq analysis of transcriptome dynamics during petal development in Rosa chinensis. Sci. Rep. *7*.

Hart, T., Komori, H.K., LaMere, S., Podshivalova, K., and Salomon, D.R. (2013). Finding the active genes in deep RNA-seq gene expression studies. BMC Genomics *14*, 778.

Houry, A., Briandet, R., Aymerich, S., and Gohar, M. (2010). Involvement of motility and flagella in *Bacillus cereus* biofilm formation. Microbiology *156*, 1009–1018.

Hussain, M.A. (2016). Food Contamination: Major Challenges of the Future. Foods *5*.

Iber, D., Clarkson, J., Yudkin, M.D., and Campbell, I.D. (2006). The mechanism of cell differentiation in *Bacillus subtilis*. Nature *441*, 371–374.

Kobayashi, K. (2007). *Bacillus subtilis* Pellicle Formation Proceeds through Genetically Defined Morphological Changes. J. Bacteriol. *189*, 4920–4931.

Lemon, K.P., Earl, A.M., Vlamakis, H.C., Aguilar, C., and Kolter, R. (2008). Biofilm development with an emphasis on *Bacillus subtilis*. Curr. Top. Microbiol. Immunol. *322*, 1–16.

López, D., Vlamakis, H., and Kolter, R. (2010). Biofilms. Cold Spring Harb. Perspect. Biol. *2*.

Magee, R., Loher, P., Londin, E., and Rigoutsos, I. (2017). Threshold-seq: a tool for determining the threshold in short RNA-seq datasets. Bioinforma. Oxf. Engl. *33*, 2034–2036.

Magnusson, M., Christiansson, A., and Svensson, B. (2007). *Bacillus cereus* spores during housing of dairy cows: factors affecting contamination of raw milk. J. Dairy Sci. *90*, 2745–2754.

Nadell, C.D., Drescher, K., Wingreen, N.S., and Bassler, B.L. (2015). Extracellular matrix structure governs invasion resistance in bacterial biofilms. ISME J. *9*, 1700–1709.

Verplaetse, E., Slamti, L., Gohar, M., and Lereclus, D. (2015). Cell Differentiation in a *Bacillus thuringiensis* Population during Planktonic Growth, Biofilm Formation, and Host Infection. MBio *6*, e00138-00115.

Vlamakis, H., Chai, Y., Beauregard, P., Losick, R., and Kolter, R. (2013). Sticking together: building a biofilm the *Bacillus subtilis* way. Nat. Rev. Microbiol. *11*, 157–168.

Webb, J.S., Thompson, L.S., James, S., Charlton, T., Tolker-Nielsen, T., Koch, B., Givskov, M., and Kjelleberg, S. (2003). Cell death in *Pseudomonas aeruginosa* biofilm development. J. Bacteriol. *185*, 4585–4592.

Wehrl, W., Niederweis, M., and Schumann, W. (2000). The FtsH protein accumulates at the septum of *Bacillus subtilis* during cell division and sporulation. J. Bacteriol. *182*, 3870–3873.

Yan, F., Yu, Y., Wang, L., Luo, Y., Guo, J.-H., and Chai, Y. (2016). The comER Gene Plays an Important Role in Biofilm Formation and Sporulation in both *Bacillus subtilis* and *Bacillus cereus*. Front. Microbiol. *7*, 1025.

CHAPTER VI

FUNCTIONAL CHARACTERIZATION OF TWO EXOPOLYSACCHARIDES PRODUCED IN *B. cereus*

1. INTRODUCTION

The biofilm extracellular matrix is composed mainly of proteins, extracellular DNA and exopolysaccharides. The importance of each component for biofilm formation depends on the species, but usually these three elements confer co-ordinately the diverse physic-chemical features defining the extracellular matrix (López et al., 2010).

Among the diverse components of the bacterial extracellular matrix are the exopolysaccharides (EPS), large molecules with complex structures and diverse chemical properties, which cover a variety of functions relevant for the bacterial physiology and multicellular lifestyle. Some are related to the architecture of the biofilm, conditioning the colony morphology and providing robustness to the biofilm (Chung et al., 2003; Irie et al., 2010; Limoli et al., 2015; Wang et al., 2016). Other functions endorsed to exopolysaccharides are adhesion of cells to biotic and abiotic surfaces, which for instance determines the ability to efficiently colonize the plant rhizosphere (Berne et al., 2015; Dertli et al., 2015; Labbate et al., 2007; Shea et al., 1991; Silva et al., 2014). Interaction among bacterial cells have been also described to be promoted by exopolysaccharides, which induce cellular aggregation (Dorken et al., 2012; Sutherland, 2001). EPS may also trap molecules present in the medium, preventing their entry inside the bacterial cells, an effect that serves the colony to defend against the toxicity of heavy metal ions, antimicrobial compounds produced by competitors, medical chemotherapy, or other sanitizers used to clean biofilms in the industry (Arciola et al., 2005; Geisinger and Isberg, 2015; Gupta and Diwan, 2016; Ryu and Beuchat, 2005; Zegans et al., 2012). EPS are also

known to participate in bacterial colony migration and motility, either functioning as rails over which bacteria move or work as a lubricant that reduce friction, facilitating the displacement of either single cells or the entire community in a sort of social movement called swarming or sliding, depending on other bacterial factors involved (Berleman et al., 2016; Gibiansky et al., 2013; Hu et al., 2016; Liu et al., 2016; Lu et al., 2005). Resistance to different stresses have been widely reported, including osmotic stress, desiccation, cryoprotection or oxidative stress (Casillo et al., 2017; Ionescu and Belkin, 2009; Roberson and Firestone, 1992; Schnider-Keel et al., 2001; Yang et al., 2015). The protection offered by exopolysaccharides is also extensive against phages in some cases. However, polysaccharides can also work as a target for phages, which recognize specific polysaccharide composition and are enzymatically degraded by phage capsid proteins previous to the infection (Drulis-Kawa et al., 2012; Roach et al., 2013; Scholl et al., 2005). Apart from resistance to sanitizers, detergents, antimicrobials and their implication in human pathologies, exopolysaccharides are responsible of corrosion over stainless steel, a material over which *B. cereus* is favourable to establish a biofilm. This material is very common in the food industry, tanks, pipes or sheep hulls, which complete the pull of human concerns on this bacterial species and biofilms (S. Bragadeeswaran, 2011).

The variety of functions of the exopolysaccharides are reflective of the differences of their exact chemical composition. Different sugar residues, chemical bond types, ramifications, sugar modifications or chain length, which involve complex biosynthesis processes (Whitfield

et al., 2015). In this way, we can find common polysaccharides like cellulose, present in species of different genus, or others that can be even strain specific (Okshevsky Mira et al., 2017; Römling and Galperin, 2015). The study of the bacterial factors involved in biofilm formation is useful to understand their functionality in the bacterial physiology and ecology, including the interaction with hosts. Additionally, these studies offer potential bacterial targets for the development of strategies oriented to minimize the negative impact of bacterial biofilms. Studies on *B. cereus* biofilm have highlighted the relevant contribution of exopolysaccharides to the total composition of the extracellular matrix, although, its origin remains still uncertain (Houry et al., 2012). Some reports have focused on the characterization of spore polysaccharides (Li et al., 2017), or the secondary cell wall polysaccharide, which seems to be strain dependent (Forsberg et al., 2011). In the phylogenetically related species *B. subtilis*, the operon *epsA-O* codifies for a group of genes in charge of the synthesis of the biofilm exopolysaccharide, and the deletion of the operon leads to impairment in biofilm formation (Branda et al., 2001; Elsholz et al., 2014). *B. cereus* possesses a homologous region (henceforth *eps1*), which we have confirmed to be irrelevant to biofilm formation in the strain ATCC14579 (Chapter IV of this thesis), a finding also supported in studies of the strain *B. cereus* 905 (Gao et al., 2015a). However, it appears that deletion of some of the genes of this region impaired biofilm formation in the strain ATCC10987 (Okshevsky Mira et al., 2017), a discordancy that reveals the heterogeneity existing among bacterial strains of the same species.

Prompted by the influence of EPS in bacterial physiology and ecology, and the divergence in terms of exact chemical composition and function, in this work we studied the different genomic regions apparently encoding for proteins carrying the synthesis of two polysaccharides, and their implication in *B. cereus* multicellularity. We previously found in a transcriptomic analysis (Chapter IV) that an additional region of the genome of *B. cereus* ATCC14579 was overexpressed in biofilm cells compared to floating cells, to which we will refer as *eps2*. This region is annotated as involved in the production of a capsular exopolysaccharide. However, *B. cereus ATCC14579* lacks capsule. Our analysis indicates that *eps1* promotes swarming mobility, while the *eps2* is involved in biofilm maturation, cell-to-cell interaction and aggregation. Studies on the protection properties of these exopolysaccharides showed that both of them contribute to the immunity of *B. cereus* biofilms to diverse antimicrobials and disinfectants.

2. RESULTS

1. The regions *eps1* and *eps2* are differentially expressed in biofilm of *B. cereus*

Results from RNAseq and proteomic analysis showed that the differential expression of *eps1*, homologous to *eps*A-O of *B. subtilis*, was statistically insignificant at 24 and 48 h between biofilm and planktonic cells (Fig. 1A). However, we found that a group of genes (*BC1583-BC1591*) annotated as 'capsular polysaccharide biosynthesis', and absent in *B. subtilis*, were surprisingly upregulated in biofilm cells. This finding along with the fact that *B. cereus* ATCC14579 does not possess capsule (Fig. 1B), led to us to investigate this new region and the putative implication in biofilm formation.

Before initiating specific studies oriented to determine the functionality of each region, we studied their genetic organization. The *eps1* region of *B. cereus* was compared with the *epsA-O* of *B. subtilis* to look for similitudes as it had been reported in other works (Gao et al., 2015b). Comparison of both genetic regions showed a poor homology, with odd genes in both species and duplications, what would help explaining the lack of phenotype in a knock-out mutant (Fig. 2).

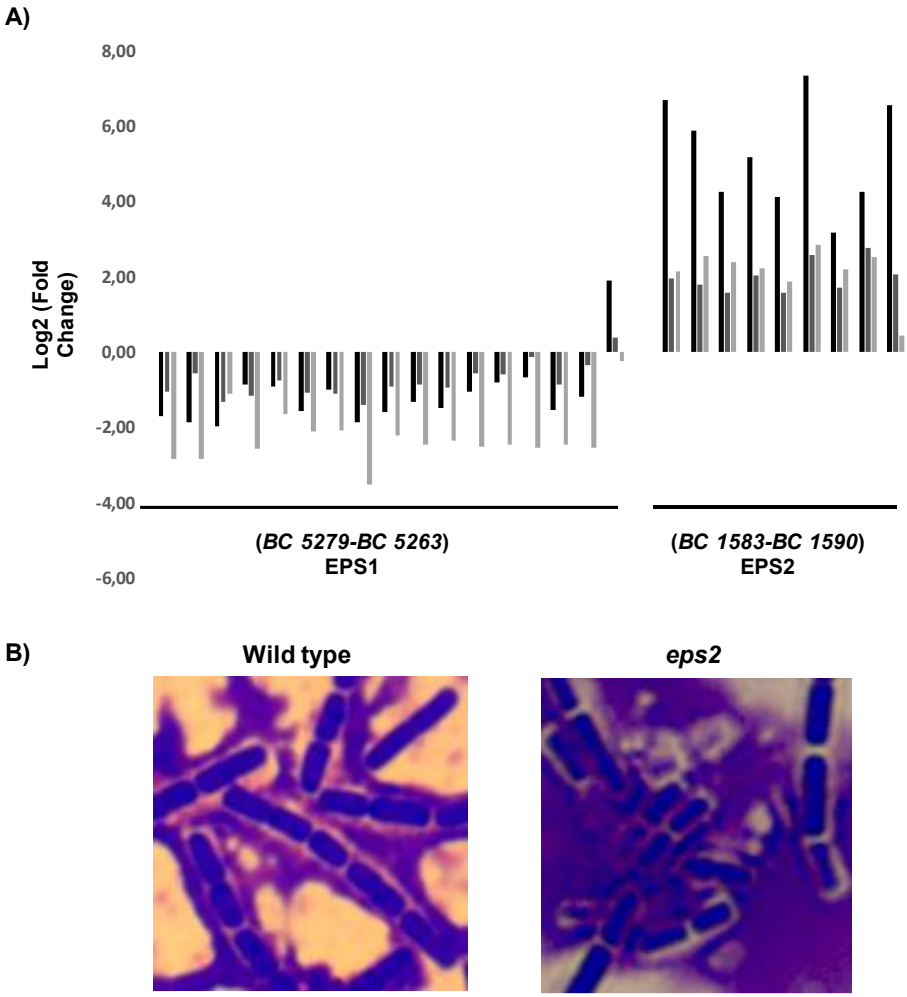

Figure 1. Two genomic regions of *B. cereus* hypothetically committed to production of exopolysaccharides are differentially expressed in biofilm cells. **A)** Transcriptomic analysis showed the specific overexpression of genes of the *eps2* region but not the *eps1* in biofilm cells compared to floating cells at 24 h (black), 48 h (dark grey) and 72 h (clear grey). **B)** Pictures taken of cells stained with the Anthony method and bright field microscopy showed the absence of capsule in *B. cereus* WT or *eps2*.

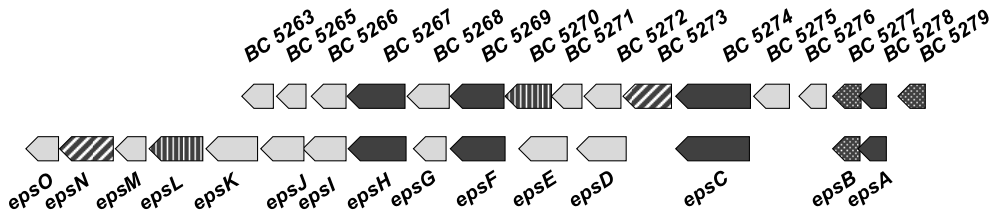

Figure 2. Comparison of the genetic structure of *eps1* of *B. cereus* and *B. subtilis epsA-O* operon. Conserved genes are in black and weave, odd genes are marked in grey. Top, Gene cluster predicted to be involved in production of an EPS in *B. cereus*. Bottom, the operon involved in the synthesis of the biofilm EPS in *B. subtilis*.

To determine if this region constitute an operon, we did RT-PCR over total RNA isolated from a liquid culture of *B. cereus* grown at 30ºC for 24h (Fig. 3). The results indicated that the *eps1* region is apparently composed of three transcriptional units and an orphan tyrosine-protein kinase: i) *BC5279*; ii) *BC5278-BC5277*; iii) *BC5276-BC5267*; iv) *BC5266-BC5263*. (Fig.3 and 4). The *in silico* analysis on this region predicted three putative promoter regions (arrows) at the beginning of each of the transcriptional units (Fig. 3B).

The same analysis on the *eps2* region revealed the organization of the nine genes in a unique transcriptional unit (Fig. 4). To confirm that any gene was excluded from the operon, we did further *in silico* analysis with the software ORFfinder of the 843 base pairs of the intergenic region upstream the locus *BC1583*. RT-PCR analysis confirmed that the poly-cistronic mRNA includes the three putative ORFs.

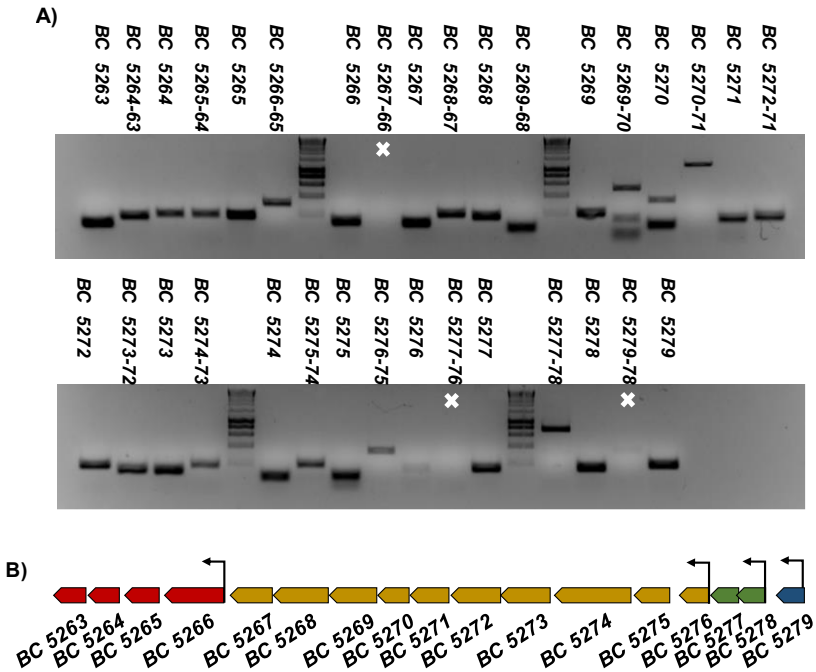

BC 5263: UDP-glucose 4-epimerase
BC 5264: EPSX protein
BC 5265: Membrane-bound transcriptional regulator LytR
BC 5266: Heteropolysaccharide repeat-containing protein

BC 5267: Glycosyltransferase
BC 5268: Secreted polysaccharide polymerase
BC 5269: Amylovoran biosynthesis AmsK
BC 5270: Undecaprenyl-phosphate galactosephosphotransferase
BC 5271: UDP-N-acetylglucosamine 4-epimerase
BC 5272: Carbamoylphosphate synthase small subunit
BC 5273: UDP-bacillosamine synthetase
BC 5274: UDP-N-acetylglucosamine 4,6-dehydratase
BC 5275: UTP--glucose-1-phosphate uridylyltransferase
BC 5276: Phosphotyrosine-protein phosphatase (capsular polysaccharide biosynthesis)

BC 5277: Tyrosine-protein kinase
BC 5278: Capsular polysaccharide chain length regulator

BC 5279: Tyrosine-protein kinase

Figure 3. The *eps1* region is organized in diverse transcriptional units. **A)** RT-PCR over cDNA obtained from RNA isolated from a broth culture of *B. cereus* grown for 24 h at 30ºC. **B)** Genetic structure determined from the RT-PCR results and automatic annotation of the genes of the *eps1* region. Arrows indicate the hypothetical promoter region of each transcriptional unit.

A)

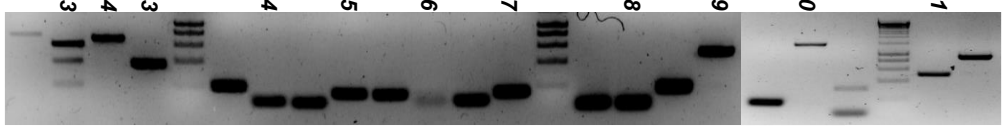

B)

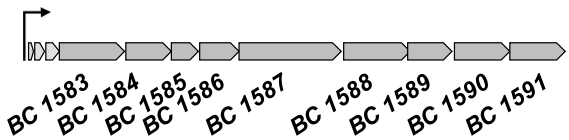

BC 1583: Acyltransferase
BC 1584: Capsular polysaccharide protein CpsC
BC 1585: Tyrosine-protein kinase cpsD
BC 1586: Undecaprenyl-phosphate galactosephosphotransferase
BC 1587: Oligosaccharide translocase
BC 1588: Secreted polysaccharide polymerase
BC 1589: N-acetylgalactosaminyl-diphosphoundecaprenol glucuronosyltransferase
BC 1590: Mannosyl transferase
BC 1591: Hypothetical protein

C)

	Label	Strand	Frame	Start	Stop	Length (nt | aa)
◗	ORF9	+	2	182	271	90 | 29
◗	ORF10	+	2	317	496	180|59
▷	ORF16	+	3	543	734	192 | 63

Figure 4. The *eps2* region is organized in a unique transcriptional unit. **A)** RT-PCR over cDNA obtained from RNA isolated from a broth culture of *B. cereus* grown for 24 h at 30ºC. Arrow indicates the hypothetical promoter region of the operon. **B)** Genetic structure determined from the RT-PCR results and automatic annotation of the genes included in the operon. **C)** Upstream putative ORFs found in ORF-Finder analysis and included as integrant of the operon.

2. The region *eps2*, but not *eps1*, is involved in biofilm formation

Previous data led us to propose a major contribution of *eps2* to biofilm formation. To confirm our hypothesis, we constructed knock-out mutants in each region. Deletion of the loci *BC5279-BC5274 of eps1*, that includes the promoter of the larger transcriptional unit, resulted in the absence of transcripts of the region *BC5279-BC5265*. The region *eps2* was completely deleted (*BC1583-BC1591*). Besides, double mutants were obtained in order to look for collaborative functions.

Biofilm assays in shaken liquid cultures showed a defect in the quantity, consistency and continuity of the air-liquid interphase biofilm ring adhered to the glass formed by the strain *Δeps*2 (Fig 5A). Reflective of its distinct expression among biofilm and floating cells (Fig. 1), the strain *Δeps1* was not impaired in biofilm formation compared to WT. Accordingly to our hypothesis, double mutant *Δeps1, Δeps2* mimicked the phenotype of the single mutant *Δeps2* (Fig. 5A). In parallel to the evaluation of the adhered biomass, we also observed a major sediment of bacterial cells in cultures of the wild type and *Δeps1* strains (Fig. 5B). Accordingly, aliquots of the supernatants observed in phase contrast microscope showed the presence of bacterial clumps in WT and *Δeps1,* but not in spent medium of *Δeps2* or double *Δeps1, Δeps2* (Fig. 5B).

Prompted by the well know staining properties of certain exopolysaccharides, we performed biofilm assays in agar and static liquid cultures in the presence of Congo Red, a dye commonly used to reveal the presence of EPS (Fig. 5C) (Jung et al., 2015; Lu et al., 2005; McKinney, 1953). Two distinctive phenotypes emerged from the

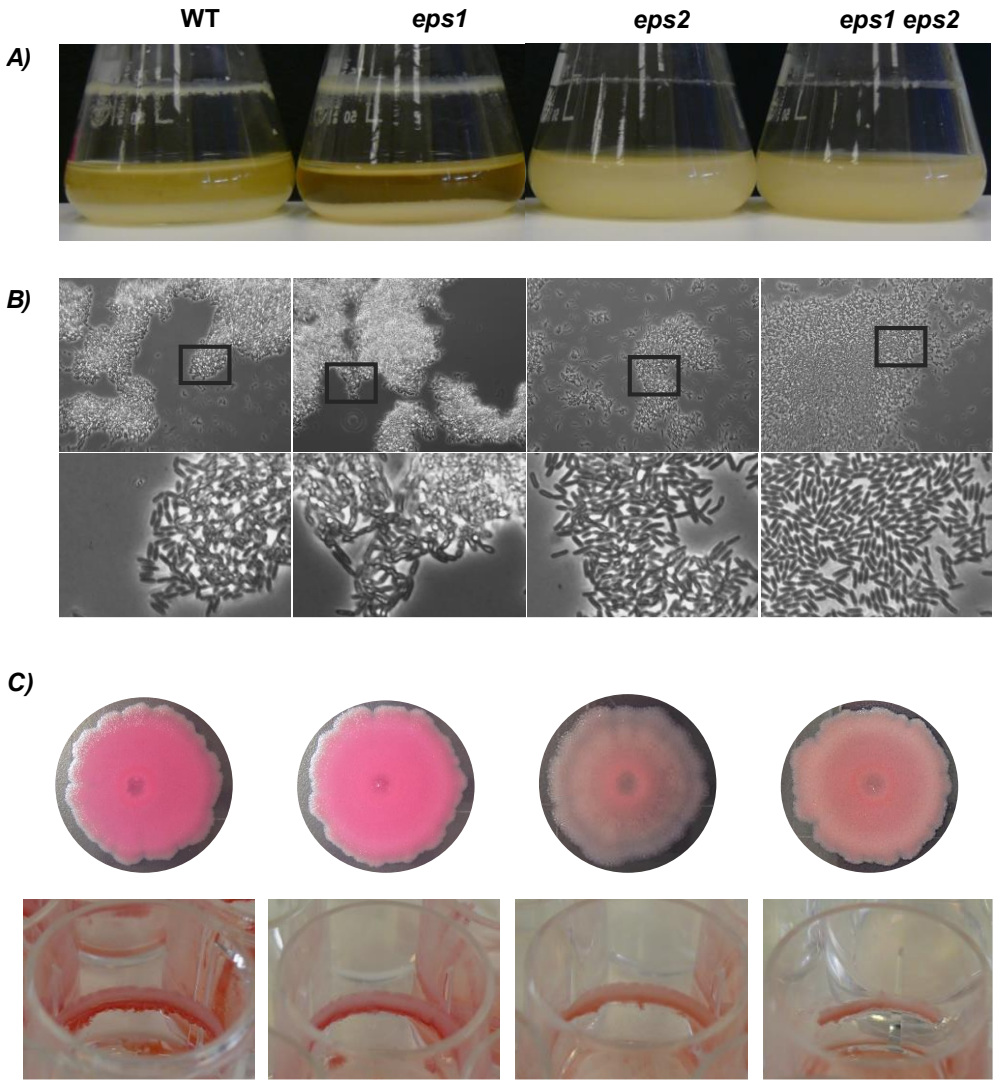

Figure 5. **Biofilm phenotypes of wild type and mutants in the *eps* regions.** **A)** Liquid cultures on Ty medium at 28ºC, 150 rpm shaking incubated during 24 h, shows the major amount of biomass attached to the wells of the flask. **B)** Images of contract phase microscopy of the spent medium of the liquid cultures shows the presence of bacterial clumps in WT and *Δeps1*. Bottom pictures are closer views of the squared areas in original pictures **C)** Congo Red biofilm assays in Ty agar plates (28ºC, 72 h) and liquid culture supplemented with Congo Red, without shaking (28ºC, 6 days).

experiments in agar plates: the absence of pinkie staining and the major spread of the colonies of *Δeps2* and double *Δeps1 Δeps2* mutants (Fig. 5C, top). The Congo Red staining associated to *eps2* was also visible in biofilm growth in static liquid culture. All the mutants developed almost similar biomass associated to the wall of the wells in static cultures, however, a clearly defined red zone was visible in the wild type and *eps1* mutant, which was absent in *Δeps2* or double *Δeps1 Δeps2* (Fig. 5C, bottom).

These findings clearly indicated a differential function of the two EPS, while EPS2 seems to be related to the development of the static life featured of biofilm formation; EPS1 is apparently more prone to promote bacterial colony motility.

3. *B. cereus eps1* and *eps2* regions are not directly involved in cellular auto-aggregation

Exopolysaccharides are known to possess adhesive properties, promoting the cell-to-cell interaction, a previous step in the formation and maturation of bacterial biofilms (Sorroche et al., 2012). Bacterial clumps observed in the spent medium of agitated cultures of WT and *Δeps1* mutant, led us to think on the major implication of the EPS2 in cell aggregation. To assess these differences, we performed an auto aggregation assay using two different and complementary methods described previously: i) recording the variation of the optical density (OD) of the upper part of the liquid culture over time (Chauhan et al., 2013), and ii) measuring the OD at a determined deep in the liquid

culture at the end of the experiments (Roux et al., 2005). Bacterial cells were grown overnight at 28ºC, and after adjusting OD, cell suspensions were incubated at room temperature with no agitation, taking samples every 15 minutes. For the second method, the OD was measured at the same deep of the cell suspensions after 9 h of incubation. The absence of any of the EPS led to a faster kinetic of aggregation than the wild-type, and this effect was amplified in the double mutant *Δeps1 Δeps2* during the first 5 hours (Fig. 6A-B). Accordingly, the OD values obtained with the second method were lower in the mutants compared to the WT after nine hours of incubation (Fig. 6C). Besides, after 24 h of incubation, a sediment at the bottom of the tubes was visible in the cultures of the mutants but not in the wild type (Fig. 6A).

These results rested relevance to the role of *eps1* and *eps2* in cellular aggregation, and indicated that other cell surfaces factors probably hidden by the presence of EPS are implicated in this cellular process. Thus, when any of the EPS is retired, cells interact increasing the sedimentation rate, an indirectly way to control cell aggregation by EPSs.

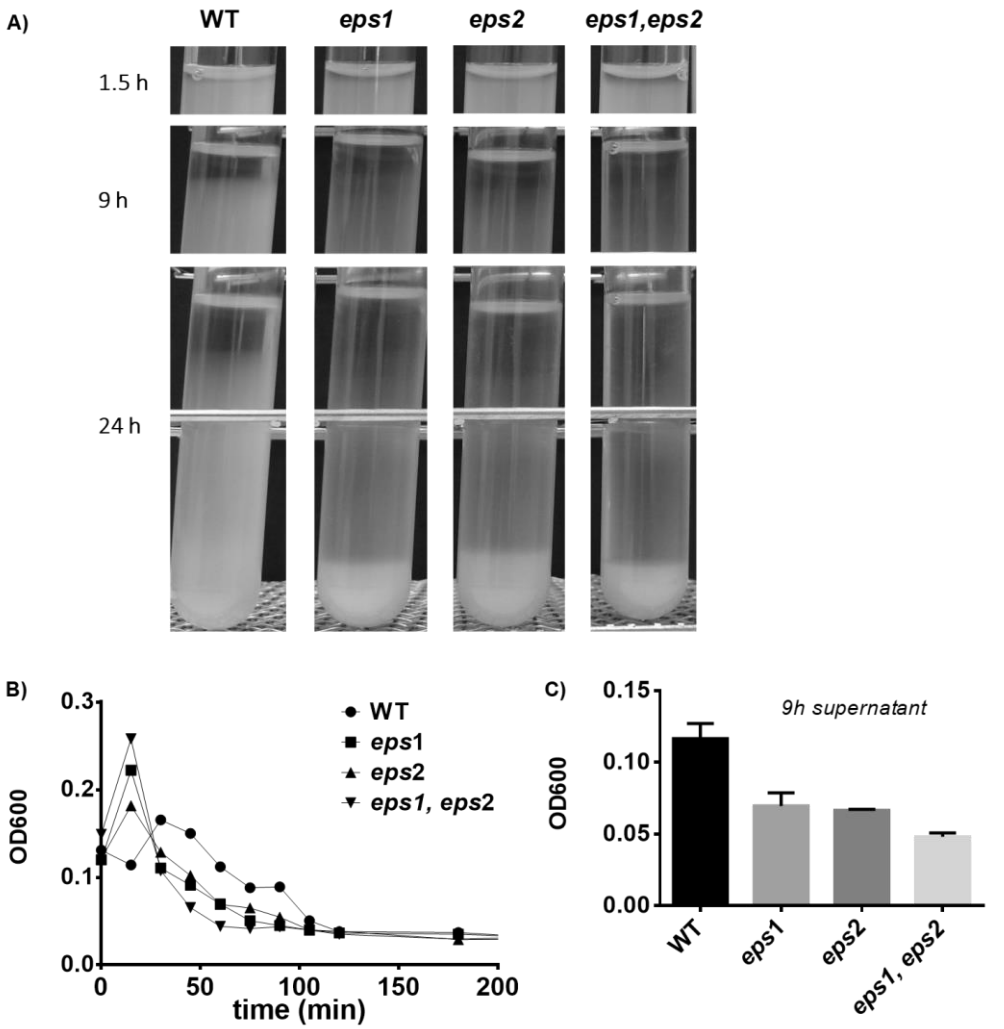

Figure 6. Eps1 and Eps2 prevent cellular auto-aggregation. Optical Density (OD) of cultures (28 ºC,16 h, 150 rpm) were adjusted to OD=3 before the experiments were initiated. **A)** OD measures of the air-liquid interface of cell suspensions in static at room temperature. **B)** OD measures of the liquid culture after 9 h sampling at the height of the grade bar. **C)** Pictures of the tubes at different times of incubation after adjustment of the OD.

4. The regions *eps1* and *eps2* are involved in cell motility

Several exopolysaccharides have been reported to play a relevant role in mobility in different strains and we previously noticed certain differences among mutants in colony sizes in agar plates. To assess if EPS1 and EPS2 were involved in this function, we seeded spots of bacterial suspension of wild type and mutants in 0.3% or 0.7% agar plates to assay swimming or swarming motility respectively (Fig. 7). *Δeps2* mutant did swim more than wild type or *Δeps1* mutant, and a synergistic effect was observed in the double mutant, which showed an increased spread of the colony by 50% (Fig. 7A). This result point to a negative effect of EPS2 in swimming, in accordance with the propensity for cell-cell clumping seen in liquid cultures at 24 h, which have an opposite effect on individual cell motility. In swarming agar plates, single *Δeps1* and double-mutant colonies spread less than the WT, and the deletion of *eps2* did not result in any noticeable modification of colony spread (Fig. 7B). Taken together, these findings suggest that Eps2 must antagonize individual cell motility, while Eps1 seems to promote social movement.

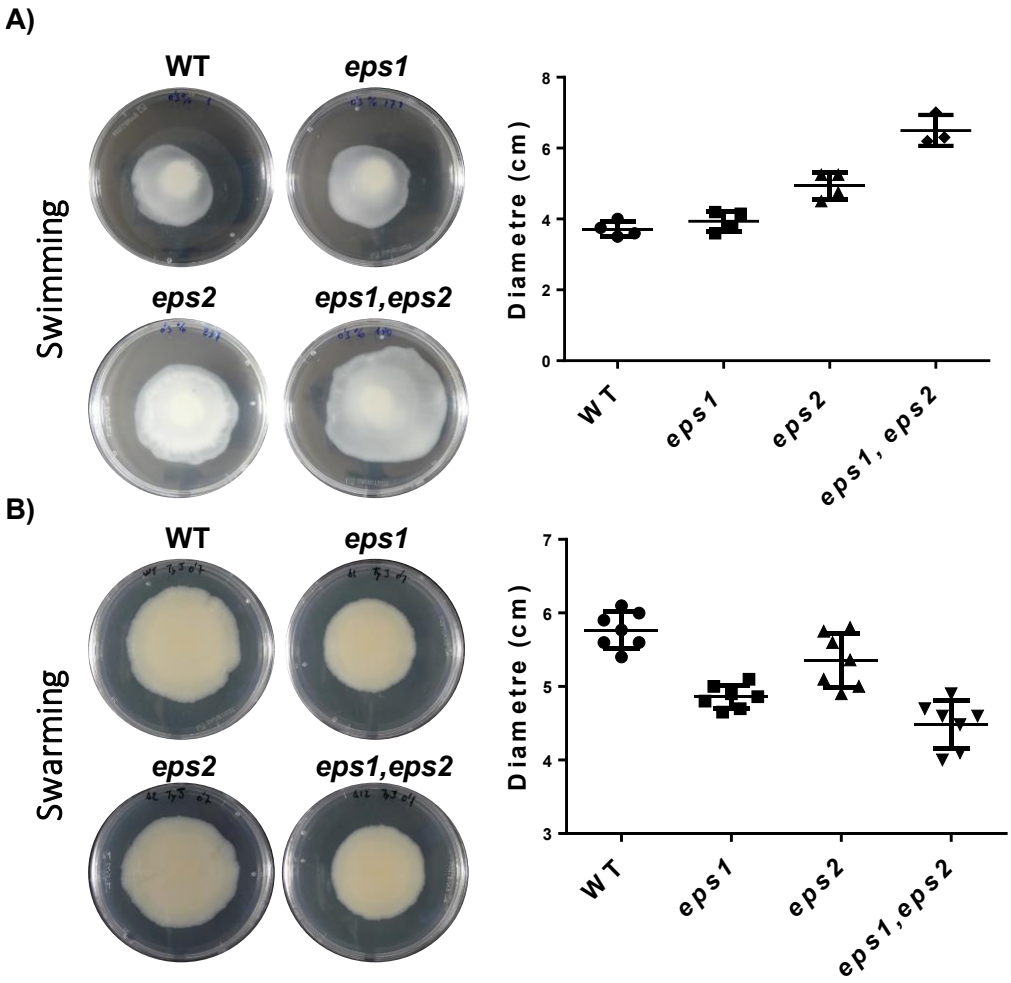

Figure 7. EPS1 and EPS2 contribute differentially to bacterial cell motility. A cell suspension was spot in the centre of the plate and incubated at 28ºC before examining motility. **A)** Images taken from swimming agar plates (0.3% Ty agar plates, 24h). **B)** Images taken from swarming agar plates (0.7% Ty, 72 h). Graphs are values of colony size at the end of the experiments.

Mutants in each *eps* region showed a differentiable phenotype, suggestive of their specific implication in different and complementary aspects of *B. cereus* social behaviour. Thus, we reasoned that the mixture of cells from each strain should rescue the WT phenotype. To test this hypothesis, we performed strain complementation experiments in swarming agar plates supplemented with Congo Red and tested for reversion of swarming motility and staining (Fig. 8). When both of the strains tested possessed *eps2* region, the colony colour was homogeneous (reddish). When one of the strains lack *eps2* region, colour sectors appeared, which reached always the colony border when none or both strains possessed *eps1*. However, these sectors decayed from the centre to the border when only one strain lacks *eps1* (Fig 8A). These results confirmed that EPS1 is necessary for social aspect of the swarming motility, given that the strains lacking *eps1* remained delayed in their movement and set aside in the centre of the colony.

There were still two strain mixtures, WT + *Δeps1* (reddish) and *Δeps2* + *Δeps1Δeps2* (pinkie) that showed no sectors, given that the colour phenotype of both strains was similar. To differentiate the strains, they were transformed with replicative plasmids expressing constitutively *yfp* or *cfp*. Fluorescent microscopy analysis confirmed the formation of sectors in the mixtures and also supported the hypothesis posted of the role of EPS1 in swarming. Mixtures of wild type and *Δeps1* revealed a reduced fitness of cells lacking *eps1,* which got delayed in the colony advance, resulting in a border dominated by wild type bacteria (Fig. 8B). Similarly, the double mutant *Δeps1 Δeps2* was less competitive when combined with *Δeps2*.

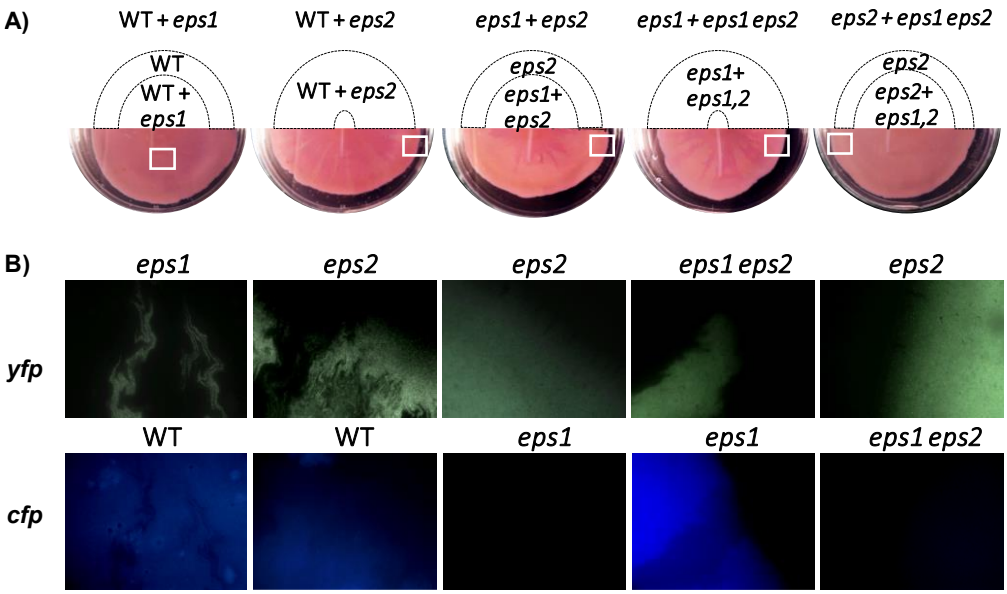

Figure 8. External complementation assays of mutants in *eps1, eps2* and *eps1eps2* regions. A) Congo Red agar plates for swarming (agar concentration 0.7%). **B)** Fluorescent microscopy images of the sections marked with a white square in A).

These results indicate that only cells producing the EPS1 show enhanced movement, which led us to state that the function of EPS1 in motility is at individual cell level and not as a good for the entire community as seen with surfactants or other exopolysaccharides which are secreted by a part of the population and affect mobility of the non-producer cells (Garcia-Betancur et al., 2012).

5. EPSs provide resistant to some antimicrobials and disinfectants

The extracellular matrix of a biofilm provides bacteria cells with protection against several stresses, and specifically resistance to antibiotic has been reported for exopolysaccharides in other bacteria species (Campos et al., 2004; Jeon et al., 2009; Oh and Jeon, 2015). The chemical features of EPS seem to trap certain antibiotics, preventing or reducing the amount of molecules that reach the bacterial cells. To assess if any of these regions contribute to antimicrobial resistance we tested their sensitive to a battery of antimicrobials in commercial Biolog® plates PM12B (Fig. 9). In general, we observed that each EPS provided protection against specific molecules, although the contribution of EPS2 was more relevant. The *eps2* provided specifically protection against carbenicillin (penicillin family) or dodecyl trimethyl ammonium (cationic detergent). A similar protection was observed for each EPS against novobiocin (aminocoumarin antibiotic) or benzethonium chloride (cationic detergent). No clear protection was noticed of any EPS against fluorootic acid (toxic for bacteria with complete uracil biosynthesis pathway), although a clear effect was seen in the double mutant. Interestingly, the protection provided was always synergistically and potentiated by the presence of the two EPSs.

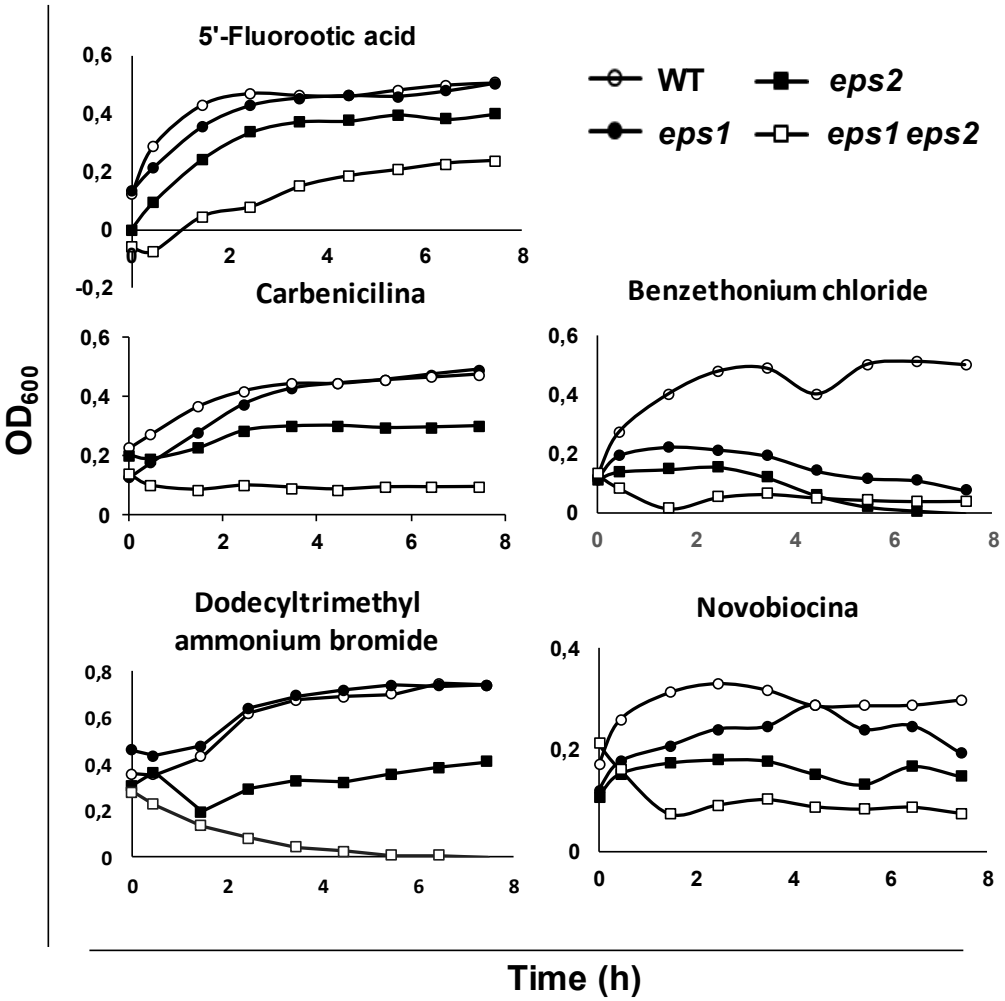

Figure 9. The EPS contribute to protect cells against antimicrobials. Growth curves of *B. cereus* wild type and mutants *eps1*, *eps2*, and *eps1 eps2* in liquid culture in Biolog® Plates PM12B containing antimicrobial compounds. Double mutants always show higher sensitivity to all antimicrobial tested.

6. EPS2 affects host adhesion specificity

The experiments done *in vitro*, suggested a major contribution of *eps2* to adhesion to abiotic surfaces. Thus, we wanted to examine if these findings were extensive to biotic surfaces. Considering the implications of *B. cereus* in human intoxications, we initially tested the adhesion ability of these strains to Hela or MDA cell lines as epithelial human infection model (Fig. 11). As expected from *in vitro* experiments, the *eps2* strain was severely impaired in adhesion, and *eps1* behaved as the wild type. Similarly, the double mutant showed a reduced adhesion ability to both epithelial cell lines.

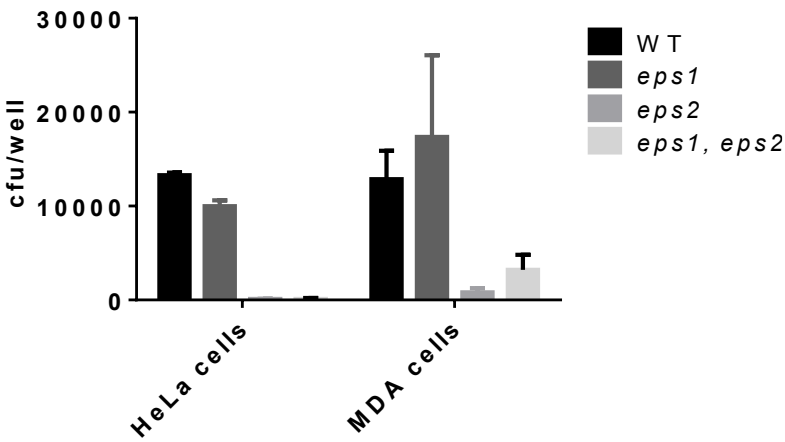

Figure 11. The EPS2 is more relevant for adhesion of *B. cereus* to human cells. Adhesion assays to human cell cultures of HeLa and MDA epithelial cell lines.

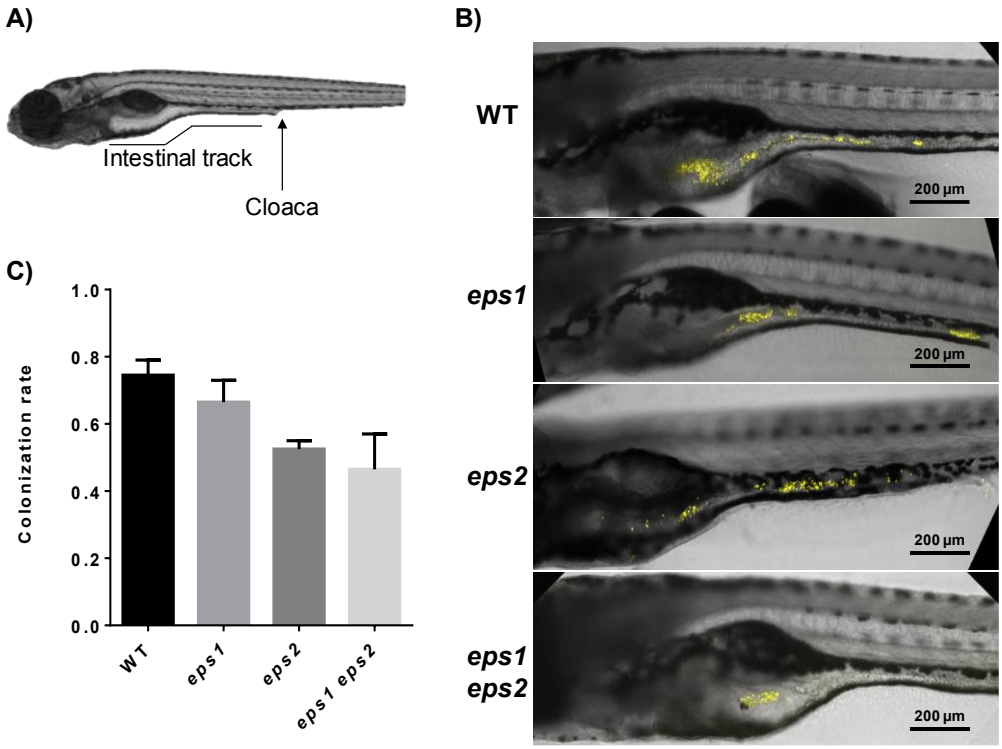

Figure 12. **The EPS2 is more relevant for adhesion of *B. cereus* to Zebrafish gut. A)** Zebrafish picture of a 6 days post infection (dpf) larvae. **B)** Fluorescent Z-stack and bright field merged confocal microscopy images. Bacteria strains were transformed with a plasmid harbouring *yfp* gene under a constitutive promoter. **C)** Rate (± SEM) of zebrafish larvae of 6 dpf harbouring fluorescent bacteria in the GI track 24 h after feeding with *B. cereus* wild type, *Δeps1, Δeps2* and the double mutant (1 E8 ucf/ml).

Confirmed the adhesive properties of EPS2 to biotic surfaces, we tested the role of this EPSs in adhesion to a complex biotic surface, using the Zebra Fish (*Danio rerio*) as an intestinal model due to the similarities with mammal's gut. For instance, the presence of finger like protrusions (villi) in the intestinal epithelium or several factors of the immune response (Brugman, 2016). After feeding zebrafish larvae with wild type,

single and double mutant strains harbouring a reporter plasmid containing yfp fused to a constitutively expressed promoter, it was assessed the presence of bacteria in the gut by observation under confocal fluorescence microscopy. The examinations of the fishes, showed that after 24 h, 74% of larvae retained fluorescent bacteria in the gut. Larvae fed with bacteria mutants in *eps1, eps2* and double mutants showed a decreased proportion of 67%, 53% and 46% respectively. These experiment confirmed the expected role of EPS2 in the adhesion of *B. cereus* to the intestinal epithelium (Fig. 12).

Given that the implication of EPS2 in biofilm and host colonization occur in different environments with variable temperature, we asked if differences in temperature culture conditions would reflect different levels of expression of the EPSs. The qRT-PCR analysis revealed that both *eps* regions were comparatively more expressed at 30ºC than at 37ºC, especially *eps2,* that showed almost 5-folds higher expression at 30ºC (Fig. 13). Comparison of *eps1* and *eps2* indicated that *eps1* expression is less sensitive to temperature changes. Thus, we think that *eps1* could be constitutively expressed

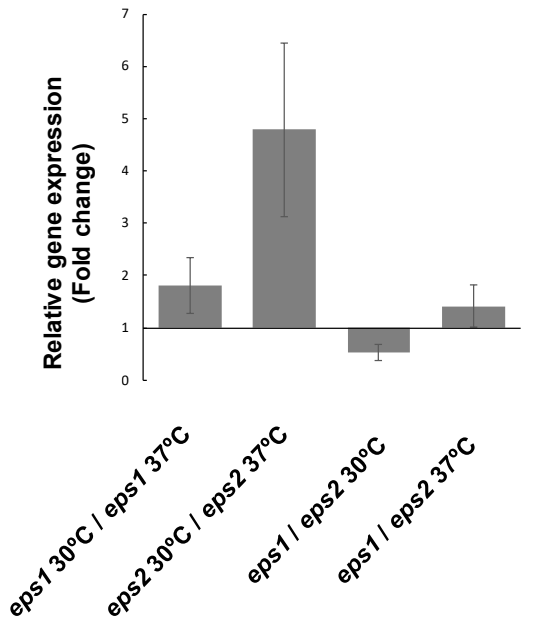

Figure 13. *eps2* expression is more sensitive to temperature. Level of expression of the *eps* regions at different temperatures. Relative amount of RNA was estimated by qRT-PCR. Results are means of fold change ± ES (n= 9) ($t^2_{0.001,3}$<0.2).

3. DISCUSSION

Bacteria usually possess a pull of genetic regions devoted to the synthesis of different polysaccharides (Yang et al., 2015). These polymers can play functions of cell wall covering, capsule formation, spore surface decoration, adhesion or structural support for biofilm, but also provide extra benefits against different stresses, storage of carbon or protection against host defence (Hidalgo-Cantabrana et al., 2014, 2014; Sims et al., 2011). In *B. cereus* it has been described the existence of: i) exopolysaccharides associated to sporulation (genes *BC0484-90)* (Li et al., 2016), ii) two spore-decorating sugars (genes *BC3358-61*) (Li et al., 2017) and iii) two secondary cell wall polysaccharides (SCWP) (genes unknown) (Candela et al., 2011). In this work, we have investigated two genomic regions putatively dedicated to produce two different polysaccharides, referred as *eps1* and *eps2.*

Data obtained from our study indicate that the two polysaccharides play different roles in *B. cereus*, with a major implication of EPS1 in motility and EPS2 in adhesion and maturation of biofilms. The results obtained from the motility assays indicates that *eps2* negatively impact swimming, most probably due to the adhesive properties mediating the cell-cell interaction leading to the formation of cell clumps (Limoli et al., 2015), while *eps1* is important for an efficient swarming motility. The synergistic effect of *eps1* in double mutant in swimming assay suggests certain EPS stratification, resulting in a different surface exposure. Complementation experiments in which two strains are co-seeded revealed the loss of fitness of *eps1* mutants in competition with the other

strains, remaining delayed and finally isolated in the centre of the colony. This element may result determinant in the colonization of vegetable tissues as swarming has been described as the major element in migration in root colonization in *B. subtilis* (Gao et al., 2016). Similar to the root, the gut of insects of mammals in which *B. cereus* also grows is a very competitive environment in which it can be speculated that swarming may play a similar role.

Auto-aggregation assay shows an opposite effect and the lack of any *eps* region result in increased sedimentation rates, suggesting that EPS1 may mask bacterial surface structures responsible for cell-cell interaction, a phenomena also reported in other bacterial species (Dertli et al., 2015; Horn et al., 2013). Data of aggregation in flasks and auto-aggregation experiments may be contradictory at a first glance. However, it is important to notice that each experiment was performed at different time points of the cultures, which is highly probable conditioning the physiological state of the cells. Auto-aggregation assay is performed after 16 h of incubation, thus previous to a visible biofilm ring formation, while aggregation observed in flasks occurred after 24 h of incubation in vigorous shaking and with visible well-developed biofilm rings. Therefore, both experiments should be conceived as complementary reporting auto-aggregation properties of planktonic cells and aggregation of a matured culture in which bacteria enter into a state prone to biofilm formation. Our data also suggest that additional elements to EPSs may be implicated in attraction and repulsion, forces regulated in response to the culture conditions and controlling auto-aggregation and cell-cell interaction (Aslim et al., 2007). For instance,

in *B. thuringiensis* cultures the S-layer is released at stationary phase, changing the surface bacteria characteristics (Luckevich and Beveridge, 1989). Nevertheless, biofilm assay in shaking flask clearly showed that the lack of *eps2* resulted in reduced aggregation and reduced biofilm formation, in accordance with some works in which auto-aggregation has been directly correlated to biofilm formation (Sorroche et al., 2012).

The study of other benefits provided by EPSs revealed their definite contribution to antimicrobial resistance, which showed a synergistic effect among both *eps* regions, the lack of *eps1* usually had a low effect when *eps2* is still present, but double mutant shows higher sensitivity than *eps2* mutant, pointing to a collaborative role with prevalence of *eps2*.

Expression quantification experiments using qRT-PCR suggest that *eps1* is constitutively expressed and may participate in the synthesis of one of those EPS described in the SCWP (Candela et al., 2011). On the other hand, *eps2* expression is highly sensitive to temperature, showing a decrease in expression at 37ºC. Likewise, in the mammal niche, *B. cereus* is more prone to attack and remain in a planktonic state instead of forming a biofilm as discussed in Chapter IV. Unless another factor influences *eps2* expression, in this scenario in which *B. cereus* prefers attack, huge amounts of EPS2 would not be necessary. Although, little amount of EPS2 seems to play a determinant role in the adhesion of *b. cereus* to epithelial cells of mammals. Results in the gut of zebrafish are in accordance with results of adhesion obtained *in vitro*. However, differences are less evident probably due to the complex environment

of the gut, were a mucus layer cover the lumen and other microorganisms may be present and interact with *B. cereus* (Brugman, 2016) Other factor affecting this experiment is the fact that Firmicutes do not find optimal the conditions of the zebrafish gut as reported by studies revealing that this species can colonize *Danio rerio* gut but remains in a low proportion compared with the total microbiota, dominated by Proteobacteria (Semova et al., 2012). Conversely, the gut of mice and humans harbour big proportions of Bacteroidetes and Firmicutes (*Bacillus spp.*) (Rawls et al., 2006). In this way, for further confirmation of the implication of EPS2 in the colonization of the gut of mammals it would be desirable to use mice as a model organism to mimic the human gut.

In summary, our results reveal the implication of *eps2* in adhesion, biofilm formation, cell-cell cohesion and host interaction, while *eps1* plays a role in social motility. Given that the only function found for *eps1* in promoting swarming seems mild, we wondered for an extra function of this EPS. The *eps1* region shows similitudes with the one in *B. subtilis* codifying the synthesis of structural EPS in biofilm. Some works has reported that this EPS exhibit induction over anti-inflammatory M2 macrophages, inhibiting T cell activation (Paynich et al., 2017). We hypothesize that in *B. cereus eps1* region might evolve to produce an even enhanced effect in immunology modulation response, having lost the structural functions in the evolution process.

4. METHODS AND MATERIAL

Bacterial strains and culture conditions

The bacteria used in this study are listed in Annex Table 1. Bacteria were routinely grown in TY broth (1% tryptone, OXOID), 0.5% yeast extract (OXOID), 0.5% NaCl, 10 mM MgSO4, and 0.1 mM MnSO4). Biofilm assays were performed in TY.

Construction of B. cereus mutants

B. cereus mutants were obtained by electroporation using the plasmid pMAD (Arnaud et al., 2004). Primers used to generate the mutagenesis constructs are listed in Annex Table 2. The constructs were created by joining PCR. In the first step, regions flanking the target genes were amplified separately, purified, and used for the joining PCRs. These PCR products were digested and cloned into the pMAD vector digested with the same enzymes. The resulting suicide plasmids were used to transform *B. cereus* electrocompetent cells as described previously (Kahrs, 1977) with some modifications. Electroporation was performed with 10 µg of plasmids in 100 µL of electrocompetent *B. cereus* in 0.2-cm cuvettes using the following electroporation parameters: voltage 1400 kV, capacitance 25µF, resistance 400 Ω. After electroporation, cells were incubated in LB for 5 hours, and then seeded in LB medium supplemented with X-Gal and erythromycin for 72 h at 30°C. Blue colonies were selected and streaked to trigger allele replacement. Finally, white colonies that were sensitive to MLS were selected, and

deletion of the target gene was verified by colony PCR analysis and sequencing of the amplicons.

Plasmids for fluorescence microscopy

The plasmid pHCMC02 (Nguyen et al., 2005) was modified cloning the fluorescent proteins Yfp and Cfp under the constitutively expressed promoter of the gene *upp* from *B. cereus,* using the primers listed in Annex table 3. Wild type strain, as well as mutants in *eps1, eps2* and double mutants were transformed with the constructed vectors and positive clones were isolated.

Biofilm assays

B. cereus biofilm formation was monitored by testing bacterial adhesion to abiotic surfaces in 24-well plates and 250 mL flask (O'Toole et al., 1999). Cultures were grown in Ty at 30ºC with or without agitation.

Congo Red assay

Staining of *B. cereus* colonies with the amyloid dye Congo Red (CR) was performed as described above but using Ty agar medium supplemented with Congo Red and Coomassie Brilliant Blue G at final concentrations of 20 µg/ml and 10 µg/ml; the dyes were filtered and added to autoclaved Ty medium (Romero et al., 2014).

Auto-aggregation assay

Flasks with 25 ml of Ty were inoculated with B. cereus strains and incubated at 28 200 rpm shaking o/n. Culture were divided in two fractions. OD600 of 10 ml culture of every strain were adjusted to 3 using the supernatant from centrifuging the other fraction. Tubes were incubated vertically at RT without moving. At each sampling time, 10 µL were carefully taken from air-liquid interface of the medium and diluted in 90 µL of Ty to measure OD_{600} in a plate reader (Omega).

Swarming and swimming motility

Petri dishes with Ty broth containing 0.7% (for swarming) and 0.3% (for swimming) agar and 20 µg/ml of CR were used to assess colony expansion. Plates were incubated at 28 during 24, 48 and 72 h. Diameters of colony were measured and data were treated statistically to obtain average and SD, n=6-9.

RT-PCR and qPCR

Total RNA was isolated following the protocol described in Methods and Materials of Chapter IV. The quality of the RNA extraction was tested by spectrometry using NanoVue GE equipment and electrophoresis in agarose gel. From total RNA samples, cDNA was obtained using Titan One RT-PCR System (Roche). To test mRNA extent of the operons which integrate *eps1* and *eps2* regions it was performed PCR using as

template cDNA and primers listed in Annex Table 4. Positive controls for each primer pair were included using genomic DNA as template and for negative controls RNA extraction as template to ensure that RNA extraction was not contaminated with genomic DNA.

For quantitative real-time PCR we measured the transcript levels of the *eps1* (*Bc5274*) and *eps2* (*Bc1583*) at 28 and 37ºC using qRT-PCR. The reaction was performed using the Power SYBR Green Master Mix (Bio-RP) following the manufacturer's recommendations. Reactions were done in triplicates in 96-well plates and 20 µL of reaction volume containing 1 µL of cDNA, 10 µL of SYBR Green Master Mix, 0.6 µL of 10 nM of each primer, and 7,8 µL of dH_2O. The reaction was started with an initial denaturation at 95 °C for 3 min and 40 cycles of amplification of 95 °C for 20 s, 56 °C for 20 s and 72 °C for 30 s.

Anthony´s method for capsule staining

An overnight culture of *B. cereus* was spread in a microscope slide and let to air dry. After that, bacteria were stained with 1% crystal violet for 2 minutes and then rinsed with a solution of copper sulphate 20%. After air dry, micrographs were taken under oil immersion.

Antibiotic resistance assay

Biolog® Plates PM12B were used to grow *B. cereus* strains and assess antibiotic resistance measuring OD_{600} every hour during 8 h after plate inoculation following manufactured instructions.

Cell culture adhesion

MDA-MB-231 breast adenocarcinoma cells and Hela cancer cervix cells were obtained from the ATCC and were grown in RPMI 1640 and DEMEM glucose (4.5 g/L) medium cultures respectively, supplemented with glutamine (2 mM), penicillin (50 IU/mL), streptomycin (50 mg/L), amphotericin (1.25 mg/L), and 10% FBS, at 37 °C with 5% CO2 in air. Cells were seeded at 2000 and 1500 cells/well in a 96-well plate and incubated 72h at 37ºC and 5% CO2 to achieve confluence and a cell density of 1·104 cells/well. Hela and MDA cells medium culture was replaced with ´assay culture´ (supplemented with glutamine and FBS, without antibiotics or antifungals), cells were incubated two hours and them the culture medium was replaced again with assay culture before bacteria inoculation. *B. cereus* ATCC14579 and EPS mutants were streaked in LB agar plate and incubated 24h at 28ºC. Tubes with 5 ml of TyJ were inoculated with *B. cereus* ATCC14579 and EPS mutants and incubated o/n 28ºC with vigorous shaking. Bacteria were washed trice with sterile PBS and OD600 was adjusted to 1 (aprox. 10^7 ucf/ml). Human cell cultures 96-well plates were inoculated with 10 µl of bacterial suspensions, using a MOI of 10:1. Plates were centrifuged at 2000 g 1 min to force bacteria to contact with human cells and avoid bias of motility. After 45 minutes of incubation, plates were washed 5 times with sterile PBS to remove non adhered bacteria. Cells were lysed with Triton x-100 0,1%, 10 min. Serial dilutions of each well were plated on LB agar to tittle the number of bacteria adhered to cells.

Danio rerio gut adhesion assay

Zebrafish larvae of 6 dpf (days post fertilization) were used for the experiment to assess the proportion of individuals harbouring *B. cereus* individuals allocated in the gut at 24 h post feeding with bacteria strains. In 50 ml tubes with 30 ml of E3 medium without disinfectant 30-40 larvae bacteria were inoculated to a final concentration of 1.0e8 ucf/ml (approx. OD=1). Larvae were incubated at RT for 12 minutes. After that, tubes were cold on ice until larvae decanted to the bottom to retire the medium with bacteria (six times). Larvae were observed one by one at the microscope and 10-15 individuals with a visible mass of bacteria in the anterior intestine (intestinal bulb) were selected to continue with the experiment. Larvae were then incubated at 28ºC for 24 h. Previous to the observation by confocal microscopy (Nikon Eclipse Ti Fluorescence Microscope equipment) to obtain the rate of presence of bacteria in the gut / total observations, larvae were incubated on ice for 3 minutes and fixated for 1 hour in cold PFA 4% to facilitate observation. For image analysis, ImageJ Fiji software was used to construct a Z-stack of images from fluorescence emission merged with bright field images.

5. ANNEX

Table 1. Table of strain used in this study.

Strain	Derivative strain	Genotype	Reference
Bacillus cereus ATCC 14579	WT	Type strain	
Bacillus cereus ATCC 14579	Δ*eps1*	Δ*BC_5279 – BC_5274*	This study
Bacillus cereus ATCC 14579	Δ*eps2*	Δ*BC_1583 – BC_1591*	This study
Bacillus cereus ATCC 14579	Δ*eps1,* Δ*eps2*	Δ*BC_1583 – BC_1591* and Δ*BC_5274 – BC_5279*	This study
Escherichia coli DH5α			(Boyer and Roulland-Dussoix, 1969)

Table 2. Table of primes used to mutate *eps* regions.

Mutation	Name	Primer sequence
Δ*BC_1583– 1591*	Forward.up.BamHI	AAAAGGATCCGGGATGTTGCATA AGTCGAAC
Δ*BC_1583– 1591*	Reverse .up	ATTGGCATTAATCCAGCAAGGC CACGAGCGATTAAACCATTC
Δ*BC_1583– 1591*	Forward.down	CCTTGCTGGATTAATGCCAAT
Δ*BC_1583– 1591*	Reverse.down.NcoI	AAAACCATGGCTCTTT TTCATTACCTATATCCCACTA
Δ*BC_5279- 5274*	Forward.up.BamHI	AAAAGGATCCTTTGAAAGAACT AAGGCTGACG
Δ*BC_5279- 5274*	Reverse .up	TGGTTTTCTTTTCTTTCTCCCG AACATAT T
Δ*BC_5279- 5274*	Forward.down	AAACCATTACGACAATTAATTA CACATCAGATGAGTCAAGA GAGTATTAGGAAAACC
Δ*BC_5279- 5274*	Reverse.down.NcoI	AAAACCATGGATGCAAAGGTAA CGTGATTTCATT

Table 3. Table of primes used for the construction of the plasmid pHCMC02-*Pupp-yfp.*

Name	Primer sequence
Prom.upp.Fw	AAAAAGCTAGCGGATGAAATTGCGTCA
Prom.upp-yfp.Rv	CATAGTAGTTCCTCCTTATGTAGATGATA TTCATGCGTTTGC
yfp.Fw	ACATAAGGAGGAACTACTATGAGT
yfp.Rv	GCGCTCACCCGGGTTATTTGTATAG

Table 4. Table of primes used for RT-PCR.

Name	Primer sequence
BC_1583_fw	TGTTTTGAGCGGATTTGTTTTGT
BC_1583_rv	GTCCACGAGCGATTAAACCA
Interg_83-84_fw	ATTCAGAAAAGGGCGGTGAAAT
Interg_83-84_rv	AGCGGTTAAACAACACATCGT
BC_1584_fw	AAAATCTCGGTTGTGAATACGG
BC_1584_rv	GATTGCTCTGCCAATGTCTTT
Interg_84-85_fw	TCGAGGTGAACATGTCGATG
Interg_84-85_rv	CACCTCTGTCCTTCGTTGAA
BC_1585_fw	ACATACAGGGACGCCTTTAGT
BC_1585_rv	AACCACTCCATCGCATTTCC
Interg_85-86_fw	TTGAATGTGGGGGTAACGAT
Interg_85-86_rv	CAAACAAGCGTTTTACACTTCG
BC_1586_fw	CCCTAGACCAGAGAGAGAGTTTT
BC_1586_rv	CCCTCCATTTATTTGTGCCCA
Interg_86-87_fw	TGAACGGTAATGGTGCAAGA
Interg_86-87_rv	AAACTGACGGCCTGAAGAAG
BC_1587_fw	GAATGCAGTAGAACCACTCCAAA
BC_1587_rv	CGTCGTTAAACCGTCAGCAA
Interg_87-88_fw	CGCAAAAAGGATTATATTACGAA
Interg_87-88_rv	GAAGAATAATCCATCCCATTGA
BC_1588_fw	CGCAGCATACTTTGTTTCGTG
BC_1588_rv	ACCATCTATCTTTCCCCTTCCTT
Interg_88-89_fw	CGCAGCATACTTTGTTTCGTG
Interg_88-89_rv	GAAGAATAATCCATCCATCCATCCCATTGA
BC_1589_fw	TGTTCAACCGACCAATCTGC
BC_1589_rv	TGCGGCAACCATATATCATCAC
Interg_89-90_fw	GAAGAATAATCCATCCATCCATCCCATTGA
Interg_89-90_rv	GCCATCGCTTCAATTACTACCA
BC_1590_fw	ATTTCAGAGCCGCATGAGTTT
BC_1590_rv	GCCATCGCTTCAATTACTACCA
Interg_90-91_fw	TTTAATATCTGAATATTGCGAAT
Interg_90-91_rv	AATTTGCAGGGTTACGGTAGG
BC_1591_fw	TTTAATATCTGAATATTGCGAAT

BC_1591_rv	TTGGACCTGCTGCCATTAAG
BC_5279_fw	TCGGACAACAAGGAAAGAAAGT
BC_5279_rv	TTGGACCTGCTGCCATTAAG
Interg_79-78_fw	CTCGGAGTCGTTTTGAATGAT
Interg_79-78_rv	CGAGGATCATTGCTAAACGTT
BC_5278_fw	GCTTCAGTTGGTCTTGCATTCT
BC_5278_rv	TCTTGATGATGGAGCGTGTGA
Interg_78-77_fw	GCTTCAGTTGGTCTTGCATTCT
Interg_78-77_rv	AGAAGCATCACATACATTTGCCA
BC_5277_fw	ATCCCACCAAATCCAGCAGA
BC_5277_rv	AGAAGCATCACATACATTTGCCA
Interg_77-76_fw	TATTACTACGGTGCAAACTAG
Interg_77-76_rv	GTGACAATGTAAATCTATCAT
BC_5276_fw	GCACAAAAAGCCGCTTCAGA
BC_5276_rv	TAACCTGACTTCTTGCCCCG
Interg_76-75_fw	TGGTGATGTCTCCTAACCGT
Interg_76-75_rv	TAATGAGAGCCGTCTTCGATA
BC_5275_fw	GCAAGGAACAGCACCATCAA
BC_5275_rv	CCCGCACCTGTTTGTTGATT
Interg_75-74_fw	TGTTGGGGAGAAGTTTGGAT
Interg_75-74_rv	ACTCAATATACCTGTTCCCTTCT
BC_5274_fw	CTAGGGAGAGAGCCTGTTCA
BC_5274_rv	CCCCAGCACCCGTTATTAAA
Interg_74-73_fw	CCTTATTAGATTTTGCGAATA
Interg_74-73_rv	GTCTGGTGGAGAAAACGGGA
BC_5273_fw	CCGTTTTCTCCACCAGACATT
BC_5273_rv	ACCGCTTTATTTGTCCCAACA
Interg_73-72_fw	AATGAAATCACGTTACCTTTGCA
Interg_73-72_rv	TGAACTGCTGCAACTCCTAG
BC_5272_fw	ACAAGGGCAAAGAGGGGTAA
BC_5272_rv	CCAAGTTTCTCTATCGGACGC
Interg_72-71_fw	CGTCCAGTAAATGGTAAAAATGA
Interg_72-71_rv	TAGAAAACCCGTTCCACCAG
BC_5271_fw	TTGGCCTGTGAGCATATTGG
BC_5271_rv	TCACCATGAAATGCTTGTCTGA
Interg_71-70_fw	TTGGCCTGTGAGCATATTGG

Interg_71-70_rv	CAGAGGCTGCCGTTAAGAAT
BC_5270_fw	ACAATGGAGCAACGTGTGAA
BC_5270_rv	CAGAGGCTGCCGTTAAGAAT
Interg_70-69_fw	ACAATGGAGCAACGTGTGAA
Interg_70-69_rv	ACATCCATTGCACGACTTTCA
BC_5269_fw	GGACTGTCCCTGAAAATGTTGT
BC_5269_rv	ACATCCATTGCACGACTTTCA
Interg_69-68_fw	CTTGGGAAGTCTAGTTCTGGG
Interg_69-68_rv	TGCAAGTCCTATTACCCTCCT
BC_5268_fw	TTAGGAGCCTGGATGTGTCT
BC_5268_rv	CGTTGTCGTTTGAACCCTTTT
Interg_68-67_fw	AAAAAAGGGTTCAAACGACAAC
Interg_68-67_rv	TCTGTAGATCCGTCATTTACCA
BC_5267_fw	TTGGTAAATGACGGATCTACAGA
BC_5267_rv	TCAATCCTACATTTCTCGCAGA
Interg_67-66_fw	GAATGCTAAACCAAGTAACTAA
Interg_67-66_rv	TAGCAATAAATGTATAAGAG
BC_5266_fw	TTTCCTGCTTTACGTCGTACATC
BC_5266_rv	CGGTAACCACGCTGATAGGA
Interg_66-65_fw	ATGCTCATGAAATCTAAATGA
Interg_66-65_rv	AATAGGATTTTCTTTTTCAT
BC_5265_fw	CAGTTGGTGGGGTAGATGTCA
BC_5265_rv	AACAGCTTGCATCACTTGGC
Interg_65-64_fw	GAGCGCATCTTGAAGTGACC
Interg_65-64_rv	CGCTCACAATCGAAGCAACA
BC_5264_fw	GCAACAGGACAAACGAGTGA
BC_5264_rv	TGCCTTTTTATCCTCAGCAGC
Interg_64-63_fw	GGACATGATGTTTGGGCGAA
Interg_64-63_rv	TATAGCCAGCTCCACCACAG
BC_5263_fw	CTGTGGTGGAGCTGGCTATA
BC_5263_rv	CGCCTTCCGTAATTGCATCT

6. REFERENCES

Arciola, C.R., Campoccia, D., Gamberini, S., Donati, M.E., Pirini, V., Visai, L., Speziale, P., and Montanaro, L. (2005). Antibiotic resistance in exopolysaccharide-forming Staphylococcus epidermidis clinical isolates from orthopaedic implant infections. Biomaterials *26*, 6530–6535.

Arnaud, M., Chastanet, A., and Débarbouillé, M. (2004). New Vector for Efficient Allelic Replacement in Naturally Nontransformable, Low-GC-Content, Gram-Positive Bacteria. Appl. Environ. Microbiol. *70*, 6887–6891.

Aslim, B., Onal, D., and Beyatli, Y. (2007). Factors influencing autoaggregation and aggregation of Lactobacillus delbrueckii subsp. bulgaricus isolated from handmade yogurt. J. Food Prot. *70*, 223–227.

Berleman, J.E., Zemla, M., Remis, J.P., Liu, H., Davis, A.E., Worth, A.N., West, Z., Zhang, A., Park, H., Bosneaga, E., et al. (2016). Exopolysaccharide microchannels direct bacterial motility and organize multicellular behavior. ISME J. *10*, 2620–2632.

Berne, C., Ducret, A., Hardy, G.G., and Brun, Y.V. (2015). Adhesins involved in attachment to abiotic surfaces by Gram-negative bacteria. Microbiol. Spectr. *3*.

Boyer, H.W., and Roulland-Dussoix, D. (1969). A complementation analysis of the restriction and modification of DNA in Escherichia coli. J. Mol. Biol. *41*, 459–472.

Branda, S.S., Gonzalez-Pastor, J.E., Ben-Yehuda, S., Losick, R., and Kolter, R. (2001). Fruiting body formation by Bacillus subtilis. Proc. Natl. Acad. Sci. *98*, 11621–11626.

Brugman, S. (2016). The zebrafish as a model to study intestinal inflammation. Dev. Comp. Immunol. *64*, 82–92.

Campos, M.A., Vargas, M.A., Regueiro, V., Llompart, C.M., Alberti, S., and Bengoechea, J.A. (2004). Capsule Polysaccharide Mediates Bacterial Resistance to Antimicrobial Peptides. Infect. Immun. *72*, 7107–7114.

Candela, T., Maes, E., Garénaux, E., Rombouts, Y., Krzewinski, F., Gohar, M., and Guérardel, Y. (2011). Environmental and Biofilm-dependent Changes in a Bacillus cereus Secondary Cell Wall Polysaccharide. J. Biol. Chem. *286*, 31250–31262.

Casillo, A., Parrilli, E., Sannino, F., Mitchell, D.E., Gibson, M.I., Marino, G., Lanzetta, R., Parrilli, M., Cosconati, S., Novellino, E., et al. (2017). Structure-activity relationship of the exopolysaccharide from a psychrophilic bacterium: a strategy for cryoprotection. Carbohydr. Polym. *156*, 364–371.

Chauhan, A., Sakamoto, C., Ghigo, J.-M., and Beloin, C. (2013). Did I Pick the Right Colony? Pitfalls in the Study of Regulation of the Phase Variable Antigen 43 Adhesin. PLoS ONE *8*, e73568.

Chung, J.W., Altman, E., Beveridge, T.J., and Speert, D.P. (2003). Colonial Morphology of Burkholderia cepacia Complex Genomovar III: Implications in Exopolysaccharide Production, Pilus Expression, and Persistence in the Mouse. Infect. Immun. *71*, 904–909.

Dertli, E., Mayer, M.J., and Narbad, A. (2015). Impact of the exopolysaccharide layer on biofilms, adhesion and resistance to stress in Lactobacillus johnsonii FI9785. BMC Microbiol. *15*.

Dorken, G., Ferguson, G.P., French, C.E., and Poon, W.C.K. (2012). Aggregation by depletion attraction in cultures of bacteria producing exopolysaccharide. J. R. Soc. Interface *9*, 3490–3502.

Drulis-Kawa, Z., Majkowska-Skrobek, G., Maciejewska, B., Delattre, A.-S., and Lavigne, R. (2012). Learning from Bacteriophages - Advantages and Limitations of Phage and Phage-Encoded Protein Applications. Curr. Protein Pept. Sci. *13*, 699–722.

Elsholz, A.K.W., Wacker, S.A., and Losick, R. (2014). Self-regulation of exopolysaccharide production in Bacillus subtilis by a tyrosine kinase. Genes Dev. *28*, 1710–1720.

Forsberg, L.S., Choudhury, B., Leoff, C., Marston, C.K., Hoffmaster, A.R., Saile, E., Quinn, C.P., Kannenberg, E.L., and Carlson, R.W. (2011).

Secondary cell wall polysaccharides from Bacillus cereus strains G9241, 03BB87 and 03BB102 causing fatal pneumonia share similar glycosyl structures with the polysaccharides from Bacillus anthracis. Glycobiology *21*, 934–948.

Gao, S., Wu, H., Yu, X., Qian, L., and Gao, X. (2016). Swarming motility plays the major role in migration during tomato root colonization by Bacillus subtilis SWR01. Biol. Control *98*, 11–17.

Gao, T., Foulston, L., Chai, Y., Wang, Q., and Losick, R. (2015a). Alternative modes of biofilm formation by plant-associated *Bacillus cereus*. MicrobiologyOpen *4*, 452–464.

Gao, T., Foulston, L., Chai, Y., Wang, Q., and Losick, R. (2015b). Alternative modes of biofilm formation by plant-associated *Bacillus cereus*. MicrobiologyOpen *4*, 452–464.

Garcia-Betancur, J.C., Yepes, A., Schneider, J., and Lopez, D. (2012). Single-cell analysis of Bacillus subtilis biofilms using fluorescence microscopy and flow cytometry. J. Vis. Exp. JoVE.

Geisinger, E., and Isberg, R.R. (2015). Antibiotic Modulation of Capsular Exopolysaccharide and Virulence in Acinetobacter baumannii. PLoS Pathog. *11*.

Gibiansky, M.L., Hu, W., Dahmen, K.A., Shi, W., and Wong, G.C.L. (2013). Earthquake-like dynamics in Myxococcus xanthus social motility. Proc. Natl. Acad. Sci. U. S. A. *110*, 2330–2335.

Gupta, P., and Diwan, B. (2016). Bacterial Exopolysaccharide mediated heavy metal removal: A Review on biosynthesis, mechanism and remediation strategies. Biotechnol. Rep. *13*, 58–71.

Hidalgo-Cantabrana, C., Sánchez, B., Milani, C., Ventura, M., Margolles, A., and Ruas-Madiedo, P. (2014). Genomic Overview and Biological Functions of Exopolysaccharide Biosynthesis in Bifidobacterium spp. Appl. Environ. Microbiol. *80*, 9–18.

Horn, N., Wegmann, U., Dertli, E., Mulholland, F., Collins, S.R.A., Waldron, K.W., Bongaerts, R.J., Mayer, M.J., and Narbad, A. (2013). Spontaneous mutation reveals influence of exopolysaccharide on Lactobacillus johnsonii surface characteristics. PloS One *8*, e59957.

Houry, A., Gohar, M., Deschamps, J., Tischenko, E., Aymerich, S., Gruss, A., and Briandet, R. (2012). Bacterial swimmers that infiltrate and take over the biofilm matrix. Proc. Natl. Acad. Sci. U. S. A. *109*, 13088–13093.

Hu, W., Gibiansky, M.L., Wang, J., Wang, C., Lux, R., Li, Y., Wong, G.C.L., and Shi, W. (2016). Interplay between type IV pili activity and exopolysaccharides secretion controls motility patterns in single cells of Myxococcus xanthus. Sci. Rep. *6*.

Ionescu, M., and Belkin, S. (2009). Overproduction of Exopolysaccharides by an Escherichia coli K-12 rpoS Mutant in Response to Osmotic Stress. Appl. Environ. Microbiol. *75*, 483–492.

Irie, Y., Starkey, M., Edwards, A.N., Wozniak, D.J., Romeo, T., and Parsek, M.R. (2010). Pseudomonas aeruginosa biofilm matrix polysaccharide Psl is regulated transcriptionally by RpoS and post-transcriptionally by RsmA. Mol. Microbiol. *78*, 158–172.

Jeon, B., Muraoka, W., Scupham, A., and Zhang, Q. (2009). Roles of lipooligosaccharide and capsular polysaccharide in antimicrobial resistance and natural transformation of Campylobacter jejuni. J. Antimicrob. Chemother. *63*, 462–468.

Jung, Y.-G., Choi, J., Kim, S.-K., Lee, J.-H., and Kwon, S. (2015). Embedded Biofilm, a New Biofilm Model Based on the Embedded Growth of Bacteria. Appl. Environ. Microbiol. *81*, 211–219.

Labbate, M., Zhu, H., Thung, L., Bandara, R., Larsen, M.R., Willcox, M.D.P., Givskov, M., Rice, S.A., and Kjelleberg, S. (2007). Quorum-Sensing Regulation of Adhesion in Serratia marcescens MG1 Is Surface Dependent. J. Bacteriol. *189*, 2702–2711.

Li, Z., Hwang, S., and Bar-Peled, M. (2016). Discovery of a Unique Extracellular Polysaccharide in Members of the Pathogenic Bacillus That Can Co-form with Spores. J. Biol. Chem. *291*, 19051–19067.

Li, Z., Mukherjee, T., Bowler, K., Namdari, S., Snow, Z., Prestridge, S., Carlton, A., and Bar-Peled, M. (2017). A Four-gene Operon in Bacillus cereus Produces Two Rare Spore-decorating Sugars. J. Biol. Chem. jbc.M117.777417.

Limoli, D.H., Jones, C.J., and Wozniak, D.J. (2015). Bacterial Extracellular Polysaccharides in Biofilm Formation and Function. Microbiol. Spectr. *3*.

Liu, A., Mi, Z.-H., Zheng, X.-Y., Yu, Y., Su, H.-N., Chen, X.-L., Xie, B.-B., Zhou, B.-C., Zhang, Y.-Z., and Qin, Q.-L. (2016). Exopolysaccharides Play a Role in the Swarming of the Benthic Bacterium Pseudoalteromonas sp. SM9913. Front. Microbiol. *7*.

López, D., Vlamakis, H., and Kolter, R. (2010). Biofilms. Cold Spring Harb. Perspect. Biol. *2*.

Lu, A., Cho, K., Black, W.P., Duan, X.-Y., Lux, R., Yang, Z., Kaplan, H.B., Zusman, D.R., and Shi, W. (2005). Exopolysaccharide biosynthesis genes required for social motility in Myxococcus xanthus. Mol. Microbiol. *55*, 206–220.

Luckevich, M.D., and Beveridge, T.J. (1989). Characterization of a dynamic S layer on Bacillus thuringiensis. J. Bacteriol. *171*, 6656–6667.

McKinney, R.E. (1953). STAINING BACTERIAL POLYSACCHARIDES1. J. Bacteriol. *66*, 453–454.

Nguyen, H.D., Nguyen, Q.A., Ferreira, R.C., Ferreira, L.C.S., Tran, L.T., and Schumann, W. (2005). Construction of plasmid-based expression vectors for Bacillus subtilis exhibiting full structural stability. Plasmid *54*, 241–248.

Oh, E., and Jeon, B. (2015). Contribution of surface polysaccharides to the resistance of Campylobacter jejuni to antimicrobial phenolic compounds. J. Antibiot. (Tokyo) *68*, 591–593.

Okshevsky Mira, Louw Matilde Greve, Lamela Elena Otero, Nilsson Martin, Tolker-Nielsen Tim, and Meyer Rikke Louise (2017). A transposon mutant library of Bacillus cereus ATCC 10987 reveals novel genes required for biofilm formation and implicates motility as an important factor for pellicle-biofilm formation. MicrobiologyOpen *0*, e00552.

O'Toole, G.A., Pratt, L.A., Watnick, P.I., Newman, D.K., Weaver, V.B., and Kolter, R. (1999). Genetic approaches to study of biofilms. Methods Enzymol. *310*, 91–109.

Paynich, M.L., Jones-Burrage, S.E., and Knight, K.L. (2017). Exopolysaccharide fromBacillus subtilisInduces Anti-Inflammatory M2 Macrophages That Prevent T Cell-Mediated Disease. J. Immunol. Baltim. Md 1950 *198*, 2689–2698.

Rawls, J.F., Mahowald, M.A., Ley, R.E., and Gordon, J.I. (2006). Reciprocal Gut Microbiota Transplants from Zebrafish and Mice to Germ-free Recipients Reveal Host Habitat Selection. Cell *127*, 423–433.

Roach, D.R., Sjaarda, D.R., Castle, A.J., and Svircev, A.M. (2013). Host Exopolysaccharide Quantity and Composition Impact Erwinia amylovora Bacteriophage Pathogenesis. Appl. Environ. Microbiol. *79*, 3249–3256.

Roberson, E.B., and Firestone, M.K. (1992). Relationship between Desiccation and Exopolysaccharide Production in a Soil Pseudomonas sp. Appl. Environ. Microbiol. *58*, 1284–1291.

Römling, U., and Galperin, M.Y. (2015). Bacterial cellulose biosynthesis: diversity of operons, subunits, products and functions. Trends Microbiol. *23*, 545–557.

Roux, A., Beloin, C., and Ghigo, J.-M. (2005). Combined Inactivation and Expression Strategy To Study Gene Function under Physiological Conditions: Application to Identification of New Escherichia coli Adhesins. J. Bacteriol. *187*, 1001–1013.

Ryu, J.-H., and Beuchat, L.R. (2005). Biofilm Formation by Escherichia coli O157:H7 on Stainless Steel: Effect of Exopolysaccharide and Curli Production on Its Resistance to Chlorine. Appl. Environ. Microbiol. *71*, 247–254.

S. Bragadeeswaran (2011). Exopolysaccharide production by Bacillus cereus GU812900, a fouling marine bacterium. Afr. J. Microbiol. Res. *5*.

Schnider-Keel, U., Lejbølle, K.B., Baehler, E., Haas, D., and Keel, C. (2001). The sigma factor AlgU (AlgT) controls exopolysaccharide production and tolerance towards desiccation and osmotic stress in the biocontrol agent Pseudomonas fluorescens CHA0. Appl. Environ. Microbiol. *67*, 5683–5693.

Scholl, D., Adhya, S., and Merril, C. (2005). Escherichia coli K1's Capsule Is a Barrier to Bacteriophage T7. Appl. Environ. Microbiol. *71*, 4872–4874.

Semova, I., Carten, J.D., Stombaugh, J., Mackey, L.C., Knight, R., Farber, S.A., and Rawls, J.F. (2012). Microbiota Regulate Intestinal Absorption and Metabolism of Fatty Acids in the Zebrafish. Cell Host Microbe *12*, 277–288.

Shea, C., Nunley, J.W., Williamson, J.C., and Smith-Somerville, H.E. (1991). Comparison of the adhesion properties of Deleya marina and the exopolysaccharide-defective mutant strain DMR. Appl. Environ. Microbiol. *57*, 3107–3113.

Silva, V.O., Soares, L.O., Silva Júnior, A., Mantovani, H.C., Chang, Y.-F., and Moreira, M.A.S. (2014). Biofilm Formation on Biotic and Abiotic Surfaces in the Presence of Antimicrobials by Escherichia coli Isolates from Cases of Bovine Mastitis. Appl. Environ. Microbiol. *80*, 6136–6145.

Sims, I.M., Frese, S.A., Walter, J., Loach, D., Wilson, M., Appleyard, K., Eason, J., Livingston, M., Baird, M., Cook, G., et al. (2011). Structure and functions of exopolysaccharide produced by gut commensal Lactobacillus reuteri 100-23. ISME J. *5*, 1115.

Sorroche, F.G., Spesia, M.B., Zorreguieta, Á., and Giordano, W. (2012). A Positive Correlation between Bacterial Autoaggregation and Biofilm Formation in Native Sinorhizobium meliloti Isolates from Argentina. Appl. Environ. Microbiol. *78*, 4092–4101.

Sutherland, I.W. (2001). Exopolysaccharides in biofilms, flocs and related structures. Water Sci. Technol. J. Int. Assoc. Water Pollut. Res. *43*, 77–86.

Wang, C., Saito, M., Ogawa, M., and Yoshida, S. (2016). Colony types and virulence traits of Legionella feeleii determined by exopolysaccharide materials. FEMS Microbiol. Lett. *363*.

Whitfield, G.B., Marmont, L.S., and Howell, P.L. (2015). Enzymatic modifications of exopolysaccharides enhance bacterial persistence. Front. Microbiol. *6*.

Yang, H., Deng, J., Yuan, Y., Fan, D., Zhang, Y., Zhang, R., and Han, B. (2015). Two novel exopolysaccharides from Bacillus amyloliquefaciens C-1: antioxidation and effect on oxidative stress. Curr. Microbiol. *70*, 298–306.

Zegans, M.E., Wozniak, D., Griffin, E., Toutain-Kidd, C.M., Hammond, J.H., Garfoot, A., and Lam, J.S. (2012). Pseudomonas aeruginosa Exopolysaccharide Psl Promotes Resistance to the Biofilm Inhibitor Polysorbate 80. Antimicrob. Agents Chemother. *56*, 4112–4122.

CHAPTER VII

FINAL DISCUSSION

Multicellularity is a common feature in all bacteria species, which even cross the line of biological kingdoms. Fungus and algae can also assemble biofilms, and are able to form inter kingdom biofilms (Barranguet et al., 2005; Dutton et al., 2014; Fanning and Mitchell, 2012; García-Meza et al., 2005; Rajendran and Hu, 2016). This fact cannot be casual since such distributed strategy provides a plethora of benefits in terms of adhesion, colonization, competition, adaptation, resilience, virulence, defence, survival, cell differentiation, efficiency and genetic exchange (Jefferson, 2004; Watnick and Kolter, 2000). In the last four decades, studies on biofilms have captured most of the attention in the field of microbiology, because of the basic biological questions posted and their implications in public health (Dasgupta and Costerton, 1989; McCoy et al., 1981; Rittmann and McCarty, 1982). During these years, much knowledge has been accumulated about biofilm development, physiology, ecology and molecular biology, especially about selected bacterial species models like *E. coli,* the paradigm of pathogenic gram-negative bacteria, or *B. subtilis* a harmless specie in the gram-positive group (Lo et al., 2017; Mielich-Süss and Lopez, 2015; Tan et al., 2017). Although studies with model microbes have revealed the main guidelines of biofilm assembly, there are many specificities for each bacteria species, and also at a strain level (Blanchette-Cain et al., 2013; Borucki et al., 2003). Up to date, it has been described 2552 genus and around 14.000 species of bacteria, that gives an idea on how variable can be the biofilms in terms of structure, physical properties, regulation and functions associated to this physiological state.

The evolutionary distance between *B. cereus* and the closer model microbe *B. subtilis* can be evidenced in their ecology. *B. subtilis* lives as a saprophyte in the soil and in association with plants, while *B. cereus* is also a mammal pathogen and also lives in the gut of insects (Song et al., 2014). In terms of molecular differences, there are several structural and regulatory elements implicated in biofilm formation which also diverge: i) the EPS operon of *B. subtilis* show low similitude with the homologous region in *B. cereus* (Gao et al., 2015a); ii) the absence of the protein TapA, necessary for the amyloid fibre assembly in *B. subtilis* (Diehl et al., 2018; Romero et al., 2014), iii) the presence of two paralogous of TasA (Gao et al., 2015a); iv) the absence in *B. cereus* of the hydrophobic biofilm-coating protein BslA (Hobley et al., 2013); v) the lack of the regulatory subnetworks II and III controlled by SlrA and DegU (Vlamakis et al., 2013), and the gain of the pleiotropic regulator PlcR involved in virulence and biofilm (Gohar et al., 2008); vii) the absence in *B. cereus* of the lipoprotein Med associated to the kinase KinD phosphorylation activity, which triggers biofilm formation (Banse et al., 2011). All these differences evidence the necessity of reliable data to have a clear image of *B. cereus* biofilm development. On the general structural components of *B. cereus* biofilms, only eDNA had been studied in detail. This work state that this molecule is essential for biofilm formation (Vilain et al., 2006). The knowledge about protein and polysaccharide elements implicated in biofilms remains blurred as only detailed information about the closer taxonomically model *B. subtilis* was accessible to understand *B. cereus* biofilms.

A proteomic study was developed in early stages biofilms in comparison with planktonic cells of *B. cereus* DL5, however it was done using 2D electrophoresis, revealing only differences in some metabolic enzymes and in a regulator of stress/energy depletion (Oosthuizen et al., 2002). This technique is known to possess low sensitivity, and usually one visible dot masks a multitude of proteins, hiding potential differences. Deeper knowledge on biofilm formation of this bacterium species will let us understand better its behaviour, weaknesses and strengths, a very useful information to develop strategies to prevent, reduce or manage problems and threatens with origin in *B. cereus* biofilms. On the other hand, *B. cereus* lives in the soil as a saprophyte or in association with plants in the rhizosphere, supposing a dual concern as a reservoir of spores and vegetative cells and as a beneficial bacterium for plants, both situations related to biofilm formation (Bottone, 2010; Brillard and Lereclus, 2007).

During the development of this thesis, some studies appeared reporting clues on *B. cereus* biofilm formation. The confirmation that the homologue region in *B. cereus* to the EPS synthesis region in *B. subtilis* is not relevant for biofilm formation (Gao et al., 2015a) opened important questions about which is the exopolysaccharide that really works as a structural and adhesion element in biofilm. Besides, if that region is not involved in biofilm formation, what is the function of this genomic region codifying for genes involved in polysaccharide synthesis? A transposon mutant library using *Bacillus cereus* ATCC 10987 pointed out several genes with putative implication in biofilm formation (Okshevsky Mira et al., 2017). The implication in biofilm was assessed as the presence or

absence of pellicle and crystal violet for submerged biofilm, techniques which omit the effects that a gene deletion might have in biomass quantity, rheology, thickness, strength, morphology, and adhesion of the pellicle or the submerged biofilm. In the same way, positive deviations over biofilm formation would remain unnoticed.

Within the structural gaps in our knowledge of biofilm assembly in *B. cereus*, no study was focused on the protein components. In *B. subtilis* the signal peptidase SipW recognise the signal peptides at the N-terminal position of the proteins TasA and TapA, which are extruded and polymerize into fibres mainly made of TasA, working TapA as the anchoring protein to the cell surfaces (Romero et al., 2010, 2011). A search in *B. cereus* genome for orthologous to TasA and TapA yielded three genes with considered similarity to *tasA*, identified as *BC1279, BC1281* and *BC4868*, and also a homologue to *sipW* identified as *BC1278.* However, no gene was found with homology to *tapA.* As *BC1278 (sipW)* and *BC1279 (tasA)* genetic structure resembled the same operon in *B. subtilis,* and *BC1281 (calY)* is a duplication of *BC1279*, we launched the hypothesis of this region (*sipW*-TO-*claY)* to contribute to the protein component of biofilm of *B. cereus*. Bioinformatic analysis of the protein codified by *BC4868* (annotated as a metalloprotease) reveals: i) sequence similarity to TasA and CalY; ii) parallel pattern of secondary structure based on predictions with SOPMA software; and iii) putative amyloidogenic regions (Pasta 2.0). Although BC4868 would retain all the potential to behave as an amyloid protein polymerizing into fibrils, it should not be involved in biofilm structural fibres formation, a fact supported by two complementary

evidences: the expression is not under the control of the biofilm master regulator SinR (Fagerlund et al., 2014), and we did not observe changes in the level of expression of the gene either at transcriptomic or proteomic levels in biofilm associated cells. It would be interesting in future studies to dig into the ability of this protein to form other kind of amyloid structures; to assess if it has a dual role as a metalloprotease and amyloid; or even if it has a residual role in the final fibre formation on the biofilm protein fibres.

We initially focused on the role of the region *sipW*-TO-*calY* in biofilm formation (Chapter I). Single mutants in *sipW* resulted in a low ring-shape biomass in the air-liquid interface biofilm, which also was poorly adhered to the wall of the well and did not show fibres under transmission electron microscopy (TEM). On the other hand, mutants in *tasA* showed a bigger biofilm biomass but poorly adhered; and *calY* mutant showed a similar development of the biofilm but also poorly adhered, at least at later stages. Both *tasA* and *calY* mutants showed fibre formation under TEM visualization, although they were more abundant and thicker in *calY* mutant, suggesting a major contribution of TasA to fibre formation. These results also suggest that both proteins are involved in biofilm formation, given that adhesion is impaired in both *tasA* and *calY* mutants.

To answer the questions about the role of these proteins individually and clarify if other elements are playing an unnoticed role in fibre formation in *B. cereus*, a strain of *B. subtilis* lacking the *tapA* operon or only *tasA* were used for heterologous expression. These strains fail in

the formation of floating and wrinkly pellicles and binding of Congo red dye (CR) when added to the medium. Unexpectedly, none of them restored the phenotype, what led us to wonder if the little signal peptide differences would make each SipW orthologue to be specific over its cognate proteins. Certainly, the heterologous expression of *sipW-tasA* in a *tasA* mutant restored the pellicle formation, CR staining and fibre formation, although the wrinkled phenotype was not restored. Expression of *sipW-calY* in a *tasA* mutant resulted in the same effect, although the pellicle was considerably thinner. The heterologous expression of *B. cereus* genes in a full *sipW-tapA-tasA* mutant of *B. subtilis* suggested that TapA might be interacting with the proteins of *B. cereus* promoting their polymerization. Expression of *sipW-tasA* or *sipW-calY* was unsuccessful in promoting strong pellicle formation or CR staining, although fibres were observed in TEM in the case of *sipW-tasA*. Only the expression of the complete region *sipW*-TO-*calY* was able to completely restore the phenotypes in pellicle, wrinkles, CR and fibre observation in TEM. These results confirmed that this region is responsible for the synthesis of structural fibre formation in *B. cereus* biofilm. It also revealed that this amyloid system has evolved to a mode of action independent of an accessory protein, like TapA in *B. subtilis* for anchoring and polymerization (Romero et al., 2014). Although, within this region it is included the locus *BC1280*, annotated as a hypothetical protein and with unknown function. RT-PCR analysis showed that this gene was not expressed under our experimental conditions, a finding contrary to the results from RNAseq and iTRAQ which revealed that this gene was actually overexpressed in biofilm (Chapter V). Ongoing

research in our group is trying to find the accommodation to these contradictory findings. Bioinformatic analysis also revealed that this protein possesses even more amyloidogenic regions than TasA and CalY. In fact, mutants in *BC1280* show the same phenotype as mutants in the complete region or *sipW,* suggesting a role of this protein in fibre polymerization. The characterization of the proteins TasA and CalY shed light over its role on fibre formation, although the study of protein *BC1280* has not been included in this thesis.

We attempted the expression and purification of the proteins TasA and CalY from *E. coli* bacterial cultures, as is routinely done for protein characterization (Rosano and Ceccarelli, 2014) that also allowed us to do the *in vitro* study of the secondary structure, amyloid properties, and polymerization of both proteins TasA and CalY (Chapter II). The use of several bioinformatic tools together with the results from mutants in *B. cereus* and the heterologous expression of *tasA* and *calY* in *B. subtilis* suggested that these proteins probably possess amyloid properties. Both proteins showed a high percentage of unstructured amino acid sequence, regions with a tendency to turn into β-sheets secondary structures due to the internal interactions of the protein and with other units of TasA or CalY. This refolding happens in a similar way with the protein CsgA in the formation of the amyloid curli in *E. coli* (Van Gerven et al., 2015). The hypothesis of the amyloid properties of TasA and CalY were initially supported by the results on the Thioflavin T and Congo red spectrums of fluorescent emission and absorbance respectively of purified proteins, common probes used to determine amyloid properties (Girych et al., 2016).

Further biophysics finding obtained with ATR-FTIR and ECD demonstrated the enrichment in β-sheets secondary structures of polymerized proteins and in β-sheets (Cheatum et al., 2004; Greenfield, 2006). TEM imaging led us to suggest that both proteins purified from *E. coli* polymerize into fibres with different morphology: TasA is prone to form large fibres and CalY have a tendency to form highly brunched polymers and grids. In *B. subtilis*, the mixture of TapA and TasA results in faster polymerization kinetic than isolated TasA and in a higher fluorescent emission of the mixture, suggesting that the interaction of both proteins increase their amyloid folding pattern (Romero et al., 2014). The *in vitro* interaction of TasA and CalY at pH 6 in the presence of Congo red resulted in huge aggregations visible to eye and absent in each single protein homogenate, suggestive of similarities to TasA and TapA interactions. Contrary to this, the intensity of fluorescent emission of Thioflavin T of the mixtures was always between the values of single TasA or single CalY homogenates. The interaction was confirmed in TEM analysis, revealing that only a 10% of CalY induced in TasA a propensity to polymerize in a grid pattern. Besides, Dynamic Light Scattering (DLS) proved an accelerated polymerization progress of the mixture. Final confirmation of the collaborative role between TasA and CalY emerged with experiments *in vivo*, in which addition of both proteins to a mutant in *tasA* induced the formation of a big floating biofilm biomass. The polymerization process should be fine-tuned given that addition of these proteins to the wild type did not make any change to the biofilm development. In the light of the characteristics of a mutant in *tasA,* expressing more flagella and enhanced chaining, it might also

be answered why the addition of amyloidogenic material results in such huge biofilm biomass.

Both forms of polymerization in grids and fibre shapes are compatible biologically and may play a protective function. We have seen that both proteins can yield both polymerization typologies, TasA seems to be prone to form fibres and CalY to assemble grids. The local conditions in which *B. cereus* produce structural amyloids are difficult to determine and reproduce *in vitro*. Analysing images of *in vivo* fibres and those formed *in vitro*, it is strongly suggestive of the co-existence of both structures *in vivo* and similarity to those formed *in vitro* (Fig.1). Immuno-

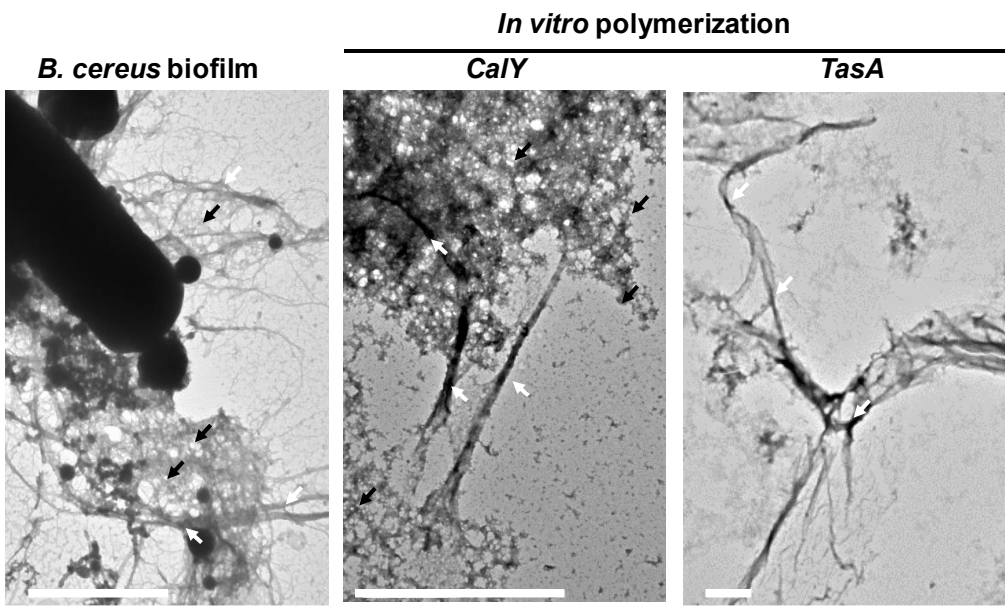

Figure 1. TEM images of *B. cereus* biofilm samples and TasA and CalY purified proteins after polymerization *in vitro*. White arrows indicate large fibres and black arrows indicate grid polymers. Bars equal 1µm.

gold labelling studies ongoing in our lab using antibodies raised against differential epitope of both proteins are trying to really determine whether these two structures are made of TasA, CalY or both.

Besides these structural proteins, the assembly of the biofilm is a complex multicellular program that implies radical changes in the lifestyle. Planktonic cells are swimmers and move responding to gradients of molecules which act as chemoattractant, like nutrients, or as chemo repellents, like toxic compounds (Eisenbach Michael, 2001; Pandey and Jain, 2002; Yamamoto et al., 1990). Sessile lifestyle requires dealing with the impossibility of moving to nutrients or fleeing from toxics, less energy consumption devoted to movement and a redirection of the metabolic flux to the assembly of the extracellular matrix. The gap in the knowledge about the physiological changes associated with the change of lifestyle led us to explore how *B. cereus* face the challenge to develop a sessile way of life. Firstly, we developed a methodology to efficiently separate biofilm and planktonic cells, avoiding the contamination with submerged biofilm individuals that might introduce noise or even mask differences between both populations. With the help of high-throughput techniques, we performed total mRNA sequencing and proteomic analysis using Isobaric Tag for Relative and Absolute Quantitation (iTRAQ) over both bacteria populations, and searched for differences reflective of their physiological state. Many of the genes with significant expression changes could be also detected in the proteomic analysis, in which the vast majority of the pattern of gene expression was confirmed.

Due to the mayor sensitivity and the advantages of reproducibility, transcriptomic analysis was our reference experiment, using the proteomic study as a tool to confirm the huge amount of entries obtained from the RNAseq (Łabaj and Kreil, 2016). In bacteria, transcription and translation are efficiently associated, although, mRNA half-life and protein recycling can alter the final protein quantities, giving a biased idea of the functional settings of bacteria (Gowrishankar and Harinarayanan, 2004; Kristoffersen et al., 2012). Nevertheless, other factors may affect the functionality of enzymes, which accurate activity needs to be assessed by metabolomic analysis.

The total number of genes with a change in the relative expression using a conservative threshold of log2 (fold change) >|2| arose to 1292 entries, representing the 23.5% of the total genes annotated in *B. cereus* ATCC1457 genome. This number gives an idea of the complexity of the changes suffered by planktonic cells when turns into biofilm inhabitants. It should have to be taken into account the cell differentiation occurring within a biofilm and that each population can display a different gene expression pattern. In this way, these analyses consider the average expression patterns for each gene and protein among the pull of individuals of biofilm and floating cells (Vlamakis et al., 2013). All the changes can be resumed in three groups which comprises: i) elements required to build the biofilm structure; ii) elements to attack competitors and to survive to competitor's attack; iii) and elements for bacterial-host interaction, which include attack and defense. The strategies used by *B. cereus* biofilm cells, usually address multiple advantages for several purposes. For instance,

exopolysaccharide works as adhesive material, serves as structural element, retains antimicrobial molecules and can protect cells against host attack (Nwodo et al., 2012). Production of all these elements suppose a change in the requirement of nutrients and energy, what is addressed redirecting the metabolic fluxes when a planktonic cell change to a sessile lifestyle.

Among the structural elements, we found several architectural changes. The bacterial cell wall plays an important role in bacterial physiology as a barrier that protects the cell. Furthermore, in a biofilm state, the cell wall is the basement platform to which exopolysaccharides and protein fibers are anchored. We found that *B. cereus* biofilm cells increase their cell wall thickness by 33.4%. We hypothesize that this strategy allows bacteria to support the physical forces that produce bacterial piling and those transmitted through the protein and polysaccharide anchored to the cell wall. The proteins TasA and CalY, as seen in chapter II, work also as adhesins. Apart from these elements, we also found the overexpression of collagen like proteins and collagen adhesion proteins, adhesins which had never been described before in *B. cereus,* but have been reported to play important roles in adhesion, aggregation, host colonization, persistence and biofilm formation in other species (Abranches et al., 2011; Miller et al., 2015; Tang et al., 2016; Zhao et al., 2015). About exopolysaccharides, a region that we called *eps1* was not overexpressed in biofilm cells, in accordance with previous results of mutants in this region, which did not show a biofilm phenotype (Gao et al., 2015b). The overexpression of the region named *eps2* and annotated as capsular polysaccharide biosynthesis suggested that this

region could be involved in biofilm formation, which was further confirmed and will be discussed forward. The third general component of extracellular matrix is the extracellular DNA. Several elements of the eDNA synthesis machinery were to be overexpressed in biofilm cells, especially at early stages of biofilm formation. In later stages, purines biosynthesis pathways remained active probably to support the synthesis of secondary messengers implicated in biofilm formation and bacteria-host interactions like ppGpp or C-di-GMP, c-GMP-AMP (Jenal et al., 2017).

In nature, biofilms are usually multispecific, cohabiting a multitude of different species in the same space (Elias and Banin, 2012; Yadav et al., 2017; Yang et al., 2011). *B. cereus* is a common inhabitant of the soil, the rhizosphere or the gut of animals, three niches also occupied by thousands of different species which compete for space and nutrients (Majed et al., 2016). Competition in these environments can be translated into a perpetual warfare that results in the deployment of attack and defense strategies. Biofilm cells of *B. cereus* were found to overexpress a pull of putative antimicrobials, including the already known thiocillin (Acker et al., 2009). We confirmed the major synthesis of this molecule in biofilm cells by mass spectrometry analysis, supporting the idea of biofilm attack mood against competitors. On the other hand, RNAseq revealed a wide strategy to survive the attack from competitors: i) overexpression of genes annotated as antimicrobial resistance genes; ii) enhancement of the rigidity of the cell membrane increasing its cardiolipin composition, what might confer resistance against surfactin (a surfactant produced by *B.* subtilis) or other

potassium leakers (Dubois-Brissonnet et al., 2016; Seydlová et al., 2013) ; iii) ROS antimicrobial mediated killing prevention strategy (Van Acker and Coenye, 2017), which includes overexpression of the complex I of the electron transport chain, downregulation of the complex II, downregulation of the TCA cycle, upregulation of the TCA cycle shunt, increase of the NAD^+ concentrations, overexpression of the ROS detoxification machinery and maintaining of a reduced environment; iv) the synthesis of the extracellular matrix, which sequesters antimicrobials by sorption, prevents their penetration into the cytoplasm or reduces their diffusion constant (Potera, 1999; Stewart, 2015; Tseng et al., 2013); v) increase of the cell wall thickness, which may provide an advantageous position against β-lactams antimicrobials (Bush, 2012). The expected overexpression of sporulation within the biofilm completes the survival strategies of biofilm cells, producing a subpopulation of resistant and adherent forms which can germinate in locations far from the original localization of the colony. In relation to sporulation, we found a time-controlled progression of the sporulation program, with an evident arrest at 72 h of biofilm development, controlled by reduced quantities of the regulator Spo0A, upregulation of the phosphatase of the active regulator SpoOA-P and upregulation of the sporulation inhibitor, comprising a complete pull of elements to control the sporulation arrest.

In the context of bacteria-host interactions, we found an outstanding overexpression of the attacking feature of planktonic cells, which overexpress almost the complete pull of toxins, oriented to accomplish a fast and efficient attack to the host. An example of the aggressiveness

that *B. cereus* may display, in a clinical case, only 13 h after ingestion of a salad dish contaminated with *B. cereus* was enough to kill a healthy patient and induce a grievous bodily harm condition to other members of the same family (Dierick et al., 2005). The vast majority of these virulence factors are downregulated in biofilm cells, with the only exception of hemolysin III, which is independent from PlcR regulation (Gohar et al., 2008). Internalization of *B. cereus* has been reported to happen in a low rate, suggesting that only a subpopulation acquires this strategy of invasion (Minnaard et al., 2004; Rolny et al., 2017). We also found that planktonic cells overexpress sphingomyelin phosphodiesterase and 1-phosphatidylinositol phosphodiesterase, two enzymes involved in liberation from the phagolysosome (Faulstich et al., 2015; Shivanna et al., 2015; Wei et al., 2005). On the other hand, biofilm cells are more prone to defend from the host attack, overexpressing beta-lysine acetyltransferase, which neutralize beta-lysine produced by platelets against gram-positive bacteria (Hamzeh-Cognasse et al., 2015), and several immune inhibitor precursors, which cleave the antibacterial humoral factors attacins and cecropins, produced by insects (Lövgren et al., 1990; Pflughoeft et al., 2014). All these findings yielded by the molecular analysis of biofilm and planktonic cells depict a detailed picture of all the processes implicated in biofilm formation, revealing that most of the changes are aimed to a strategy of attack and defence (Fig. 2). There is an especially remarkable result, the sophisticated and wide strategy of biofilm cells to prevent ROS damage. This might be a clue revealing the weakness of biofilms, pointing to a new target to design antimicrobial compounds

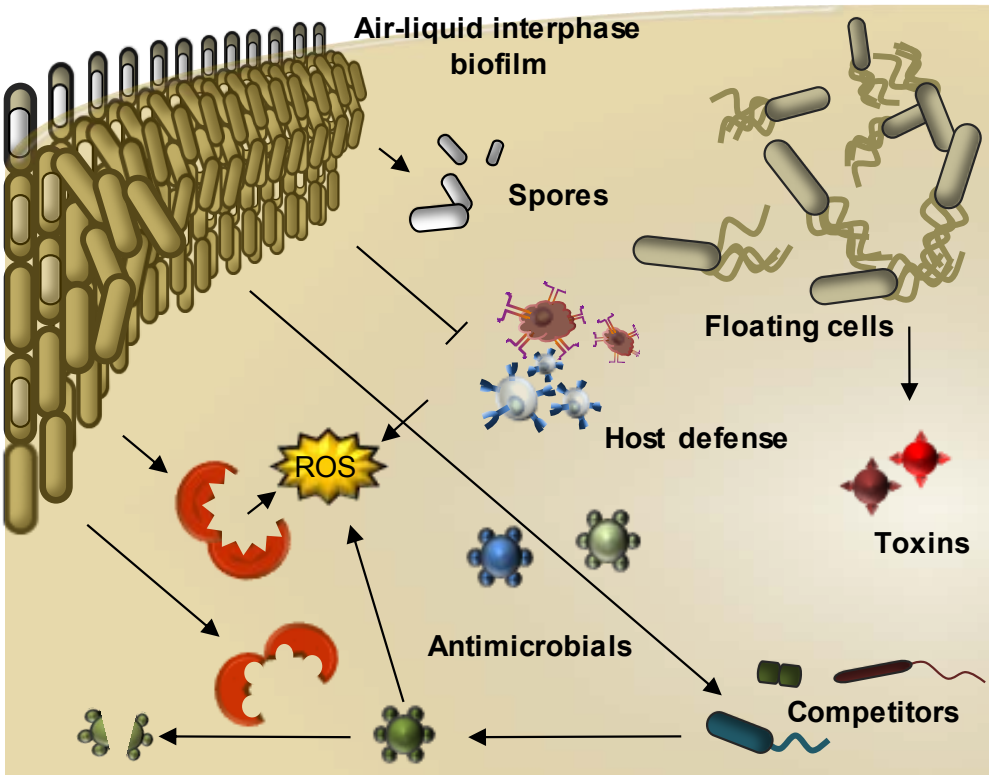

Figure 2. Scheme of the attack and defence strategies displayed by biofilm and planktonic cells of *b. cereus.*

or ROS enhancers combined with commercial antimicrobials and anti-biofilm agents.

The conclusions obtained from the comparison of transcriptomic and proteomic analysis of biofilm and planktonic cells should be considered on a background of total population of these two big groups of cell types. Within the biofilm, cell differentiation takes place. In this way, our findings correspond to the average of the total population without considering the specific profile of differentiated cells. In *B. subtilis* it has

been described up to date 9 cell types (van Gestel et al., 2015; Iber et al., 2006; Kovács, 2016). Within *B. cereus* group, this differentiation is not such clear although a study in *B. thuringiensis* reported four different cell types (Verplaetse et al., 2015).

Recently, two studies reported a pull of genes involved in biofilm formation. The approach used was the construction of transposon mutant libraries and further assessment of the biofilm formation (Okshevsky Mira et al., 2017). Unfortunately, as the author noticed, the library was incomplete, leaving behind putative genes with involvement in multicellularity. A limitation of this approach is the indirect effects caused by the absence of a protein which upon interaction with other proteins may have deleterious effects over basic functions, what might indirectly result in the absence of biofilm. Besides, it would remain hidden genes involved in functional structures or metabolic rearrangement which contribute to biofilm formation but are not determinant. In another study, transposon insertion mutagenesis was combined with RNAseq analysis of bacteria cultured either in normal or biofilm-inducing cultures supplemented with glycerol and magnesium. Some of the findings were metabolic rearrangements related to glycerol, what makes difficult to discern if the effect is caused by the biofilm physiological state or the culture condition (Yan et al., 2017). Despite the methodological differences between these studies and experiment limitations, we found coincident findings with our experiments regarding the enhanced purine metabolism and amino acid biosynthesis in biofilm cells. Results about exopolysaccharides of the three studies reveals the

high variability among strains in *B. cereus*, showing several regions with different implications in biofilm formation.

In parallel to the study at molecular level by the transcriptomic and proteomic analysis of biofilm, we did a microscopic developmental study of *B. cereus* biofilm (Chapter V). Submerging partially a glass cover slide in a liquid culture offered the possibility to study the air-liquid interface biofilm by microscopic observation. After culture inoculation, image analysis was done every two hours, leading us to describe the different steps of biofilm formation. The initial adhesion occurs vertically in one of the poles of the bacteria and in a reversible way, in a similar manner as described in other bacteria species (Caiazza and O'Toole, 2004; Sjollema et al., 2017). The adhesion progresses with the horizontal attachment to the surface, what occurs in the time-scale of minutes. The micro colony formation is achieved in two different ways, ordered or disordered group of bacteria leading to the same ordered biofilm. As biofilm grows, long bacterial cell chains anchored to the biofilm develop, floating in the liquid culture and to which planktonic cell clumps seem to be recruited, turning later into fully biofilm cells. Sporulation was mainly produced in the upper part of the biofilm, close to the air and more exposed to desiccation, recalling fruiting bodies produce on the top of the pellicle wrinkles of *B. subtilis* biofilm (Branda et al., 2001). Maturation of the biofilm after 72 h results in inner areas occupied by dead cells, a condition reported in other bacteria species that might be implicated in biofilm disassembly given that the inner biofilm population support the function of surface adhesion (Asally et al., 2012; Webb et al., 2003).

In the first chapter, it was reported a characteristic biofilm formation phenotype in the *tasA* mutant strain, showing an enhanced biofilm formation despite the lack of an important adhesin involved in biofilm. This suggests a deregulation in gene expression which affects other important elements in biofilm formation. To look for deregulated genes, we performed RNAseq and iTRAQ over biofilms of *tasA* mutant and wild type strains. The analysis showed that biofilm cells in the *tasA* mutant downregulate the expression of the cell division protein *ftsH*, a protein which mutation originates in *B. subtilis* a phenotype of growth in long chains (Deuerling et al., 1997; Wehrl et al., 2000). This result is in agreement to the microscopic developmental progression of *tasA* mutant, in which it was remarkable the high-filament phenotype while all the other growing characteristics remained visually unchanged. It was also revealed that biofilm cells of the *tasA* mutant were in an intermediate state between biofilm and planktonic cells of the wild type, what make them cells to retain flagellum structures or at least in a higher proportion. Flagellum has been reported to be essential for recruitment (Houry et al., 2010), a fact that combined with the higher cell chaining would result in increased recruitment of planktonic cell clumps. This hypothesis was supported by measuring the optical density of wild type and *tasA* in the spent medium, showing around a half of planktonic cell concentration in the mutant in *tasA*.

The study of the promoter activity gave also information on the timing at which *tasA* is expressed. TasA expression was not detected until micro colonies was formed, revealing that TasA is not involved in the initial adhesion stages of biofilm.

The study of the physiological changes and the molecular machinery implicated in *B. cereus* biofilm highlighted the gap in the study of the exopolysaccharides of *B. cereus*. In *B. subtilis*, the operon *epsA-O* involved in the synthesis of exopolysaccharides has been studied in detail, playing a determinant role in biofilm formation, as mutants in this region are unable to assemble a floating pellicle (Elsholz et al., 2014). In *B. cereus* there is a region with certain homology to this region (*eps1)* which had been reported non-essential to biofilm formation (Gao et al., 2015b). Results from RNAseq data comparing biofilm and planktonic cells confirmed that the expression pattern of this region does not significantly change during biofilm formation. However, other exopolysaccharide biosynthesis regions were upregulated: two of them are related with polysaccharides associated to the spore (Li et al., 2017); and the region *eps2* comprised of several genes annotated as capsular exopolysaccharide biosynthesis. The fact that *B. cereus ATCC14579* lacks of capsule lead us to hypothesize a role of this exopolysaccharide as a structural component in biofilm. Knock-out strains of *eps1, eps2* and double mutants were obtained to search for their roles. Biofilm assays in agar plates, liquid cultures without shaking and liquid culture with shaking confirmed our hypothesis of the role in biofilm of the *eps2* region. Mutants in *eps2* show a reduced biofilm formation in shaking cultures and reduced Congo Red staining in liquid cultures and agar plates. Microscopic observation of the planktonic medium also revealed that *eps2* is involved in the cohesion of planktonic clumps.

The study of the expression pattern of both regions claimed for a relatively stable expression of the *eps1* region, in contrast with *eps2,* which shows a drastic decrease expression at 37ºC. *B. cereus* is a human pathogen, usually with a very aggressive strategy when is in contact with the host, producing a plethora of toxins mainly by cells in a planktonic state as revealed by transcriptomic and proteomic analysis. Given that *B. cereus* has a low tendency to colonize structures of the host, our results are suggestive of avoidance of biofilm formation at 37ºC, with a preference for a planktonic state prone to attack the host.

In the context of multicellularity, several works propose that some exopolysaccharides play a role in bacterial motility (Berleman et al., 2016; Zhou Tianyi and Nan Beiyan, 2016). We performed swimming and swarming motility experiments, which revealed a negative effect of *eps2* in swimming and a positive role of *eps1* in swarming. In both experiments, double mutants showed a more enhanced phenotype than single mutants, suggesting certain degree of collaboration or synergy between both exopolysaccharides. An effect that was also patent in the results of the aggregation assay, revealing that the lack of any of them induce aggregation and sedimentation. This experiment suggests an equilibrium of charges between both exopolysaccharides which is broken in the absence of any of them. Furthermore, motility and aggregation assays reveals that despite *eps2* play a major role in biofilm formation, the basal expression results in functional structures affecting tasks developed typically by planktonic cells like swimming or have an effect in planktonic cells aggregation and sedimentation.

A principal-component study with strains characterized as non-pathogenic, food poisoning isolates and clinical strains, clustered the pathogenic strains in relation to adhesion and cytotoxicity (Kamar et al., 2013). Exopolysaccharides are also implicated in adhesion to biotic surfaces. Our findings suggest that *eps1* region lacks of detectable functionality in adhesion, in which seems to be highly involved the *eps2* given the results obtained using epithelial human cell cultures to assess adhesion of the mutant strains in *eps*'s regions in comparison with the wild type. These results were confirmed in experiments with zebra fish larvae. Cells lacking the *eps2* region showed a reduction in the time of transit through the gut as the proportion of larvae harbouring fluorescently labelled bacteria was reduced 24 h after bacterial feeding, a finding that led us to propose *eps2* as a factor contributing to colonization and pathogenicity. Given the high variability in EPSs even within the *B. cereus sensu stricto* strains (Okshevsky Mira et al., 2017; Yan et al., 2017), it would be interesting to investigate the relation of EPSs with the virulence of pathogenic strains.

As mentioned above, the molecular machinery of biofilm formation comprises several strategies to survive the attack from other competitors, usually antimicrobial compounds, and the extracellular matrix is conceived as a major contributor to this antimicrobial resistance. Extracellular DNA is a major factor in the protection against the activity of aminoglycosides, fluoroquinolones and antimicrobial peptides (Chiang et al., 2013; Johnson et al., 2013; Lewenza, 2013; Tetz et al., 2009). But also exopolysaccharides play an important role in antimicrobial resistance. Again in this purpose, we found

collaboration between both exopolysaccharides, given that higher sensitivities to certain antimicrobials were detected in the absence of both *eps´s* regions. The study of extracellular structures has been usually oriented to bacteria protection despite other functions in competence, signalling or social aspects (Dragoš et al., 2017). Further research in sensitivities derived from exopolysaccharides can be very advantageous in terms of optimal use of antibiotics against pathogen, especially against the recalcitrant biofilm. Antimicrobial resistance of pathogenic strains is an important public concern which is attracting the attention of the scientific community (Ventola, 2015). Although it was not the original aim of this work, we propose a new focus to develop new strategies to target pathogenic bacteria. In the same way as resistance to beta-lactam antibiotics was solved including in the preparation inhibitors of the enzyme which degrade the antimicrobial (Sánchez Navarro, 2005), it would be interesting to explore similar strategies including inducer of ROS or polysaccharide degradation.

This thesis aimed to fill some of the gaps in our knowledge of *B. cereus* biofilm formation, and also to the close related species that comprise the *B. cereus* group. Our results shed light over the protein and exopolysaccharide components of the extracellular matrix. Furthermore, we studied the differential molecular machinery implicated in the physiology of biofilm and planktonic populations. From the molecular aspect, a zoom out stopping in the microscopic development complete a multiscale work which started with the macroscopic biofilm development of *B. cereus*. Future studies will be necessary to answer questions on the molecular interactions of TasA and CalY, the accurate

role of *Bc1280*, the mechanism of action of accessory proteins involved in biofilm formation, the function of the hypothetical proteins involved in biofilm formation, the regulatory role of CalY, or the sugar composition of the EPS1 and EPS2. Having this information in our hands, our knowledge will be boosted in terms of the understanding of *B. cereus* life cycle and, therefore, critical point and factors potentially targetable to reduce or eliminate biofilms.

REFERENCES

Abranches, J., Miller, J.H., Martinez, A.R., Simpson-Haidaris, P.J., Burne, R.A., and Lemos, J.A. (2011). The Collagen-Binding Protein Cnm Is Required for Streptococcus mutans Adherence to and Intracellular Invasion of Human Coronary Artery Endothelial Cells. Infect. Immun. *79*, 2277–2284.

Acker, M.G., Bowers, A.A., and Walsh, C.T. (2009). Generation of thiocillin variants by prepeptide gene replacement and in vivo processing by Bacillus cereus. J. Am. Chem. Soc. *131*, 17563–17565.

Asally, M., Kittisopikul, M., Rué, P., Du, Y., Hu, Z., Çağatay, T., Robinson, A.B., Lu, H., Garcia-Ojalvo, J., and Süel, G.M. (2012). Localized cell death focuses mechanical forces during 3D patterning in a biofilm. Proc. Natl. Acad. Sci. *109*, 18891–18896.

Banse, A.V., Hobbs, E.C., and Losick, R. (2011). Phosphorylation of Spo0A by the Histidine Kinase KinD Requires the Lipoprotein Med in Bacillus subtilis ▿. J. Bacteriol. *193*, 3949–3955.

Barranguet, C., Veuger, B., Beusekom, S.A.M.V., Marvan, P., Sinke, J.J., and Admiraal, W. (2005). Divergent composition of algal-bacterial biofilms developing under various external factors. Eur. J. Phycol. *40*, 1–8.

Berleman, J.E., Zemla, M., Remis, J.P., Liu, H., Davis, A.E., Worth, A.N., West, Z., Zhang, A., Park, H., Bosneaga, E., et al. (2016). Exopolysaccharide microchannels direct bacterial motility and organize multicellular behavior. ISME J. *10*, 2620–2632.

Blanchette-Cain, K., Hinojosa, C.A., Babu, R.A.S., Lizcano, A., Gonzalez-Juarbe, N., Munoz-Almagro, C., Sanchez, C.J., Bergman, M.A., and Orihuela, C.J. (2013). Streptococcus pneumoniae Biofilm Formation Is Strain Dependent, Multifactorial, and Associated with Reduced Invasiveness and Immunoreactivity during Colonization. MBio *4*, e00745-13.

Borucki, M.K., Peppin, J.D., White, D., Loge, F., and Call, D.R. (2003). Variation in Biofilm Formation among Strains of Listeria monocytogenes. Appl. Environ. Microbiol. *69*, 7336–7342.

Bottone, E.J. (2010). Bacillus cereus, a volatile human pathogen. Clin. Microbiol. Rev. *23*, 382–398.

Branda, S.S., Gonzalez-Pastor, J.E., Ben-Yehuda, S., Losick, R., and Kolter, R. (2001). Fruiting body formation by Bacillus subtilis. Proc. Natl. Acad. Sci. *98*, 11621–11626.

Brillard, J., and Lereclus, D. (2007). Characterization of a small PlcR-regulated gene co-expressed with cereolysin O. BMC Microbiol. *7*, 52.

Bush, K. (2012). Antimicrobial agents targeting bacterial cell walls and cell membranes. Rev. Sci. Tech. Int. Off. Epizoot. *31*, 43–56.

Caiazza, N.C., and O'Toole, G.A. (2004). SadB is required for the transition from reversible to irreversible attachment during biofilm formation by Pseudomonas aeruginosa PA14. J. Bacteriol. *186*, 4476–4485.

Cheatum, C.M., Tokmakoff, A., and Knoester, J. (2004). Signatures of beta-sheet secondary structures in linear and two-dimensional infrared spectroscopy. J. Chem. Phys. *120*, 8201–8215.

Chiang, W.-C., Nilsson, M., Jensen, P.O., Hoiby, N., Nielsen, T.E., Givskov, M., and Tolker-Nielsen, T. (2013). Extracellular DNA Shields against Aminoglycosides in Pseudomonas aeruginosa Biofilms. Antimicrob. Agents Chemother. *57*, 2352–2361.

Dasgupta, M.K., and Costerton, J.W. (1989). Significance of biofilm-adherent bacterial microcolonies on Tenckhoff catheters of CAPD patients. Blood Purif. *7*, 144–155.

Deuerling, E., Mogk, A., Richter, C., Purucker, M., and Schumann, W. (1997). The ftsH gene of Bacillus subtilis is involved in major cellular processes such as sporulation, stress adaptation and secretion. Mol. Microbiol. *23*, 921–933.

Diehl, A., Roske, Y., Ball, L., Chowdhury, A., Hiller, M., Molière, N., Kramer, R., Stöppler, D., Worth, C.L., Schlegel, B., et al. (2018). Structural changes of TasA in biofilm formation of Bacillus subtilis. Proc. Natl. Acad. Sci. 201718102.

Dierick, K., Van Coillie, E., Swiecicka, I., Meyfroidt, G., Devlieger, H., Meulemans, A., Hoedemaekers, G., Fourie, L., Heyndrickx, M., and Mahillon, J. (2005). Fatal Family Outbreak of Bacillus cereus-Associated Food Poisoning. J. Clin. Microbiol. *43*, 4277–4279.

Dragoš, A., Kovács, Á.T., and Claessen, D. (2017). The Role of Functional Amyloids in Multicellular Growth and Development of Gram-Positive Bacteria. Biomolecules *7*.

Dubois-Brissonnet, F., Trotier, E., and Briandet, R. (2016). The Biofilm Lifestyle Involves an Increase in Bacterial Membrane Saturated Fatty Acids. Front. Microbiol. *7*.

Dutton, L.C., Nobbs, A.H., Jepson, K., Jepson, M.A., Vickerman, M.M., Alawfi, S.A., Munro, C.A., Lamont, R.J., and Jenkinson, H.F. (2014). O-Mannosylation in Candida albicans Enables Development of Interkingdom Biofilm Communities. MBio *5*, e00911-14.

Eisenbach Michael (2001). Bacterial Chemotaxis. ELS.

Elias, S., and Banin, E. (2012). Multi-species biofilms: living with friendly neighbors. FEMS Microbiol. Rev. *36*, 990–1004.

Elsholz, A.K.W., Wacker, S.A., and Losick, R. (2014). Self-regulation of exopolysaccharide production in Bacillus subtilis by a tyrosine kinase. Genes Dev. *28*, 1710–1720.

Fagerlund, A., Dubois, T., Økstad, O.-A., Verplaetse, E., Gilois, N., Bennaceur, I., Perchat, S., Gominet, M., Aymerich, S., Kolstø, A.-B., et al. (2014). SinR Controls Enterotoxin Expression in Bacillus thuringiensis Biofilms. PLoS ONE *9*.

Fanning, S., and Mitchell, A.P. (2012). Fungal Biofilms. PLOS Pathog. *8*, e1002585.

Faulstich, M., Hagen, F., Avota, E., Kozjak-Pavlovic, V., Winkler, A.-C., Xian, Y., Schneider-Schaulies, S., and Rudel, T. (2015). Neutral sphingomyelinase 2 is a key factor for PorB-dependent invasion of Neisseria gonorrhoeae. Cell. Microbiol. *17*, 241–253.

Gao, T., Foulston, L., Chai, Y., Wang, Q., and Losick, R. (2015a). Alternative modes of biofilm formation by plant-associated *Bacillus cereus*. MicrobiologyOpen *4*, 452–464.

Gao, T., Foulston, L., Chai, Y., Wang, Q., and Losick, R. (2015b). Alternative modes of biofilm formation by plant-associated *Bacillus cereus*. MicrobiologyOpen *4*, 452–464.

García-Meza, J.V., Barrangue, C., and Admiraal, W. (2005). Biofilm formation by algae as a mechanism for surviving on mine tailings. Environ. Toxicol. Chem. *24*, 573–581.

van Gestel, J., Vlamakis, H., and Kolter, R. (2015). From cell differentiation to cell collectives: Bacillus subtilis uses division of labor to migrate. PLoS Biol. *13*, e1002141.

Girych, M., Gorbenko, G., Maliyov, I., Trusova, V., Mizuguchi, C., Saito, H., and Kinnunen, P. (2016). Combined thioflavin T-Congo red fluorescence assay for amyloid fibril detection. Methods Appl. Fluoresc. *4*, 034010.

Gohar, M., Faegri, K., Perchat, S., Ravnum, S., Økstad, O.A., Gominet, M., Kolstø, A.-B., and Lereclus, D. (2008). The PlcR Virulence Regulon of Bacillus cereus. PLoS ONE *3*, e2793.

Gowrishankar, J., and Harinarayanan, R. (2004). Why is transcription coupled to translation in bacteria? Mol. Microbiol. *54*, 598–603.

Greenfield, N.J. (2006). Using circular dichroism spectra to estimate protein secondary structure. Nat. Protoc. *1*, 2876–2890.

Hamzeh-Cognasse, H., Damien, P., Chabert, A., Pozzetto, B., Cognasse, F., and Garraud, O. (2015). Platelets and Infections – Complex Interactions with Bacteria. Front. Immunol. *6*.

Hobley, L., Ostrowski, A., Rao, F.V., Bromley, K.M., Porter, M., Prescott, A.R., MacPhee, C.E., van Aalten, D.M.F., and Stanley-Wall, N.R. (2013). BslA is a self-assembling bacterial hydrophobin that coats the Bacillus subtilis biofilm. Proc. Natl. Acad. Sci. U. S. A. *110*, 13600–13605.

Houry, A., Briandet, R., Aymerich, S., and Gohar, M. (2010). Involvement of motility and flagella in Bacillus cereus biofilm formation. Microbiology *156*, 1009–1018.

Iber, D., Clarkson, J., Yudkin, M.D., and Campbell, I.D. (2006). The mechanism of cell differentiation in Bacillus subtilis. Nature *441*, 371–374.

Jefferson, K.K. (2004). What drives bacteria to produce a biofilm? FEMS Microbiol. Lett. *236*, 163–173.

Jenal, U., Reinders, A., and Lori, C. (2017). Cyclic di-GMP: second messenger extraordinaire. Nat. Rev. Microbiol. *15*, 271–284.

Johnson, L., Horsman, S.R., Charron-Mazenod, L., Turnbull, A.L., Mulcahy, H., Surette, M.G., and Lewenza, S. (2013). Extracellular DNA-induced antimicrobial peptide resistance in Salmonella enterica serovar Typhimurium. BMC Microbiol. *13*, 115.

Kamar, R., Gohar, M., Jéhanno, I., Réjasse, A., Kallassy, M., Lereclus, D., Sanchis, V., and Ramarao, N. (2013). Pathogenic Potential of Bacillus cereus Strains as Revealed by Phenotypic Analysis. J. Clin. Microbiol. *51*, 320–323.

Kovács, Á.T. (2016). Bacterial differentiation via gradual activation of global regulators. Curr. Genet. *62*, 125–128.

Kristoffersen, S.M., Haase, C., Weil, M.R., Passalacqua, K.D., Niazi, F., Hutchison, S.K., Desany, B., Kolstø, A.-B., Tourasse, N.J., Read, T.D., et al. (2012). Global mRNA decay analysis at single nucleotide resolution reveals segmental and positional degradation patterns in a Gram-positive bacterium. Genome Biol. *13*, R30.

Łabaj, P.P., and Kreil, D.P. (2016). Sensitivity, specificity, and reproducibility of RNA-Seq differential expression calls. Biol. Direct *11*.

Lewenza, S. (2013). Extracellular DNA-induced antimicrobial peptide resistance mechanisms in Pseudomonas aeruginosa. Front. Microbiol. *4*.

Li, Z., Mukherjee, T., Bowler, K., Namdari, S., Snow, Z., Prestridge, S., Carlton, A., and Bar-Peled, M. (2017). A Four-gene Operon in Bacillus cereus Produces Two Rare Spore-decorating Sugars. J. Biol. Chem. jbc.M117.777417.

Lo, A.W., Moriel, D.G., Phan, M.-D., Schulz, B.L., Kidd, T.J., Beatson, S.A., and Schembri, M.A. (2017). “Omic” Approaches to Study Uropathogenic Escherichia coli Virulence. Trends Microbiol. *25*, 729–740.

Lövgren, A., Zhang, M., Engström, A., Dalhammar, G., and Landén, R. (1990). Molecular characterization of immune inhibitor A, a secreted virulence protease from Bacillus thuringiensis. Mol. Microbiol. *4*, 2137–2146.

Majed, R., Faille, C., Kallassy, M., and Gohar, M. (2016). Bacillus cereus Biofilms—Same, Only Different. Front. Microbiol. *7*.

McCoy, W.F., Bryers, J.D., Robbins, J., and Costerton, J.W. (1981). Observations of fouling biofilm formation. Can. J. Microbiol. *27*, 910–917.

Mielich-Süss, B., and Lopez, D. (2015). Molecular mechanisms involved in Bacillus subtilis biofilm formation. Environ. Microbiol. *17*, 555–565.

Miller, J.H., Avilés-Reyes, A., Scott-Anne, K., Gregoire, S., Watson, G.E., Sampson, E., Progulske-Fox, A., Koo, H., Bowen, W.H., Lemos, J.A., et al. (2015). The Collagen Binding Protein Cnm Contributes to Oral Colonization and Cariogenicity of Streptococcus mutans OMZ175. Infect. Immun. *83*, 2001–2010.

Minnaard, J., Lievin-Le Moal, V., Coconnier, M.-H., Servin, A.L., and Perez, P.F. (2004). Disassembly of F-Actin Cytoskeleton after Interaction of Bacillus cereus with Fully Differentiated Human Intestinal Caco-2 Cells. Infect. Immun. *72*, 3106–3112.

Nwodo, U.U., Green, E., and Okoh, A.I. (2012). Bacterial Exopolysaccharides: Functionality and Prospects. Int. J. Mol. Sci. *13*, 14002–14015.

Okshevsky Mira, Louw Matilde Greve, Lamela Elena Otero, Nilsson Martin, Tolker-Nielsen Tim, and Meyer Rikke Louise (2017). A transposon mutant library of Bacillus cereus ATCC 10987 reveals novel genes required for biofilm formation and implicates motility as an important factor for pellicle-biofilm formation. MicrobiologyOpen *0*, e00552.

Oosthuizen, M.C., Steyn, B., Theron, J., Cosette, P., Lindsay, D., von Holy, A., and Brözel, V.S. (2002). Proteomic Analysis Reveals Differential Protein Expression by Bacillus cereus during Biofilm Formation. Appl. Environ. Microbiol. *68*, 2770–2780.

Pandey, G., and Jain, R.K. (2002). Bacterial Chemotaxis toward Environmental Pollutants: Role in Bioremediation. Appl. Environ. Microbiol. *68*, 5789–5795.

Pflughoeft, K.J., Swick, M.C., Engler, D.A., Yeo, H.-J., and Koehler, T.M. (2014). Modulation of the Bacillus anthracis Secretome by the Immune Inhibitor A1 Protease. J. Bacteriol. *196*, 424–435.

Potera, C. (1999). Forging a Link Between Biofilms and Disease. Science *283*, 1837–1839.

Rajendran, A., and Hu, B. (2016). Mycoalgae biofilm: development of a novel platform technology using algae and fungal cultures. Biotechnol. Biofuels *9*, 112.

Rittmann, B.E., and McCarty, P.L. (1982). Model of steady-state-biofilm kinetics. Biotechnol. Bioeng. *24*, 2291.

Rolny, I.S., Racedo, S.M., and Pérez, P.F. (2017). Fate of Bacillus cereus within phagocytic cells. Int. Microbiol. Off. J. Span. Soc. Microbiol. *20*, 170–177.

Romero, D., Aguilar, C., Losick, R., and Kolter, R. (2010). Amyloid fibers provide structural integrity to Bacillus subtilis biofilms. Proc. Natl. Acad. Sci. *107*, 2230–2234.

Romero, D., Vlamakis, H., Losick, R., and Kolter, R. (2011). An Accessory Protein Required for Anchoring and Assembly of Amyloid Fibers in B. subtilis Biofilms. Mol. Microbiol. *80*, 1155–1168.

Romero, D., Vlamakis, H., Losick, R., and Kolter, R. (2014). Functional analysis of the accessory protein TapA in Bacillus subtilis amyloid fiber assembly. J. Bacteriol. *196*, 1505–1513.

Rosano, G.L., and Ceccarelli, E.A. (2014). Recombinant protein expression in Escherichia coli: advances and challenges. Front. Microbiol. *5*.

Sánchez Navarro, A. (2005). New formulations of amoxicillin/clavulanic acid: a pharmacokinetic and pharmacodynamic review. Clin. Pharmacokinet. *44*, 1097–1115.

Seydlová, G., Fišer, R., Čabala, R., Kozlík, P., Svobodová, J., and Pátek, M. (2013). Surfactin production enhances the level of cardiolipin in the cytoplasmic membrane of Bacillus subtilis. Biochim. Biophys. Acta BBA - Biomembr. *1828*, 2370–2378.

Shivanna, V., Kim, Y., and Chang, K.-O. (2015). Ceramide formation mediated by acid sphingomyelinase facilitates endosomal escape of caliciviruses. Virology *483*, 218–228.

Sjollema, J., van der Mei, H.C., Hall, C.L., Peterson, B.W., de Vries, J., Song, L., Jong, E.D. de, Busscher, H.J., and Swartjes, J.J.T.M. (2017). Detachment and successive re-attachment of multiple, reversibly-binding tethers result in irreversible bacterial adhesion to surfaces. Sci. Rep. *7*, 4369.

Song, F., Peng, Q., Brillard, J., Lereclus, D., and Nielsen-LeRoux, C. (2014). An insect gut environment reveals the induction of a new sugar-phosphate sensor system in Bacillus cereus. Gut Microbes *5*, 58–63.

Stewart, P.S. (2015). Antimicrobial Tolerance in Biofilms. Microbiol. Spectr. *3*.

Tan, C.H., Lee, K.W.K., Burmølle, M., Kjelleberg, S., and Rice, S.A. (2017). All together now: experimental multispecies biofilm model systems. Environ. Microbiol. *19*, 42–53.

Tang, Q., Yin, K., Qian, H., Zhao, Y., Wang, W., Chou, S.-H., Fu, Y., and He, J. (2016). Cyclic di-GMP contributes to adaption and virulence of Bacillus thuringiensis through a riboswitch-regulated collagen adhesion protein. Sci. Rep. *6*, 28807.

Tetz, G.V., Artemenko, N.K., and Tetz, V.V. (2009). Effect of DNase and Antibiotics on Biofilm Characteristics. Antimicrob. Agents Chemother. *53*, 1204–1209.

Toyofuku, M., Inaba, T., Kiyokawa, T., Obana, N., Yawata, Y., and Nomura, N. (2016). Environmental factors that shape biofilm formation. Biosci. Biotechnol. Biochem. *80*, 7–12.

Tseng, B.S., Zhang, W., Harrison, J.J., Quach, T.P., Song, J.L., Penterman, J., Singh, P.K., Chopp, D.L., Packman, A.I., and Parsek, M.R. (2013). The extracellular matrix protects Pseudomonas aeruginosa biofilms by limiting the penetration of tobramycin. Environ. Microbiol. *15*, 2865–2878.

Van Acker, H., and Coenye, T. (2017). The Role of Reactive Oxygen Species in Antibiotic-Mediated Killing of Bacteria. Trends Microbiol. *25*, 456–466.

Van Gerven, N., Klein, R.D., Hultgren, S.J., and Remaut, H. (2015). Bacterial amyloid formation: structural insights into curli biogensis. Trends Microbiol. *23*, 693–706.

Ventola, C.L. (2015). The Antibiotic Resistance Crisis. Pharm. Ther. *40*, 277–283.

Verplaetse, E., Slamti, L., Gohar, M., and Lereclus, D. (2015). Cell Differentiation in a Bacillus thuringiensis Population during Planktonic Growth, Biofilm Formation, and Host Infection. MBio *6*, e00138-00115.

Vilain, S., Luo, Y., Hildreth, M.B., and Brozel, V.S. (2006). Analysis of the Life Cycle of the Soil Saprophyte Bacillus cereus in Liquid Soil Extract and in Soil. Appl. Environ. Microbiol. *72*, 4970–4977.

Vlamakis, H., Chai, Y., Beauregard, P., Losick, R., and Kolter, R. (2013). Sticking together: building a biofilm the Bacillus subtilis way. Nat. Rev. Microbiol. *11*, 157–168.

Watnick, P., and Kolter, R. (2000). Biofilm, City of Microbes. J. Bacteriol. *182*, 2675–2679.

Webb, J.S., Thompson, L.S., James, S., Charlton, T., Tolker-Nielsen, T., Koch, B., Givskov, M., and Kjelleberg, S. (2003). Cell death in Pseudomonas aeruginosa biofilm development. J. Bacteriol. *185*, 4585–4592.

Wehrl, W., Niederweis, M., and Schumann, W. (2000). The FtsH protein accumulates at the septum of Bacillus subtilis during cell division and sporulation. J. Bacteriol. *182*, 3870–3873.

Wei, Z., Zenewicz, L.A., and Goldfine, H. (2005). Listeria monocytogenes phosphatidylinositol-specific phospholipase C has evolved for virulence by greatly reduced activity on GPI anchors. Proc. Natl. Acad. Sci. *102*, 12927–12931.

Yadav, M.K., Chae, S.-W., Go, Y.Y., Im, G.J., and Song, J.-J. (2017). In vitro Multi-Species Biofilms of Methicillin-Resistant Staphylococcus aureus and Pseudomonas aeruginosa and Their Host Interaction during In vivo Colonization of an Otitis Media Rat Model. Front. Cell. Infect. Microbiol. *7*.

Yamamoto, K., Macnab, R.M., and Imae, Y. (1990). Repellent response functions of the Trg and Tap chemoreceptors of Escherichia coli. J. Bacteriol. *172*, 383–388.

Yan, F., Yu, Y., Gozzi, K., Chen, Y., Guo, J., and Chai, Y. (2017). Genome-Wide Investigation of Biofilm Formation in Bacillus cereus. Appl. Environ. Microbiol. *83*.

Yang, L., Liu, Y., Wu, H., Høiby, N., Molin, S., and Song, Z. (2011). Current understanding of multi-species biofilms. Int. J. Oral Sci. *3*, 74–81.

Zhao, X., Wang, Y., Shang, Q., Li, Y., Hao, H., Zhang, Y., Guo, Z., Yang, G., Xie, Z., and Wang, R. (2015). Collagen-Like Proteins (ClpA, ClpB, ClpC, and ClpD) Are Required for Biofilm Formation and Adhesion to Plant Roots by Bacillus amyloliquefaciens FZB42. PLOS ONE *10*, e0117414.

Zhou Tianyi, and Nan Beiyan (2016). Exopolysaccharides promote Myxococcus xanthus social motility by inhibiting cellular reversals. Mol. Microbiol. *103*, 729–743.

VIII

THESIS CONCLUSIONS

Conclusions:

1. The genomic region containing the locus *sipW*, *tasA* and *calY,* orthologous to the *tapA* operon in the closely related species *B. subtilis*, is involved in the formation of structural fibres and adhesion of *B. cereus* biofilm to abiotic surfaces.

2. The proteins TasA and CalY expressed heterologously in *E. coli* retain biochemical and morphological features reminiscent of amyloid proteins. TasA shows a tendency to polymerize into fibres, while CalY is prone to produce a grid pattern. The combination of the two proteins accelerates the kinetic of polymerization and modifies the fibrillation pattern, a cross seeding activity also distinctive of other amyloid proteins.

3. *B. cereus* biofilm cells undergo a plethora of anatomical and structural changes, which involve cell wall reinforcement, enhanced membrane rigidity, and the assembly of an extracellular matrix. As a consequence of a sessile lifestyle, biofilms cells are reprogramed to defend from external aggressions, while floating cells are intrinsically aimed at targeting host cells.

4. The developmental program of the biofilm of *B. cereus* is based in the formation of floating cell chains from the initially attached biomass to the surface, which seems to be in charge of the recruitment of planktonic cell clumps. The study of the pattern of expression of TasA using transcriptional fusion and fluorescence microscopy indicates that TasA is not involved in the initial stages of attachment to surfaces but

in the subsequent steps of the development of the biofilm. Indeed, TasA seems to play a mild positive regulatory role over most of the physiological changes associated to biofilm cells, indicative of the tight control *B. cereus* exerts on the expression and assembly of this important protein component of the extracellular matrix.

6. The two genomic regions identified in this study and apparently implicated in the production of exopolysaccharides are functionally complementary to the multicellularity of *B. cereus*. While the *eps1* is more relevant for social motility, the exopolysaccharide region *eps2* is involved in biofilm formation, clumping and adhesion to human epithelial cells and zebrafish intestine. The role of the exopolysaccharides goes beyond the multicellular behaviour as the presence or the absence of any of these genetic regions affect the sensitivity to antimicrobials.

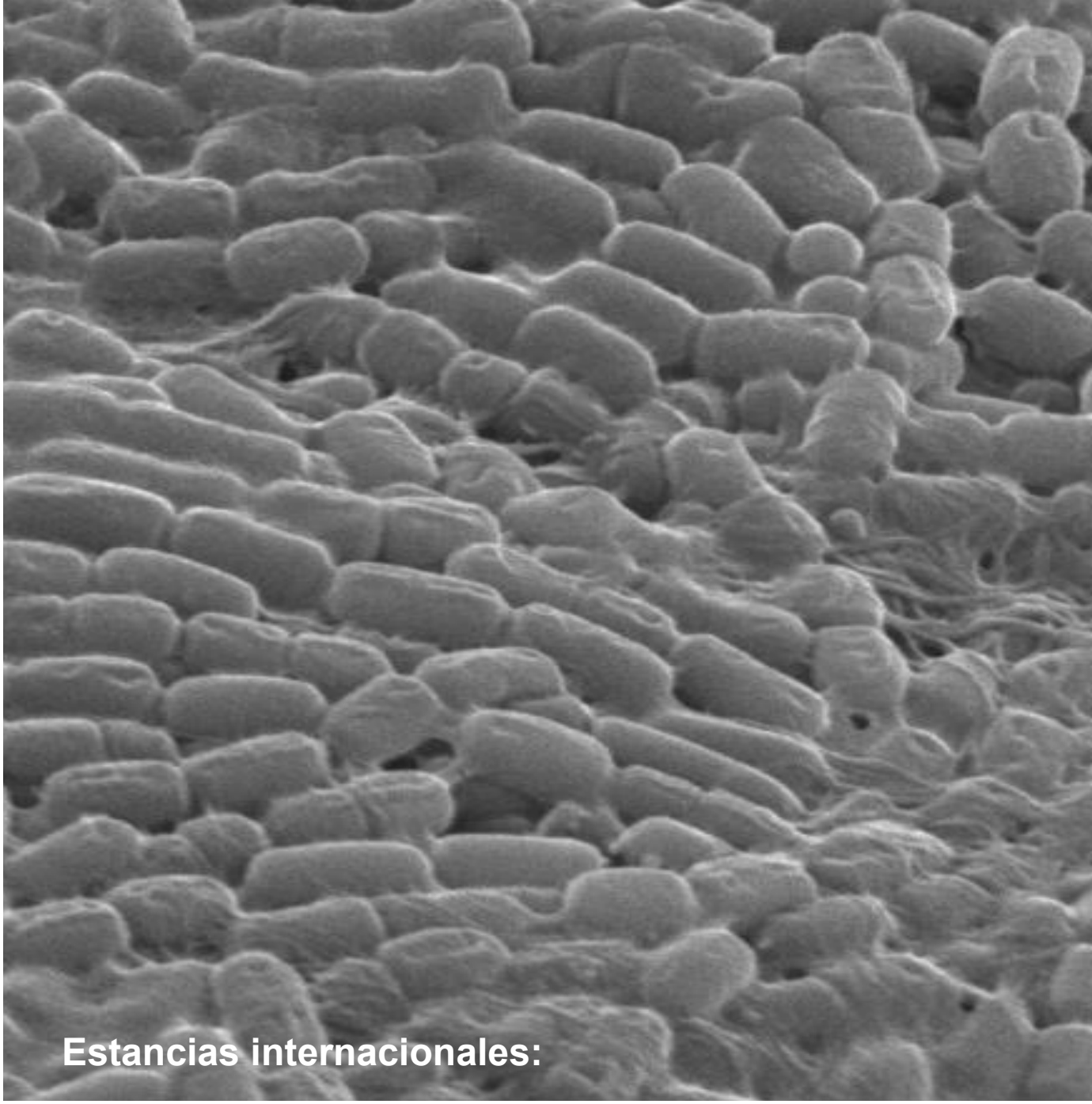

Estancias internacionales:

HARVARD MEDICAL SCHOOL

university of groningen